

UNCLASSIFIED

AD-451393

DEFENSE DOCUMENTATION CENTER

FOR

SCIENTIFIC AND TECHNICAL INFORMATION

CAMERON STATION ALEXANDRIA, VIRGINIA



UNCLASSIFIED

NOTICE: When government or other drawings, specifications or other data are used for any purpose other than in connection with a definitely related government procurement operation, the U. S. Government thereby incurs no responsibility, nor any obligation whatsoever; and the fact that the Government may have formulated, furnished, or in any way supplied the said drawings, specifications, or other data is not to be regarded by implication or otherwise as in any manner licensing the holder or any other person or corporation, or conveying any rights or permission to manufacture, use or sell any patented invention that may in any way be related thereto.

**Best
Available
Copy**

AS AD No. 451393

333154

SUBIC

PROCESSING OF DATA FROM SONAR SYSTEMS

VOLUME II

DDC
RECEIVED
NOV 24 1964
RECEIVED
DDC-IRA C

□ □ □ □ □ □ ■ □ □ □ □ □ □ □ □ □ □



VWR
RESEARCH

GENERAL DYNAMICS/ELECTRIC BOAT
Research and Development Department
Groton, Connecticut

PROCESSING OF DATA FROM
SONAR SYSTEMS

VOLUME II

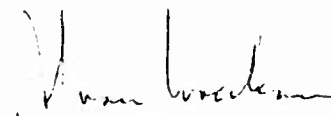
by

Allen H. Levesque
Richard A. McDonald
Peter M. Schultheiss
Theron Usher, Jr.

Dunham Laboratory
Yale University

Examined: 

C. R. DeVoe
Head, Information Processing Section

Approved: 

Dr. A. J. van Woerkom
Chief Scientist

U417-64-028
September 1, 1964



PROCESSING OF DATA FROM SONAR SYSTEMS

by

Allen H. Levesque

Richard A. McDonald

Peter M. Schultheiss

Theron Usher, Jr.

Report on work performed under Yale
University Contract 53-00-10-0231
from July 1, 1963, to July 1, 1964

General Dynamics/Electric Boat Research

DEPARTMENT OF ENGINEERING

AND APPLIED SCIENCE

YALE UNIVERSITY

FOREWORD

The work described in this report was accomplished by members of the Department of Engineering and Applied Science, Dunham Laboratory, Yale University, under subcontract to the SUBIC program (contract NOnr 2512(00)) during the period from July 1, 1963 to July 1, 1964. The Office of Naval Research is the sponsor and General Dynamics/Electric Boat is the prime contractor. Lcdr. R. N. Crawford, USN, is Project Officer for ONR; Dr. A. J. van Woerkom is Project Coordinator for Electric Boat and Chief Scientist of the Applied Sciences Department.

The SUBIC program encompasses all aspects of submarine system analysis. This report is the second of a series dealing with acoustic signal processing.

TABLE OF CONTENTS

	<u>Page</u>
FOREWORD	i
ABSTRACT	v
TEXT: Processing of Data from Sonar Systems (Report of work performed under Yale University Subcontract to EB Division 53-00-10-0231, from July 1, 1963, to July 1, 1964.	1
APPENDICES:	
A. A. H. Levesque, "Optimal Detection of a Sinusoid with Unknown Frequency and Phase," Progress Report No. 8, November 1963.	A-1
B. T. Usher, Jr., "Random Bearing Errors in Split- Beam Systems," Progress Report No. 9, December 1963.	B-1
C. P. M. Schultheiss, "Evaluation of a Suboptimal Procedure for Detecting Directional Gaussian Signals in Isotropic Gaussian Noise," Progress Report No. 10, December 1963.	C-1
D. P. M. Schultheiss, "Likelihood Ratio Detection of Gaussian Signals with Noise Varying from Element to Element of the Receiving Array," Progress Report No. 11, January 1964.	D-1
E. R. A. McDonald, "Minimum Variance Estimation of Relative Delay Between Two Random Signals in Noise," Progress Report No. 12, March 1964.	E-1
F. T. Usher, Jr., "Bearing Uncertainty for Split- Beam Sonar Arrays Due to Scattering in a Random Medium," Progress Report No. 13, March 1964.	F-1
G. A. H. Levesque, "Likelihood Ratio Detection for Long Observation Times," Progress Report No. 14, May 1964.	G-1
H. A. H. Levesque, "Optimal Detection of a Coherent Sinusoid with Unknown Frequency," Progress Report No. 15, June 1964.	H-1
I. T. Usher, Jr., "An Analysis of Bearing Errors Due to Clipping and Sampling in the PUFFS Sonar System," Progress Report No. 16, June 1964.	I-1

ABSTRACT

This report describes work concerned with the detection and determination of the bearing of a single target in an isotropic noise field. In the cases studied, the data source was assumed to be a single hydrophone or a given array of hydrophones. The problems investigated involved studies of likelihood ratio detection of sinusoidal signals in gaussian noise, likelihood ratio detection of gaussian signals in wide-band noise, and determinations of random bearing errors due to processing and also due to medium inhomogeneity for specific types of sonar systems.

I. Introduction

The studies undertaken during the period from July 1, 1963, to July 1, 1964, are described in detail in nine progress reports, which serve as appendices to the main body of this report. The subject material covered in Appendices A through I can be arranged in roughly three categories. In all three categories the work was concerned with the processing of a signal generated by a single target in a background of isotropic random noise.

In the first category, the detection of sinusoids or quasi-sinusoids of unknown center frequency in a background of gaussian, band-limited noise was considered. It is well known that surface and underwater targets emit signal components with periodic structures as well as components with wide-band random structures. Appendices A, G, and H give the results of basic studies involving the detection of sinusoidal signals or of very narrow-band random signals having a center frequency known only within a band of uncertainty. The signal source is a single hydrophone, and likelihood-ratio techniques are employed. The assumptions and results are described in more detail in Section II.

In the second category, the studies involved the detection of a wide-band directional gaussian signal in a similar background of isotropic noise. This work, carried out in Appendices C and D, contains extensions of studies reported earlier by Yale University.¹ In Appendix C, the performance of a suboptimal detector is compared to that of a likelihood-ratio detector. Since the completion of Appendix C, a slightly different scheme has been evaluated by Knapp.² In Appendix D, the performance of a likelihood-ratio scheme is evaluated for the detection of gaussian signals

for the situation in which the average noise power varies from hydrophone to hydrophone. The performance of the likelihood-ratio detector is compared to that of an array with infinite clippers and a standard detector.³ The assumptions and results are described in more detail in Section III.

Finally, in the third category, the computation of random bearing errors was considered. Appendices B, E, F, and I are studies in this category. Appendix E contains a fundamental study for determining the minimum variance of the relative delay between signals generated by two hydrophones, by using statistical estimation techniques. Since the bearing of a single signal source in a medium is directly related to the relative delay between signals generated by two transducers separated by a known distance, this study essentially determines the lower bound for random bearing error for the simple array due to processing techniques. In Appendices F and I, the random bearing errors due to processing techniques for particular types of sonar systems are evaluated. In Appendix G, the bearing uncertainty caused by the scattering effect of a medium with a randomly varying refraction index is studied. The assumptions and results are described in more detail in Section IV.

II. Optimal Detection of Sinusoids or Quasi-Periodic Signals in Noise

In Appendix A, the detection of a sinusoidal signal of known amplitude, but unknown frequency and phase, in additive gaussian noise is considered. Middleton's⁴ development of the likelihood-ratio (hereafter LR) detector, using time-sampled functions, is closely followed. Two cases for the distribution of the unknown frequency are considered: (1) The frequency is equally likely to be one of m different frequencies. (2) The frequency has a uniform probability density function over a band Ω rad/sec wide centered at ω_0 rad/sec.

The LR formed by the optimum detector is

$$\ell(\underline{v}) = \frac{\langle f(\underline{v}/\underline{s}) \rangle_{\underline{s}}}{f(\underline{v}/\underline{o})} \quad (1)$$

where \underline{s} is the desired signal vector, \underline{n} is the noise vector, $\underline{v} = \underline{s} + \underline{n}$ is the received signal, and $f(\underline{v}/\underline{s})$ and $f(\underline{v}/\underline{o})$ are conditional probability density functions. The operation $\langle \rangle_{\underline{s}}$ indicates averaging over the signal parameters of phase and frequency. The detection scheme is essentially one of energy measurement, that is, an incoherent scheme, since $\langle \underline{s} \rangle_{\underline{s}} = 0$. The logarithm of the LR is used as the test statistic because it is more easily interpretable.

The performance index defined in Eq. (2) is used to make appropriate comparisons, and has been used previously.

$$R = \frac{\left[\langle \log \ell(\underline{v}) \rangle_{\underline{S+N}} - \langle \log \ell(\underline{v}) \rangle_{\underline{N}} \right]^2}{\left\langle \left[\log \ell(\underline{v}) \right]^2 \right\rangle_{\underline{N}} - \left\langle \log \ell(\underline{v}) \right\rangle_{\underline{N}}^2} \quad (2)$$

The index R is an output signal-to-noise ratio (hereafter SNR) for the LR detector. The operations $\langle \rangle_{S+N}$ and $\langle \rangle_N$ indicate further averages taken with signal and noise present, and with signal absent respectively.

In the series expansion of $\log \ell(\underline{v})$, if only the terms representing quadratic operations on \underline{v} are retained for the LR detector, we have

$$\log \ell(\underline{v}) \approx \frac{1}{2} \underline{v}' \underline{\bar{G}} \underline{v} - \frac{1}{2} \text{tr}(\underline{K} \underline{\bar{G}}) - \frac{1}{4} \text{tr}(\underline{K} \underline{\bar{G}})^2 \quad (3)$$

where

$$\underline{\bar{G}} = \underline{K}^{-1} \langle \underline{s} \underline{s}' \rangle_S \underline{K}^{-1} \quad (4)$$

and \underline{K} is the covariance matrix for the noise. The last two terms in Eq. (3) represent bias terms of the detector. This approximation is justified in the literature on the basis of small signal-to-noise ratio.

For the situation in which the noise is white and ideally band-limited, and the unknown frequency has the discrete distribution, the variable term of Eq. (3) is

$$\frac{1}{2} \underline{v}' \underline{\bar{G}} \underline{v} \approx \frac{A^2}{4mN^2\Delta^2} \sum_{k=1}^m \left[\left(\int_0^T v(t) \cos \omega_k t dt \right)^2 + \left(\int_0^T v(t) \sin \omega_k t dt \right)^2 \right] \quad (5)$$

where A is the signal amplitude, N is the noise power, T is the observation time, and Δ is the time interval dictated by the sampling theorem. From Eq. (5) the detector is seen to consist of a bank of m correlators and squarers (Figure 1, Appendix A).

Next, for the case in which the statistics of the unknown frequency are given by uniform probability density function over a band Ω rad/sec wide, the variable term in Eq. (3) is given by the quadratic form

$$\frac{1}{2} \underline{v}^T \underline{\bar{G}} \underline{v} = \frac{A^2}{4N^2} \sum_{i=1}^n \sum_{j=1}^n v_i v_j \operatorname{sinc} \bar{\Phi}(t_i - t_j) \cos \omega_0(t_i - t_j) \quad (6)$$

where

$$\bar{\Phi} = \frac{\Omega}{2\pi} \quad \text{and} \quad \operatorname{sinc} a = \frac{\sin \pi a}{\pi a}$$

The output SNR is given by

$$\begin{aligned} R &= \frac{1}{2} \operatorname{tr}(\underline{K} \underline{\bar{G}})^2 = \frac{A^4}{8N^2} \sum_{i=1}^n \sum_{j=1}^n \left[\operatorname{sinc} \bar{\Phi}(t_i - t_j) \cos \omega_0(t_i - t_j) \right]^2 \\ &\approx \frac{A^4}{4N_0^2 \Omega^2} \int_0^{\bar{\Phi}T} dx \int_0^{\bar{\Phi}T} dy \operatorname{sinc}^2(x - y) \\ &\approx \frac{A^4}{4N_0^2 \Omega^2} \bar{\Phi}T \end{aligned} \quad (7)$$

if $\omega_0 \gg \Omega$, $\omega_0 T \gg 1$, $\bar{\Phi}T \gg 1$, and $N = N_0 \Omega$.

Finally, for the situation in which the noise has a bandwidth equal to that of the signal uncertainty, it is shown that the optimum detector is a square-law device followed by an integrator. The SNR is

$$R \approx \frac{A^4 T^2}{16 \pi^2 N_0^2 \int_0^{\bar{\Phi}T} dx \int_0^{\bar{\Phi}T} dy \operatorname{sinc}^2(x - y)} \quad (8)$$

Both the results of Eqs. (8) and (7) are plotted in Fig. 2 of Appendix A. The optimal narrow-band detection index is slightly greater than that for the wide-band case, because it is assumed that the ideal profiler

necessary to process the wide-band noise to a narrow-band noise has been operating on the received signal for an infinite time, not just in the observation interval $(0, T)$.

The previous results apply to the received signal from a single hydrophone. For an array of M hydrophones, the detection index is M^2 times the above expressions. Expressions are also derived in Appendix A for the case of non-white background noise, and a general expression is given for the output signal-to-noise ratio for suboptimum incoherent detectors.

The neglect of the higher-order terms in the expansion of $\log \ell(\underline{y})$ is based on the assumption that low predetection SNR $(A^2/2N)$ makes the higher-order terms negligible. This is the usual assumption made in the literature. However, for certain classes of signals, namely the one considered in Appendix A, long integration or observation time can make the higher-order terms for the expansion of $\log \ell(\underline{y})$ become predominant, even though the predetection SNR is low.

In Appendix G, a study is carried out of the conditions under which the higher-order terms in the series for $\log \ell(\underline{y})$ do not become negligible. Three different signal cases are considered:

- 1) A gaussian random signal which has a flat spectral density over a band of width Ω rad/sec.
- 2) A narrow-band gaussian random signal with bandwidth Ω_b rad/sec and center frequency ω_c rad/sec. In this case ω_c is unknown and has a uniform probability density function over the band Ω and $\Omega_b \ll \Omega$.
- 3) A sinusoid of constant amplitude, unknown frequency and phase, the frequency having a uniform probability density function

over the band Ω . This is the case treated partially in Appendix A.

In each case the noise is assumed gaussian and has a flat spectral density over Ω , the "band" of the signal.

Since the noise is white, and the signals described above are incoherent in the sense that $\langle \underline{s} \rangle_S = 0$, the averaged LR and the test statistic are found to be

$$\ell(\underline{v}) = \exp \left(-\frac{1}{2N} \sum_{i=1}^n s_i^2 \right) \left\langle 1 + \frac{1}{2!} (\underline{s}' \underline{K}^{-1} \underline{v})^2 + \frac{1}{4!} (\underline{s}' \underline{K}^{-1} \underline{v})^4 + \dots \right\rangle \quad (9)$$

and

$$\begin{aligned} \log \ell(\underline{v}) = & -\frac{1}{2N} \sum_{i=1}^n s_i^2 + \frac{1}{2} \left\langle (\underline{s}' \underline{K}^{-1} \underline{v})^2 \right\rangle \\ & + \frac{1}{4!} \left\langle (\underline{s}' \underline{K}^{-1} \underline{v})^4 \right\rangle - \frac{1}{8} \left\langle (\underline{s}' \underline{K}^{-1} \underline{v})^2 \right\rangle^2 \\ & + O(\underline{s}^6) \end{aligned} \quad (10)$$

Equation (10) is exact for terms through $O(\underline{s}^4)$.

In order to justify either using or neglecting higher-order terms for the signal in Eq. (10), the change or deflection in these terms must be examined in going from the "noise-only" condition to the "signal-plus-noise" condition. The total change or deflection is the numerator term $\langle \log \ell(\underline{v}) \rangle_{S+N} - \langle \log \ell(\underline{v}) \rangle_N$ in Eq. (2). For each of the three signal cases, the following deflections (ΔE) are calculated:

$$\Delta E \left[O(\underline{s}^2) \right] = \Delta E \left[\frac{1}{2} \left\langle (\underline{s}' \underline{K}^{-1} \underline{v})^2 \right\rangle \right] \quad (11)$$

$$\Delta E \left[O(\underline{s}^4) \right] = \Delta E \left[\frac{1}{4!} \left\langle (\underline{s}' \underline{K}^{-1} \underline{v})^4 \right\rangle - \frac{1}{8} \left\langle (\underline{s}' \underline{K}^{-1} \underline{v})^2 \right\rangle^2 \right] \quad (12)$$

and

$$\Delta E \left[\text{largest term in } O(\underline{s}^6) \right] = \Delta E \left[\frac{1}{6!} \left\langle (\underline{s}' \underline{K}^{-1} \underline{v})^6 \right\rangle \right] \quad (13)$$

The computations of the deflections, especially for higher-order terms, are extremely complicated. The results of the computations are summarized in Table 1, in which the predetection SNR, $R_1 = \frac{A^2}{2N}$.

Signal Description	$\Delta E \left[O(\underline{s}^2) \right]$	$\Delta E \left[O(\underline{s}^4) \right]$	$\Delta E \left[\text{largest } O(\underline{s}^6) \right]$
1. Random gaussian Bandwidth Ω	$R_1^2 \Phi T$	$-R_1^3 \Phi T$	$\propto \Phi T$
2. Random gaussian Bandwidth Ω_b $b = \frac{\Omega_b}{\Omega} \ll 1$	$R_1^2 \Phi T$	$R_1^4 \left[\left(\frac{1}{3b} - \frac{1}{2} \right) (\Phi T)^2 + \left(\frac{1}{2b^2} - \frac{3}{8b} \right) (\Phi T) \right]$ $- R_1^3 \Phi T$	not computed
3. Sinusoid of constant amplitude Unknown frequency and phase	$R_1^2 \Phi T$	$\frac{2}{3} R_1^4 (\Phi T)^3 - R_1^4 (\Phi T)^2$ $- R_1^3 \Phi T$	$\frac{1}{3} R_1^6 (\Phi T)^5$

Table 1 Deflections of Series Terms for $\log \ell(\underline{v})$

From Table 1 it can be seen that only the random signal having bandwidth Ω satisfies the assumptions made in Appendix A. All deflection terms for this signal are proportional to $\bar{\Phi}T$, and higher-order terms depend on higher powers of R_1 . Thus, for small R_1 , the approximation by terms of the $O(\underline{s}^2)$ is sufficient. The narrow-band gaussian signal with uncertain center frequency has $\Delta E[O(\underline{s}^4)]$ increasing primarily as $(\bar{\Phi}T)^2$ and the same deflection for the steady sinusoidal signal increases as $(\bar{\Phi}T)^3$. Higher-order deflections increase with higher powers of $\bar{\Phi}T$.

For a numerical example, let $R_1 = .1$, $b = .1$, and $\bar{\Phi}T = 100$. The numerical results from direct substitution into the expressions in Table 1 are given in Table 2.

Signal Description	$\Delta E[O(\underline{s}^2)]$	$\Delta E[O(\underline{s}^4)]$	$\Delta E[\text{largest } O(\underline{s}^6)]$
1. Random gaussian Bandwidth Ω	1.0	-.1	-
2. Random gaussian Bandwidth Ω_b	1.0	3.19	-
3. Sinusoid of constant amplitude	1.0	66.6	3333

Table 2 Numerical Values for Deflections

$$R_1 = .1, b = .1, \bar{\Phi}T = 100$$

The numerical values chosen above are used because the output SNR for the random signal of bandwidth Ω has the same expression as that for $\Delta E[O(\underline{s}^2)]$. The table thus gives a rather marginal output SNR for detection purposes. For the other signals, the deflections for higher-order terms are much larger than that for $\Delta E[O(\underline{s}^2)]$ and therefore cannot be neglected.

The latter two signal cases are nonergodic and if one were to construct an efficient detector, the operations corresponding to the higher-order terms of Eq. (10) would have to be built into the detector. A consideration of the higher-order terms for a signal whose center frequency is equally likely to be any one of m different frequencies suggests a band-splitting detector containing m filters, and nonlinear operation on the output of each of the detectors. Such a technique is examined in Appendix H.

In Appendix H the optimum detector structure is determined for the case in which the signal is assumed to be a sinusoid with known amplitude and phase and unknown frequency. The frequency is assumed to take on any one of m equally likely values. The phase is assumed to be known in order to keep the mathematical development relatively simple.

The averaged LR where one parameter is unknown and may take on only discrete values can be expressed as

$$\ell(\underline{v}) = \sum_{i=1}^m p_i \exp \left[\log L(\underline{v}, \omega_i) \right] \quad (14)$$

where ω_i are the possible frequencies, p_i are the respective probabilities of occurrence, and $L(\underline{v}, \omega_i)$ are the LR's for particular values of frequency. The decision scheme consists of comparing $\ell(\underline{v})$ with a pre-set threshold k : if $\ell(\underline{v}) < k$, "no signal" is the decision; if $\ell(\underline{v}) > k$, "signal present" is the decision. The quantities $\log L(\underline{v}, \omega_i)$ in Eq. (14) are considered as coordinates of an m -dimensional space for the received signal \underline{v} . The boundary

$$\sum_{i=1}^m p_i \exp \left[\log L(\underline{v}, \omega_i) \right] = k$$

divides this space into the "signal" and "no signal" regions.

The decision scheme is examined in detail for the two-frequency case.

The boundary between the decision regions is given by

$$\log L(\underline{v}, \omega_2) = \log \left\{ 2k - \exp \left[\log L(\underline{v}, \omega_1) \right] \right\} \quad (15)$$

The curves are shown in Appendix H, Figure 1, and are asymptotic to the straight lines $\log L(\underline{v}, \omega_1) = \log 2k$ and $\log L(\underline{v}, \omega_2) = \log 2k$.

Conditional false-alarm and conditional false-dismissal probabilities are calculated for the optimum detector and for a suboptimum detector for which the decision boundary is

$$\log L(\underline{v}, \omega_1) + \log L(\underline{v}, \omega_2) = 2 \log k - \frac{d}{2} \quad (16)$$

where

$$d = \frac{1}{\pi N_0} \int_0^T s^2(t) dt \quad (17)$$

The quantity d is a detection index and may be considered the post-detection SNR.

For large values of d , the boundary given by Eq. (15) may be replaced by its straight line asymptotes, and the false-alarm and false-dismissal probabilities are given by

$$\alpha \approx \frac{1}{2} \left[1 - \Phi \left(\sqrt{\frac{d}{4}} + \frac{1}{\sqrt{d}} \log 2k \right) \right] \left[\frac{3}{2} + \frac{1}{2} \Phi \left(\sqrt{\frac{d}{4}} + \frac{1}{\sqrt{d}} \log 2k \right) \right] \quad (18)$$

$$\beta \approx \frac{1}{4} \left[1 - \Phi \left(\sqrt{\frac{d}{4}} - \frac{1}{\sqrt{d}} \log 2k \right) \right] \left[1 + \Phi \left(\sqrt{\frac{d}{4}} + \frac{1}{\sqrt{d}} \log 2k \right) \right] \quad (19)$$

where $\Phi(x)$ is the normal probability integral.⁵

For the "sum-and-test" detector, defined by the decision boundary in Eq. (16), α and β are given by

$$\alpha = \frac{1}{2} \left[1 - \Phi \left(\sqrt{\frac{d}{8}} + \frac{1}{\sqrt{2d}} \log k \right) \right] \quad (20)$$

$$\beta = \frac{1}{2} \left[1 - \Phi \left(\sqrt{\frac{d}{8}} - \frac{1}{\sqrt{2d}} \log k \right) \right] \quad (21)$$

From Appendix H, Fig. 4, the performance of the sum-and-test detector becomes progressively poorer than the optimum detector as d becomes larger. It should be noted that the optimum detector for large d becomes a band-splitting detector by virtue of the separate-decision criteria. The sum-and-test detector is derived by omitting higher-order terms in the series expansion for $\log \ell(\underline{y})$. Thus Fig. 4 shows the effect of this omission.

The optimum or band-splitting decision scheme and the sum-and-test decision scheme are also examined and compared for the general or m -frequency case, where $p_i = \frac{1}{m}$. The decision boundary surface for the m -dimensional space is given by

$$\frac{1}{m} \sum_{i=1}^m \exp \left[\log L(\underline{y}, \omega_i) \right] = k \quad (22)$$

and that for the sub-optimum "sum-and-test" scheme by

$$\sum_{i=1}^m \log L(\underline{y}, \omega_i) = m \log k - (m-1) \frac{d}{2} \quad (23)$$

The comparison between the performance of the two detectors is carried out by evaluating the ratio of the output SNR's for both systems for equal false-alarm and false-dismissal probabilities. This gives the

ratio of the observation times necessary to achieve identical detection performance in each case. These results are given in Appendix H, Fig. 6, and are reproduced in Table 3, for $\alpha = \beta = .01$.

Ratio of detection indices or integration times $\frac{d_{\text{sum}}}{d_{\text{opt}}}$	1	1.8	11	72
Number of signal frequencies - m	1	2	16	128

Table 3 Ratio of Detection Indices for "Sum-and-Test"
and "Band-Splitting" Detectors; $\alpha = \beta = .01$

It can be seen from Table 3 that the advantage of the band-splitting technique becomes greater and greater as the number of possible frequencies increases. Thus the penalty paid by neglecting higher-order terms in the series expansion for $\log \ell(\underline{y})$ can be quite large.

III. Detection of Directional Gaussian Signals in Isotropic Noise

In Appendix C a suboptimum detection scheme for processing the outputs of M hydrophones is evaluated. Non-zero correlation of the noise components of the hydrophone outputs is assumed. The suboptimum scheme consists of summing the outputs, and then passing the resulting voltage through an Eckart filter, squarer, and low-pass filter.

The index used to compare the performance of the suboptimum detector to that for the LR detector is the output signal-to-noise ratio defined in a manner similar to that found in Eq. (2):

$$r = \frac{(\text{av. output with signal}) - (\text{av. output--noise only})}{\text{standard deviation of output with noise only}} = \frac{\Delta(\text{av. output})}{D(\text{output})} \quad (24)$$

The index defined in Eq. (24) is actually analogous to the square root of that found in Eq. (2). The denominator is evaluated with noise only since we are concerned with threshold detection problems.

For the optimum or LR detector, the index has been shown to be¹

$$r_{\text{opt}} = \left(\frac{T}{2\pi} \right)^{1/2} \left[\int_0^{\infty} \left(\frac{S(\omega)}{N(\omega)} G(\omega) \right)^2 d\omega \right]^{1/2} \quad (25)$$

where $S(\omega)$ and $N(\omega)$ are the signal and the noise spectral densities respectively and $G(\omega)$ is the array gain defined by Bryn⁶ and is given by

$$G(\omega_n) = \text{Tr} \left[P(n) Q^{-1}(n) \right] \quad (26)$$

In Eq. (26) $P(n)$ and $Q(n)$ are the normalized correlation matrices of signal and noise respectively. For the array steered on target and no correlation between the noise outputs at each hydrophone, we have

$$r_{\text{opt}} = \left(\frac{T}{2\pi} \right)^{1/2} M \left[\int_0^{\infty} \left(\frac{S(\omega)}{N(\omega)} \right)^2 d\omega \right]^{1/2} \quad (27)$$

The optimum detector for the case of no cross-correlation for the noise components is identical to the suboptimum detector described previously. The purpose of the study is the evaluation of the effects of cross-correlation for the noise components of different hydrophones.

The detection index for the suboptimum system having a general filter with the response function $H(j\omega)$ is found to be

$$r = \left(\frac{T}{2\pi} \right)^{1/2} M^2 \frac{\int_0^{\infty} S(\omega) |H(j\omega)|^2 d\omega}{\left[\int_0^{\infty} |H(j\omega)|^4 \left| \sum_{i=1}^M \sum_{h=1}^M G_{ih}(\omega) \right|^2 d\omega \right]^{1/2}} \quad (28)$$

In Eq. (28), $G_{ih}(\omega)$ is the cross-spectral density for the noise components of the i^{th} and h^{th} hydrophones respectively. For a spherically isotropic noise field, where d_{ih} is the distance between hydrophones i and h ,

$$G_{ih}(\omega) = N(\omega) \frac{\sin \omega \tau_{ih}}{\omega \tau_{ih}} \quad (29)$$

and

$$\tau_{ih} = \frac{d_{ih}}{c} \quad (30)$$

The Eckart filter has the characteristic

$$|H(j\omega)|^2 = \Lambda \frac{S(\omega)}{N^2(\omega)}$$

If one assumes further that

$$\frac{S(\omega)}{N(\omega)} = \begin{cases} \frac{S}{N} & |\omega| \leq \omega_0 \\ 0 & |\omega| > \omega_0 \end{cases} \quad (31)$$

then Eq. (28) reduces to

$$r_1 = \left(\frac{T}{2\pi} \right)^{1/2} M \frac{S}{N} \frac{\omega_0}{\left[\int_0^{\omega_0} \left| 1 + \frac{2}{M} \sum_{\ell=1}^{M-1} (M-\ell) \frac{\sin \ell \omega \tau_0}{\ell \omega \tau_0} \right|^2 d\omega \right]^{1/2}} \quad (32)$$

for a linear array with elements having equal spacing d and $\tau_0 = \frac{d}{c}$.

The best linear filter function for maximizing r in Eq. (28) is, however, not the Eckart filter, but is found in Eq. (33) by means of the calculus of variations.²

$$|H(j\omega)|^2 = B \frac{S(\omega)}{\left| \sum_{i=1}^M \sum_{h=1}^M G_{ih}(\omega) \right|^2} \quad (33)$$

For this situation, and utilizing the assumptions in Eqs. (29) and (31), Eq. (28) reduces to

$$r_2 = \left(\frac{T}{2\pi} \right)^{1/2} M \frac{S}{N} \frac{\omega_0}{\left[\int_0^{\omega_0} \left| 1 + \frac{2}{M} \sum_{\ell=1}^{M-1} (M-\ell) \frac{\sin \ell \omega \tau_0}{\ell \omega \tau_0} \right|^2 d\omega \right]^{1/2}} \quad (34)$$

Table 5 gives the results of a numerical evaluation of Eqs. (25), (32) and (34) for a five-element linear array with 2-ft. spacing. The results are normalized with respect to $(T\omega_0/2\pi)^{1/2} M (S/N)$.

detector \ Upper cut-off frequency kcp/s	1	2	3	5	10	15
1. Likelihood ratio detector Eq. (25)	.75	1.05	1.05	1.04	1.01	1.005
2. Power detector with Eckart filter Eq. (32)	.25	.47	.55	.64	.75	.81
3. Power detector with optimum filter Eq. (34)	.49	.90	.99	1.01	1.00	1.00

Table 5 Normalized Performance Indices
as Functions of Upper Cut-Off
Frequency for Three Detectors

From Table 5 it is easily seen that the detector with the Eckart filter is measurably inferior to the other two detector systems, even for reasonably high cut-off frequencies. However, the index for the power detector with the optimum prefilter approaches that for the LR detector even for reasonably low cut-off frequencies.

It is suspected that any simple prefilter having high-pass characteristics with a cut-off frequency in the vicinity of 1250 cps would yield a system with a performance index closely approaching that of the detector with the optimum prefilter. All the optimum prefilter does is to attenuate the frequency band over which appreciable correlation exists between the noise components from different hydrophones. Most sonar systems are designed with high-pass characteristics, so it is unlikely that significant improvement can be obtained by changing present system design.

For the study in Appendix D, it is assumed that the noise outputs of different hydrophones are not correlated, and that the noise power outputs from different hydrophones are not the same. Likelihood-ratio detection is examined and the results are compared to those for a system using infinite clippers, which has been examined previously.^{1,3}

The detection index defined in Eq. (24) for the LR detector is

$$r_{\text{opt}} = \left(\frac{T}{2\pi} \right) \left[\sum_{i=1}^M \frac{S}{N_i} \right] \left[\int_0^{\infty} \left(\frac{g_s(\omega)}{g_n(\omega)} \right)^2 d\omega \right]^{1/2} \quad (35)$$

In Eq. (35), S is the signal power at each hydrophone, N_i is the noise power at the i^{th} hydrophone, and $g_s(\omega)$ and $g_n(\omega)$ are the normalized signal and noise spectral densities respectively. The result in Eq. (35) is equal to that in Eq. (27) for a LR detector with input SNR

$$\frac{S}{N} = \frac{1}{M} \sum_{i=1}^M \frac{S}{N_i}$$

at each hydrophone. However, as stated previously, the LR detector with the same SNR at each hydrophone and no noise correlation between hydrophones is equivalent to a simple power detector preceded by an Eckart filter.

Thus the LR detector for the case of different noise powers at each hydrophone is instrumented by a gain control following each hydrophone, followed by the power detector with an Eckart prefilter. The gain settings are such that the SNR after summation for the system with different noise powers at each hydrophone is equal to that for the system

with equal noise powers at each hydrophone. With the use of this equivalence, the gain settings k_i are found to be

$$k_i = \frac{1}{N_i} \quad (36)$$

and the average power at the output of each gain control varies as $\frac{1}{N_i}$ ($\sigma^2 \ll N_i$).

The comparison between the LR detector and the power detector with infinite clippers following the hydrophones is accomplished by comparing each to a power detector without clippers. A ratio of performance indices is used for the comparison. The ratio of the performance index for the LR detector with the k_i determined by Eq. (36) to that for a power detector with an Eckart prefilter ($k_i = 1$) is

$$F_1 = \frac{r_{\text{opt}}}{r_{\text{unclipped}}} = \frac{1}{M^2} \sum_{i=1}^M N_i \sum_{i=1}^M (N_i)^{-1} \quad (37)$$

From previous work,³ the ratio of the SNR for a power detector with infinite clippers following the hydrophones to that for a detector without the clippers can be found to be

$$F_2 = \frac{r_{\text{clipped}}}{r_{\text{unclipped}}} = .89 \frac{2}{M^2 (M^2 - M)^{1/2}} \sum_{i=1}^M \sum_{j=i+1}^M (N_i N_j)^{-1/2} \left[\sum_{i=1}^M N_i \right] \quad (38)$$

For a simple numerical computation, it is assumed that exactly pM hydrophones take on a high noise value N_H and $(1-p)M$ hydrophones take on a low noise value N_L . This seems reasonable since the noise values are determined by known patterns of flow noise. Other statistical descriptions are considered in Appendix D. If $b = N_H/N_L$, Eq. (37) reduces to

$$F_1 = p^2 + (1-p)^2 + p(1-p)(b + b^{-1}) \quad (39)$$

and for large M Eq. (38) becomes

$$F_2 = .89 \left[p(b^{-1/2} - 1) + 1 \right]^2 \left[p(b - 1) + 1 \right] \quad (40)$$

Equations (39) and (40) are evaluated in Table 6 for $p = \frac{1}{2}$, which yields the maximum value of F_1 and close to the maximum value of F_2 .

$\frac{N_H}{N_L} = b$	1	3	10	100	1000
$\frac{r_{\text{opt}}}{r_{\text{unclipped}}} = F_1$	1	1.25	3.02	25	250
$\frac{r_{\text{clipped}}}{r_{\text{unclipped}}} = F_2$.89	1.11	2.17	13.6	118

Table 6 Ratios of Performance Indices
for Different Values of Noise
Power Ratio

The results in Table 6 represent extreme values of improvement for systems in which the noise powers are known to vary between two limits. The improvement factor F_1 for the LR detector as $N_H/N_L \rightarrow \infty$ is only $2/.89$ times the improvement factor for the standard detector with infinite clippers.

Since practical situations involve noise powers distributed inside a relative range of usually no more than 100 to 1, with most of the noise

powers near the lower level, the advantage gained by using the instrumentation to set k_1 would be significantly less than 2/.89 . Moreover, the possibilities of nonstationarity, coupled with the complexity of estimating N_i to drive automatic gain control circuits, makes the simplicity of the infinite clipper attractive.

IV. Random Bearing Errors

Appendix E contains a basic study for determining the minimum variance in estimating the time delay δ between the signal components of the outputs of two hydrophones. The total outputs for the hydrophones are given by $s(t) + n_1(t)$ and $s(t - \delta) + n_2(t)$. It is assumed that signal and noise are gaussian and ideally limited to a band W cps wide, and the noise components are not correlated. Signal and noise are thus completely described by $2TW$ samples for an observation time T .

The data available to the estimator are given by the row vector

$$\underline{\ell} = (\underline{x}, \underline{y}) \quad (41)$$

where

$$\underline{x} = (x_1, x_2, x_3, \dots, x_{2TW}) \quad (42)$$

$$\underline{y} = (y_1, y_2, y_3, \dots, y_{2TW}) \quad (43)$$

and

$$x_i = s\left(\frac{i}{2W}\right) + n_1\left(\frac{i}{2W}\right) \quad (44)$$

$$y_i = s\left(\frac{i}{2W} - \frac{k}{2W}\right) + n_2\left(\frac{i}{2W}\right) \quad (45)$$

A well-known theorem⁷ of statistical estimation states that the best estimate, k^* , of normalized time delay, k , has a variance given by

$$E \left[(k^* - k)^2 \right] \geq \left[E \left\{ \left(\frac{\partial}{\partial k} \left[\log P(\underline{\ell}; k) \right] \right)^2 \right\} \right]^{-1} \quad (46)$$

where $P(\underline{\ell}; k)$ is the probability density function for $\underline{\ell}$, and is a function of the parameter to be estimated. The density function is gaussian and has $4TW$ dimensions.

$$P(\underline{\ell}; k) = \frac{1}{(2\pi)^{2TW} |M_k|^{1/2}} \exp \left\{ -\frac{1}{2} \underline{\ell} M_k^{-1} \underline{\ell} \right\} \quad (47)$$

In Eq. (47), M_k is the covariance matrix for $\underline{\ell}$.

The operations on $P(\underline{\ell}; k)$ described in Eq. (46) are tedious and require extensive matrix manipulation. The result obtained for the case $k = 0$ is

$$E \left[(k^* - k)^2 \right] \geq \frac{(S + N_1)(S + N_2) - S^2}{2S^2} \left[2WT \frac{\pi^2}{6} - \log(2WT - 1) - .5772 \right]^{-1} \quad (48)$$

When the usual assumptions $WT \gg 1$ and $\frac{S}{N_1}, \frac{S}{N_2} \ll 1$ are made, the expression in Eq. (48) may be simplified and translated to a bearing uncertainty with the relation

$$\sigma_\theta^2 = \left(\frac{c}{d} \cdot \frac{1}{2W} \right)^2 E \left[(k^* - k)^2 \right] \quad (49)$$

Thus

$$\sigma_\theta \geq \frac{c}{d} \frac{(N_1 N_2)^{1/2}}{S} \cdot \left(\frac{3}{8\pi^2} \right)^{1/2} W^{-3/2} T^{-1/2} \quad (50)$$

If the minimum estimation error given by Eq. (48) is attainable, it can be attained by a maximum likelihood estimator. For maximum likelihood estimation,

$$\frac{\partial}{\partial k} \log P(\underline{\ell}; k) = 0$$

must be solved for k as a function of $\underline{\ell}$. This is extremely difficult to do, but a nearly equivalent technique is to steer the array physically or electronically until $\delta = 0$. Since conventional estimation techniques produce the minimum value of σ_0 in Eq. (50), errors involved in this steering technique are not investigated.

The effects of nonstationary signal strength and also delay errors due to the medium are also discussed briefly in Appendix E.

Appendix B contains an analysis of the bearing uncertainty due to processing errors in a conventional split-beam sonar system. In this system (Fig. 1, Appendix B) the outputs of each set of M hydrophones from a linear, equally spaced array of $2M$ hydrophones are summed, and each sum is fed into a linear filter. The frequency response functions of these filters are related in that there is 90° phase shift between the response functions at all frequencies. The filtered sums are passed through infinite clippers, the results are multiplied, and the product averaged with a low-pass filter. The signal and noise are gaussian, and the noise components from different transducers are uncorrelated.

The voltages following the summing operation are given by

$$v_A(t) = \sum_{i=1}^K \left\{ s_1[t - (i-1)T] + n_i(t) \right\} \quad (51)$$

$$v_r(t) = \sum_{j=1}^M \left\{ s_1[t - (j+M-1)T] + n_{M+j}(t) \right\} \quad (52)$$

where T is the signal time delay between adjacent hydrophones. The frequency response functions of the linear filters enjoy the simple minimum phase relation

$$H_A(j\omega) = j\omega k H_B(j\omega) \quad (53)$$

where k is a proportionality constant.

The average output of the low-pass filter is

$$\bar{y} = \frac{2}{\pi} \arcsin \left[\frac{R_{x_A x_B}(0)}{\left\{ R_{x_A}(0) R_{x_B}(0) \right\}^{1/2}} \right] \quad (54)$$

in which $R_{x_A x_B}$, R_{x_A} , and R_{x_B} are cross- and autocorrelation functions for the output voltages of the filters described in Eq. (53).

For threshold signal conditions $\left(\frac{SM}{N} \ll 1 \right)$ Eq. (54) reduces to

$$\bar{y} \approx - \frac{2}{\pi} \frac{SM}{N} \frac{\int_{-\infty}^{\infty} \omega |H_B(j\omega)|^2 g_s(\omega) \sin \omega MT \operatorname{sinc}^2 \frac{\omega MT}{2\pi} d\omega}{\left[\int_{-\infty}^{\infty} \omega^2 |H_B(j\omega)|^2 g_n(\omega) d\omega \right]^{1/2} \left[\int_{-\infty}^{\infty} |H_B(j\omega)|^2 g_n(\omega) d\omega \right]^{1/2}} \quad (55)$$

in which $g_s(\omega)$ and $g_n(\omega)$ are normalized signal and noise spectral densities, as defined previously. It is easy to see that $\bar{y} = 0$ for $T = 0$.

The bearing uncertainty is defined by

$$\sigma_\theta = \frac{c}{d} \sigma_z \left| \frac{d\bar{y}}{dT} \right|_{T=0}^{-1} \quad (56)$$

where σ_z is the standard deviation for the output of the final low-pass filter.

Evaluation of the terms in Eq. (56) yields

$$\sigma_{\theta} \approx \frac{c}{Md} \left(\frac{SM}{N} \right)^{-1} (\omega_L)^{1/2} \frac{\left[2 \int_{-\infty}^{\infty} \omega^2 |H_B(j\omega)|^4 \epsilon_n^2(\omega) d\omega \right]^{1/2}}{\int_{-\infty}^{\infty} \omega^2 |H_B(j\omega)|^2 \epsilon_s(\omega) d\omega} \quad (57)$$

Employing the calculus of variations, one finds the minimum bearing uncertainty to be

$$\sigma_{\theta \min} = \frac{c}{Md} \left(\frac{SM}{N} \right)^{-1} (\omega_L)^{1/2} \left[\int_0^{\infty} \omega^2 \left(\frac{\epsilon_s(\omega)}{\epsilon_n(\omega)} \right)^2 d\omega \right]^{-1/2} \quad (58)$$

for

$$|H_B(j\omega)|^2 = k_B \frac{\epsilon_s(\omega)}{\epsilon_n^2(\omega)} \quad (59)$$

In Eqs. (57) and (58), ω_L is the noise bandwidth of the low-pass filter.

In obtaining Eq. (57), an approximation is made which causes the result to be approximately 20 per cent lower than the actual answer due to the infinite clipping action. Also it is demonstrated in Appendix F that the result in Eq. (58) holds for even more general filter response functions, $H_A(j\omega)$ and $H_B(j\omega)$.

With the use of the spectral model⁸

$$\epsilon_s(\omega) = \epsilon e^{-\omega^2 \alpha r} \quad \epsilon_n(\omega) = \frac{1}{\pi \omega_0} \frac{\epsilon e^{-\omega^2 \alpha r}}{1 + \left(\frac{\omega}{\omega_0} \right)^2} \quad (60)$$

it is found that the minimum bearing uncertainty is

$$\sigma_{\theta_{\min}} = \frac{c}{Md} \left(\frac{SM}{N} \right)^{-1} (\omega_L)^{1/2} \left(\frac{2}{\pi} \right)^{1/4} (4\pi r)^{3/4} \text{ radians} \quad (61)$$

For $M = 25$, $c = 5000$ ft/sec, $d = 2$ ft, $\omega_L = 1$ rad/sec, $r = 10$ kyd, $\alpha = 6 \times 10^{-11}$, $\frac{SM}{N} = 0.1$, we have $\sigma_{\theta_{\min}} = .013$ degrees.

Two comparisons are carried out between systems with suboptimum filters and the system with the filters specified by Eqs. (59) and (53).

In one case, for the system with the bandpass filter function

$$H_B(j\omega) = b \frac{\left(1 + j \frac{\omega}{\omega_0} \right) \left(j \frac{\omega}{30,000} \right)}{\left(1 + j \frac{\omega}{30,000} \right) \left(1 + j \frac{\omega}{45,000} \right) \left(1 + j \frac{\omega}{60,000} \right)} \quad (62)$$

the ratio of the bearing uncertainty to the minimum value is below 2 from ranges of 20 kyd to below 1 kyd. At 3.3 kyd the ratio is 1.03. This investigation shows that optimum filter characteristics need not be met exactly if performance closely approaching the optimum is desired. This investigation also supports to some extent the statement in Section III concerning the approximation of the characteristic required by Eq. (33).

Since the bearing error calculated above is not particularly large, it is highly possible that other sources, such as medium inhomogeneities, contribute significant amounts.

A comparison with the result in Eq. (50) for the maximum likelihood estimator is also possible. If we set $M = 1$, $\omega_L = \frac{\pi}{T}$, $E_S(\omega)/E_N(\omega) = 1$ for $|\omega| \leq \pi W$ and zero elsewhere, $N_1 = N_2 = N$, then Eqs. (58) and

(50) become identical. The bearing uncertainty for the split-beam system considered here is therefore about 20 per cent greater than that for the maximum-likelihood estimator due to approximations involved in obtaining Eq. (57). The approximations were made for mathematical expressions that were generated due to the infinite clipping action.

Appendix I contains a study of the bearing errors generated by the processing techniques of a PUFFS tracking sonar system. The basic elements of a PUFFS system are shown in Fig. 1, Appendix I, and consist of two hydrophones, two DELay LINE Time Compressors,⁹ a polarity coincidence indicator and summer, a digital-to-analog converter, and a nonlinear filter called a WOX-1A tracker. The analysis of the system is carried out in general terms, and reference to specific numbers, which might characterize particular systems, is not emphasized. The operation of the system is described in detail in Appendix I, Section I.

The system operation is such that the output voltage of the hydrophone amplifiers are infinitely clipped and time-sampled. These samples from both channels are processed in such a way as to give a real-time estimate of the cross-correlation function between the signals generated by the hydrophones. The usual assumptions of gaussian input signals and noise, and zero noise correlation between channels, are made. The input SNR is also assumed to be small. The WOX-1A tracker determines the time value of the peak of the estimated cross-correlation function by employing a gate circuit which makes use of area subtraction and a nonlinear error-correction technique.

The analysis centers on determining the expressions for (1) the K-point correlation estimate generated by the two DELTIC processors and

the polarity coincidence indicator and summer, (2) the expected gate circuit output, (3) the variance of the gate circuit output, and (4) the variance of the tracker output. The bearing uncertainty is calculated from a relation almost identical to Eq. (56). The bearing uncertainty represented by the random output of the gate circuit can be directly compared to results obtained in Appendix F.

A number of general results for bearing uncertainty are obtained in Appendix I, but the simplest to present in this summary are found in Eqs. (63) and (64).

$$\sigma_{\theta_i} = \frac{\pi}{2\sqrt{2}} \cdot \frac{c}{d} \frac{N}{S} K^{-1/2} T \left(\frac{G}{T} - \frac{3}{4} \right)^{1/2} \quad \frac{G}{T} = 1, 2, 3, \dots \quad (63)$$

$$\sigma_{\theta_h} = \frac{\pi}{2\sqrt{2}} \cdot \frac{c}{d} \frac{N}{S} K^{-1/2} T \cdot \frac{\pi}{2} \cdot \frac{4 \left(\frac{G}{T} \right)^2 - 1}{4 \left(\frac{G}{T} \right)^2 + (-1)^{G/T} - 1} \left(\frac{G}{T} - \frac{21}{32} \right)^{1/2} \quad (64)$$

$$\frac{G}{T} = 2, 3, 4, \dots$$

Equation (63) represents a lower bound on bearing uncertainty and Eq. (64), an upper bound for the following condition:

$$g_s(\omega) = g_n(\omega) = \begin{cases} \frac{1}{2\omega_0} & |\omega| \leq \omega_0 \\ 0 & |\omega| > \omega_0 \end{cases} \quad (65)$$

Also $\omega_0 T = \pi$, T is the time between signal samples, K is the number of signal samples in the observation period, and G is the width of the gate circuit in Eqs. (63) and (64). The results hold only for integer values of $\frac{G}{T}$.

In order to compare these results to those in Eq. (57), we let $H_B(j\omega) = 1$, $\omega_L = \frac{\pi}{KT}$, and $\omega_0 = \frac{\pi}{T}$. We get

$$\sigma_{\theta_L} = \frac{3^{1/2}}{\pi} \frac{c}{d} \frac{N}{S} K^{-1/2} T \quad (66)$$

The ratios of the results in Eqs. (63) and (64) to those in Eq. (66) give

$$\frac{\sigma_{\theta}}{\sigma_{\theta_L}} \left\{ \begin{array}{l} < \frac{\pi^3}{4 \cdot 6^{1/2}} \frac{4 \left(\frac{G}{T}\right)^2 - 1}{4 \left(\frac{G}{T}\right)^2 + (-1)^{G/T} - 1} \left(\frac{G}{T} - \frac{21}{32}\right)^{1/2} \\ > \frac{\pi^2}{2 \cdot 6^{1/2}} \left(\frac{G}{T} - \frac{3}{4}\right)^{1/2} \end{array} \right. \quad (67)$$

For $\frac{G}{T} = 1$, for which the gate width is approximately equal to the process correlation time, the ratio above has an upper bound of 3 and a lower bound of unity. The ratio increases approximately as $\left(\frac{G}{T}\right)^{1/2}$ for higher $\frac{G}{T}$.

These results and others included in Appendix I indicate that it is desirable to use a fairly large gate width G for high gain or sensitivity. However, for gate widths larger than the process correlation time, the sensitivity does not increase greatly. The results also show that the bearing uncertainty increases as gate width gets larger than the process correlation time, but remains relatively constant for gate widths less than the correlation time. Thus a gate width equal to the correlation time of the process provides good sensitivity and low bearing uncertainty. This choice seems to have been used in the design of the present PUFFS systems.

The effect of the WOX-1A tracker as a nonlinear filter that increases observation time and decreases random bearing error is also discussed.

In Appendix F, the evaluation of bearing errors due to scattering in a medium with a fluctuating refractive index is accomplished for a split-beam system identical to that described in Appendix B. Results taken from work by Chernov¹⁰ are employed in the analysis.

In particular, Chernov assumes a single-frequency plane-wave propagating through a medium in which the variance of the refractive index is $\langle \mu^2 \rangle$. For typical sonar reception conditions, the variance of the phase and log amplitude of the received signal at one location after traveling through the random medium a distance of r feet are respectively

$$\langle \gamma^2 \rangle = \langle \beta^2 \rangle = \frac{\pi^{1/2}}{2} \langle \mu^2 \rangle \frac{\omega^2}{c^2} a r \quad (68)$$

In Eq. (68) a is the correlation distance for the spatial fluctuations of the refractive index. Also the following normalized cross-correlation function holds for the outputs of two hydrophones broadside to the direction of propagation:

$$R_{\beta_{1,2}} = R_{\gamma_{1,2}} = e^{-\frac{\ell^2}{a^2}} \quad (69)$$

where ℓ is the separation of the two hydrophones.

The bearing uncertainty for the split-beam array of $2M$ hydrophones broadside to the direction of propagation is

$$\sigma_{\theta} = \left(\pi^{1/2} \langle \mu^2 \rangle a \right)^{1/2} \frac{r^{1/2}}{M^2 (Md)} \left[\sum_{i=1}^M \sum_{p=1}^M R_{(p-i)} - \sum_{i=1}^M \sum_{k=1}^M R_{(k+M-i)} \right]^{1/2} \quad (70)$$

where

$$R_{(\alpha)} = \epsilon \frac{a^2 d^2}{a^2} \quad (71)$$

The bearing uncertainty is seen to satisfy the inequality

$$K \frac{r^{1/2}}{M^{3/2} (Md)} < \sigma_\theta \ll K \frac{r^{1/2}}{M(Md)} \quad (72)$$

If $M = 25$, $d = 2$ ft, $r = 30,000$ ft or 10 kyd, $a = 2$ ft, $\langle \mu^2 \rangle = 5 \times 10^{-9}$, then Eq. (70) gives $\sigma_\theta = 2.8 \times 10^{-4}$ degrees.

This numerical result is an extremely small bearing error. Quite possibly the assumed value¹⁰ of $\langle \mu^2 \rangle$ is several orders of magnitude too small, because more fluctuation of signal power is experimentally observed than that given by Eq. (68) with $\langle \mu^2 \rangle = 5 \times 10^{-9}$. It is also worth noting that the analysis holds for single-frequency signals. It is expected that fluctuations for broadband random signals are even smaller. Certainly more work needs to be done in this area.

REFERENCES

1. McDonald, R. A., P. M. Schultheiss, F. B. Tuteur, and T. Usher, Jr., "Processing of Data from Sonar Systems," SUBIC Report U417-63-045, September 1, 1963.
2. Knapp, C., "A Power Detector with Optimal Prefiltering for Detecting Directional Gaussian Signals in Gaussian Noise Fields," GD/EB Report U417-64-009, February 18, 1964.
3. Usher, T., "Signal Detection by Arrays in Noise Fields with Local Variations," JASA 36, 8, August 1964.
4. Middleton, D., An Introduction to Statistical Communication Theory, McGraw-Hill Book Company, Inc., New York, 1960.
5. National Bureau of Standards, Tables of Normal Probability Functions, Applied Math. Series, No. 23, Washington, 1953.
6. Bryn, F., "Optimal Signal Processing of Three-Dimensional Arrays Operating on Gaussian Signals and Noise," JASA 34, 3, pp. 289-297, March 1962.
7. Cramér, H., Mathematical Methods of Statistics, Ch. 32, Princeton University Press, 1946.
8. Eckart, Carl, "Optimal Rectifier Systems for the Detection of Steady Signals," Marine Laboratory, Scripps Institute of Oceanography, SIO Reference 52-11, University of California, March 4, 1952.
9. Anderson, V. C., "Delay Line Time Compressor (DELTIC)", U. S. Patent No. 2,958,039, October 25, 1960.
10. Chernov, L. A., Wave Propagation in a Random Medium, McGraw-Hill Book Company, Inc., New York, 1960.



OPTIMAL DETECTION OF A SINUSOID
WITH UNKNOWN FREQUENCY AND PHASE

by

Allen H. Levesque

Progress Report No. 8

General Dynamics/Electric Boat Research

(53-00-10 -0231)

November 1963

DEPARTMENT OF ENGINEERING
AND APPLIED SCIENCE
YALE UNIVERSITY

I. Introduction

Earlier reports^{1,2} have dealt with the optimum detection of signals which were assumed to be gaussian random processes. It is known, however, that various signals with more or less coherent time structure are sometimes observed. Tuteur² considered the detection of a gaussian signal whose power is amplitude modulated by a low frequency sinusoid of known amplitude, phase and frequency. This report considers the optimum detection of certain baseband signals which are typically observed in the frequency range near 100 c.p.s. There is reason to believe that these signals are periodic time functions with coherent phase structure, but the frequencies are not known precisely.

For convenience in this analysis the signal is taken to be a steady sinusoid with known amplitude but unknown frequency and phase. Since in practice the amplitude of such a signal would not be known precisely, the results are to be considered as upper bounds on the performance of the detection system.

Two general cases are considered, one in which the frequency of the sinusoid is known to be one of a finite discrete set of frequencies, the other in which the frequency is given by a flat, unimodal probability density function (p.d.f.) over the band of frequency uncertainty.

II. Likelihood Ratio Detection of General Signals in Additive Gaussian Noise

The general theory of likelihood ratio (hereafter LR) detection of signals in additive gaussian noise has been outlined by several authors.^{3,4} In this section we follow rather closely Middleton's⁴ development of the form of the optimum LR detector.

Here and throughout this report we shall assume the following:

1) The desired signal is deterministic, though its functional form will in general include certain parameters the values of which are not known except statistically. The stochastic parameters are assumed independent.

2) The noise is additive and gaussian with zero mean.

3) The signal and noise processes are independent.

The general technique for developing the form of the optimum detector can be applied equally well for continuous signals or for discrete (sampled) signals. However, in order to keep the derivation simple and to obviate the necessity of discussing integral equations, we shall treat the discrete case. The various time-sampled signal functions and noise functions then take the forms of signal vectors and noise vectors. The samples are assumed to be uniformly spaced in time, though we do not make use of this assumption in this section.

The received signal vector is given by

$$\underline{v} = \underline{s} + \underline{n} \quad (1)$$

where \underline{s} is the "desired signal" vector and \underline{n} is the noise vector (hereafter simply referred to as the received signal, the desired signal and the noise).

The optimum detector forms the LR

$$\ell(\underline{v}) = \frac{\langle f(\underline{v}/\underline{s}) \rangle_{\underline{s}}}{f(\underline{v}/\underline{o})} \quad (2)$$

$f(\underline{v}/\underline{s})$ and $f(\underline{v}/\underline{o})$ are conditional probability density functions (p.d.f.'s) for the received signal given that the desired signal is present and given

no signal present, respectively. The averaging operation $\langle \rangle_S$ indicates a statistical average over the set S of signal parameters. Since the noise is additive and gaussian with zero mean, we have

$$f(\underline{v}/\underline{s}) = \frac{1}{(2\pi)^{n/2} (\det \underline{K})^{n/2}} e^{-\frac{1}{2}(\underline{v}-\underline{s})' \underline{K}^{-1}(\underline{v}-\underline{s})} \quad (3)$$

and

$$f(\underline{v}/\underline{o}) = \frac{1}{(2\pi)^{n/2} (\det \underline{K})^{n/2}} e^{-\frac{1}{2}\underline{v}' \underline{K}^{-1} \underline{v}} \quad (4)$$

where \underline{K} is the covariance matrix of the noise. From Eq. (2) we can write

$$\ell(\underline{v}) = \left\langle e^{-\frac{1}{2}(\underline{v}-\underline{s})' \underline{K}^{-1}(\underline{v}-\underline{s})} \right\rangle_S e^{\frac{1}{2}\underline{v}' \underline{K}^{-1} \underline{v}} \quad (5)$$

$$= \left\langle e^{-\frac{1}{2}\underline{s}' \underline{K}^{-1} \underline{s} + \underline{s}' \underline{K}^{-1} \underline{v}} \right\rangle_S \quad (6)$$

The LR thus calculated is compared to a fixed threshold and if the threshold is exceeded, the decision is made that the desired signal is present.

To derive the form of the optimum detector, we 1) expand the exponential form in Eq. (6) in a power series, 2) perform the averaging $\langle \rangle_S$ term by term, and 3) expand $\ln \ell(\underline{v})$ in another power series. The quantity $\ln \ell(\underline{v})$, rather than $\ell(\underline{v})$, is usually taken to be the test statistic in a LR detector. One reason is that $\ln \ell(\underline{v})$ is more readily interpretable in terms of electronic correlation and filtering operations. For the case of low input signal-to-noise ratio, we shall be able to find a suitable approximation to the optimum detector by neglecting certain higher order terms in the signal.

The aforementioned steps are straightforward, and the following expansion can easily be verified:

$$\begin{aligned}
 \ln \ell(\underline{v}) = & \langle \underline{s}' \underline{K}^{-1} \underline{v} \rangle \\
 & - \frac{1}{2} \langle \underline{s}' \underline{K}^{-1} \underline{s} \rangle + \frac{1}{2} \left[\langle (\underline{s}' \underline{K}^{-1} \underline{v})^2 \rangle - \langle \underline{s}' \underline{K}^{-1} \underline{v} \rangle^2 \right] \\
 & + \frac{1}{2} \left[\langle \underline{s}' \underline{K}^{-1} \underline{s} \rangle \langle \underline{s}' \underline{K}^{-1} \underline{v} \rangle - \langle \underline{s}' \underline{K}^{-1} \underline{s} \underline{s}' \underline{K}^{-1} \underline{v} \rangle \right] \\
 & + \left[\frac{1}{6} \langle (\underline{s}' \underline{K}^{-1} \underline{v})^3 \rangle - \frac{1}{2} \langle \underline{s}' \underline{K}^{-1} \underline{v} \rangle \langle (\underline{s}' \underline{K}^{-1} \underline{v})^2 \rangle + \frac{1}{3} \langle \underline{s}' \underline{K}^{-1} \underline{v} \rangle^3 \right] \\
 & + \frac{1}{8} \left[\langle (\underline{s}' \underline{K}^{-1} \underline{s})^2 \rangle - \langle \underline{s}' \underline{K}^{-1} \underline{s} \rangle^2 \right] \\
 & + \frac{1}{4} \left[\langle \underline{s}' \underline{K}^{-1} \underline{s} \rangle \langle (\underline{s}' \underline{K}^{-1} \underline{v})^2 \rangle - \langle (\underline{s}' \underline{K}^{-1} \underline{v})^2 \underline{s}' \underline{K}^{-1} \underline{s} \rangle \right] \\
 & + \frac{1}{2} \left[\langle \underline{s}' \underline{K}^{-1} \underline{s} \underline{s}' \underline{K}^{-1} \underline{v} \rangle \langle \underline{s}' \underline{K}^{-1} \underline{v} \rangle - \langle \underline{s}' \underline{K}^{-1} \underline{s} \rangle \langle \underline{s}' \underline{K}^{-1} \underline{v} \rangle^2 \right] \\
 & + \left[\frac{1}{24} \langle (\underline{s}' \underline{K}^{-1} \underline{v})^4 \rangle - \frac{1}{6} \langle (\underline{s}' \underline{K}^{-1} \underline{v})^3 \rangle \langle \underline{s}' \underline{K}^{-1} \underline{v} \rangle - \frac{1}{8} \langle (\underline{s}' \underline{K}^{-1} \underline{v})^2 \rangle^2 \right. \\
 & \quad \left. + \frac{1}{4} \langle \underline{s}' \underline{K}^{-1} \underline{v} \rangle^4 \right] \\
 & + O(\underline{s}^5)
 \end{aligned} \tag{7}$$

where $\langle \rangle$ implies $\langle \rangle_{\underline{s}}$ throughout. Equation (7) is exact through

$O(\underline{s}^4)$. We note that if the structure of the desired signal is known completely, the averaging operation $\langle \rangle_{\underline{s}}$ over unknown signal parameters is trivial, and each of the seven bracketed terms in Eq. (7) is identically equal to zero. In such a case the optimum detector would perform the following operation:

$$\ln \ell(\underline{v}) = \underline{s}' \underline{K}^{-1} \underline{v} - \frac{1}{2} \underline{s}' \underline{K}^{-1} \underline{s} \quad (8)$$

a result which can be verified from Eq. (6).

Noting that

$$\left\langle \underline{s}' \underline{K}^{-1} \underline{v} \right\rangle_S = \left\langle \underline{s} \right\rangle_S' \underline{K}^{-1} \underline{v} \quad (9)$$

we can distinguish two different classes of optimum detection:

1) If $\left\langle \underline{s} \right\rangle_S \neq 0$, the optimum detection process is considered to be "coherent." In such a case, Eq. (7) contains a term which is linear in \underline{v} . In the threshold case of low input SNR, the principal contribution to $\ln \ell(\underline{v})$ is from the linear term and the higher order terms can be neglected or replaced by appropriate average values. The optimum detection operation is then approximately a cross-correlation of the received signal with a replica of the desired signal.

2) If $\left\langle \underline{s} \right\rangle_S = 0$, the optimum detection process is said to be "incoherent." In such a case, the linear term in Eq. (7) disappears and the principal contribution to $\ln \ell(\underline{v})$ is from a second order term representing a square law operation on the received signal. As in case 1), higher order terms in $(\underline{s}' \underline{K}^{-1} \underline{v})^2$ are either neglected or replaced by appropriate average values, such average values being taken into the bias in the threshold comparison.

III. LR Detection of a Sine Wave with Unknown Frequency and Phase-- Discrete Frequency Distribution

In this section we shall consider the problem of detecting, in the presence of additive gaussian noise, a steady sine wave whose amplitude is known but whose frequency and phase are statistically described.

III. 1. The Form of the Detector

We consider the desired signal, in continuous form, to be

$$s(t) = A \cos(\omega t - \phi) \quad (10)$$

In sampled form,

$$\underline{s} = A \left\{ \cos(\omega t_i - \phi) \right\} \quad (11)$$

The radian frequency ω and the phase ϕ are unknown but their probability distributions are known. Let us assume that the phase ϕ is uniformly distributed from 0 to 2π , i.e.,

$$p(\phi) = \begin{cases} \frac{1}{2\pi} & 0 \leq \phi \leq 2\pi \\ 0 & \text{elsewhere} \end{cases} \quad (12)$$

We shall assume that the frequency is equally likely to be one of m different frequencies:

$$P(\omega_i) = \frac{1}{m}, \quad i = 1, 2, \dots, m \quad (13)$$

In deriving the form of the optimum detector, we are concerned with two terms which represent linear and square law operations on the received signal, respectively. They are:

$$\left\langle \underline{s}^T \underline{K}^{-1} \underline{v} \right\rangle_S = \left\langle \underline{s} \right\rangle_S^T \underline{K}^{-1} \underline{v} \quad (14)$$

and

$$\begin{aligned} \frac{1}{2} \left\langle \left(\underline{s}^T \underline{K}^{-1} \underline{v} \right)^2 \right\rangle_S &= \frac{1}{2} \left\langle \underline{v}^T \underline{K}^{-1} \underline{s} \underline{s}^T \underline{K}^{-1} \underline{v} \right\rangle_S \\ &= \frac{1}{2} \underline{v}^T \underline{K}^{-1} \left\langle \underline{s} \underline{s}^T \right\rangle_S \underline{K}^{-1} \underline{v} \\ &= \frac{1}{2} \underline{v}^T \underline{G} \underline{v} \end{aligned} \quad (15)$$

where

$$\bar{G} = \underline{K}^{-1} \left\langle \underline{s} \underline{s}^i \right\rangle_S \underline{K}^{-1} \quad (16)$$

We see then that the desired signal \underline{s} enters into the detector operation through the forms $\left\langle \underline{s} \right\rangle_S$ and $\left\langle \underline{s} \underline{s}^i \right\rangle_S$. Averaging over phase first,

$$\begin{aligned} \left\langle \underline{s} \right\rangle_{\phi} &= \left\{ \frac{A}{2\pi} \int_0^{2\pi} \cos(\omega t_1 - \phi) d\phi \right\} \\ &= \{0\} \end{aligned} \quad (17)$$

Thus the optimum detection is "incoherent." Turning to the nonlinear term,

$$\begin{aligned} \left\langle \underline{s} \underline{s}^i \right\rangle_{\phi} &= \left\{ \frac{A^2}{2\pi} \int_0^{2\pi} \cos(\omega t_1 - \phi) \cos(\omega t_j - \phi) d\phi \right\} \\ &= \left\{ \frac{A^2}{2\pi} \int_0^{2\pi} \frac{1}{2} \cos[\omega(t_1 + t_j) - 2\phi] d\phi + \frac{A^2}{2\pi} \int_0^{2\pi} \frac{1}{2} \cos \omega(t_1 - t_j) d\phi \right\} \\ &= \left\{ \frac{A^2}{2} \cos \omega(t_1 - t_j) \right\} \end{aligned} \quad (18)$$

and, averaging over frequency,

$$\left\langle \underline{s} \underline{s}^i \right\rangle_{\phi, \omega} = \left\{ \frac{A^2}{2m} \sum_{k=1}^m \cos \omega_k(t_i - t_j) \right\} \quad (19)$$

In Eq. (7) the linear term and the third order terms (in \underline{s}) disappear.

The most significant fourth order terms (in \underline{s}) are replaced by their averages taken in the absence of desired signal. The detector operation is then approximately

$$\begin{aligned}
\ln \ell(\underline{v}) \cong & \frac{1}{2} \underline{v} \underline{\bar{G}} \underline{v} - \frac{1}{2} \left\langle \underline{s} \underline{\bar{K}}^{-1} \underline{s} \right\rangle_S \\
& + \left\langle \left[-\frac{1}{8} \left\langle \underline{s} \underline{\bar{K}}^{-1} \underline{s} \right\rangle_S^2 + \frac{1}{4} \left\langle \underline{s} \underline{\bar{K}}^{-1} \underline{s} \right\rangle_S \left\langle \underline{s} \underline{\bar{K}}^{-1} \underline{v} \right\rangle_S - \frac{1}{8} \left\langle \underline{s} \underline{\bar{K}}^{-1} \underline{v} \right\rangle_S^2 \right] \right\rangle_N
\end{aligned}
\quad (20)$$

We note that

$$\begin{aligned}
\left\langle \underline{s} \underline{\bar{K}}^{-1} \underline{s} \right\rangle_S &= \left\langle \sum_i \sum_j s_i s_j K_{ij}^{-1} \right\rangle_S \\
&= \sum_i \sum_j \langle s_i s_j \rangle_S K_{ij}^{-1} \\
&= \text{tr} (\underline{K} \underline{\bar{G}})
\end{aligned}
\quad (21)$$

$$\begin{aligned}
\left\langle \left\langle \underline{s} \underline{\bar{K}}^{-1} \underline{v} \right\rangle_S^2 \right\rangle_N &= \left\langle \underline{v} \underline{\bar{G}} \underline{v} \right\rangle_N \\
&= \text{tr} (\underline{K} \underline{\bar{G}})
\end{aligned}
\quad (22)$$

$$\begin{aligned}
-\frac{1}{8} \left\langle \left\langle \underline{s} \underline{\bar{K}}^{-1} \underline{v} \right\rangle_S^2 \right\rangle_N &= -\frac{1}{8} \left\langle (\underline{v} \underline{\bar{G}} \underline{v})^2 \right\rangle_N \\
&= -\frac{1}{8} \left\langle \underline{v} \underline{\bar{G}} \underline{v} \underline{v} \underline{\bar{G}} \underline{v} \right\rangle_N \\
&= -\frac{1}{4} \text{tr} (\underline{K} \underline{\bar{G}})^2 - \frac{1}{8} \text{tr}^2 (\underline{K} \underline{\bar{G}})
\end{aligned}
\quad (23)$$

Substituting Eqs. (21), (22) and (23) into Eq. (20), we obtain

$$\ln \ell(\underline{v}) \cong \frac{1}{2} \underline{v} \underline{\bar{G}} \underline{v} - \frac{1}{2} \text{tr} (\underline{K} \underline{\bar{G}}) - \frac{1}{4} \text{tr} (\underline{K} \underline{\bar{G}})^2$$

(24)

The operation of the optimum detector for the case of a sine wave with unknown frequency and unknown phase is given by the incoherent form Eq. (24), where $\underline{\bar{G}}$ is given by Eq. (16) and $\left\langle \underline{s} \underline{s}' \right\rangle_S$ by Eq. (19).

Output Signal-to-Noise Ratio

Since we shall be concerned in this report with cases of incoherent detection, we shall now derive an expression for a performance index which we can use to make comparison among various optimum and sub-optimum detection schemes. A definition of output signal-to-noise ratio which has been used in earlier reports is

$$R = \frac{\left[\left\langle \ln \ell(\underline{v}) \right\rangle_{S+N} - \left\langle \ln \ell(\underline{v}) \right\rangle_N \right]^2}{\left\langle \left[\ln \ell(\underline{v}) \right]^2 \right\rangle_N - \left\langle \ln \ell(\underline{v}) \right\rangle_N^2} \quad (25)$$

For convenience, we shall use this definition here.

From Eq. (24), above,

$$\begin{aligned} \left\langle \ln \ell(\underline{v}) \right\rangle_{S+N} &= \frac{1}{2} \left\langle \underline{v}' \underline{\bar{G}} \underline{v} \right\rangle_{S+N} - \frac{1}{2} \text{tr} (\underline{K} \underline{\bar{G}}) - \frac{1}{4} \text{tr} (\underline{K} \underline{\bar{G}})^2 \\ &= \frac{1}{2} \left\langle (\underline{s}' + \underline{n}') \underline{\bar{G}} (\underline{s} + \underline{n}) \right\rangle_{S+N} - \frac{1}{2} \text{tr} (\underline{K} \underline{\bar{G}}) - \frac{1}{4} \text{tr} (\underline{K} \underline{\bar{G}})^2 \\ &= \frac{1}{2} \left\langle \underline{s}' \underline{\bar{G}} \underline{s} \right\rangle_{S+N} + \left\langle \underline{s}' \underline{\bar{G}} \underline{n} \right\rangle_{S+N} + \frac{1}{2} \left\langle \underline{n}' \underline{\bar{G}} \underline{n} \right\rangle_{S+N} - \frac{1}{2} \text{tr} (\underline{K} \underline{\bar{G}}) - \frac{1}{4} \text{tr} (\underline{K} \underline{\bar{G}})^2 \\ &= \frac{1}{2} \text{tr} (\underline{K} \underline{\bar{G}})^2 + \frac{1}{2} \text{tr} (\underline{K} \underline{\bar{G}}) - \frac{1}{2} \text{tr} (\underline{K} \underline{\bar{G}}) - \frac{1}{4} \text{tr} (\underline{K} \underline{\bar{G}})^2 \\ &= \frac{1}{4} \text{tr} (\underline{K} \underline{\bar{G}})^2 \end{aligned} \quad (26)$$

$$\begin{aligned}
\langle \ell_n \ell(\underline{v}) \rangle_N &= \frac{1}{2} \langle \underline{v}' \underline{\bar{G}} \underline{v} \rangle_N - \frac{1}{2} \text{tr} (\underline{K} \underline{\bar{G}}) - \frac{1}{4} \text{tr} (\underline{K} \underline{\bar{G}})^2 \\
&= \frac{1}{2} \text{tr} (\underline{K} \underline{\bar{G}}) - \frac{1}{2} \text{tr} (\underline{K} \underline{\bar{G}}) - \frac{1}{4} \text{tr} (\underline{K} \underline{\bar{G}})^2 \\
&= -\frac{1}{4} \text{tr} (\underline{K} \underline{\bar{G}})^2
\end{aligned} \tag{27}$$

Therefore,

$$\langle \ell_n \ell(\underline{v}) \rangle_{S+N} - \langle \ell_n \ell(\underline{v}) \rangle_N = \frac{1}{2} \text{tr} (\underline{K} \underline{\bar{G}})^2 \tag{28}$$

Also

$$\begin{aligned}
\langle [\ell_n \ell(\underline{v})]^2 \rangle_N &= \frac{1}{4} \langle \underline{v}' \underline{\bar{G}} \underline{v} \underline{v}' \underline{\bar{G}} \underline{v} \rangle_N - \left[\frac{1}{2} \text{tr} (\underline{K} \underline{\bar{G}}) - \frac{1}{4} \text{tr} (\underline{K} \underline{\bar{G}})^2 \right] \langle \underline{v}' \underline{\bar{G}} \underline{v} \rangle_N \\
&\quad + \left[\frac{1}{2} \text{tr} (\underline{K} \underline{\bar{G}}) + \frac{1}{4} \text{tr} (\underline{K} \underline{\bar{G}})^2 \right]^2 \\
&= \frac{1}{2} \text{tr} (\underline{K} \underline{\bar{G}})^2 + \frac{1}{4} [\text{tr} \underline{K} \underline{\bar{G}}]^2 - \frac{1}{2} [\text{tr} (\underline{K} \underline{\bar{G}})]^2 \\
&\quad - \frac{1}{4} \text{tr} (\underline{K} \underline{\bar{G}})^2 \text{tr} (\underline{K} \underline{\bar{G}}) + \left[\frac{1}{2} \text{tr} (\underline{K} \underline{\bar{G}}) + \frac{1}{4} \text{tr} (\underline{K} \underline{\bar{G}})^2 \right]^2 \\
&= \frac{1}{2} \text{tr} (\underline{K} \underline{\bar{G}})^2 + \frac{1}{16} [\text{tr} (\underline{K} \underline{\bar{G}})^2]^2
\end{aligned} \tag{29}$$

Therefore,

$$\langle [\ell_n \ell(\underline{v})]^2 \rangle_N - \langle \ell_n \ell(\underline{v}) \rangle_N^2 = \frac{1}{2} \text{tr} (\underline{K} \underline{\bar{G}})^2 \tag{30}$$

and, from Eq. (25),

$$R = \frac{1}{2} \text{tr} (\underline{K} \underline{\bar{G}})^2 \tag{31}$$

III. 2. Detection in White Noise

If the background noise is white and wide-sense stationary, the covariance matrix for the noise, K , is a diagonal matrix and is given by

$$K = N \underline{I} \quad (32)$$

where N is the noise power and \underline{I} is the unit matrix. Therefore,

$$\underline{G} = \frac{A^2}{2mN} \left\{ \sum_{k=1}^m \cos \omega_k (t_i - t_j) \right\} \quad (33)$$

The operation on the received signal is then

$$\begin{aligned} \frac{1}{2} \underline{v}^T \underline{G} \underline{v} &= \frac{A^2}{4mN} \sum_{i=1}^n \sum_{j=1}^n v_i v_j \left\{ \sum_{k=1}^m \cos \omega_k (t_i - t_j) \right\} \\ &= \frac{A^2}{4mN} \sum_{k=1}^m \left[\sum_{i=1}^n \sum_{j=1}^n v_i v_j \left\{ \cos \omega_k (t_i - t_j) \right\} \right] \\ &= \frac{A^2}{4mN} \sum_{k=1}^m \left[\sum_{i=1}^n \sum_{j=1}^n v_i v_j \cos \omega_k t_i \cos \omega_k t_j \right. \\ &\quad \left. + \sum_{i=1}^n \sum_{j=1}^n v_i v_j \sin \omega_k t_i \sin \omega_k t_j \right] \\ &= \frac{A^2}{4mN} \sum_{k=1}^m \left[\left(\sum_{i=1}^n v_i \cos \omega_k t_i \right)^2 + \left(\sum_{i=1}^n v_i \sin \omega_k t_i \right)^2 \right] \end{aligned} \quad (34)$$

It is informative to approximate the inner summations by integrations:

$$\frac{1}{2} \underline{v}^T \underline{G} \underline{v} \approx \frac{A^2}{4mN} \sum_{k=1}^m \left[\left(\int_0^T v(t) \cos \omega_k t dt \right)^2 + \left(\int_0^T v(t) \sin \omega_k t dt \right)^2 \right] \quad (35)$$

where Δ is the time interval between uniformly spaced samples and T is the observation time of the received signal.

Thus the optimum detector consists of a bank of m pairs of correlators and squarers followed by an adder and a threshold device. These operations are shown in Figure 1. The correlators in the detector, shown typically in the dashed box in Fig. 1, can be implemented by matched filters.

It is clear that if the uncertainty about the frequency of the sine wave is enlarged to a greater and greater number of discrete frequencies, we simply incorporate more and more pairs of correlators and squarers into the detector. It is also clear from Eq. (35) that if the probabilities of the m discrete frequencies are not uniform, the m terms in the summation are simply weighted according to the probabilities of the various frequencies. In terms of the actual detector, the m inputs to the adder are appropriately weighted.

III. 3. Detection in Non-White Noise

If the noise background is non-white, the covariance matrix \underline{K} is no longer diagonal, and the matrix $\underline{\bar{G}}$ becomes in general

$$\begin{aligned}
 \underline{\bar{G}} &= \underline{K}^{-1} \left\langle \underline{s} \underline{s}' \right\rangle_S \underline{K}^{-1} \\
 &= \underline{K}^{-1} \left\{ \frac{A^2}{2m} \sum_{k=1}^m \cos \omega_k (t_1 - t_j) \right\} \underline{K}^{-1} \\
 &= \frac{A^2}{2m} \sum_{k=1}^m \underline{K}^{-1} \left\{ \cos \omega_k t_1 \cos \omega_k t_j + \sin \omega_k t_1 \sin \omega_k t_j \right\} \underline{K}^{-1} \quad (36)
 \end{aligned}$$

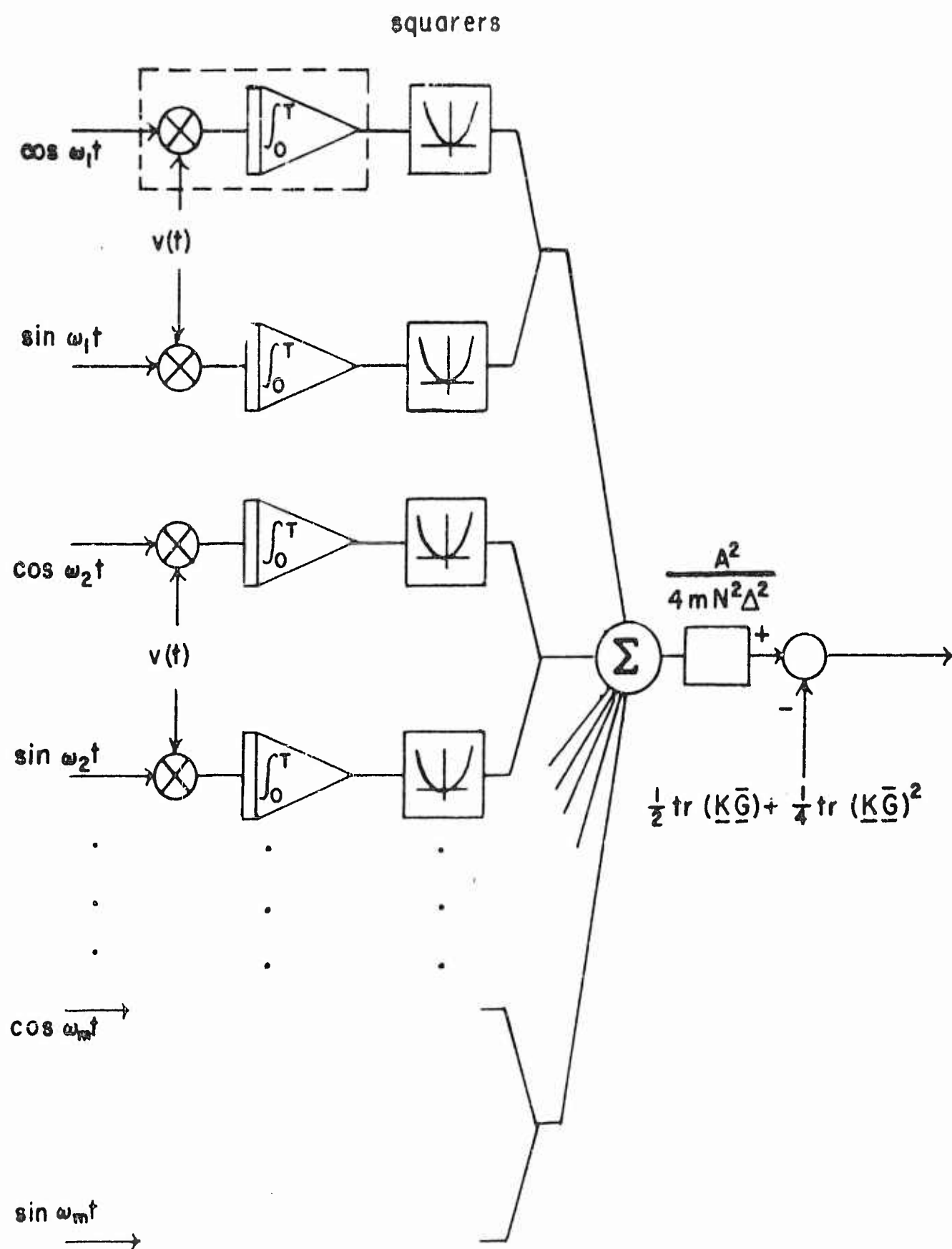


FIG. 1 Optimum Detector

The operation on the received signal then becomes

$$\begin{aligned}
 \frac{1}{2} \underline{v}' \underline{G} \underline{v} &= \frac{A^2}{4m} \sum_{k=1}^m \underline{v}' \underline{K}^{-1} \left\{ \cos \omega_k t_i \cos \omega_k t_j \right\} \underline{K}^{-1} \underline{v} \\
 &\quad + \frac{A^2}{4m} \sum_{k=1}^m \underline{v}' \underline{K}^{-1} \left\{ \sin \omega_k t_i \sin \omega_k t_j \right\} \underline{K}^{-1} \underline{v} \\
 &= \frac{A^2}{4m} \sum_{k=1}^m \left(\sum_{i=1}^n \sum_{j=1}^n v_i K_{ij}^{-1} \cos \omega_k t_j \right)^2 \\
 &\quad + \frac{A^2}{4m} \sum_{k=1}^m \left(\sum_{i=1}^n \sum_{j=1}^n v_i K_{ij}^{-1} \sin \omega_k t_j \right)^2
 \end{aligned} \tag{37}$$

IV. LR Detection of a Sine Wave with Unknown Frequency and Phase-- Continuous Frequency Distribution

A more general kind of uncertainty about the frequency of the sine wave is one in which the unknown frequency has a p.d.f. over a range of the spectrum. In this section we assume that the frequency is known only to lie between certain upper and lower limits. For convenience we shall assume that the p.d.f. is flat and unimodal.

IV. 1. The Form of the Optimum Detector

As in sections III.1 through III.3, the desired signal in continuous form is taken to be

$$s(t) = A \cos (\omega t - \phi) \tag{38}$$

and in sampled form,

$$\underline{s} = A \left\{ \cos (\omega t_i - \phi) \right\} \tag{39}$$

The phase ϕ is assumed to be uniformly distributed over $0, 2\pi$ and the radian frequency ω to be uniformly distributed over a band Ω rad/sec wide centered at ω_0 rad/sec, i.e.,

$$p(\phi) = \begin{cases} \frac{1}{2\pi} & 0 \leq \phi \leq 2\pi \\ 0 & \text{elsewhere} \end{cases} \quad (40)$$

and

$$p(\omega) = \begin{cases} \frac{1}{\Omega} & \omega_0 - \frac{\Omega}{2} \leq \omega \leq \omega_0 + \frac{\Omega}{2} \\ 0 & \text{elsewhere} \end{cases} \quad (41)$$

As before [see Eq. (17)],

$$\langle \underline{s} \rangle_{\phi} = \begin{Bmatrix} 0 \end{Bmatrix} \quad (42)$$

and the optimum detector is termed "incoherent." The operation on the received signal is thus

$$\frac{1}{2} \underline{v}' \underline{\bar{G}} \underline{v} = \frac{1}{2} \underline{v}' \underline{K}^{-1} \langle \underline{s} \underline{s}' \rangle_{\phi} \underline{K}^{-1} \underline{v} \quad (43)$$

Carrying out the averaging $\langle \underline{s} \underline{s}' \rangle_{\phi}$ over ϕ and ω , we have first [see Eq. (18)]

$$\langle \underline{s} \underline{s}' \rangle_{\phi} = \begin{Bmatrix} \frac{A^2}{2} \cos \omega(t_1 - t_j) \end{Bmatrix} \quad (44)$$

Averaging over ω ,

$$\begin{aligned} \langle \underline{s} \underline{s}' \rangle_{\phi, \omega} &= \begin{Bmatrix} \frac{A^2 \sin \omega(t_1 - t_j)}{2\Omega(t_1 - t_j)} \left| \begin{matrix} \omega = \omega_0 + \frac{\Omega}{2} \\ \omega = \omega_0 - \frac{\Omega}{2} \end{matrix} \right. \end{Bmatrix} \\ &= \frac{A^2}{2} \left\{ \frac{\sin(\omega_0 + \frac{\Omega}{2})(t_1 - t_j) - \sin(\omega_0 - \frac{\Omega}{2})(t_1 - t_j)}{2(t_1 - t_j)} \right\} \\ &= \frac{A^2}{2} \left\{ \frac{\sin \frac{\Omega}{2}(t_1 - t_j)}{\frac{\Omega}{2}(t_1 - t_j)} \cos \omega_0(t_1 - t_j) \right\} \end{aligned}$$

$$= \frac{A^2}{2} \left\{ \text{sinc} \frac{\Omega(t_i - t_j)}{2\pi} \cos \omega_0(t_i - t_j) \right\} \quad (45)$$

where

$$\text{sinc } x = \frac{\sin \pi x}{\pi x} \quad (46)$$

and

$$\bar{\Phi} = \frac{\Omega}{2\pi} \quad (47)$$

The operation of the optimum detector upon the received signal is therefore given by

$$\frac{1}{2} \underline{v}^T \underline{G} \underline{v} = \frac{A^2}{4} \underline{v}^T \underline{K}^{-1} \left\{ \text{sinc} \bar{\Phi} (t_i - t_j) \cos \omega_0(t_i - t_j) \right\} \underline{K}^{-1} \underline{v} \quad (48)$$

IV. 2. Detection in White Noise

Broadband Low-Pass White Noise

We shall now consider a case in which the power density spectrum of the noise is flat with amplitude N_0 watts/rad/sec over the frequency range $0, W$ rad/sec and contains no power in frequencies greater than W , i.e.,

$$N = W N_0 \quad (49)$$

Using well-known results⁵ of sampling analysis, we can assume that samples of the noise $n(t)$ will be uncorrelated (and hence statistically independent, since the noise is gaussian) if samples are taken at time intervals

$$\Delta = \frac{1}{2 \times \text{bandwidth in c.p.s.}} \quad (50)$$

$$\Delta = \frac{\pi}{W} \quad (51)$$

It is assumed that W is greater than the highest possible signal frequency, i.e., $W \geq \omega_0 + \frac{\Omega}{2}$, and that $WT \gg 1$. Under these assumptions, all of the information in the received continuous signal $v(t)$, observed during the interval $(0, T)$, will be contained in the samples taken at intervals of $\frac{\pi}{W}$.

For the noise spectrum and sampling procedure described, the covariance matrix K is diagonal and Eq. (48) becomes

$$\begin{aligned} \frac{1}{2} \underline{v}^T \underline{G} \underline{v} &= \frac{A^2}{4N^2} \underline{v}^T \left\{ \text{sinc } \Phi(t_1 - t_j) \cos \omega_0(t_1 - t_j) \right\} \underline{v} \\ &= \frac{A^2}{4N^2} \sum_{i=1}^n \sum_{j=1}^n v_i v_j \text{sinc } \Phi(t_i - t_j) \cos \omega_0(t_i - t_j) \end{aligned} \quad (52)$$

The operation of the optimum detector upon the received signal is thus given by the quadratic form Eq. (52). The output signal-to-noise ratio R , from Eq. (31), is

$$\begin{aligned} R &= \frac{1}{2} \text{tr} (\underline{K} \underline{G})^2 = \frac{1}{2} \text{tr} \left(\left\langle \underline{s} \underline{s}^T \right\rangle_S \underline{K}^{-1} \right)^2 \\ &= \frac{A^4}{8N^2} \sum_{i=1}^n \sum_{j=1}^n \left[\text{sinc } \Phi(t_i - t_j) \cos \omega_0(t_i - t_j) \right]^2 \end{aligned} \quad (53)$$

For purposes of computation, we obtain an approximation to R : for $\omega_0 \gg \Omega$ and $\omega_0 T \gg 1$, $\cos^2 \omega_0(t_i - t_j)$ can be replaced by its average value, $\frac{1}{2}$, and

$$R \approx \frac{A^4}{16N^2} \sum_{i=1}^n \sum_{j=1}^n \left[\text{sinc } \Phi(t_i - t_j) \right]^2 \quad (54)$$

Replacing the double summation in Eq. (54) by a double integration we obtain a further approximation:

$$\begin{aligned}
 R &\approx \frac{A^4}{16N_o^2} \cdot \frac{W^2}{\pi^2} \int_0^T dt \int_0^T d\sigma \operatorname{sinc}^2 \Phi(t - \sigma) \\
 &= \frac{A^4}{4 N_o^2 \Omega^2} \int_0^{\Phi T} dx \int_0^{\Phi T} dy \operatorname{sinc}^2(x - y)
 \end{aligned} \tag{55}$$

The output SNR, as given by Eq. (54), is plotted in Fig. 2 for $W = 10 \Omega$. As the noise bandwidth W becomes very much larger than Ω , the summation in Eq. (53) converges to the integral in Eq. (55). Eq. (55) can thus be regarded as the output SNR for the case of continuous filtering.

From the figure it can be seen that a suitable approximation to R for reasonably long integration time, i.e., for $\Phi T \gg 1$, is

$$R \approx \frac{A^4}{4 N_o^2 \Omega^2} \Phi T \tag{55a}$$

Rewriting Eq. (55a) slightly,

$$R \approx \frac{A^4 T}{8\pi N_o^2 \Omega} \tag{55b}$$

In this form we see that R is proportional to observation time T and inversely proportional to the bandwidth of signal frequency uncertainty Ω .

Ideally Filtered White Noise

If at the detector it is known with certainty that the frequency of the desired signal lies between the strict limits $\omega_o - \frac{\Omega}{2}$, $\omega_o + \frac{\Omega}{2}$, then prior to detection, the incoming signal should be filtered to remove all noise power outside those frequency limits. We shall now consider

such a case and shall assume that the filtering is ideal, so that the noise spectral level after filtering is N_0 within $\omega_0 - \frac{\Omega}{2}$, $\omega_0 + \frac{\Omega}{2}$, and is zero elsewhere. We then have $N = N_0 \Omega$.

For such strictly band-limited noise, we can choose a sampling interval so that the samples of the noise will be completely uncorrelated. Sampling theory dictates* that such samples be taken at intervals $\frac{1}{\Phi}$ where $\Omega = 2\pi \Phi$. In order that the noise be completely specified by the sample values, it is necessary to sample both the noise waveform $n(t)$ and its Hilbert transform $h(t)$. These sample values, taken at the same sampling instant, are combined into a "complex sample," $n(t_i) + j h(t_i)$.

Applying these ideas to the detection problem at hand, we can simply replace \underline{v} in Eq. (52) by $\underline{v} + j \underline{u}$ where \underline{u} represents the sampled Hilbert transform of $v(t)$. For $\Phi T \gg 1$, all of the information in the received signal $v(t)$ will be contained in the complex samples $v(t_i) + j u(t_i)$ taken at intervals $\frac{1}{\Phi}$. The noise covariance matrix is again diagonal.

Thus, rewriting Eq. (52) for the band-pass case,

$$\begin{aligned} & \frac{1}{2} (\underline{v}' - j \underline{u}') \bar{\underline{G}} (\underline{v} + j \underline{u}) \\ &= \frac{A^2}{4N^2} \sum_{i=1}^n \sum_{j=1}^n (v_i v_j + u_i u_j) \text{sinc } \Phi (t_i - t_j) \cos \omega_0 (t_i - t_j) \quad (56) \end{aligned}$$

where, now, $n = \Phi T$.

*For an excellent discussion of sampling analysis, see Woodward.⁵

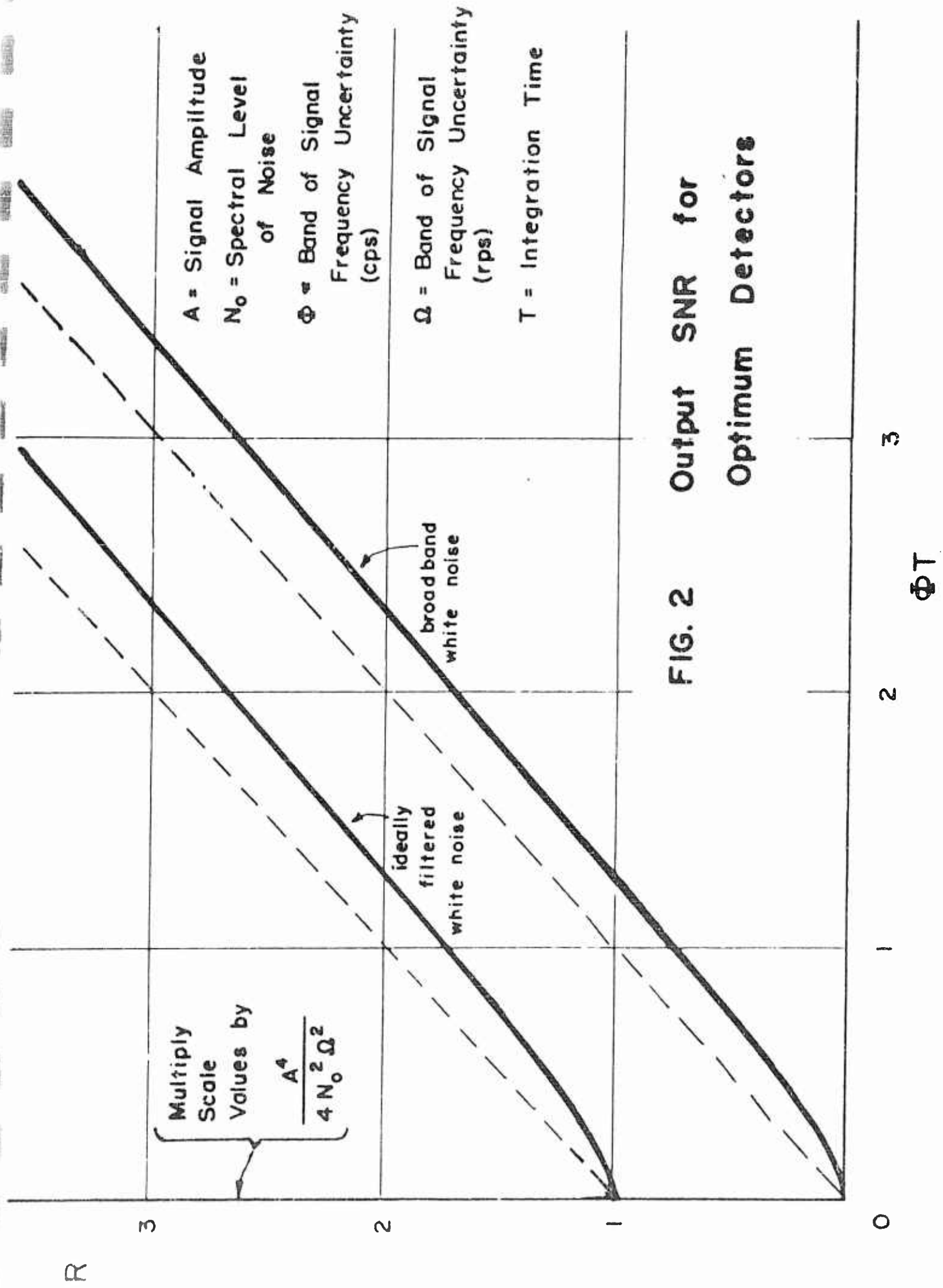


FIG. 2 Output SNR for Optimum Detectors

However, we note that

$$\text{sinc } \bar{\Phi}(t_i - t_j) = \begin{cases} 1 & t_i = t_j \\ 0 & (t_i - t_j) = k \frac{1}{\bar{\Phi}} \end{cases} \quad (57)$$

Therefore all the cross-terms in Eq. (56) disappear, and we are left with

$$\frac{1}{2} (\underline{v}' - j \underline{u}') \bar{\underline{G}} (\underline{v} + j \underline{u}) = \frac{A^2}{4N^2} \sum_1^n (v_1^2 + u_1^2) \quad (58)$$

But⁵

$$\sum_{i=1}^{\bar{\Phi}T} \left[v^2 \left(\frac{1}{\bar{\Phi}} \right) + u^2 \left(\frac{1}{\bar{\Phi}} \right) \right] = \sum_{i=1}^{2\bar{\Phi}T} v^2 \left(\frac{1}{2\bar{\Phi}} \right) \quad (59)$$

and Eq. (58) can be rewritten as

$$\frac{1}{2} \underline{v}' \bar{\underline{G}} \underline{v} = \frac{A^2}{4N^2} \sum_{i=1}^n v_i^2 = \frac{A^2}{4N^2} \underline{v}' \underline{I} \underline{v} \quad (60)$$

where $n = 2 \bar{\Phi} T$. The expressions in Eq. (60) are recognized as discrete forms of the operations performed by a square-law device and integrator. We conclude then that the optimum detector for the case of white noise ideally filtered to the band of signal frequency uncertainty is a square law device followed by an integrator.

Output SNR

To calculate the output SNR, we shall consider the square-law device in its continuous form, i.e., the detector output is taken to be $\int_0^T v^2(t) dt$.

The derivation of R is straightforward, and the result is given here, the details being left to Appendix A.

However, we note that

$$\text{sinc } \frac{\Phi}{T} (t_1 - t_j) = \begin{cases} 1 & t_1 = t_j \\ 0 & (t_1 - t_j) = k \frac{1}{\frac{\Phi}{T}} \end{cases} \quad (57)$$

Therefore all the cross-terms in Eq. (56) disappear, and we are left with

$$\frac{1}{2} (\underline{v}' - j \underline{u}') \bar{\underline{G}} (\underline{v} + j \underline{u}) = \frac{A^2}{4N^2} \sum_j (v_1^2 + u_1^2) \quad (58)$$

But⁵

$$\sum_{i=1}^{\frac{\Phi}{T}} \left[v^2 \left(\frac{1}{\frac{\Phi}{T}} \right) + u^2 \left(\frac{1}{\frac{\Phi}{T}} \right) \right] = \sum_{i=1}^{2\frac{\Phi}{T}} v^2 \left(\frac{1}{2\frac{\Phi}{T}} \right) \quad (59)$$

and Eq. (58) can be rewritten as

$$\frac{1}{2} \underline{v}' \bar{\underline{G}} \underline{v} = \frac{A^2}{4N^2} \sum_{i=1}^n v_1^2 = \frac{A^2}{4N^2} \underline{v}' \underline{I} \underline{v} \quad (60)$$

where $n = 2 \frac{\Phi}{T}$. The expressions in Eq. (60) are recognized as discrete forms of the operations performed by a square-law device and integrator. We conclude then that the optimum detector for the case of white noise ideally filtered to the band of signal frequency uncertainty is a square law device followed by an integrator.

Output SNR

To calculate the output SNR, we shall consider the square-law device in its continuous form, i.e., the detector output is taken to be $\int_0^T v^2(t) dt$.

The derivation of R is straightforward, and the result is given here, the details being left to Appendix A.

$$R \approx \frac{A^4 T^2}{16 \pi^2 N_0^2 \int_0^{\bar{\Phi} T} dx \int_0^{\bar{\Phi} T} dy \operatorname{sinc}^2(x - y)} \quad (61)$$

This is plotted in Fig. 2 as a function of $\bar{\Phi} T$. It is seen from the figure that the curve for R vs. $\bar{\Phi} T$ for this case of ideally filtered white noise is identical in form to the corresponding curve for the case of broadband white noise, except for a constant vertical displacement. This result is misleading since it seems to indicate that one can improve upon the performance of the optimum detector derived for the broadband white noise case simply by pre-filtering the noise to the band of signal frequency uncertainty. However, this cannot be the case in view of the known optimality of LR detection. The cause of this discrepancy lies in the assumed nature of the ideal pre-filtering operation. In deriving Eq. (61) it was assumed that the filter was operating in a steady-state condition, i.e., that the received signal was applied to the filter a long time before the start of the observation period $(0, T)$. This, however, is a false assumption, since the received signal is available only during the period $(0, T)$. An analysis which takes into account the transient operation of the filter is rather involved and is taken up in Appendix B. The output SNR for such a short-term filter followed by a squarer and integrator is derived but is not easily evaluable. However, it can be shown that for large and small values of $\bar{\Phi} T$ respectively, the SNR behaves as does R for the original case of optimum detection in broadband white noise.

It is therefore conjectured that the optimum procedure for the detection of a steady sine wave of unknown frequency in a background of

white noise consists of a filtering of the received signal to the band of signal frequency uncertainty followed by squaring and integration.

V. Comparison with the Optimal Detection of a Gaussian Signal

It is of interest to compare the results obtained thus far with the case of optimal detection of a gaussian random signal in a background of gaussian noise. The question to be answered is whether or not a periodic signal with unknown frequency is more detectable than a gaussian random signal of the same average power having a power spectral density over the same band of uncertainty. The results of Tuteur² are applicable in this case.

Adapting Tuteur's Eq. (13) we find that the operation to be performed by the LR detector to detect a gaussian signal in gaussian noise is

$$\ln \ell(\underline{v}) = \frac{1}{2} \underline{v}' \underline{K}^{-1} \underline{P} \underline{K}^{-1} \underline{v} + \text{Bias terms} \quad (62)$$

where \underline{P} is the covariance matrix of the signal. If the power spectral density of the signal is flat over the frequency band $(\omega_0 - \frac{\Omega}{2}, \omega_0 + \frac{\Omega}{2})$ with total average power $\frac{A^2}{2}$, then

$$\underline{P} = \left\{ \frac{A^2}{2} \text{sinc} \frac{\Omega}{2} (t_i - t_j) \cos \omega_0 (t_i - t_j) \right\} \quad (63)$$

But this is seen to be identical to the matrix $\left\langle \underline{s} \underline{s}' \right\rangle_S$ derived in Section IV.1. Therefore

$$\begin{aligned} \frac{1}{2} \underline{v}' \underline{K}^{-1} \underline{P} \underline{K}^{-1} \underline{v} &= \frac{1}{2} \underline{v}' \underline{K}^{-1} \left\langle \underline{s} \underline{s}' \right\rangle_S \underline{K}^{-1} \underline{v} \\ &= \frac{1}{2} \underline{v}' \underline{G} \underline{v} \end{aligned} \quad (64)$$

Thus the optimum detector for the case of a gaussian signal with a flat spectral density over a given frequency band is identical to the detector derived in Section IV.1 for the case of a sine wave whose frequency has a flat p.d.f. over the same band. The same gaussian noise background is assumed in each case. The output SNR, R , is also the same in the two cases [See Tuteur, Eq. (20)]. We therefore conclude that if the desired signal is known only to lie between certain upper and lower frequency limits, there is no advantage to be gained from knowledge that the signal is periodic rather than random and gaussian. In either case, the optimum detector consists of a filter matched to the signal band followed by a squarer and integrator

VI. Detection with a Hydrophone Array

We have up to this point considered signal processing with a single hydrophone. Let us now assume that an array of M hydrophones is used to detect the desired signal in a three-dimensional isotropic gaussian noise field. For such a noise background, it can be shown⁶ that the cross-correlation function for noise outputs from two separated hydrophones is given by

$$R(\tau, \tau_s) = \frac{1}{2\tau_s} \int_{\tau - \tau_s}^{\tau + \tau_s} R'(\tau') d\tau' \quad (65)$$

where $\tau_s = \frac{d}{c}$ is the time required for a signal to travel the spacing, d , between the two hydrophones when the speed of sound in water is c . $R'(\tau')$ is the a.c.f. for the noise arriving at any one hydrophone. We note that Eq. (65) simply represents the average value of $R'(\tau')$ over an interval $2\tau_s$ wide centered at τ .

The various signal and noise vectors \underline{v} , \underline{s} and \underline{n} are now taken to be $n \times M$ -dimensional vectors and the matrices \underline{K} , $\langle \underline{s} \underline{s}^t \rangle_S$, $\underline{\bar{G}}$ and \underline{I} are taken to be $n \times M$ -dimensional matrices. It will be assumed that the array is being steered "on target" so that the matrix $\langle \underline{s} \underline{s}^t \rangle_S$ will consist of an $M \times M$ matrix of identical $n \times n$ submatrices.

Broadband White Noise Background--Hydrophone Array

If the noise background is white with finite power and essentially infinite bandwidth, it can easily be shown that the noise covariance matrix \underline{K} is diagonal. Assuming the desired signal to be as described in Section IV, i.e., a steady sine wave whose phase and frequency are described by p.d.f.'s, the matrix $\langle \underline{s} \underline{s}^t \rangle_S$ is an $M \times M$ matrix of $n \times n$ submatrices, each identical to the form in Eq. (45), derived for the case of a single hydrophone. The $n \times M$ matrix $\underline{\bar{G}}$ for the array case is given by

$$\underline{\bar{G}} = \frac{1}{N^2} \langle \underline{s} \underline{s}^t \rangle_S \quad (66)$$

and is itself a matrix of identical submatrices.

Thus it can easily be verified that the optimum detector sums the signals picked up at the M hydrophones, and performs the quadratic operation $\underline{v}^t \underline{\bar{G}} \underline{v}$ where \underline{v} is now the output of the summer and $\underline{\bar{G}}$ is identical to the form originally derived in Section IV.2 for the single hydrophone case. We have previously conjectured that the continuous form of the operation $\underline{v}^t \underline{\bar{G}} \underline{v}$ consists of a filtering to the signal band $(\omega_0 - \frac{\Omega}{2}, \omega_0 + \frac{\Omega}{2})$ followed by squaring and integrating.

The $n \times M$ matrix $\underline{K} \underline{\bar{G}}$ is

$$\underline{K} \underline{\bar{G}} = \frac{1}{N} \langle \underline{s} \underline{s}^t \rangle_S \quad (67)$$

It can readily be verified that for the array case

$$\frac{1}{2} \text{tr} (\underline{K} \underline{G})^2 = \frac{M^2 A^4}{4N_0^2 \Omega^2} \int_0^{\Phi_T} dx \int_0^{\Phi_T} dy \text{sinc}^2(x - y) \quad (68)$$

In other words, for the case of broadband white noise, the output signal-to-noise ratio with the array of M hydrophones is M^2 times that with a single hydrophone [compare with Eq. (55)].

Note on the Threshold Analysis

In obtaining the form of the optimum detection operation from Eq. (7), for the case of a single hydrophone, we assumed that threshold conditions prevailed, i.e., the input SNR was low and higher order terms in the SNR could be neglected. In terms of the specific problems treated this implied for the single hydrophone case

$$\frac{A^2}{2N} \ll 1 \quad (69)$$

It should be noted that for the M-array case, the equivalent condition is that

$$\frac{MA^2}{2N} \ll 1 \quad (70)$$

VII. Output SNR with a Sub-optimum Incoherent Detector

One may wish to compare the performance of the optimum incoherent detector with some sub-optimum detector. For that purpose we next shall derive a compact expression for the output SNR, R , of a general incoherent detector which forms the test statistic

$$d(\underline{v}) = \underline{v}^T \underline{F} \underline{v} \quad (71)$$

The matrix \underline{F} is an $n \times n$ matrix in the single hydrophone case, which we shall consider first. The quantity $\underline{v}' \underline{F} \underline{v}$ can be thought of (in continuous form) as the squared output of a filter which is not necessarily time-invariant, subsequently integrated over the observation time of the received signal. The interpretation of \underline{F} can be made as follows:

Let the discrete form of the filter weighting function be an $n \times n$ matrix \underline{H} , and let the output of the filter be the vector $\underline{Y} = \underline{H} \underline{v}$.^{*} The squared and summer filter output is then $\underline{v}' \underline{H}' \underline{H} \underline{v}$. Thus, letting

$$\underline{v}' \underline{H}' \underline{H} \underline{v} = \underline{v}' \underline{F} \underline{v} \quad (72)$$

we have

$$\underline{F} = \underline{H}' \underline{H} \quad (73)$$

Now the output SNR is to be found. The calculations of the required averages are similar to those in deriving Eqs. (26), (27) and (29). The following can easily be shown:

$$\langle d(\underline{v}) \rangle_{S+N} = \text{tr} \left(\langle \underline{s} \underline{s}' \rangle_S \underline{F} \right) + \text{tr} (\underline{K} \underline{F}) \quad (74)$$

$$\langle d(\underline{v}) \rangle_N = \text{tr} (\underline{K} \underline{F}) \quad (75)$$

$$\langle [d(\underline{v})]^2 \rangle_N = 2 \text{tr} (\underline{K} \underline{F})^2 + \text{tr}^2 (\underline{K} \underline{F}) \quad (76)$$

Thus, from Eq. (25),

$$R = \frac{\left[\text{tr} \left(\langle \underline{s} \underline{s}' \rangle_S \underline{F} \right) \right]^2}{2 \text{tr} (\underline{K} \underline{F})^2} \quad (77)$$

^{*}More explicitly, $Y_i = \sum_j H_{ij} v_j$. If the filter is to be realizable, then $Y_i = 0$ for $i < j$, for any \underline{v} . This is assured if $H_{ij} = 0$ for $i < j$, thus \underline{H} is "lower diagonal" in such a case.

Let us now use Eq. (77) to calculate the output SNR for the case considered earlier, i.e., the case of a steady sinusoid whose frequency lies somewhere in a band Ω rad/sec wide centered at ω_0 . Let us assume the noise is white and strictly cut-off at W rad/sec. In such a case, $\langle \underline{s} \underline{s} \rangle$ is given by Eq. (45) as before. Here \underline{F} simply represents the square-and-add operation and so

$$\underline{F} = \underline{I} \quad (78)$$

Since the noise is white,

$$K = N \underline{I} \quad (79)$$

Thus, from Eq. (77) we have

$$R = \frac{nA^4}{8N^2} = \frac{A^4}{8\pi N^2} WT \quad (80)$$

where $n = \frac{WT}{\pi}$. It is clear of course that the result Eq. (80) does not depend in any way upon the uncertainty about signal frequency. However, Eq. (80) can be rewritten in a more interesting form:

$$R = \frac{A^4}{4N_0^2 \Omega^2} \left(\frac{\Omega}{W} \right) \overline{\Phi} T, \quad W \geq \Omega \quad (81)$$

This is seen to be identical to Eq. (55a) except for the factor $\frac{\Omega}{W}$. Thus we can summarize:

If the background noise is white over a band $(0, W)$, the optimum LR detector consists of a filter matched to the band of signal frequency uncertainty Ω , where $W > \Omega$, followed by a squarer and an integrator. If, however, the received signal is not filtered before detection but is simply squared and integrated, the output SNR derived for the optimum detector must be multiplied by the factor $\frac{\Omega}{W}$.

VIII. Sub-optimum Detection--Hydrophone Array

If an M-hydrophone array is used, the operation equivalent to $\underline{v}' \underline{F} \underline{v}$ in Eq. (71) consists of summing the outputs from the M hydrophones and then using the summer output in the quadratic form $\underline{v}' \underline{F} \underline{v}$.

If the background noise is broadband white, and the array is steered on target, it can easily be verified that the output SNR is

$$R = \frac{M^2 A^4}{4 N_0^2 \Omega^2} \left(\frac{\Omega}{W} \right) \Phi T \quad (82)$$

IX. Conclusions

There is evidence that the low frequency portion of received signal spectrum contains certain coherent signals which may be used as a basis for detection. It had been hoped that advantage could be taken of the periodic nature of these signals to perform some form of coherent detection and thereby enhance signal detectability. However, the lack of precise knowledge about the frequency of the periodicity is a stumbling block. If the frequency is known only to lie within certain upper and lower limits, then the optimum detection procedure is an incoherent one, i.e., an energy measurement of the received signal. Coherent detection is, generally speaking, cross-correlation with a replica of the desired signal. However, effective cross-correlation requires at least a knowledge of the frequency or fundamental frequency of the signal. This in a nutshell is why the optimum detection scheme for the case we have considered is not a coherent scheme.

A comparison of the case of a sinusoidal signal of unknown frequency and phase with the case of a gaussian random signal shows that in either case the optimum LR detector has the same form, i.e., a purely incoherent

detector. This indicates that a periodic signal of unknown frequency is no more detectable than a gaussian random signal of the same power confined to the same frequency band. This is a surprising result, but one which follows quite clearly from a straightforward application of the general theory of optimal (minimum average risk) detection as outlined by Middleton.

Even though the unknown signal frequency may have a value anywhere in a given region of uncertainty, it seems intuitively that one should be able to make use of the fact that in the observation interval at hand, the signal frequency takes on but one of its possible values for the entire interval. With this idea in mind, a detection scheme has been considered in which the overall band of signal frequency uncertainty is split up into a number of sub-bands. The SNR is thus enhanced in one sub-band, that which contains the signal. Each of the sub-bands is then processed by means of an incoherent threshold detector and a final decision is made on the basis of the outputs of the sub-band detectors. Preliminary results indicate that this scheme would perform better than the "optimum" detector derived in this report. Presumably, the same improvement would be exhibited if the signal were not a pure sinusoid but a narrow-band signal whose center frequency was not known exactly. In such a case the width of each sub-band would be chosen approximately equal to the width of the narrow-band signal.

This result brings up some serious questions regarding the supposed optimality of LR detection, since this arbitrary band-splitting operation is not dictated by the results of the general optimum detection analysis. Therefore the general detection problem, as analyzed from the Bayes' risk point of view, is presently being re-examined. This investigation, as well as the analysis of the band-splitting scheme, will be subjects of later reports.

Appendix A

Square Law Detector I--Ideal Filtering

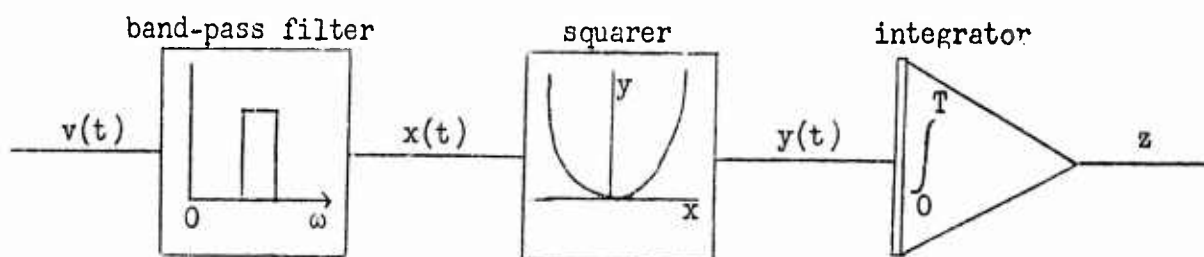


Figure A-1 Square Law Detector

The detector output, i.e., the test statistic to be used in the threshold comparison, is

$$z = \int_0^T x^2(t) dt \quad (A-1)$$

where

$$x(t) = \int_{-\infty}^t v(\tau) h(t - \tau) d\tau \quad (A-2)$$

and $h(\tau)$ is the weighting function for a rectangular filter matched to the band of signal frequency uncertainty. The $(-\infty)$ value of the lower limit in Eq. (A-2) implies that the filter is operating in a "steady-state" condition. The background noise contained in $v(t)$ is assumed to be flat over a broad band.

The output SNR will be taken as normalized deflection-squared, as before. The necessary averages are calculated as follows:

$$\begin{aligned} \langle z \rangle_{S+N} &= \left\langle \int_0^T dt \left[s^2(t) + 2 s(t) n_F(t) + n_F^2(t) \right] \right\rangle_{S+N} \\ &= \frac{A^2}{2} T + N_o \Omega T \end{aligned} \quad (A-3)$$

where $n_F(t)$ is the noise at the output of the filter.

$$\begin{aligned} \left\langle z \right\rangle_N &= \left\langle \int_0^T dt n_F^2(t) \right\rangle_N \\ &= N_0 \Omega T \end{aligned} \quad (A-4)$$

$$\begin{aligned} \left\langle z^2 \right\rangle_N &= \left\langle \int_0^T dt \int_0^T d\sigma n_F^2(t) n_F^2(\sigma) \right\rangle_N \\ &= \int_0^T dt \int_0^T d\sigma \left\langle n_F^2(t) n_F^2(\sigma) \right\rangle_N \\ &= \int_0^T dt \int_0^T d\sigma \left[N_0^2 \Omega^2 + 2 R^2(t - \sigma) \right] \\ &= N_0^2 \Omega^2 T^2 + 2 \int_0^T dt \int_0^T d\sigma R_F^2(t - \sigma) \end{aligned} \quad (A-5)$$

where $R_F(\tau)$ is the a.c.f. for $n_F(t)$.

Thus,

$$R = \frac{A^4 T^2}{8 \int_0^T dt \int_0^T d\sigma R_F^2(t - \sigma)} \quad (A-6)$$

For the rectangular filter with flat response over $(\omega_0 - \frac{\Omega}{2}, \omega_0 + \frac{\Omega}{2})$,

$$R_F(t - \sigma) = N_0 \Omega \text{sinc } \frac{\Omega}{2} (t - \sigma) \cos \omega_0 (t - \sigma) \quad (A-7)$$

Thus in this case

$$R = \frac{A^4 T^2}{8 N_o^2 \Omega^2 \int_0^T dt \int_0^T d\sigma \operatorname{sinc}^2 \Phi(t - \sigma) \cos^2 \omega_o(t - \sigma)}$$

$$\approx \frac{A^4 T^2}{4 N_o^2 \Omega^2 \int_0^T dt \int_0^T d\sigma \operatorname{sinc}^2 \Phi(t - \sigma)} \quad (\text{A-8})$$

or,

$$R \approx \frac{A^4 T^2}{16 \pi^2 N_o^2 \int_0^T dx \int_0^T dy \operatorname{sinc}^2(x - y)} \quad (\text{A-9})$$

Appendix B

Square Law Detector II--Short-Term Filtering

In this Appendix we assume that the pre-detection filter cannot operate on the infinite past history of the received signal $v(t)$ as was assumed in the previous Appendix [See Eq. (A-2)]. Instead, the filter is allowed to weight only as much of $v(t)$ as is available at any time in the observation interval $(0 \leq t \leq T)$. With this restriction, $x(t)$ now takes the form

$$x(t) = \int_0^t v(\tau) h(t - \tau) d\tau \quad (B-1)$$

Again,

$$z = \int_0^T x^2(t) dt \quad (B-2)$$

Now,

$$\begin{aligned} z &= \int_0^T dt \left[\int_0^T d\tau v(\tau) h(t - \tau) \right] \left[\int_0^t d\sigma v(\sigma) h(t - \sigma) \right] \\ &= \int_0^T dt \int_0^t d\tau \int_0^t d\sigma v(\tau) v(\sigma) h(t - \tau) h(t - \sigma) \end{aligned} \quad (B-3)$$

The output SNR R is required. We obtain the appropriate averages as follows:

$$\langle z \rangle_{S+N} = \left\langle \int_0^T dt \int_0^t d\tau [s(\tau) + n(\tau)] h(t - \tau) \int_0^t d\sigma [s(\sigma) + n(\sigma)] h(t - \sigma) \right\rangle_{S+N}$$

$$= \int_0^T dt \left[\int_0^t d\tau \int_0^t d\sigma \left\langle s(\tau) s(\sigma) \right\rangle_S h(t - \tau) h(t - \sigma) + \int_0^t d\tau \int_0^t d\sigma R(\tau - \sigma) h(t - \tau) h(t - \sigma) \right] \quad (B-4)$$

$$\langle z \rangle_N = \int_0^T dt \int_0^t d\tau \int_0^t d\sigma R(\tau - \sigma) h(t - \tau) h(t - \sigma) \quad (B-5)$$

Thus,

$$\langle z \rangle_{S+N} - \langle z \rangle_N = \int_0^T dt \int_0^t d\tau \int_0^t d\sigma \left\langle s(\tau) s(\sigma) \right\rangle_S h(t - \tau) h(t - \sigma) \quad (B-6)$$

Letting

$$\left\langle s(\tau) s(\sigma) \right\rangle_S = R_S(\tau - \sigma) \quad (B-7)$$

we can write

$$\langle z \rangle_{S+N} - \langle z \rangle_N = \int_0^T dt \int_0^t d\tau \int_0^t d\sigma R_S(\tau - \sigma) h(\tau) h(\sigma) \quad (B-8)$$

Calculating the variance of z given that only noise is present,

$$\begin{aligned} \langle z^2 \rangle_N &= \left\langle \int_0^T dt \left[\int_0^t d\tau v(\tau) h(t - \tau) \int_0^t d\sigma v(\sigma) h(t - \sigma) \right] \right. \\ &\quad \cdot \left. \int_0^T ds \left[\int_0^s d\eta v(\eta) h(s - \eta) \int_0^s d\xi v(\xi) h(s - \xi) \right] \right\rangle_N \end{aligned}$$

$$\begin{aligned}
&= \int_0^T dt \int_0^T ds \int_0^t d\tau \int_0^t d\sigma \int_0^s d\eta \int_0^s d\xi \left\langle v(\tau) v(\sigma) v(\eta) v(\xi) \right\rangle_N \\
&\quad \cdot h(t - \tau) h(t - \sigma) h(s - \eta) h(s - \xi)
\end{aligned} \tag{B-9}$$

If the noise before filtering is white,

$$\left\langle v(x) v(y) \right\rangle_N = \pi N_0 \delta(x - y) \tag{B-10}$$

If the noise is also gaussian,

$$\begin{aligned}
\left\langle z^2 \right\rangle_N &= \pi^2 N_0^2 \int_0^T dt \int_0^T ds \left\{ \int_0^t d\tau h^2(t - \tau) \int_0^s d\eta h^2(s - \eta) \right. \\
&\quad + \int_0^t d\tau h(t - \tau) h(s - \tau) \int_0^t d\sigma h(t - \sigma) h(s - \sigma) \\
&\quad \left. + \int_0^t d\tau h(t - \tau) h(s - \tau) \int_0^t d\sigma h(t - \sigma) h(s - \sigma) \right\} \\
&= \pi^2 N_0^2 \left[\int_0^T dt \int_0^t d\tau h^2(t - \tau) \right]^2 + \pi^2 N_0^2 \left[\int_0^t d\tau h(t - \tau) h(s - \tau) \right]^2
\end{aligned} \tag{B-11}$$

Thus,

$$R = \frac{\left[\int_0^T dt \int_0^t d\tau \int_0^t d\sigma R_s(\tau - \sigma) h(\tau) h(\sigma) \right]^2}{2\pi^2 N_o^2 \int_0^T dt \int_0^T ds \left[\int_0^t d\tau n(t - \tau) h(s - \tau) \right]^2}$$

(B-12)

List of Symbols

- A = signal amplitude
- $\{B(t_i)\}$ = a vector
- $\{B(t_i, t_j)\}$ = a matrix
- c = velocity of sound in water
- d = distance between two hydrophones
- $d(\underline{v})$ = test statistic in sub-optimum detection
- $\delta(x)$ = Dirac delta function
- Δ = sampling interval
- \underline{F} = coefficient matrix of sub-optimum quadratic form
- $f(\underline{v}/\underline{o})$ = conditional probability density of \underline{v} with no signal present
- $f(\underline{v}/\underline{s})$ = conditional probability density of \underline{v} with signal present
- \underline{B} = bandwidth of signal frequency uncertainty in cps
- ϕ = phase of desired signal
- \underline{G} = coefficient matrix of optimum quadratic form
- \underline{H} = filter weighting matrix
- $h(\tau)$ = filter weighting function
- $h(t_i)$ = sample of Hilbert transform of $n(t)$
- \underline{I} = identity matrix
- \underline{K} = noise covariance matrix
- K_{ij}^{-1} = element of inverse covariance matrix
- $\ell(\underline{v})$ = likelihood ratio
- M = number of hydrophones in an array
- m = number of possible discrete signal frequencies
- N = noise power
- N_o = noise spectrum level in watts/rps

n = number of time samples

\underline{n} = noise vector

$n(t)$ = noise signal in continuous form

$n_F(t)$ = noise signal after filtering

$\theta(x)$ = "at most on the order of x "

$P(x_1)$ = probability function

$p(x)$ = probability density function

R = output signal-to-noise ratio

$R'(\tau')$ = autocorrelation function of noise at a hydrophone

$R(\tau, \tau_s)$ = cross-correlation function for noise signals at two different hydrophones

$R_F(\tau)$ = a.c.f. of noise after filtering

S = set of unknown signal parameters

\underline{s} = desired signal vector

\underline{s}' = transpose of vector \underline{s}

$s(t)$ = desired signal in continuous form

T = observation time of received signal

τ_s = time delay between two hydrophones

\underline{u} = sampled Hilbert transform of $v(t)$

\underline{v} = received signal vector

$v(t)$ = received signal in continuous form

W = noise bandwidth in rps

$x(t)$ = received waveform after filtering

Ω = bandwidth of signal frequency uncertainty in rps

ω = signal frequency

ω_0 = center of band of signal frequency uncertainty

\underline{Y} = filter output in sub-optimum detection

$y(t)$ = received waveform after squarer

z = integrator output

$\det \underline{A}$ = determinant of matrix \underline{A}

$\left\langle \right\rangle_N$ = statistical average, conditioned on presence of noise only

$\left\langle \right\rangle_{S+N}$ = statistical average, conditioned on presence of both signal and noise

$\text{tr } \underline{A}$ = trace of matrix \underline{A}

Abbreviations

a.c.f. = autocorrelation function

LR = likelihood ratio

p.d.f. = probability density function

SNR = signal-to-noise ratio

References

1. Schultheiss, P. M., "Optimal Detection of Directional Gaussian Signals in an Isotropic Gaussian Noise Field," Progress Report No. 3, General Dynamics/Electric Boat Research, Yale University, May 1963.
2. Tuteur, F. B., "Detection of Wide-Band Signals Modulated by a Low-Frequency Sinusoid," Progress Report No. 5, General Dynamics/Electric Boat Research, Yale University, June 1963.
3. Peterson, W. W., T. G. Birdsall, and W. C. Fox, "The Theory of Signal Detectability," IRE Trans. on Information Theory, vol. IT-4, pp. 171-212, September 1954.
4. Middleton, D., An Introduction to Statistical Communication Theory, McGraw-Hill Book Company, New York, 1960.
5. Woodward, P. M., Probability and Information Theory, With Applications to Radar, McGraw-Hill Book Company, New York, 1953; cf. Chapter 2.
6. Faran, J. J., and R. Hills, "The Application of Correlation Techniques to Acoustic Receiving Systems," Technical Memo. No. 28, Acoustics Research Laboratory, Harvard University, Cambridge, Massachusetts, November 1952.



RANDOM BEARING ERRORS IN SPLIT-BEAM SYSTEMS

by

Theron Usher, Jr.

Progress Report No. 9

General Dynamics/Electric Boat Research

(53-00-10-0231)

December 1963

DEPARTMENT OF ENGINEERING
AND APPLIED SCIENCE
YALE UNIVERSITY

I. Introduction

The determination of the bearing of a plane-wave random signal in a background of isotropic random noise, by means of so-called "split-beam" systems of transducers, has been popular because a null output is obtained when the transducers are steered "on target." Such systems are of great value in automatic tracking applications.

However, the random fluctuation of the output of such systems causes uncertainty in the determination of the bearing of signal source. It is the purpose of this report to determine general mathematical relations for the computation of the bearing uncertainty, and from these relations to determine system parameters which optimize or minimize the bearing uncertainty.

The problem of determining bearing uncertainty has been treated in Reference 1, but the analysis is somewhat restricted in that the system is not quite as general as the one considered here. The problem of minimizing bearing uncertainty has not been treated previously, but the analysis is parallel to that done by Eckart in Reference 2. There also seems to be an error in Reference 1 in the analysis concerning multi-element arrays.

II. Definitions and Assumptions

The system to be analyzed is shown in Fig. 1. The outputs of each set of M transducers from an array of $2M$ transducers are summed and each sum is then fed into a linear filter. The frequency response functions of the filters are related in that there is a 90° phase shift between the response functions at all frequencies. The filtered sums

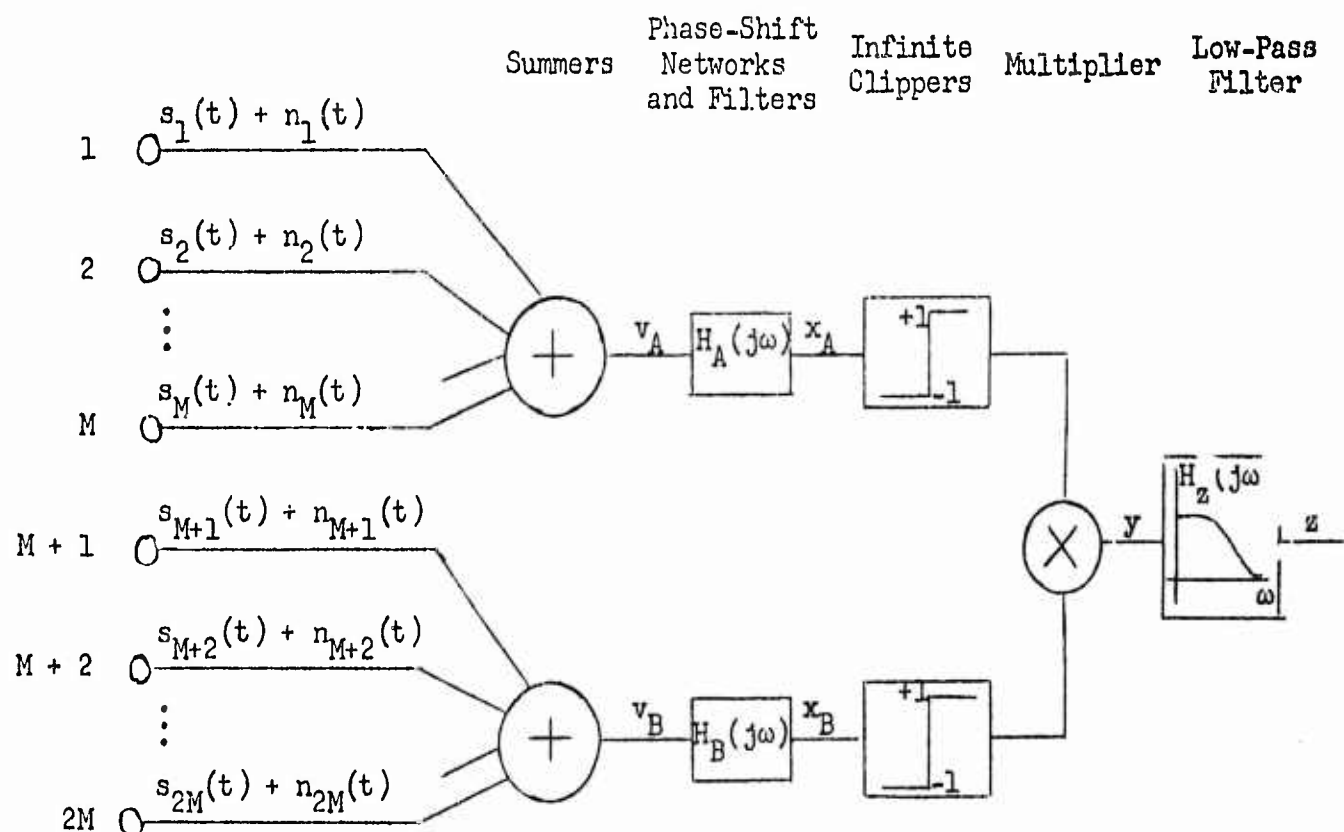


Fig. 1 Typical Split-Beam System

are then passed through infinite clippers, the results are multiplied and the product is averaged by means of a low-pass filter. The average output of the low-pass filter as the array is steered gives the bearing response pattern for the system.

Following are the major assumptions inherent in the analysis:

- 1) The transducers in the array have omnidirectional characteristics.
- 2) The array of $2M$ transducers is a linear array, with equal spacing between transducers.
- 3) The signal in the medium is a plane wave.
- 4) The noise is isotropic in the medium and the cross-correlation between the noise components of the outputs of different transducers is assumed to be zero.

5) The signal and noise are Gaussian and stationary, and signal and noise are independent.

6) The spectral density of the signal need not be the same as that for the noise at the output of any transducer.

III. Bearing Response Pattern

Since the signal is a plane wave, the array is linear with equal spacing between transducers, and the transducers are omnidirectional, the relation in Eq. (1) holds for the signal component from the i^{th} transducer.

$$s_i(t) = s_1[t - (i - 1)T] \quad (1)$$

The time T is the spatial time delay of the signal between adjacent transducers. When $T = 0$, the bearing of the signal is perpendicular to the line of the array.

The outputs of the summing amplifiers in Fig. 1 are given by

$$v_A(t) = \sum_{i=1}^M \left\{ s_1[t - (i - 1)T] + n_i(t) \right\} \quad (2)$$

$$v_B(t) = \sum_{k=1}^M \left\{ s_1[t - (k + M - 1)T] + n_{M+k}(t) \right\} \quad (3)$$

The autocorrelation function of $v_A(t)$ and $v_B(t)$ may be expressed in terms of the autocorrelation functions of the signal and noise at any transducer by means of the following relations.

$$\begin{aligned}
R_{v_A}(\tau) &= \sum_{i=1}^M \sum_{\ell=1}^M E \left[\left\{ s_1[t - (i-1)T] + n_1(t) \right\} \left\{ s_1[t - (\ell-1)T + \tau] + n_\ell(t + \tau) \right\} \right] \\
&= \sum_{i=1}^M \sum_{\ell=1}^M R_S[\tau + (i-\ell)T] + M N \rho_n(\tau) \\
&= S \sum_{i=1}^M \sum_{\ell=1}^M \rho_S[\tau + (i-\ell)T] + M N \rho_n(\tau) \tag{4}
\end{aligned}$$

$$R_{v_B}(\tau) = R_{v_A}(\tau) \tag{5}$$

In Eq. (4) S and N are the signal and noise powers at each transducer respectively, and ρ_S and ρ_n are the corresponding normalized autocorrelation functions.

The spectral densities of v_A and v_B are the Fourier transforms of the corresponding autocorrelation functions.* In Eq. (6) $g_S(\omega)$ and $g_n(\omega)$ are the normalized spectral density functions for signal and for noise respectively at every transducer.

*The transform pair given below will be used for relating spectral densities and correlation functions throughout this report.

$$\begin{aligned}
G(\omega) &= \frac{1}{2\pi} \int_{-\infty}^{\infty} R(\tau) e^{-j\omega\tau} d\tau \\
R(\tau) &= \int_{-\infty}^{\infty} G(\omega) e^{j\omega\tau} d\omega
\end{aligned}$$

$$\begin{aligned}
G_{V_A}(\omega) &= S \sum_{i=1}^M \sum_{\ell=1}^M \frac{1}{2\pi} \int_{-\infty}^{\infty} \rho_s(\tau + (i - \ell)T) e^{-j\omega\tau} d\tau \\
&\quad + MN \frac{1}{2\pi} \int_{-\infty}^{\infty} \rho_n(\tau) e^{-j\omega\tau} d\tau \\
&= S \sum_{i=1}^M \sum_{\ell=1}^M g_s(\omega) e^{j\omega(i-\ell)T} + MN g_n(\omega)
\end{aligned} \tag{6}$$

$$G_{V_B}(\omega) = G_{V_A}(\omega) \tag{7}$$

The filter frequency response functions are related in that there is a 90° phase difference between their phase angle at every frequency. Since simple filter realizations are desirable, for the initial analysis it is assumed that

$$H_A(j\omega) = j\omega k H_B(j\omega) \tag{8}$$

where k is an arbitrary proportionality constant.

The spectral densities of the outputs of the filters are found in Eqs. (9) and (10).

$$G_{X_A}(\omega) = \omega^2 k^2 |H_B(j\omega)|^2 G_{V_A}(\omega) \tag{9}$$

$$G_{X_B}(\omega) = |H_B(j\omega)|^2 G_{V_A}(\omega) \tag{10}$$

The development in Eqs. (1) through (10) is preliminary in determining the bearing response, which is the average value of the output of the multiplier, \bar{y} . The value of \bar{y} is dependent on the time delay T , and has been found to be¹

$$\bar{y} = \frac{2}{\pi} \arcsin \left[\frac{R_{x_A x_B}(0)}{\left\{ R_{x_A}(0) R_{x_B}(0) \right\}^{1/2}} \right] \quad (11)$$

The quantity $R_{x_A x_B}(0)$ is the cross-correlation function of $x_A(t)$ and $x_B(t)$ at $\tau = 0$. The cross-correlation may be evaluated by first writing the convolution integrals which yield $x_A(t)$ and $x_B(t)$.

$$x_A(t) = \sum_{i=1}^M \int_{-\infty}^{\infty} \left\{ s_1[t - (i-1)T - \alpha] + n_1(t - \alpha) \right\} h_A(\alpha) d\alpha \quad (12)$$

$$x_B(t) = \sum_{k=1}^M \int_{-\infty}^{\infty} \left\{ s_1[t - (k+M-1)T - \beta] + n_{M+k}(t - \beta) \right\} h_B(\beta) d\beta \quad (13)$$

In Eqs. (12) and (13) $h_A(\alpha)$ and $h_B(\beta)$ are the weighting functions of the filters with frequency response functions $H_A(j\omega)$ and $H_B(j\omega)$ respectively.

The cross-correlation at $\tau = 0$ is defined by

$$R_{x_A x_B}(0) = E[x_A(t) x_B(t)] \quad (14)$$

Since there is no correlation between the noise outputs of different transducers, the noise terms disappear when Eqs. (12) and (13) are substituted into Eq. (14). Thus

$$\begin{aligned} R_{x_A x_B}(0) &= \sum_{i=1}^M \sum_{k=1}^M \int_{-\infty}^{\infty} \int_{-\infty}^{\infty} E \left\{ s_1[t - (i-1)T - \alpha] s_1[t - (k+M-1)T - \beta] \right\} \times \\ &\quad h_A(\alpha) h_B(\beta) d\alpha d\beta \\ &= S \sum_{i=1}^M \sum_{k=1}^M \int_{-\infty}^{\infty} \int_{-\infty}^{\infty} \rho_s[\alpha - \beta - (k-i+M)T] h_A(\alpha) h_B(\beta) d\alpha d\beta \quad (15) \end{aligned}$$

The matrix \underline{F} is an $n \times n$ matrix in the single hydrophone case, which we shall consider first. The quantity $\underline{v}' \underline{F} \underline{v}$ can be thought of (in continuous form) as the squared output of a filter which is not necessarily time-invariant, subsequently integrated over the observation time of the received signal. The interpretation of \underline{F} can be made as follows:

Let the discrete form of the filter weighting function be an $n \times n$ matrix \underline{H} , and let the output of the filter be the vector $\underline{Y} = \underline{H} \underline{v}$.^{*} The squared and summer filter output is then $\underline{v}' \underline{H}' \underline{H} \underline{v}$. Thus, letting

$$\underline{v}' \underline{H}' \underline{H} \underline{v} = \underline{v}' \underline{F} \underline{v} \quad (72)$$

we have

$$\underline{F} = \underline{H}' \underline{H} \quad (73)$$

Now the output SNR is to be found. The calculations of the required averages are similar to those in deriving Eqs. (26), (27) and (29). The following can easily be shown:

$$\langle d(\underline{v}) \rangle_{S+N} = \text{tr} \left(\left\langle \underline{s} \underline{s}' \right\rangle_S \underline{F} \right) + \text{tr} (\underline{K} \underline{F}) \quad (74)$$

$$\langle d(\underline{v}) \rangle_N = \text{tr} (\underline{K} \underline{F}) \quad (75)$$

$$\langle [d(\underline{v})]^2 \rangle_N = 2 \text{tr} (\underline{K} \underline{F})^2 + \text{tr}^2 (\underline{K} \underline{F}) \quad (76)$$

Thus, from Eq. (25),

$$R = \frac{\left[\text{tr} \left(\left\langle \underline{s} \underline{s}' \right\rangle_S \underline{F} \right) \right]^2}{2 \text{tr} (\underline{K} \underline{F})^2} \quad (77)$$

^{*}More explicitly, $Y_i = \sum_j H_{ij} v_j$. If the filter is to be realizable, then $Y_i = 0$ for $i < j$, for any \underline{v} . This is assured if $H_{ij} = 0$ for $i < j$, thus \underline{H} is "lower diagonal" in such a case.

Let us now use Eq. (77) to calculate the output SNR for the case considered earlier, i.e., the case of a steady sinusoid whose frequency lies somewhere in a band Ω rad/sec wide centered at ω_0 . Let us assume the noise is white and strictly cut-off at W rad/sec. In such a case, $\langle \underline{s} \underline{s} \rangle$ is given by Eq. (45) as before. Here \underline{F} simply represents the square-and-add operation and so

$$\underline{F} = \underline{I} \quad (78)$$

Since the noise is white,

$$K = N \underline{I} \quad (79)$$

Thus, from Eq. (77) we have

$$R = \frac{nA^4}{8N^2} = \frac{A^4}{8\pi N^2} WT \quad (80)$$

where $n = \frac{WT}{\pi}$. It is clear of course that the result Eq. (80) does not depend in any way upon the uncertainty about signal frequency. However, Eq. (80) can be rewritten in a more interesting form:

$$R = \frac{A^4}{4N_0^2 \Omega^2} \left(\frac{\Omega}{W} \right) \Phi T, \quad W \geq \Omega \quad (81)$$

This is seen to be identical to Eq. (55a) except for the factor $\frac{\Omega}{W}$. Thus we can summarize:

If the background noise is white over a band $(0, W)$, the optimum LR detector consists of a filter matched to the band of signal frequency uncertainty Ω , where $W > \Omega$, followed by a squarer and an integrator. If, however, the received signal is not filtered before detection but is simply squared and integrated, the output SNR derived for the optimum detector must be multiplied by the factor $\frac{\Omega}{W}$.

VIII. Sub-optimum Detection--Hydrophone Array

If an M-hydrophone array is used, the operation equivalent to $\underline{v}' \underline{F} \underline{v}$ in Eq. (71) consists of summing the outputs from the M hydrophones and then using the summer output in the quadratic form $\underline{v}' \underline{F} \underline{v}$.

If the background noise is broadband white, and the array is steered on target, it can easily be verified that the output SNR is

$$R = \frac{M^2 A^4}{4 N_0^2 \Omega^2} \left(\frac{\Omega}{W} \right) \bar{\Phi} T \quad (82)$$

IX. Conclusions

There is evidence that the low frequency portion of received signal spectrum contains certain coherent signals which may be used as a basis for detection. It had been hoped that advantage could be taken of the periodic nature of these signals to perform some form of coherent detection and thereby enhance signal detectability. However, the lack of precise knowledge about the frequency of the periodicity is a stumbling block. If the frequency is known only to lie within certain upper and lower limits, then the optimum detection procedure is an incoherent one, i.e., an energy measurement of the received signal. Coherent detection is, generally speaking, cross-correlation with a replica of the desired signal. However, effective cross-correlation requires at least a knowledge of the frequency or fundamental frequency of the signal. This in a nutshell is why the optimum detection scheme for the case we have considered is not a coherent scheme.

A comparison of the case of a sinusoidal signal of unknown frequency and phase with the case of a gaussian random signal shows that in either case the optimum LR detector has the same form, i.e., a purely incoherent

detector. This indicates that a periodic signal of unknown frequency is no more detectable than a gaussian random signal of the same power confined to the same frequency band. This is a surprising result, but one which follows quite clearly from a straightforward application of the general theory of optimal (minimum average risk) detection as outlined by Middleton.

Even though the unknown signal frequency may have a value anywhere in a given region of uncertainty, it seems intuitively that one should be able to make use of the fact that in the observation interval at hand, the signal frequency takes on but one of its possible values for the entire interval. With this idea in mind, a detection scheme has been considered in which the overall band of signal frequency uncertainty is split up into a number of sub-bands. The SNR is thus enhanced in one sub-band, that which contains the signal. Each of the sub-bands is then processed by means of an incoherent threshold detector and a final decision is made on the basis of the outputs of the sub-band detectors. Preliminary results indicate that this scheme would perform better than the "optimum" detector derived in this report. Presumably, the same improvement would be exhibited if the signal were not a pure sinusoid but a narrow-band signal whose center frequency was not known exactly. In such a case the width of each sub-band would be chosen approximately equal to the width of the narrow-band signal.

This result brings up some serious questions regarding the supposed optimality of LR detection, since this arbitrary band-splitting operation is not dictated by the results of the general optimum detection analysis. Therefore the general detection problem, as analyzed from the Bayes' risk point of view, is presently being re-examined. This investigation, as well as the analysis of the band-splitting scheme, will be subjects of later reports.

Appendix A

Square Law Detector I--Ideal Filtering

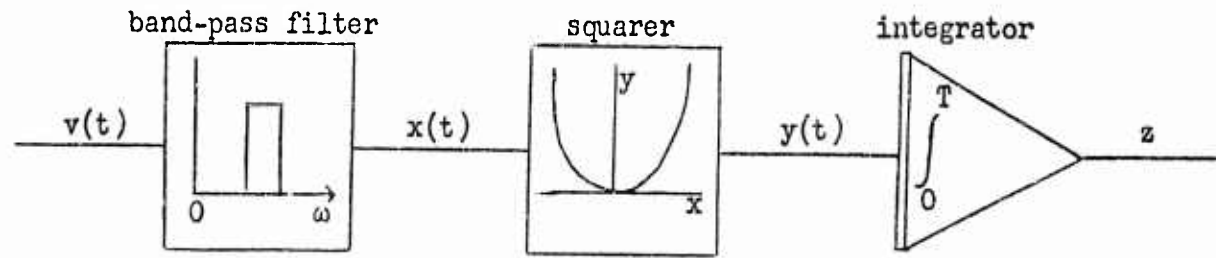


Figure A-1 Square Law Detector

The detector output, i.e., the test statistic to be used in the threshold comparison, is

$$z = \int_0^T x^2(t) dt \quad (A-1)$$

where

$$x(t) = \int_{-\infty}^t v(\tau) h(t - \tau) d\tau \quad (A-2)$$

and $h(\tau)$ is the weighting function for a rectangular filter matched to the band of signal frequency uncertainty. The $(-\infty)$ value of the lower limit in Eq. (A-2) implies that the filter is operating in a "steady-state" condition. The background noise contained in $v(t)$ is assumed to be flat over a broad band.

The output SNR will be taken as normalized deflection-squared, as before. The necessary averages are calculated as follows:

$$\begin{aligned} \langle z \rangle_{S+N} &= \left\langle \int_0^T dt \left[s^2(t) + 2 s(t) n_F(t) + n_F^2(t) \right] \right\rangle_{S+N} \\ &= \frac{A^2}{2} T + N_0 \Omega T \end{aligned} \quad (A-3)$$

where $n_F(t)$ is the noise at the output of the filter.

$$\begin{aligned} \left\langle z \right\rangle_N &= \left\langle \int_0^T dt \, u_F^2(t) \right\rangle_N \\ &= N_0 \Omega T \end{aligned} \quad (A-4)$$

$$\begin{aligned} \left\langle z^2 \right\rangle_N &= \left\langle \int_0^T dt \int_0^T d\sigma \, n_F^2(t) n_F^2(\sigma) \right\rangle_N \\ &= \int_0^T dt \int_0^T d\sigma \, \left\langle n_F^2(t) n_F^2(\sigma) \right\rangle_N \\ &= \int_0^T dt \int_0^T d\sigma \left[N_0^2 \Omega^2 + 2 R^2(t - \sigma) \right] \\ &= N_0^2 \Omega^2 T^2 + 2 \int_0^T dt \int_0^T d\sigma R_F^2(t - \sigma) \end{aligned} \quad (A-5)$$

where $R_F(\tau)$ is the a.c.f. for $n_F(t)$.

Thus,

$$R = \frac{A^4 T^2}{8 \int_0^T dt \int_0^T d\sigma R_F^2(t - \sigma)} \quad (A-6)$$

For the rectangular filter with flat response over $(\omega_0 - \frac{\Omega}{2}, \omega_0 + \frac{\Omega}{2})$,

$$R_F(t - \sigma) = N_0 \Omega \text{sinc} \frac{\Omega}{2} (t - \sigma) \cos \omega_0 (t - \sigma) \quad (A-7)$$

Thus in this case

$$R = \frac{A^4 T^2}{8 N_o^2 \Omega^2 \int_0^T dt \int_0^T d\sigma \operatorname{sinc}^2 \Phi(t - \sigma) \cos^2 \omega_o(t - \sigma)}$$

$$\approx \frac{A^4 T^2}{4 N_o^2 \Omega^2 \int_0^T dt \int_0^T d\sigma \operatorname{sinc}^2 \Phi(t - \sigma)} \quad (\text{A-8})$$

or,

$$R \approx \frac{A^4 T^2}{16 \pi^2 N_o^2 \int_0^T dx \int_0^T dy \operatorname{sinc}^2(x - y)} \quad (\text{A-9})$$

Appendix B

Square Law Detector II--Short-Term Filtering

In this Appendix we assume that the pre-detection filter cannot operate on the infinite past history of the received signal $v(t)$ as was assumed in the previous Appendix [See Eq. (A-2)]. Instead, the filter is allowed to weight only as much of $v(t)$ as is available at any time in the observation interval $(0 \leq t \leq T)$. With this restriction, $x(t)$ now takes the form

$$x(t) = \int_0^t v(\tau) h(t - \tau) d\tau \quad (B-1)$$

Again,

$$z = \int_0^T x^2(t) dt \quad (B-2)$$

Now,

$$\begin{aligned} z &= \int_0^T dt \left[\int_0^T d\tau v(\tau) h(t - \tau) \right] \left[\int_0^t d\sigma v(\sigma) h(t - \sigma) \right] \\ &= \int_0^T dt \int_0^t d\tau \int_0^t d\sigma v(\tau) v(\sigma) h(t - \tau) h(t - \sigma) \end{aligned} \quad (B-3)$$

The output SNR R is required. We obtain the appropriate averages as follows:

$$\langle z \rangle_{S+N} = \left\langle \int_0^T dt \int_0^t d\tau \left[s(\tau) + n(\tau) \right] h(t - \tau) \int_0^t d\sigma \left[s(\sigma) + n(\sigma) \right] h(t - \sigma) \right\rangle_{S+N}$$

$$= \int_0^T dt \left[\int_0^t d\tau \int_0^t d\sigma \langle s(\tau) s(\sigma) \rangle_S h(t-\tau) h(t-\sigma) + \int_0^t d\tau \int_0^t d\sigma R(\tau-\sigma) h(t-\tau) h(t-\sigma) \right] \quad (B-4)$$

$$\langle z \rangle_N = \int_0^T dt \int_0^t d\tau \int_0^t d\sigma R(\tau-\sigma) h(t-\tau) h(t-\sigma) \quad (B-5)$$

Thus,

$$\langle z \rangle_{S+N} - \langle z \rangle_N = \int_0^T dt \int_0^t d\tau \int_0^t d\sigma \langle s(\tau) s(\sigma) \rangle_S h(t-\tau) h(t-\sigma) \quad (B-6)$$

Letting

$$\langle s(\tau) s(\sigma) \rangle_S = R_s(\tau-\sigma) \quad (B-7)$$

we can write

$$\langle z \rangle_{S+N} - \langle z \rangle_N = \int_0^T dt \int_0^t d\tau \int_0^t d\sigma R_s(\tau-\sigma) h(\tau) h(\sigma) \quad (B-8)$$

Calculating the variance of z given that only noise is present,

$$\begin{aligned} \langle z^2 \rangle_N &= \left\langle \int_0^T dt \left[\int_0^t d\tau v(\tau) h(t-\tau) \int_0^t d\sigma v(\sigma) h(t-\sigma) \right] \right. \\ &\quad \left. \cdot \int_0^T ds \left[\int_0^s d\eta v(\eta) h(s-\eta) \int_0^s d\xi v(\xi) h(s-\xi) \right] \right\rangle_N \end{aligned}$$

$$= \int_0^T dt \left[\int_0^t d\tau \int_0^t d\sigma \langle s(\tau) s(\sigma) \rangle_S h(t - \tau) h(t - \sigma) + \int_0^t d\tau \int_0^t d\sigma R(\tau - \sigma) h(t - \tau) h(t - \sigma) \right] \quad (B-4)$$

$$\langle z \rangle_N = \int_0^T dt \int_0^t d\tau \int_0^t d\sigma R(\tau - \sigma) h(t - \tau) h(t - \sigma) \quad (B-5)$$

Thus,

$$\langle z \rangle_{S+N} - \langle z \rangle_N = \int_0^T dt \int_0^t d\tau \int_0^t d\sigma \langle s(\tau) s(\sigma) \rangle_S h(t - \tau) h(t - \sigma) \quad (B-6)$$

Letting

$$\langle s(\tau) s(\sigma) \rangle_S = R_s(\tau - \sigma) \quad (B-7)$$

we can write

$$\langle z \rangle_{S+N} - \langle z \rangle_N = \int_0^T dt \int_0^t d\tau \int_0^t d\sigma R_s(\tau - \sigma) h(\tau) h(\sigma) \quad (B-8)$$

Calculating the variance of z given that only noise is present,

$$\langle z^2 \rangle_N = \left\langle \int_0^T dt \left[\int_0^t d\tau v(\tau) h(t - \tau) \int_0^t d\sigma v(\sigma) h(t - \sigma) \right] \cdot \int_0^T ds \left[\int_0^s d\eta v(\eta) h(s - \eta) \int_0^s d\xi v(\xi) h(s - \xi) \right] \right\rangle_N$$

$$\begin{aligned}
&= \int_0^T dt \int_0^T ds \int_0^t d\tau \int_0^t d\sigma \int_0^s d\eta \int_0^s d\xi \left\langle v(\tau) v(\sigma) v(\eta) v(\xi) \right\rangle_N \\
&\quad \cdot h(t - \tau) h(t - \sigma) h(s - \eta) h(s - \xi)
\end{aligned} \tag{B-9}$$

If the noise before filtering is white,

$$\left\langle v(x) v(y) \right\rangle_N = \pi N_0 \delta(x - y) \tag{B-10}$$

If the noise is also gaussian,

$$\begin{aligned}
\left\langle z^2 \right\rangle_N &= \pi^2 N_0^2 \int_0^T dt \int_0^T ds \left\{ \int_0^t d\tau h^2(t - \tau) \int_0^s d\eta h^2(s - \eta) \right. \\
&\quad + \int_0^t d\tau h(t - \tau) h(s - \tau) \int_0^t d\sigma h(t - \sigma) h(s - \sigma) \\
&\quad \left. + \int_0^t d\tau h(t - \tau) h(s - \tau) \int_0^t d\sigma h(t - \sigma) h(s - \sigma) \right\} \\
&= \pi^2 N_0^2 \left[\int_0^T dt \int_0^t d\tau h^2(t - \tau) \right]^2 + \pi^2 N_0^2 \left[\int_0^t d\tau h(t - \tau) h(s - \tau) \right]^2
\end{aligned} \tag{B-11}$$

Thus,

$$R = \frac{\left[\int_0^T dt \int_0^t d\tau \int_0^t d\sigma R_s(\tau - \sigma) h(\tau) h(\sigma) \right]^2}{2\pi^2 N_0^2 \int_0^T dt \int_0^T ds \left[\int_0^t d\tau h(t - \tau) h(s - \tau) \right]^2}$$

(B-12)

List of Symbols

A = signal amplitude

$\{B(t_i)\}$ = a vector

$\{B(t_i, t_j)\}$ = a matrix

c = velocity of sound in water

d = distance between two hydrophones

$d(\underline{v})$ = test statistic in sub-optimum detection

$\delta(x)$ = Dirac delta function

Δ = sampling interval

\underline{F} = coefficient matrix of sub-optimum quadratic form

$f(\underline{v}/\underline{o})$ = conditional probability density of \underline{v} with no signal present

$f(\underline{v}/\underline{s})$ = conditional probability density of \underline{v} with signal present

$\underline{\Theta}$ = bandwidth of signal frequency uncertainty in cps

ϕ = phase of desired signal

\underline{G} = coefficient matrix of optimum quadratic form

\underline{H} = filter weighting matrix

$h(\tau)$ = filter weighting function

$h(t_1)$ = sample of Hilbert transform of $n(t)$

\underline{I} = identity matrix

\underline{K} = noise covariance matrix

K_{ij}^{-1} = element of inverse covariance matrix

$\ell(\underline{v})$ = likelihood ratio

M = number of hydrophones in an array

m = number of possible discrete signal frequencies

N = noise power

N_o = noise spectrum level in watts/rps

n = number of time samples

\underline{n} = noise vector

$n(t)$ = noise signal in continuous form

$n_F(t)$ = noise signal after filtering

$\theta(x)$ = "at most on the order of x "

$P(x_1)$ = probability function

$p(x)$ = probability density function

R = output signal-to-noise ratio

$R'(\tau')$ = autocorrelation function of noise at a hydrophone

$R(\tau, \tau_s)$ = cross-correlation function for noise signals at two different hydrophones

$R_F(\tau)$ = a.c.f. of noise after filtering

S = set of unknown signal parameters

\underline{s} = desired signal vector

\underline{s}' = transpose of vector \underline{s}

$s(t)$ = desired signal in continuous form

T = observation time of received signal

τ_s = time delay between two hydrophones

\underline{u} = sampled Hilbert transform of $v(t)$

\underline{v} = received signal vector

$v(t)$ = received signal in continuous form

W = noise bandwidth in rps

$x(t)$ = received waveform after filtering

Ω = bandwidth of signal frequency uncertainty in rps

ω = signal frequency

ω_0 = center of band of signal frequency uncertainty

\underline{Y} = filter output in sub-optimum detection

$y(t)$ = received waveform after squarer

z = integrator output

$\det \underline{A}$ = determinant of matrix \underline{A}

$\left\langle \right\rangle_N$ = statistical average, conditioned on presence of noise only

$\left\langle \right\rangle_{S+N}$ = statistical average, conditioned on presence of both signal and noise

$\text{tr } \underline{A}$ = trace of matrix \underline{A}

Abbreviations

a.c.f. = autocorrelation function

LR = likelihood ratio

p.d.f. = probability density function

SNR = signal-to-noise ratio

References

1. Schultheiss, P. M., "Optimal Detection of Directional Gaussian Signals in an Isotropic Gaussian Noise Field," Progress Report No. 3, General Dynamics/Electric Boat Research, Yale University, May 1963.
2. Tuteur, F. B., "Detection of Wide-Band Signals Modulated by a Low-Frequency Sinusoid," Progress Report No. 5, General Dynamics/Electric Boat Research, Yale University, June 1963.
3. Peterson, W. W., T. G. Birdsall, and W. C. Fox, "The Theory of Signal Detectability," IRE Trans. on Information Theory, vol. IT-4, pp. 171-212, September 1954.
4. Middleton, D., An Introduction to Statistical Communication Theory, McGraw-Hill Book Company, New York, 1960.
5. Woodward, P. M., Probability and Information Theory, With Applications to Radar, McGraw-Hill Book Company, New York, 1953; cf. Chapter 2.
6. Faran, J. J., and R. Hills, "The Application of Correlation Techniques to Acoustic Receiving Systems," Technical Memo. No. 28, Acoustics Research Laboratory, Harvard University, Cambridge, Massachusetts. November 1952.



RANDOM BEARING ERRORS IN SPLIT-BEAM SYSTEMS

by

Theron Usher, Jr.

Progress Report No. 9

General Dynamics/Electric Boat Research

(53-00-10-0231)

December 1963

DEPARTMENT OF ENGINEERING
AND APPLIED SCIENCE

YALE UNIVERSITY

I. Introduction

The determination of the bearing of a plane-wave random signal in a background of isotropic random noise, by means of so-called "split-beam" systems of transducers, has been popular because a null output is obtained when the transducers are steered "on target." Such systems are of great value in automatic tracking applications.

However, the random fluctuation of the output of such systems causes uncertainty in the determination of the bearing of signal source. It is the purpose of this report to determine general mathematical relations for the computation of the bearing uncertainty, and from these relations to determine system parameters which optimize or minimize the bearing uncertainty.

The problem of determining bearing uncertainty has been treated in Reference 1, but the analysis is somewhat restricted in that the system is not quite as general as the one considered here. The problem of minimizing bearing uncertainty has not been treated previously, but the analysis is parallel to that done by Eckart in Reference 2. There also seems to be an error in Reference 1 in the analysis concerning multi-element arrays.

II. Definitions and Assumptions

The system to be analyzed is shown in Fig. 1. The outputs of each set of M transducers from an array of $2M$ transducers are summed and each sum is then fed into a linear filter. The frequency response functions of the filters are related in that there is a 90° phase shift between the response functions at all frequencies. The filtered sums

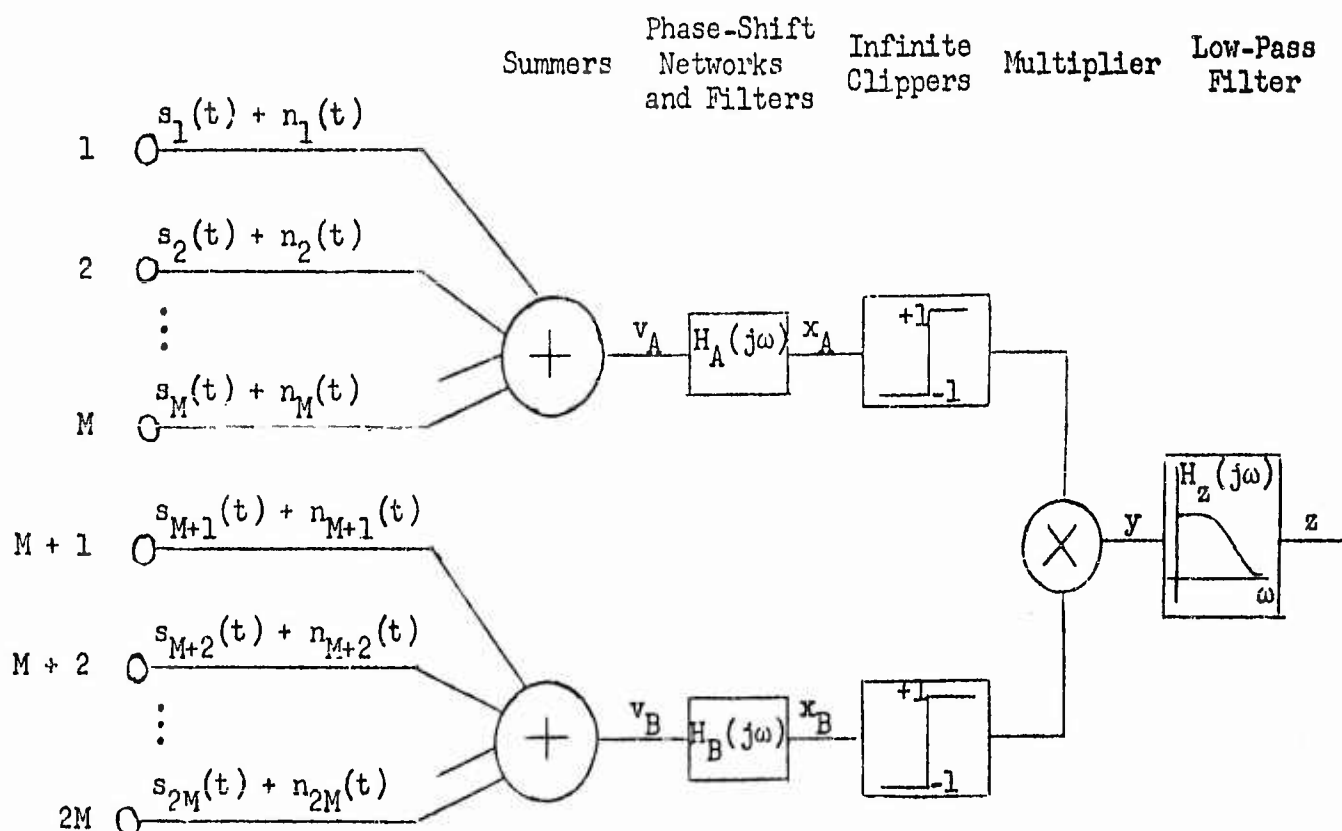


Fig. 1 Typical Split-Beam System

are then passed through infinite clippers, the results are multiplied and the product is averaged by means of a low-pass filter. The average output of the low-pass filter as the array is steered gives the bearing response pattern for the system.

Following are the major assumptions inherent in the analysis:

- 1) The transducers in the array have omnidirectional characteristics.
- 2) The array of $2M$ transducers is a linear array, with equal spacing between transducers.
- 3) The signal in the medium is a plane wave.
- 4) The noise is isotropic in the medium and the cross-correlation between the noise components of the outputs of different transducers is assumed to be zero.

5) The signal and noise are Gaussian and stationary, and signal and noise are independent.

6) The spectral density of the signal need not be the same as that for the noise at the output of any transducer.

III. Bearing Response Pattern

Since the signal is a plane wave, the array is linear with equal spacing between transducers, and the transducers are omnidirectional, the relation in Eq. (1) holds for the signal component from the i^{th} transducer.

$$s_i(t) = s_1[t - (i - 1)T] \quad (1)$$

The time T is the spatial time delay of the signal between adjacent transducers. When $T = 0$, the bearing of the signal is perpendicular to the line of the array.

The outputs of the summing amplifiers in Fig. 1 are given by

$$v_A(t) = \sum_{i=1}^M \left\{ s_1[t - (i - 1)T] + n_i(t) \right\} \quad (2)$$

$$v_B(t) = \sum_{k=1}^M \left\{ s_1[t - (k + M - 1)T] + n_{M+k}(t) \right\} \quad (3)$$

The autocorrelation function of $v_A(t)$ and $v_B(t)$ may be expressed in terms of the autocorrelation functions of the signal and noise at any transducer by means of the following relations.

$$\begin{aligned}
R_{v_A}(\tau) &= \sum_{i=1}^M \sum_{\ell=1}^M E \left[\left\{ s_1[t - (i-1)T] + n_1(t) \right\} \left\{ s_1[t - (\ell-1)T + \tau] + n_\ell(t + \tau) \right\} \right] \\
&= \sum_{i=1}^M \sum_{\ell=1}^M R_s[\tau + (i-\ell)T] + M R_n(\tau) \\
&= S \sum_{i=1}^M \sum_{\ell=1}^M \rho_s[\tau + (i-\ell)T] + M N \rho_n(\tau) \tag{4}
\end{aligned}$$

$$R_{v_B}(\tau) = R_{v_A}(\tau) \tag{5}$$

In Eq. (4) S and N are the signal and noise powers at each transducer respectively, and ρ_s and ρ_n are the corresponding normalized autocorrelation functions.

The spectral densities of v_A and v_B are the Fourier transforms of the corresponding autocorrelation functions.* In Eq. (6) $g_s(\omega)$ and $g_n(\omega)$ are the normalized spectral density functions for signal and for noise respectively at every transducer.

*The transform pair given below will be used for relating spectral densities and correlation functions throughout this report.

$$\begin{aligned}
G(\omega) &= \frac{1}{2\pi} \int_{-\infty}^{\infty} R(\tau) e^{-j\omega\tau} d\tau \\
R(\tau) &= \int_{-\infty}^{\infty} G(\omega) e^{j\omega\tau} d\omega
\end{aligned}$$

$$\begin{aligned}
G_{v_A}(\omega) &= S \sum_{i=1}^M \sum_{\ell=1}^M \frac{1}{2\pi} \int_{-\infty}^{\infty} \rho_s(\tau + (i - \ell)T) e^{-j\omega\tau} d\tau \\
&\quad + MN \frac{1}{2\pi} \int_{-\infty}^{\infty} \rho_n(\tau) e^{-j\omega\tau} d\tau \\
&= S \sum_{i=1}^M \sum_{\ell=1}^M g_s(\omega) e^{j\omega(i - \ell)T} + MN g_n(\omega)
\end{aligned} \tag{6}$$

$$G_{v_B}(\omega) = G_{v_A}(\omega) \tag{7}$$

The filter frequency response functions are related in that there is a 90° phase difference between their phase angle at every frequency. Since simple filter realizations are desirable, for the initial analysis it is assumed that

$$H_A(j\omega) = j\omega k H_B(j\omega) \tag{8}$$

where k is an arbitrary proportionality constant.

The spectral densities of the outputs of the filters are found in Eqs. (9) and (10).

$$G_{x_A}(\omega) = \omega^2 k^2 |H_B(j\omega)|^2 G_{v_A}(\omega) \tag{9}$$

$$G_{x_B}(\omega) = |H_B(j\omega)|^2 G_{v_A}(\omega) \tag{10}$$

The development in Eqs. (1) through (10) is preliminary in determining the bearing response, which is the average value of the output of the multiplier, \bar{y} . The value of \bar{y} is dependent on the time delay T , and has been found to be¹

$$\bar{y} = \frac{2}{\pi} \arcsin \left[\frac{R_{x_A x_B}(0)}{\left\{ R_{x_A}(0) R_{x_B}(0) \right\}^{1/2}} \right] \quad (11)$$

The quantity $R_{x_A x_B}(0)$ is the cross-correlation function of $x_A(t)$ and $x_B(t)$ at $\tau = 0$. The cross-correlation may be evaluated by first writing the convolution integrals which yield $x_A(t)$ and $x_B(t)$.

$$x_A(t) = \sum_{i=1}^M \int_{-\infty}^{\infty} \left\{ s_1[t - (i-1)T - \alpha] + n_1(t - \alpha) \right\} h_A(\alpha) d\alpha \quad (12)$$

$$x_B(t) = \sum_{k=1}^M \int_{-\infty}^{\infty} \left\{ s_1[t - (k+M-1)T - \beta] + n_{M+k}(t - \beta) \right\} h_B(\beta) d\beta \quad (13)$$

In Eqs. (12) and (13) $h_A(\alpha)$ and $h_B(\beta)$ are the weighting functions of the filters with frequency response functions $H_A(j\omega)$ and $H_B(j\omega)$ respectively.

The cross-correlation at $\tau = 0$ is defined by

$$R_{x_A x_B}(0) = E[x_A(t) x_B(t)] \quad (14)$$

Since there is no correlation between the noise outputs of different transducers, the noise terms disappear when Eqs. (12) and (13) are substituted into Eq. (14). Thus

$$\begin{aligned} R_{x_A x_B}(0) &= \sum_{i=1}^M \sum_{k=1}^M \int_{-\infty}^{\infty} \int_{-\infty}^{\infty} E \left\{ s_1[t - (i-1)T - \alpha] s_1[t - (k+M-1)T - \beta] \right\} \times \\ &\quad h_A(\alpha) h_B(\beta) d\alpha d\beta \\ &= S \sum_{i=1}^M \sum_{k=1}^M \int_{-\infty}^{\infty} \int_{-\infty}^{\infty} \rho_s[\alpha - \beta - (k-i+M)T] h_A(\alpha) h_B(\beta) d\alpha d\beta \quad (15) \end{aligned}$$

Since

$$\rho_s[a - \beta - (k - I + M)T] = \int_{-\infty}^{\infty} g_s(\omega) e^{j\omega a} e^{-j\omega \beta} e^{-j\omega(k-i+M)T} d\omega \quad (16)$$

Equation (15) becomes

$$\begin{aligned} R_{x_A x_B}(0) &= S \sum_{i=1}^M \sum_{k=1}^M \int_{-\infty}^{\infty} g_s(\omega) e^{-j\omega(k-i+M)T} d\omega \int_{-\infty}^{\infty} h_A(\alpha) e^{j\omega \alpha} d\alpha \int_{-\infty}^{\infty} h_B(\beta) e^{-j\omega \beta} d\beta \\ &= S \sum_{i=1}^M \sum_{k=1}^M \int_{-\infty}^{\infty} H_A^*(j\omega) H_B(j\omega) g_s(\omega) e^{-j\omega(k-i+M)T} d\omega \end{aligned} \quad (17)$$

From Eq. (8), Eq. (17) becomes

$$R_{x_A x_B}(0) = S \sum_{i=1}^M \sum_{k=1}^M \int_{-\infty}^{\infty} j\omega k |H_B(j\omega)|^2 g_s(\omega) e^{-j\omega(k-i+M)T} d\omega \quad (18)$$

The denominator terms of Eq. (11) may be determined by performing inverse transformations on Eqs. (9) and (10).

$$R_{x_A}(0) = \int_{-\infty}^{\infty} k^2 \omega^2 |H_B(j\omega)|^2 G_{V_A}(\omega) d\omega \quad (19)$$

$$R_{x_B}(0) = \int_{-\infty}^{\infty} |H_B(j\omega)|^2 G_{V_A}(\omega) d\omega \quad (20)$$

Substitution of the results in Eqs. (6) and (7) into Eqs. (19) and (20) yields

$$\begin{aligned} R_{x_A}(0) &= S \sum_{i=1}^M \sum_{\ell=1}^M \int_{-\infty}^{\infty} k^2 \omega^2 |H_B(j\omega)|^2 g_s(\omega) e^{j\omega(i-\ell)T} d\omega \\ &\quad + MN \int_{-\infty}^{\infty} k^2 \omega^2 |H_B(j\omega)|^2 g_n(\omega) d\omega \end{aligned} \quad (21)$$

$$R_{x_B}(0) = S \sum_{k=1}^M \sum_{m=1}^M \int_{-\infty}^{\infty} |H_B(j\omega)|^2 g_s(\omega) e^{j\omega(k-m)T} d\omega$$

$$+ MN \int_{-\infty}^{\infty} |H_B(j\omega)|^2 g_n(\omega) d\omega \quad (22)$$

The bearing response results from the combination of Eqs. (11), (18), (21), and (22)

$$\bar{y} = -\frac{2}{\pi} \arcsin \left\{ \frac{\sum_{i=1}^M \sum_{k=1}^M \int_{-\infty}^{\infty} j\omega k |H_B|^2 g_s e^{-j\omega(k-i+M)T} d\omega}{\left[\sum_{i=1}^M \sum_{\ell=1}^M \int_{-\infty}^{\infty} k^2 \omega^2 |H_B|^2 g_s e^{j\omega(i-\ell)T} d\omega + \frac{MN}{S} \int_{-\infty}^{\infty} k^2 \omega^2 |H_B|^2 g_n d\omega \right]^{1/2}} \times \right.$$

$$\left. \left[\sum_{k=1}^M \sum_{m=1}^M \int_{-\infty}^{\infty} |H_B|^2 g_s e^{j\omega(i-\ell)T} d\omega + \frac{MN}{S} \int_{-\infty}^{\infty} |H_B|^2 g_n d\omega \right]^{1/2} \right\} \quad (23)$$

The expected result of $\bar{y} = 0$ when $T = 0$ is easily confirmed from Eq. (23).

If M is sufficiently large, the double summations in Eq. (23) reduce to

$$\sum_{i=1}^M \sum_{\ell=1}^M e^{j\omega(i-\ell)T} \approx M^2 \operatorname{sinc}^2 \frac{\omega MT}{2\pi} \quad (24)$$

and

$$\sum_{i=1}^M \sum_{k=1}^M e^{-j\omega(k-i+M)T} \approx (\cos \omega MT - j \sin \omega MT) M^2 \operatorname{sinc}^2 \frac{\omega MT}{2\pi} \quad (25)$$

where

$$\operatorname{sinc} x = \frac{\sin \pi x}{\pi x} \quad (26)$$

Substitution of the results of Eqs. (24) and (25) into Eq. (23) yields

$$\bar{y} = -\frac{2}{\pi} \arcsin \left\{ \frac{\int_{-\infty}^{\infty} \omega |H_B|^2 g_s \sin \omega MT \operatorname{sinc}^2 \frac{\omega MT}{2\pi} d\omega}{\left[\int_{-\infty}^{\infty} \omega^2 |H_B|^2 g_s \operatorname{sinc}^2 \frac{\omega MT}{2\pi} d\omega + \frac{N}{SM} \int_{-\infty}^{\infty} \omega^2 |H_B|^2 g_n d\omega \right]^{1/2} \left[\int_{-\infty}^{\infty} |H_B|^2 g_s \operatorname{sinc}^2 \frac{\omega MT}{2\pi} d\omega + \frac{N}{SM} \int_{-\infty}^{\infty} |H_B|^2 g_n d\omega \right]^{1/2}} \right\} \quad (27)$$

Furthermore, if $\frac{S}{N} \ll \frac{1}{M}$, Eq. (27) reduces to

$$\bar{y} \approx -\frac{2}{\pi} \frac{SM}{N} \frac{\int_{-\infty}^{\infty} \omega |H_B(j\omega)|^2 g_s(\omega) \sin \omega MT \operatorname{sinc}^2 \frac{\omega MT}{2\pi} d\omega}{\left[\int_{-\infty}^{\infty} \omega^2 |H_B(j\omega)|^2 g_n(\omega) d\omega \right]^{1/2} \left[\int_{-\infty}^{\infty} |H_B(j\omega)|^2 g_n(\omega) d\omega \right]^{1/2}} \quad (28)$$

The result in Eq. (28) is not unduly restricted, since threshold signal detection is important. For computational purposes, it should be remembered that $g_s(\omega)$ and $g_n(\omega)$ are normalized spectra and that normalization requires

$$\int_{-\infty}^{\infty} g_s(\omega) d\omega = \int_{-\infty}^{\infty} g_n(\omega) d\omega = 1 \quad (29)$$

IV. Bearing Uncertainty

The relation between target bearing θ and the time delay T is

$$T = \frac{d}{c} \sin \theta \quad (30)$$

where d is the separation between transducers, c is the speed of wave propagation in the medium, and θ is the angle between the direction of wave propagation and a plane perpendicular to the line of the array.

It has been shown¹ that the bearing uncertainty σ_θ is given by

$$\sigma_\theta = \sigma_z \left| \frac{d\bar{y}}{dT} \right|_{T=0} \cdot \left| \frac{dT}{d\theta} \right|_{\theta=0}^{-1} = \frac{c}{d} \sigma_z \left| \frac{d\bar{y}}{dT} \right|_{T=0}^{-1} \quad (31)$$

In Eq. (31), σ_z is the standard deviation of the output $z(t)$ of the split-beam system, shown in Fig. 1. For the computation of σ_z , it will be assumed that $\frac{S}{N} \ll \frac{1}{M}$ and that only noise \times noise terms make significant contribution to its value.

We have

$$\sigma_z = \left[\int_{-\infty}^{\infty} G_y(\omega) |H_z(j\omega)|^2 d\omega \right]^{1/2} \quad (32)$$

where $G_y(\omega)$ is the spectral density of $y(t)$ and $H_z(j\omega)$ is the frequency response function of the low-pass filter. Since the bandwidth of the low-pass filter is much narrower than the bandwidth of $G_y(\omega)$,

$$\sigma_z \approx \left[G_y(0) \int_{-\infty}^{\infty} |H_z(j\omega)|^2 d\omega \right]^{1/2} \quad (33)$$

The integral in Eq. (33) is simply twice the equivalent bandwidth of the low-pass filter for random signals [if $H_z(0) = 1$] and will be given the symbol $2\omega_L$. Also

$$G_y(0) = \frac{1}{2\pi} \int_{-\infty}^{\infty} R_y(\tau) d\tau \quad (34)$$

The autocorrelation function for $y(t)$ is defined by

$$R_y(\tau) = E \left[\left\{ \text{sgn } x_A(t) \cdot \text{sgn } x_B(t) \right\} \left\{ \text{sgn } x_A(t + \tau) \cdot \text{sgn } x_B(t + \tau) \right\} \right] \quad (35)$$

If $\frac{S}{N} \ll \frac{1}{M}$ only the noise \times noise terms in Eq. (35) are significant.

The functions $x_A(t)$ and $x_B(t)$ are not correlated so that

$$\begin{aligned} R_y(\tau) &= E \left[\text{sgn } x_A(t) \text{sgn } x_A(t + \tau) \right] E \left[\text{sgn } x_B(t) \text{sgn } x_B(t + \tau) \right] \\ &= \frac{4}{\pi^2} \arcsin \rho_{x_A}(\tau) \arcsin \rho_{x_B}(\tau) \end{aligned} \quad (36)$$

In Eq. (36) $\rho_{x_A}(\tau)$ and $\rho_{x_B}(\tau)$ are the normalized autocorrelation functions for $x_A(t)$ and $x_B(t)$ respectively. For small values of $\frac{S}{N}$ the normalized autocorrelation functions become

$$\rho_{x_A}(\tau) = \frac{R_{x_A}(\tau)}{R_{x_A}(0)} = \frac{\int_{-\infty}^{\infty} k^2 \omega^2 |H_B(j\omega)|^2 g_n(\omega) e^{j\omega\tau} d\omega}{\int_{-\infty}^{\infty} k^2 \omega^2 |H_B(j\omega)|^2 g_n(\omega) d\omega} \quad (37)$$

and

$$\rho_{x_B}(\tau) = \frac{R_{x_B}(\tau)}{R_{x_B}(0)} = \frac{\int_{-\infty}^{\infty} |H_B(j\omega)|^2 g_n(\omega) e^{j\omega\tau} d\omega}{\int_{-\infty}^{\infty} |H_B(j\omega)|^2 g_n(\omega) d\omega} \quad (38)$$

Equations (21) and (22) help to determine the final form of Eqs. (37) and (38).

Combination of Eqs. (33), (34), (36), (37) and (38) yields σ_z :

$$\sigma_z = \frac{2}{\pi} \left[\frac{2\omega_L}{2\pi} \int_{-\infty}^{\infty} \arcsin \left(\frac{\int_{-\infty}^{\infty} \omega^2 |H_B|^2 g_n \varepsilon^{j\omega\tau} d\omega}{\int_{-\infty}^{\infty} \omega^2 |H_B|^2 g_n d\omega} \right) \arcsin \left(\frac{\int_{-\infty}^{\infty} |H_B|^2 g_n \varepsilon^{j\omega\tau} d\omega}{\int_{-\infty}^{\infty} |H_B|^2 g_n d\omega} \right) d\tau \right]^{1/2} \quad (39)$$

Equation (39) can be simplified considerably if the product of the arcsin functions is replaced by the product of their arguments. Since the value of the arcsin function exceeds the value of its argument by a maximum of 57%, the use of the above-mentioned approximation will cause an error in σ_z amounting to much less than 57% because an integration process is involved. Thus Eq. (39) becomes

$$\sigma_z \approx \frac{2}{\pi} \left(\frac{\omega_L}{\pi} \right)^{1/2} \frac{\left[\int_{-\infty}^{\infty} \alpha^2 |H_B(j\alpha)|^2 g_n(\alpha) d\alpha \int_{-\infty}^{\infty} |H_B(j\beta)|^2 g_n(\beta) d\beta \int_{-\infty}^{\infty} \varepsilon^{j(\alpha+\beta)\tau} d\tau \right]^{1/2}}{\left[\int_{-\infty}^{\infty} \omega^2 |H_B(j\omega)|^2 g_n(\omega) d\omega \right]^{1/2} \left[\int_{-\infty}^{\infty} |H_B(j\omega)|^2 g_n(\omega) d\omega \right]^{1/2}} \quad (40)$$

It is seen that the frequency variable, ω , in the numerator of Eq. (39) has been replaced by α and β in Eq. (40) so that the integration over τ can be performed first. We then have

$$\int_{-\infty}^{\infty} \varepsilon^{j(\alpha+\beta)\tau} d\tau = 2\pi \delta(\alpha + \beta) \quad (41)$$

where $\delta(\alpha + \beta)$ is a unit delta function occurring at $\beta = -\alpha$. Next, performing the integration in the numerator of Eq. (40), we find that the triple integral resolves to

$$\int_{-\infty}^{\infty} \alpha^2 |H_B(j\alpha)|^2 g_n(\alpha) |H_B(-j\alpha)|^2 g_n(-\alpha) d\alpha$$

Since $|H_B(j\omega)|^2$ and $g_n(\omega)$ are even functions, Eq. (40) becomes

$$\sigma_z \approx \frac{2}{\pi} (\omega_L)^{1/2} \left[\frac{2 \int_{-\infty}^{\infty} \omega^2 |H_B(j\omega)|^4 g_n^2(\omega) d\omega}{\left(\int_{-\infty}^{\infty} \omega^2 |H_B(j\omega)|^2 g_n(\omega) d\omega \right) \left(\int_{-\infty}^{\infty} |H_B(j\omega)|^2 g_n(\omega) d\omega \right)} \right]^{1/2} \quad (42)$$

The slope of the bearing response pattern found in Eq. (31) can best be determined by differentiating Eq. (23). Under the restriction that $\frac{S}{N} \ll \frac{1}{M}$, the double summation terms in the denominator disappear, so that

$$\left. \frac{d\bar{y}}{dT} \right|_{T=0} \approx -\frac{2}{\pi} \frac{S}{MN} \frac{\sum_{i=1}^M \sum_{k=1}^M (k-i+M) \int_{-\infty}^{\infty} \omega^2 |H_B|^2 g_s d\omega}{\left[\int_{-\infty}^{\infty} \omega^2 |H_B|^2 g_n d\omega \right]^{1/2} \left[\int_{-\infty}^{\infty} |H_B|^2 g_n d\omega \right]^{1/2}} \quad (43)$$

$\left(\frac{SM}{N} \ll 1 \right)$

But

$$\sum_{i=1}^M \sum_{k=1}^M (k-i+M) = M^3 \quad (44)$$

The bearing uncertainty is then found by combining Eqs. (42), (43), and (44) with Eq. (31).

$$\sigma_{\theta} \approx \frac{c}{M_d} \left(\frac{SM}{N} \right)^{-1} (\omega_L)^{1/2} \frac{\left[2 \int_{-\infty}^{\infty} \omega^2 |H_B(j\omega)|^4 \xi_n^2(\omega) d\omega \right]^{1/2}}{\int_{-\infty}^{\infty} \omega^2 |H_B(j\omega)|^2 g_s(\omega) d\omega} \text{ radians} \quad (45)$$

In Eq. (45), M_d is half the total aperture of the split-beam array, and $\frac{SM}{N}$ is the signal-to-noise ratio in either channel, after summation of the signals from the M transducers. The ratio of the integral terms at the end of Eq. (45) yields a result with the dimensions of $[\text{rad/sec}]^{-3/2}$. The result without the exponent is some measure of effective system bandwidth. The following section deals with minimizing the bearing uncertainty.

V. Minimum Bearing Uncertainty

According to Eq. (45) the bearing uncertainty may be decreased by increasing the array aperture ($2 M_d$), by increasing the number of transducers inside a fixed aperture, and by decreasing the noise bandwidth of the final low-pass filter. However, increasing the number of transducers within a fixed aperture without limit does not cause a continuing decrease in bearing uncertainty because the assumption that there is zero correlation between noise outputs of different transducers is no longer realistic for close transducer spacing. For very close transducer spacing, the signal-to-noise ratio after summation no longer is represented by $\frac{SM}{N}$ because of the non-negligible cross-correlation.

However, if the array spacing, number of transducers, and low-pass filter characteristics are fixed, the bearing uncertainty is still a function of $H_B(j\omega)$. The following analysis yields the optimum filter function, $H_{B_C}(j\omega)$, that minimizes the ratio of the integrals in Eq. (45).

In Eq. (45) $|H_B(j\omega)|^2$ is replaced by $|H_{B_0}(j\omega)|^2 + \lambda |H_B''(j\omega)|^2$ where $H_{B_0}(j\omega)$ is the frequency response function that provides a stationary point for the ratio of the integrals, and $H_B''(j\omega)$ is any arbitrary frequency response function. We have

$$\sigma_0 \approx A \frac{\left[2 \int_{-\infty}^{\infty} \omega^2 \left(|H_{B_0}|^2 + \lambda |H_B''|^2 \right)^2 g_n^2(\omega) d\omega \right]^{1/2}}{\int_{-\infty}^{\infty} \omega^2 \left(|H_{B_0}|^2 + \lambda |H_B''|^2 \right) g_s(\omega) d\omega} \quad (46)$$

For a stationary point of σ_0 to exist,

$$\left. \frac{d\sigma_0}{d\lambda} \right|_{\lambda=0} = 0 \quad (47)$$

Performing the operation indicated in Eq. (47), we obtain

$$\begin{aligned} & \left[\int_{-\infty}^{\infty} \omega^2 |H_{B_0}|^2 |H_B''|^2 g_n^2 d\omega \right] \left[\int_{-\infty}^{\infty} \omega^2 |H_{B_0}|^2 g_s d\omega \right] \\ & - \left[\int_{-\infty}^{\infty} \omega^2 |H_{B_0}|^4 g_n^2 d\omega \right] \left[\int_{-\infty}^{\infty} \omega^2 |H_B''|^2 g_s d\omega \right] = 0 \quad (48) \end{aligned}$$

Rearranging Eq. (48) to obtain separation of terms involving $g_s(\omega)$ and $g_n(\omega)$, we get

$$\frac{\int_{-\infty}^{\infty} \omega^2 |H_{B0}|^2 |H_B''|^2 g_n^2 d\omega}{\int_{-\infty}^{\infty} \omega^2 |H_{B0}|^4 g_n^2 d\omega} = \frac{\int_{-\infty}^{\infty} \omega^2 |H_B''|^2 g_s d\omega}{\int_{-\infty}^{\infty} \omega^2 |H_{B0}|^2 g_s d\omega} \quad (49)$$

Equation (49) is satisfied for any arbitrary $|H_B''|^2$ if

$$|H_{B0}|^2 = k_B \frac{g_s(\omega)}{g_n^2(\omega)} \quad (50)$$

where k_B is an arbitrary constant.

Also

$$|H_{A0}|^2 = k_A \omega^2 \frac{g_s(\omega)}{g_n^2(\omega)} \quad (51)$$

The results in Eqs. (50) and (51) are almost identical to those obtained by Eckart in Reference 2. The ratio of integrals in Eq. (45) is also quite similar to the ratio found in Eq. (8) in Reference 2.

Under the conditions given in Eqs. (50) and (51), the minimum bearing uncertainty becomes

$$\sigma_{\theta_{\min}} \approx \frac{c}{Md} \left(\frac{SM}{N} \right)^{-1} (\omega_L)^{1/2} \left[\int_0^{\infty} \omega^2 \left(\frac{g_s(\omega)}{g_n(\omega)} \right)^2 d\omega \right]^{-1/2} \quad (52)$$

The result in Eq. (52) is also quite similar to the corresponding result obtained in Reference 2.

The application and further investigation of the results in Eqs. (50), (51), and (52) are deferred to a later section of this report. In the next section, the effect of using a non-minimum phase network to provide the 90° phase shift between channels is investigated. The results given previously depend on the minimum phase assumption in Eq. (8).

VI. Minimum Bearing Uncertainty with Non-Minimum Phase Filters

In this section it will be assumed that the non-minimum phase relationship between the two filters is given by

$$H_A'(j\omega) = j H_B'(j\omega) \quad (53)$$

The primes are used to indicate the fact that a non-minimum phase relation holds. The 90° phase shift without change in amplitude characteristics can be accomplished over a fairly wide band of frequencies by means of a complicated active all-pass structure.

The analysis follows exactly the same steps taken in Sections III, IV, and V, and for this reason only a skeleton set of equations will be listed here.

$$\text{Since } |H_A'|^2 = |H_B'|^2,$$

$$G_{x_A}(\omega) = G_{x_B}(\omega) = |H_B'|^2 G_{v_A}(\omega) \quad (54)$$

With the use of Eq. (17) the cross-correlation between $x_A(t)$ and $x_B(t)$ becomes

$$R_{x_A x_B}(0) = -S \sum_{i=1}^M \sum_{k=1}^M \left[\int_0^\infty j |H_B'|^2 g_s e^{-j\omega(k-i+M)T} d\omega - \int_{-\infty}^0 j |H_B'|^2 g_s e^{-j\omega(k-i+M)T} d\omega \right] \quad (55)$$

Also

$$R_{x_A}(0) = R_{x_B}(0) \approx MN \int_{-\infty}^{\infty} |H_B'|^2 g_n(\omega) d\omega \quad \text{if } \frac{SM}{N} \ll 1 \quad (56)$$

The bearing response equation for small signal-to-noise ratios

$\frac{SM}{N} \ll 1$ is

$$\bar{y} = -\frac{2}{\pi} \arcsin \left\{ \frac{\sum_{i=1}^M \sum_{k=1}^M \left[\int_0^{\infty} |H_B'|^2 g_s \varepsilon^{-j\omega(k-i+M)T} d\omega - \int_{-\infty}^0 |H_B'|^2 g_s \varepsilon^{-j\omega(k-i+M)T} d\omega \right]}{\frac{MN}{S} \int_{-\infty}^{\infty} |H_B'|^2 g_n d\omega} \right\} \quad (57)$$

Equation (57) reduces to

$$\bar{y} \approx -\frac{2}{\pi} \frac{SM}{N} \left\{ \frac{2 \int_0^{\infty} |H_B'|^2 g_s \sin \omega MT \operatorname{sinc}^2 \frac{\omega MT}{2\pi} d\omega}{\int_{-\infty}^{\infty} |H_B'|^2 g_n d\omega} \right\} \quad (58)$$

The normalized autocorrelation functions $\rho_{x_A}(\tau)$ and $\rho_{x_B}(\tau)$ are

$$\rho_{x_A}(\tau) = \rho_{x_B}(\tau) = \frac{\int_{-\infty}^{\infty} |H_B'|^2 g_n(\omega) \varepsilon^{j\omega\tau} d\omega}{\int_{-\infty}^{\infty} |H_B'|^2 g_n(\omega) d\omega} \quad (59)$$

Thus

$$\sigma_z^2 = \frac{2}{\pi} \left[\frac{\omega_L}{2\pi} \int_{-\infty}^{\infty} \arcsin^2 \left\{ \rho_{x_A}(\tau) \right\} d\tau \right]^{1/2} \quad (60)$$

If the arcsin function is replaced by its argument, we obtain the approximate answer

$$\sigma_z \approx \frac{2}{\pi} (\omega_L)^{1/2} \frac{\left[2 \int_{-\infty}^{\infty} |H_B'|^4 g_n^2(\omega) d\omega \right]^{1/2}}{\int_{-\infty}^{\infty} |H_B'|^2 g_n(\omega) d\omega} \quad (61)$$

The derivative of Eq. (58) with respect to T gives the slope of the bearing response pattern. The "on target" slope is

$$\left. \frac{d\bar{y}}{dT} \right|_{T=0} = - \frac{2}{\pi} \frac{SM^2}{N} \frac{2 \int_0^{\infty} \omega |H_B'|^2 g_s d\omega}{\int_{-\infty}^{\infty} |H_B'|^2 g_n d\omega} \quad (62)$$

Substitution of the results in Eqs. (61) and (62) yields the equation for bearing uncertainty

$$\sigma_\theta \approx \frac{c}{Md} \left(\frac{SM}{N} \right)^{-1} (\omega_L)^{1/2} \frac{\left[\int_0^{\infty} |H_B'|^4 g_n^2(\omega) d\omega \right]^{1/2}}{\int_0^{\infty} \omega |H_B'|^2 g_s(\omega) d\omega} \quad (63)$$

A comparison of the results in Eqs. (45) and (63) together with those in Eqs. (50) and (51) shows that bearing uncertainty may be minimized by setting

$$\left| H_{A_0}'(j\omega) \right|^2 = \left| H_{B_0}'(j\omega) \right|^2 = |\omega| \frac{g_s(\omega)}{g_n^2(\omega)} \quad (64)$$

The minimum bearing uncertainty under the conditions in Eq. (64) then becomes

$$\sigma_{\theta_{\min}} \approx \frac{c}{M\dot{d}} \left(\frac{SM}{N} \right)^{-1} \omega_L^{1/2} \left[\int_0^{\infty} \omega^2 \left(\frac{g_s(\omega)}{g_n(\omega)} \right)^2 d\omega \right]^{-1/2} \quad (65)$$

A comparison of Eqs. (52) and (65) shows that the minimum bearing uncertainty under the assumption of the nonminimum phase filter in Eq. (53) is precisely the same as the minimum bearing uncertainty using minimum phase processing. The optimum frequency responses for the processing filters in each case are not the same. It can be seen from Eqs. (50), (51), and (64) that the magnitude response of both processing filters for the non-minimum phase case is the geometric mean of the magnitude response functions for the minimum phase case.

VII. Results with Optimum Filter Using Physical Model for Spectra

Physical measurements indicate that Eq. (66) is a reasonable approximation for the underwater noise spectral density.

$$G_n(\omega) = \frac{N}{\pi\omega_o} \frac{1}{1 + \left(\frac{\omega}{\omega_o} \right)^2} \quad (66)$$

In Eq. (66) ω_o is fairly low, say, 1000 rad/sec.

The signal spectral density, generated at the source, is assumed to have the same shape as the noise spectral density. However, at the transducers the signal undergoes further frequency selective attenuation. The model utilized here is that introduced by Eckart.² Thus

$$G_s(\omega) = \frac{S}{\pi\omega_o} \frac{1}{1 + \left(\frac{\omega}{\omega_o} \right)^2} e^{-\omega^2 \alpha r} \quad (67)$$

where r is the target range in kiloyards, and α is a constant whose numerical value is 6×10^{-11} . For target ranges under 100 kiloyards, the normalization of $G_s(\omega)$ is not appreciably affected by the exponential factor, so that

$$G_s(\omega) \approx \epsilon^{-\omega^2 \alpha r} G_n(\omega) = \frac{1}{\pi \omega_0} \frac{\epsilon^{-\omega^2 \alpha r}}{1 + \left(\frac{\omega}{\omega_0}\right)^2} \quad (68)$$

From Eqs. (50) and (51) the optimum minimum phase filter response functions are

$$|H_B| = \left(k_B \frac{G_s(\omega)}{G_n^2(\omega)} \right)^{1/2} = b \left[1 + \left(\frac{\omega}{\omega_0} \right)^2 \right]^{1/2} \epsilon^{-\frac{\omega^2 \alpha r}{2}} \quad (69)$$

and

$$|H_A| = \left(k_A \omega^2 \frac{G_s(\omega)}{G_n^2(\omega)} \right)^{1/2} = a \omega \left[1 + \left(\frac{\omega}{\omega_0} \right)^2 \right]^{1/2} \epsilon^{-\frac{\omega^2 \alpha r}{2}} \quad (70)$$

where a and b are arbitrary constants.

From Eq. (64), the optimum filter response functions for the system with the all-pass 90° phase shifting network are

$$|H_B'| = |H_A'| = c \omega^{1/2} \left[1 + \left(\frac{\omega}{\omega_0} \right)^2 \right]^{1/2} \epsilon^{-\frac{\omega^2 \alpha r}{2}} \quad (71)$$

Equations (69), (70) and (71) are plotted in Fig. 2 for $\omega_0 = 1000$, $\alpha = 6 \times 10^{-11}$, and $r = 10$ kyd. It can be seen that the optimum response functions have a peak value in the vicinity of the frequency at which the signal spectrum begins to attenuate. Due to the fact that the low

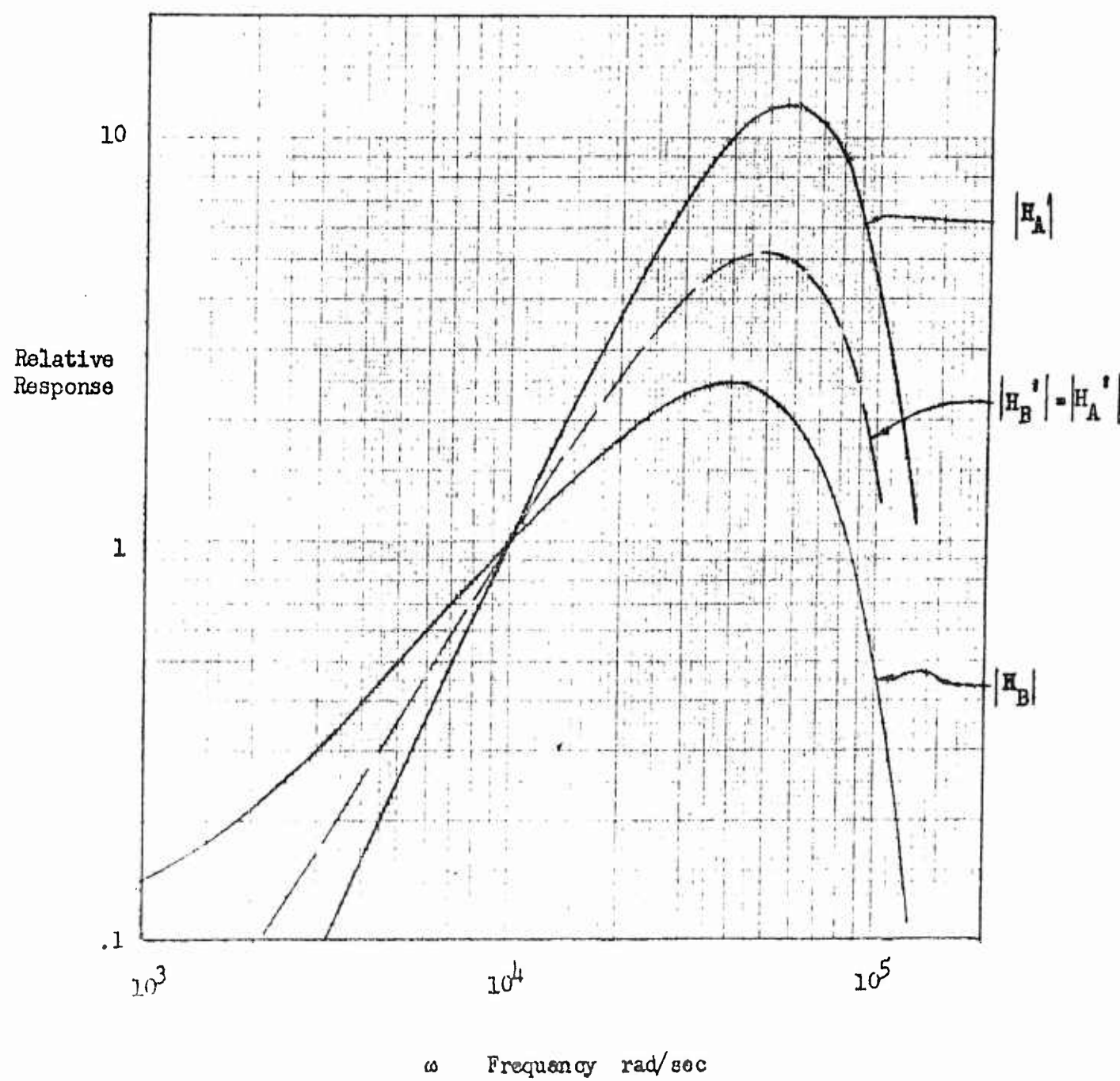


Fig. 2 Optimum Filter Response Function for $r = 10$ kyd.

frequency corner at $\omega_0 = 1000$ is practically insignificant, the peak values of the filter response functions occur at the following frequencies:

$$\text{For } |H_B| \quad \omega_{\max} = (ar)^{-1/2} \quad (72)$$

$$\text{For } |H_A| \quad \omega_{\max} = (2ar)^{-1/2} \quad (73)$$

$$\text{For } |H_B| = |H_A| \quad \omega_{\max} = \left(\frac{3}{2} ar\right)^{-1/2} \quad (74)$$

Table 1 gives the center frequencies and half-power frequencies for several values of range for $|H_B|$.

Range (kyd)	Center frequency (rad/sec)	Half-power frequencies (rad/sec)
1	131,000	63,000 ; 210,000
10	41,000	20,000 ; 66,000
100	13,100	6,300 ; 21,000

Table 1 Critical Frequencies for $|H_B|$

The minimum bearing uncertainty is obtained by substituting the information in Eq. (68) into Eq. (52). Thus

$$\begin{aligned} \sigma_{\theta_{\min}} &\approx \frac{c}{Md} \left(\frac{SM}{N}\right)^{-1} \omega_L^{1/2} \left[\int_0^\infty \omega^2 e^{-2\omega^2 ar} d\omega \right]^{-1/2} \\ &= \frac{c}{Md} \left(\frac{SM}{N}\right)^{-1} \omega_L^{1/2} \left(\frac{2}{\pi}\right)^{1/4} (4ar)^{3/4} \\ &= 5.45 \times 10^{-8} \frac{c}{Md} \left(\frac{SM}{N}\right)^{-1} \omega_L^{1/2} r^{3/4} \text{ radians} \end{aligned} \quad (75)$$

For a representative calculation, it is assumed that $M = 25$, $c = 5000$ ft/sec, $d = 2$ ft, $\omega_L = 1$ rad/sec, $r = 10$ kyd, and $SM/N = 0.1$. The last assumption puts the signal power at each receiver 24 db below the noise. From Eq. (75) we get

$$\sigma_{\theta_{\min}} = (5.45 \times 10^{-8}) \frac{5000}{(25)(2)} (10)(1)^{1/2} (10)^{3/4} = 3.08 \times 10^{-4} \text{ radians} \\ = .018 \text{ degrees} \quad (76)$$

The uncertainty in Eq. (76) seems unusually small. In the next section, the performance of specific suboptimum filters is investigated.

VIII. Results with Suboptimum Filters

The suboptimum filter to be considered first has the frequency response function

$$|H_B| = \begin{cases} b \left[1 + \left(\frac{\omega}{\omega_0} \right)^2 \right]^{1/2} & \beta\omega_H \leq \omega \leq \omega_H \\ 0 & \text{elsewhere} \end{cases} \quad (77)$$

$$H_A = kj\omega H_B \quad (78)$$

From Eq. (77), it can be seen that this filter provides the whitening of the noise spectrum as required of the optimum filter, but only passes signals in the frequency band from $\beta\omega_H$ to ω_H . The effect of the general location and width of the pass band will be investigated in this section.

From Eqs. (45), (66), (67), and (77) the bearing uncertainty is

$$\sigma_{\theta_1} \approx \frac{c}{Md} \left(\frac{SM}{N} \right)^{-1} \omega_L^{1/2} \frac{\left[\int_{\beta\omega_H}^{\omega_H} \omega^2 d\omega \right]^{1/2}}{\int_{\beta\omega_H}^{\omega_H} \omega^2 \frac{-\omega^2 ar}{\epsilon} d\omega} \quad (79)$$

Performing the integrations indicated in Eq. (79), we get

$$\sigma_{\theta_1} \approx \frac{c}{Md} \left(\frac{SM}{N} \right)^{-1} \omega_L^{1/2} \frac{(1 - \beta^3)^{1/2} \omega_H^{3/2}}{(6\pi)^{1/2} \sigma^3 \left[f' \left(\frac{\omega_H}{\sigma} \right) - f' \left(\frac{\beta \omega_H}{\sigma} \right) + \frac{1}{2} P \left(\frac{\omega_H}{\sigma} \right) - \frac{1}{2} P \left(\frac{\beta \omega_H}{\sigma} \right) \right]} \quad (80)$$

where

$$\sigma = (2ar)^{-1/2} \quad (81)$$

$$f'(X) = \left[\frac{d}{dx} \left\{ \frac{1}{\sqrt{2\pi}} e^{-\frac{x^2}{2}} \right\} \right]_{x=X} \quad (82)$$

and

$$P(X) = \frac{1}{\sqrt{2\pi}} \int_{-X}^X e^{-\frac{x^2}{2}} dx \quad (83)$$

The functions defined in Eqs. (82) and (83) are tabulated in References 3 and 4.

In order to provide a comparison with the results for the optimum filter, Eq. (80) is divided by Eq. (75) to yield the ratio of the respective bearing uncertainties.

$$\frac{\sigma_{\theta_1}}{\sigma_{\theta_{\min}}} = \frac{(1 - \beta^3)^{1/2} \left(\frac{\omega_H}{\sigma} \right)^{3/2}}{6.5 \left[f' \left(\frac{\omega_H}{\sigma} \right) - f' \left(\frac{\beta \omega_H}{\sigma} \right) + \frac{1}{2} P \left(\frac{\omega_H}{\sigma} \right) - \frac{1}{2} P \left(\frac{\beta \omega_H}{\sigma} \right) \right]} \quad (84)$$

For $\beta = 0$, two approximations are possible from Eqs. (79), (75) and (84).

$$\frac{\sigma_{\theta_1}}{\sigma_{\theta_{\min}}} \approx \begin{cases} 1.15 \left(\frac{\omega_H}{\sigma} \right)^{-3/2} & \frac{\omega_H}{\sigma} \ll 1 \\ .308 \left(\frac{\omega_H}{\sigma} \right)^{3/2} & \frac{\omega_H}{\sigma} \gg 1 \end{cases} \quad (85)$$

The minimum value of $\sigma_{\theta_1}/\sigma_{\theta_{\min}}$ occurs for a value of ω_H/σ very near the value at which the two approximations in Eq. (85) intersect.

$$\frac{\omega_H}{\sigma} = \left(\frac{1.15}{.308} \right)^{1/3} = 1.55 \quad (\beta = 0) \quad (86)$$

Substitution of the result in Eq. (86) into Eq. (84) yields

$$\left[\frac{\sigma_{\theta_1}}{\sigma_{\theta_{\min}}} \right]_{\min} = 1.17 \quad (87)$$

If the filter has a fairly narrow relative bandwidth such that β is nearly unity, then the combination of Eqs. (75) and (79) gives the following approximate result for $\sigma_{\theta_1}/\sigma_{\theta_{\min}}$:

$$\frac{\sigma_{\theta_1}}{\sigma_{\theta_{\min}}} = .667 \left(\frac{\omega_H}{\sigma} \right)^{-3/2} \frac{\omega_H^2}{\epsilon^2 \sigma^2} (1 - \beta)^{-1/2} \quad (1 - \beta) \ll 1 \quad (88)$$

The right hand side of Eq. (88) has a minimum value occurring at

$$\frac{\omega_H}{\sigma} = (1.5)^{1/2} = 1.23 \quad (1 - \beta) \ll 1 \quad (89)$$

The minimum value is

$$\left[\frac{\sigma_{\theta_1}}{\sigma_{\theta_{\min}}} \right]_{\min} = 1.04 (1 - \beta)^{-1/2} \quad (1 - \beta) \ll 1 \quad (90)$$

The figure of merit $\sigma_{\theta_1}/\sigma_{\theta_{\min}}$ for the suboptimum filter described in Eq. (77) is plotted for three values of β in Fig. 3. The results in Eqs. (84) through (90) apply to Fig. 3. It can be seen that the system performance with the suboptimum filter is good if the value of ω_H/σ is near 1.5 or, in other words, if the filter cutoff frequency matches the frequency at which the signal spectrum begins to fall off exponentially. For a fixed filter cutoff frequency, however, the relation $\omega_H/\sigma \approx 1.5$ holds only at one value of target range, and performance is not as good at other target ranges.

To illustrate this, let us assume that $\omega_H = 50,000$ rad/sec and $\beta = 0$. Table 2 shows values of $\sigma_{\theta_A}/\sigma_{\theta_{\min}}$ for various target ranges.

$\sigma_{\theta_1}/\sigma_{\theta_{\min}}$	r (kyd)	ω_H/σ
3.0	1	.55
1.18	10	1.74
4.0	100	5.5

Table 2 Figure of Merit for Various Target Ranges

The second suboptimum filter to be investigated has the frequency response function

$$H_B(j\omega) = b \frac{\left(1 + j \frac{\omega}{\omega_0}\right) \left(j \frac{\omega}{30,000}\right)}{\left(1 + j \frac{\omega}{30,000}\right) \left(1 + j \frac{\omega}{45,000}\right) \left(1 + j \frac{\omega}{60,000}\right)} \quad (91)$$

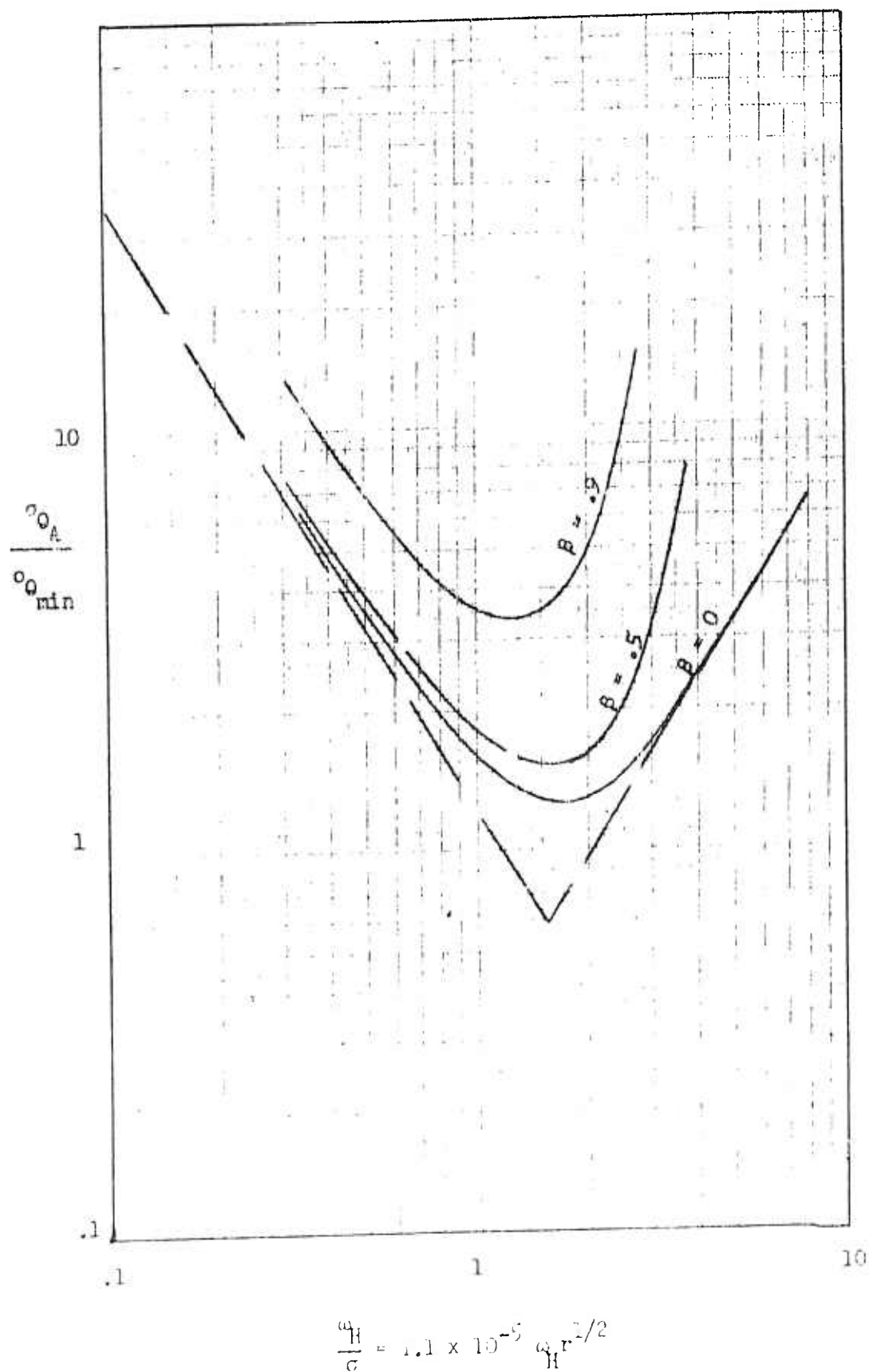


Fig. 3 Performance Index of Suboptimum System One as a Function of Normalized Filter Upper Cutoff Frequency

Also

$$H_A(j\omega) = k j\omega H_B(j\omega) \quad (92)$$

The expression in Eq. (91) is a realistic approximation to the filter in an existing system. Combining Eqs. (45), (68), and (91), we obtain the equation for bearing uncertainty

$$\sigma_{\theta_2} \approx \frac{c}{Md} \left(\frac{SM}{N} \right)^{-1} \omega_L^{1/2} \frac{\left[2 \int_{-\infty}^{\infty} \frac{\omega^6 d\omega}{\left[1 + \left(\frac{\omega}{30000} \right)^2 \right]^2 \left[1 + \left(\frac{\omega}{45000} \right)^2 \right]^2 \left[1 + \left(\frac{\omega}{60000} \right)^2 \right]^2} \right]^{1/2}}{\int_{-\infty}^{\infty} \frac{\omega^4 e^{-6 \times 10^{-11} \omega^2 r}}{\left[1 + \left(\frac{\omega}{30000} \right)^2 \right] \left[1 + \left(\frac{\omega}{45000} \right)^2 \right] \left[1 + \left(\frac{\omega}{60000} \right)^2 \right]} d\omega} \quad (93)$$

If the substitution $\omega = 10^4 u$ is made, Eq. (93) becomes

$$\sigma_{\theta_2} \approx \frac{c}{Md} \left(\frac{SM}{N} \right)^{-1} \omega_L^{1/2} 10^{-6} \frac{\left[2 \int_{-\infty}^{\infty} \frac{u^6 du}{\left[1 + \left(\frac{u}{3} \right)^2 \right]^2 \left[1 + \left(\frac{u}{4.5} \right)^2 \right]^2 \left[1 + \left(\frac{u}{6} \right)^2 \right]^2} \right]^{1/2}}{\int_{-\infty}^{\infty} \frac{u^4 e^{-6 \times 10^{-11} \omega^2 r}}{\left[1 + \left(\frac{u}{3} \right)^2 \right] \left[1 + \left(\frac{u}{4.5} \right)^2 \right] \left[1 + \left(\frac{u}{6} \right)^2 \right]} du} \quad (94)$$

The integrals in Eq. (94) have been determined numerically for different values of r . For the extreme values of r , the following approximations hold:

$$\sigma_{\theta_2} \approx 2.44 \times 10^{-8} \frac{c}{Md} \left(\frac{SM}{N} \right)^{-1} \omega_L^{1/2} \text{ radians} \quad \text{for } r \ll 1 \text{ kyd} \quad (95)$$

and

$$\sigma_{\theta_2} \approx 8.95 \times 10^{-5} r^{5/2} \frac{c}{Md} \left(\frac{SM}{N} \right)^{-1} \omega_L^{1/2} \text{ radians} \quad \text{for } r \gg 100 \text{ kyd} \quad (96)$$

The results of the numerical analysis are shown in Fig. 4, in which the ratio of the bearing uncertainty for the suboptimum filter to that for the optimum filter is plotted versus target range. The approximate ratios for extreme values of r are obtained by combining Eqs. (95) and (96) with Eq. (75).

$$\frac{\sigma_{\theta_2}}{\sigma_{\theta_{\min}}} \approx .447 r^{-3/4} \quad \text{for } r \ll 1 \text{ kyd} \quad (97)$$

and

$$\frac{\sigma_{\theta_2}}{\sigma_{\theta_{\min}}} \approx 1.64 \times 10^{-3} r^{7/4} \quad \text{for } r \gg 100 \text{ kyd} \quad (98)$$

Figure 4 shows that the minimum value of the performance ratio is approximately 1.03 at a range of 3.3 kyd. The performance ratio is less than 2 for ranges from 20 kyd to less than 1 kyd. Thus the present design should certainly be adequate for bearing determination purposes.

IX. Conclusions

Reference 1 contains a result for bearing uncertainty for narrow bandpass split-beam systems. If $|H_B|$ in Eq. (63) takes on the form of an ideal narrow band-pass filter, the result checks favorably with the corresponding result in Reference 1. However, the result in Eq. (63) is smaller by approximately 20% than the answer in Reference 1, simply because the latter analysis does not contain an approximation for the arcsin function. In Section IV of this paper, the arcsin function was approximated by its argument to allow simplification of Eq. (39).

For other forms of $|H_B|$, the approximation causes the results in Eqs. (45) and (63) to be low by approximately 20%.

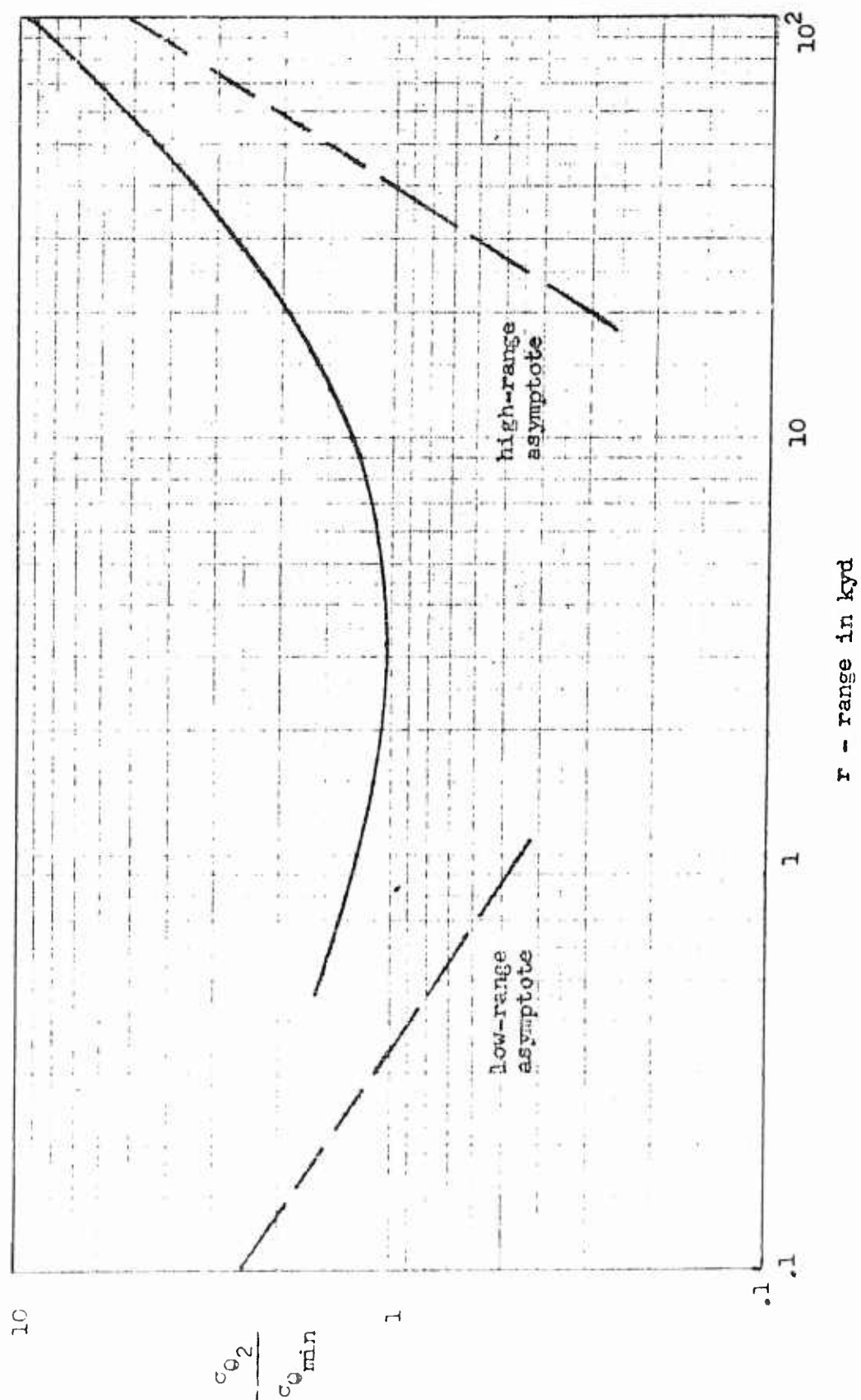


Fig. 4 Performance Index of Suboptimum System Two as a Function of Target Range

The minimization of Eqs. (45) and (63) by choosing an appropriate form for $|H_B|$ produces results nearly identical to those in Reference 2 simply because the integrals in Eqs. (45) and (63) are nearly identical to those in Reference 2. Actually, in demonstrating that the proper choice of $|H_B|$ produces a stationary point for σ_θ , it was never proved that the stationary point is actually a minimum. This consideration is somewhat academic, however, since the suboptimum systems treated in Section VIII always produce bearing uncertainties which are greater than those for the optimum system.

The calculation of a typical minimum bearing uncertainty in Section VII for a range of 10 kyd yields the extremely small uncertainty of .018 degrees. The investigation in Section VIII shows that an existing system at ranges of 10 kyd should have a bearing uncertainty about 1.3 times that of the optimum system. Actual data seem to indicate that bearing errors in automatic tracking systems are many times greater than $1.3 \times .018 = .023$ degrees. Of course, poor estimates on this author's part of the number of active transducers, average separation, signal-to-noise ratio, etc., may certainly contribute to the low value calculated.

However, another phenomenon may contribute largely to target bearing error. For split-beam arrays used in automatic tracking systems, a steady bearing error exists if the target has an angular velocity relative to the array. This steady error is inversely proportional to the loop-gain of the tracking system and, in turn, the loop-gain is dependent upon the signal-to-noise ratio as well as the target range. It is well known that the signal-to-noise ratio at the transducers varies in a random fashion with time because of signal fading. The random variation of signal-to-noise

ratio, and thus of loop-gain, can cause the "offset error" to vary in a random fashion, the variation possibly being many times greater than the bearing uncertainty computed in this report. Certainly the phenomenon should be quantitatively investigated. In some cases the random variation of the offset error may cause the automatic tracking system to lose the target.

References

1. Theoretical Limitations Imposed by System Parameters on Passive Sonar Bearing Accuracy, NavWeps Report 4732, The Raytheon Company, 10 August 1962 (Confidential).
2. Eckart, Carl, Optimal Rectifier Systems for the Detection of Steady Signals, Marine Laboratory, Scripps Institute of Oceanography, SIO Reference 52-11, University of California, 4 March 1952.
3. Tables of Normal Probability Functions, NBS Applied Mathematics Series, 23, 1953.
4. Marcum, J. I., Tables of Hermite Polynomials and the Derivatives of the Error Function, Rand Corporation, 1948.



EVALUATION OF A SUBOPTIMAL PROCEDURE FOR DETECTING
DIRECTIONAL GAUSSIAN SIGNALS IN ISOTROPIC GAUSSIAN NOISE

by

Peter M. Schultheiss

Progress Report No. 10

General Dynamics/Electric Boat Research

(53-00-10-0231)

December 1963

DEPARTMENT OF ENGINEERING
AND APPLIED SCIENCE
YALE UNIVERSITY

I. Introduction

An earlier report¹ dealt with the problem of detecting a weak, directional Gaussian signal in a very much stronger isotropic Gaussian noise field. It compared the performance of a likelihood ratio detector with that of a standard power detector and indicated that some advantage could often be gained in principle by use of likelihood ratio techniques. However, in the cases of practical interest investigated, the attainable improvement appeared to be too small to warrant the increased complexity of instrumentation. This raises two questions:

- 1) Are there situations of practical importance in which large gains can be made through use of likelihood ratio techniques?
- 2) Can one find suboptimal instrumentations that closely approximate the likelihood ratio detector in performance but are sufficiently simple to justify their use in situations where only moderate gains can be expected?

This report considers the second problem. Specifically, it shows that for the types of signal and noise spectra discussed in the earlier report the standard power detector preceded by an Eckart filter is such a suboptimal instrumentation. In the light of Bryn's² results it is of course not at all surprising that the likelihood ratio detector formally reduces to the proposed instrumentation for the special case of zero correlation between the noise disturbances at different hydrophones.

¹Progress Report No. 3, May 1963.

²F. Bryn, "Optimal Signal Processing of Three Dimensional Arrays Operating on Gaussian Signals and Noise," J.A.S.A. 34, No. 3, March 1962, pp. 289-297.

II. Output Signal to Noise Ratio of Power Detector with Eckart Filter

Consider the system shown in Fig. 1. The quantity of ultimate interest

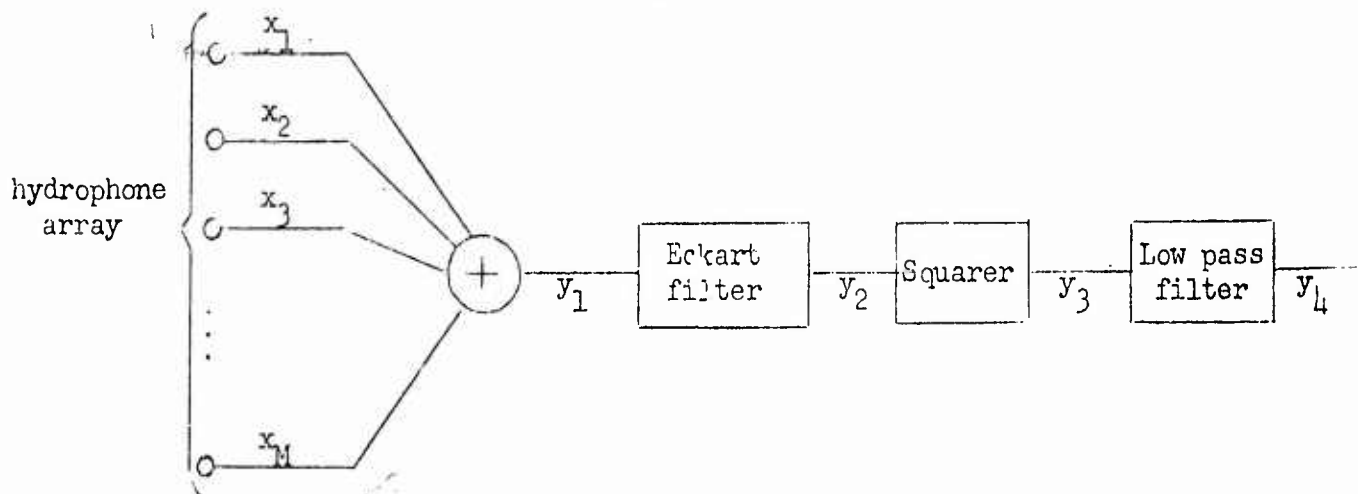


Fig. 1

is the output signal to noise ratio, the ratio of the change in average output resulting from the appearance of a signal to the rms output fluctuation. Throughout the discussion the array is assumed to be steered on target.

If the weighting function of the Eckart filter is designated by $w(t)$, the time function $y_2(t)$ at its output is given by

$$y_2(t) = \int_0^{\infty} d\tau w(\tau) \sum_{i=1}^M x_i(t - \tau) \quad (1)$$

where $x_i(t) = s(t) + n_i(t)$, the sum of the signal and noise disturbances received by the i^{th} hydrophone. The output $y_3(t)$ of the squarer is then

$$y_3(t) = \int_0^{\infty} d\tau w(\tau) \int_0^{\infty} d\sigma w(\sigma) \sum_{i=1}^M \sum_{j=1}^M [s(t - \tau) + n_i(t - \tau)] [s(t - \sigma) + n_j(t - \sigma)] \quad (2)$$

Hence the average output of the low pass filter assumes the form

$$\begin{aligned}
 E(y_4) = E(y_3) &= \int_0^\infty d\tau w(\tau) \int_0^\infty d\sigma w(\sigma) \sum_{i=1}^M \sum_{j=1}^M \overline{[s(t-\tau) + n_i(t-\tau)][s(t-\sigma) + n_j(t-\sigma)]} \\
 &= \int_0^\infty d\tau w(\tau) \int_0^\infty d\sigma w(\sigma) \sum_{i=1}^M \sum_{j=1}^M [R(\tau-\sigma) + Q_{ij}(\tau-\sigma)] \quad (3)^1
 \end{aligned}$$

$R(\tau)$ is the autocorrelation function of the signal and $Q_{ij}(\tau)$ is the cross-correlation between the noise received at the i^{th} and j^{th} hydrophones. In obtaining the last form of Eq. (3) use has been made of the assumption that signal and noise are statistically independent and have mean values of zero.

The increment in DC output resulting from the appearance of a signal is clearly

$$\Delta(\text{DC output}) = M^2 \int_0^\infty d\tau w(\tau) \int_0^\infty d\sigma w(\sigma) R(\tau-\sigma) \quad (4)$$

Expressing $R(\tau)$ in terms of the signal spectrum $S(\omega)$

$$R(\tau) = \frac{1}{2} \int_{-\infty}^{\infty} S(\omega) e^{j\omega\tau} d\omega \quad (5)$$

one obtains

$$\begin{aligned}
 \Delta(\text{DC output}) &= \frac{M^2}{2} \int_{-\infty}^{\infty} d\omega S(\omega) \int_0^\infty d\tau w(\tau) e^{j\omega\tau} \int_0^\infty d\sigma w(\sigma) e^{-j\omega\sigma} \\
 &= \frac{M^2}{2} \int_{-\infty}^{\infty} d\omega S(\omega) |H(\omega)|^2 \quad (6)
 \end{aligned}$$

¹The bar indicates an averaging operation over the random parameters of the noise.

where

$$H(\omega) = \int_0^{\infty} d\sigma w(\sigma) e^{-j\omega\sigma} \quad (7)$$

is the frequency response function of the Eckart filter.

The next step is to compute the output variance $D^2(y_4)$. As in Report No. 3 the low pass filter will be defined as a device whose output at any instant of time is the average of its input over the past T seconds. The corresponding weighting function is

$$h(t) = \begin{cases} \frac{1}{T} & 0 \leq t \leq T \\ 0 & \text{elsewhere} \end{cases} \quad (8)$$

If one assumes, still following Report No. 3, that T is large compared to the correlation time of y_3 , the desired output variance is given by

$$D^2(y_4) = \frac{1}{T} \int_{-\infty}^{\infty} [R_3(\alpha) - R_3(\infty)] d\alpha \quad (9)^1$$

$R_3(\alpha) - R_3(\infty)$ is the autocorrelation function of $y_3(t) - E[y_3(t)]$, i.e., of the fluctuating component of y_3 .

In cases of practical interest the input noise power is generally far greater than the input signal power. Hence a good approximation is obtained by considering only the contribution of the noise to $R_3(\alpha)$.

From Eq. (2)

$$\begin{aligned} R_3(\alpha) &= \sum_{i=1}^M \sum_{j=1}^M \sum_{h=1}^M \sum_{k=1}^M \int_0^{\infty} d\tau w(\tau) \int_0^{\infty} d\sigma w(\sigma) \int_0^{\infty} d\rho w(\rho) \int_0^{\infty} d\gamma w(\gamma) \\ &\quad \times n_i(t - \tau) n_j(t - \sigma) n_h(t + \alpha - \rho) n_k(t + \alpha - \gamma) \end{aligned} \quad (10)$$

¹See Report No. 3, Eqs. (39) and (40).

Recalling that $n_i(t)$ is a Gaussian random process one can write

$$\begin{aligned} n_i(t-\tau) n_j(t-\sigma) n_h(t+\alpha-\rho) n_k(t+\alpha-\gamma) = & Q_{ij}(\tau-\sigma) Q_{hk}(\rho-\gamma) \\ & + Q_{ih}(\sigma+\tau-\rho) Q_{jk}(\alpha+\sigma-\gamma) + Q_{ik}(\alpha+\tau-\gamma) Q_{jh}(\alpha+\sigma-\rho) \end{aligned} \quad (11)$$

The first term in Eq. (11) does not contain α . Upon substitution into Eq. (10) it leads to the DC component $R_3(\infty)$. The two last terms of Eq. (11) clearly make equal contributions to Eq. (10). Hence

$$\begin{aligned} R_3(\alpha) - R_3(\infty) = & 2 \sum_{i=1}^M \sum_{j=1}^M \sum_{h=1}^M \sum_{k=1}^M \int_0^\infty d\tau w(\tau) \int_0^\infty d\rho w(\rho) Q_{ih}(\alpha+\tau-\rho) \int_0^\infty d\sigma w(\sigma) \times \\ & \int_0^\infty d\gamma w(\gamma) Q_{jk}(\alpha+\sigma-\gamma) \\ = & 2 \left[\sum_{i=1}^M \sum_{h=1}^M \int_0^\infty d\tau w(\tau) \int_0^\infty d\rho w(\rho) Q_{ih}(\alpha+\tau-\rho) \right]^2 \end{aligned} \quad (12)$$

Thus from Eq. (9)

$$D^2(y_4) = \frac{2}{T} \int_{-\infty}^{\infty} d\alpha \left[\sum_{i=1}^M \sum_{h=1}^M \int_0^\infty d\tau w(\tau) \int_0^\infty d\rho w(\rho) Q_{ih}(\alpha+\tau-\rho) \right]^2 \quad (13)$$

Now using Parseval's theorem

$$D^2(y_4) = \frac{2}{T} \times \frac{\pi}{2} \int_{-\infty}^{\infty} |G(\omega)|^2 d\omega \quad (14)$$

where

$$G(\omega) = \frac{1}{\pi} \int_{-\infty}^{\infty} d\alpha e^{-j\omega\alpha} \sum_{i=1}^M \sum_{h=1}^M \int_0^{\infty} d\tau w(\tau) \int_0^{\infty} d\rho w(\rho) Q_{ih}(\alpha + \tau - \rho) \quad (15)$$

If one designates the cross-spectral density corresponding to $Q_{ih}(\tau)$ by $G_{ih}(\omega)$, i.e.,

$$G_{ih}(\omega) = \frac{1}{\pi} \int_{-\infty}^{\infty} d\alpha e^{-j\omega\alpha} Q_{ih}(\alpha) \quad (16)$$

it becomes possible to rewrite Eq. (15) in the following form.

$$G(\omega) = \frac{1}{\pi} \sum_{i=1}^M \sum_{h=1}^M \int_0^{\infty} d\tau w(\tau) e^{j\omega\tau} \int_0^{\infty} d\rho w(\rho) e^{-j\omega\rho} \int_{-\infty}^{\infty} d\alpha e^{-j\omega(\alpha+\tau-\rho)} Q_{ih}(\alpha + \tau - \rho) \quad (17)$$

Using Eqs. (7) and (16) this can be reduced to the very simple expression

$$G(\omega) = |H(\omega)|^2 \sum_{i=1}^M \sum_{j=1}^M G_{ih}(\omega) \quad (18)$$

Thus $G(\omega)$ is identified as the power spectrum of y_2 , and Eq. (14) becomes

$$D^2(y_4) = \frac{\pi}{T} \int_{-\infty}^{\infty} d\omega |H(\omega)|^4 \left| \sum_{i=1}^M \sum_{j=1}^M G_{ih}(\omega) \right|^2 \quad (19)$$

Combining Eqs. (6) and (19) one obtains the output signal to noise ratio

$$\frac{\Lambda(\text{DC output})}{D(y_4)} = \frac{\sqrt{T} M^2 \int_{-\infty}^{\infty} d\omega S(\omega) |H(\omega)|^2}{2\sqrt{\pi} \left[\int_{-\infty}^{\infty} d\omega |H(\omega)|^4 \left| \sum_{i=1}^M \sum_{j=1}^M G_{ih}(\omega) \right|^2 \right]^{1/2}} \quad (20)$$

Equation (20) makes no special assumptions concerning the linear filter which converts y_1 to y_2 . If the filter is indeed an Eckart filter as initially stated, then

$$|H(\omega)|^2 = \frac{S(\omega)}{[N(\omega)]^2} \quad (21)$$

where $N(\omega)$ is the power spectrum of the noise received by each hydrophone.

Substitution of Eq. (21) into Eq. (20) yields

$$\frac{\Delta(\text{DC output})}{D(y_4)} = \frac{\sqrt{T} M^2 \int_{-\infty}^{\infty} d\omega \left[\frac{S(\omega)}{N(\omega)} \right]^2}{2\sqrt{\pi} \left[\int_{-\infty}^{\infty} d\omega \frac{S^2(\omega)}{N^4(\omega)} \left| \sum_{i=1}^M \sum_{j=1}^M G_{ih}(\omega) \right|^2 \right]^{1/2}} \quad (22)$$

If the cross-correlation, and hence cross-spectral density, between the noise received at different hydrophones is zero, then

$$G_{ih}(\omega) = \begin{cases} 0 & \text{for } i \neq h \\ N(\omega) & \text{for } i = h \end{cases} \quad (23)$$

In that case

$$\frac{\Delta(\text{DC output})}{D(y_4)} = \frac{\sqrt{T} M \int_{-\infty}^{\infty} d\omega \left[\frac{S(\omega)}{N(\omega)} \right]^2}{2\sqrt{\pi} \left\{ \int_{-\infty}^{\infty} d\omega \left[\frac{S(\omega)}{N(\omega)} \right]^2 \right\}^{1/2}} = \sqrt{\frac{T}{2\pi}} M \sqrt{\int_0^{\infty} d\omega \left[\frac{S(\omega)}{N(\omega)} \right]^2} \quad (24)$$

This is identical with the output signal to noise ratio of the likelihood ratio detector under the same assumptions. [See Report No. 3, Eq. (32).] Thus the instrumentation of Fig. 1 is equivalent to a likelihood ratio detector if there is no noise correlation from hydrophone to hydrophone.¹

¹This can also be seen from Bryn, op. cit., Fig. 4 and associated discussion.

If there is noise correlation from hydrophone to hydrophone, it becomes necessary to compute the cross-spectral densities $G_{ih}(\omega)$. Assuming a spherically isotropic noise field,

$$Q_{ih}(\tau) = \frac{1}{2\tau_{ih}} \int_{\tau-\tau_{ih}}^{\tau+\tau_{ih}} Q(\sigma) d\sigma \quad (25)^1$$

$Q(\sigma) = Q_{ii}(\sigma)$, the autocorrelation function of the noise received at each hydrophone. $\tau_{ih} = d_{ih}/c$, where d_{ih} is the distance between the i^{th} and h^{th} hydrophones and c is the speed of sound in water. Using the symbol $u(x)$ to denote a unit step function at the origin, one can rewrite Eq. (25) as follows.

$$Q_{ih}(\tau) = \frac{1}{2\tau_{ih}} \int_{-\infty}^{\infty} Q(\sigma) \left[u(\sigma - \tau + \tau_{ih}) - u(\sigma - \tau - \tau_{ih}) \right] d\sigma \quad (26)$$

Now Fourier transforming

$$\begin{aligned} G_{ih}(\omega) &= \frac{1}{2\tau_{ih}} \frac{1}{\pi} \int_{-\infty}^{\infty} d\tau e^{-j\omega\tau} \int_{-\infty}^{\infty} d\sigma Q(\sigma) \left[u(\sigma - \tau + \tau_{ih}) - u(\sigma - \tau - \tau_{ih}) \right] \\ &= \frac{1}{2\pi\tau_{ih}} \int_{-\infty}^{\infty} d\sigma Q(\sigma) e^{-j\omega\sigma} \int_{-\infty}^{\infty} d\tau e^{-j\omega(\tau-\sigma)} \left[u(\sigma - \tau + \tau_{ih}) - u(\sigma - \tau - \tau_{ih}) \right] \\ &= \frac{1}{2\pi\tau_{ih}} \int_{-\infty}^{\infty} d\sigma Q(\sigma) e^{-j\omega\sigma} \int_{-\tau_{ih}}^{\tau_{ih}} dx e^{-j\omega x} \\ &= \frac{1}{\pi\tau_{ih}} \int_{-\infty}^{\infty} d\sigma Q(\sigma) e^{-j\omega\sigma} \left(\frac{\sin \omega\tau_{ih}}{\omega} \right) \end{aligned} \quad (27)$$

¹See Report No. 3, Eq. (60).

Hence

$$G_{ih}(\omega) = N(\omega) \frac{\sin \omega \tau_{ih}}{\omega \tau_{ih}} \quad (28)$$

Substitution of Eq. (28) into Eq. (22) yields

$$\frac{\Delta(\text{DC output})}{D(y_L)} = \frac{1}{2} \sqrt{\frac{T}{\pi}} M^2 \frac{\int_{-\infty}^{\infty} d\omega \left[\frac{S(\omega)}{N(\omega)} \right]^2}{\sqrt{\int_{-\infty}^{\infty} d\omega \left[\frac{S(\omega)}{N(\omega)} \right]^2 \left| \sum_{i=1}^M \sum_{j=1}^M \frac{\sin \omega \tau_{ih}}{\omega \tau_{ih}} \right|^2}} \quad (29)$$

A case of considerable practical interest, and one analyzed in some detail in Report No. 3, is that of signal and noise spectra sufficiently similar in shape over the frequency range containing most of the signal power so that one can write

$$\frac{S(\omega)}{N(\omega)} = \begin{cases} \frac{\mathcal{S}}{N} & \text{for } -\omega_0 \leq \omega \leq \omega_0 \\ 0 & \text{for } |\omega| > \omega_0 \end{cases} \quad (30)^1$$

\mathcal{S} and N are the total signal and noise power respectively. Substitution of Eq. (30) into Eq. (29) leads to the expression

$$\frac{\Delta(\text{DC output})}{D(y_L)} = \frac{1}{2} \sqrt{\frac{T}{\pi}} M^2 \frac{\mathcal{S}}{N} \frac{2\omega_0}{\sqrt{\int_{-\omega_0}^{\omega_0} d\omega \left| \sum_{i=1}^M \sum_{h=1}^M \frac{\sin \omega \tau_{ih}}{\omega \tau_{ih}} \right|^2}} \quad (31)$$

It is interesting to observe that actual spectra $S(\omega)$ and $N(\omega)$ are immaterial so long as their ratio remains constant.

¹An equivalent assumption is that $\frac{S(\omega)}{N(\omega)} = \frac{\mathcal{S}}{N}$ for all ω , but that only the frequency range $-\omega_0 \leq \omega \leq \omega_0$ is being processed.

III. Results for a Linear Array with Equally Spaced Elements

If the receiving array is linear and its elements are equally spaced, one can write

$$\tau_{ih} = |i - h| \tau_0 = |i - h| \frac{d}{c} \quad (32)$$

where d is the distance between adjacent hydrophones. The double sum in the denominator of Eq. (31) can now be reduced to a single sum.

$$\sum_{i=1}^M \sum_{h=1}^M \frac{\sin \omega \tau_{ih}}{\omega \tau_{ih}} = \sum_{i=1}^M \sum_{h=1}^M \frac{\sin |i - h| \omega \tau_0}{|i - h| \omega \tau_0} \quad (33)$$

With the change of variable $i - h = \ell$ this becomes

$$\sum_{i=1}^M \sum_{h=1}^M \frac{\sin \omega \tau_{ih}}{\omega \tau_{ih}} = M + 2 \sum_{\ell=1}^{M-1} (M - \ell) \frac{\sin \ell \omega \tau_0}{\ell \omega \tau_0} \quad (34)$$

Hence

$$\begin{aligned} \int_{-\omega_0}^{\omega_0} d\omega \left| \sum_{i=1}^M \sum_{h=1}^M \frac{\sin \omega \tau_{ih}}{\omega \tau_{ih}} \right|^2 &= \int_{-\omega_0}^{\omega_0} d\omega \left| M + 2 \sum_{\ell=1}^{M-1} (M - \ell) \frac{\sin \ell \omega \tau_0}{\ell \omega \tau_0} \right|^2 \\ &= 2 \omega_0^2 M^2 + 8M \sum_{\ell=1}^M (M - \ell) \int_0^{\omega_0} \frac{\sin \ell \omega \tau_0}{\ell \omega \tau_0} d\omega \\ &\quad + 4 \int_{-\omega_0}^{\omega_0} d\omega \sum_{\ell=1}^{M-1} \sum_{k=1}^{M-1} (M - \ell)(M - k) \frac{\sin \ell \omega \tau_0}{\ell \omega \tau_0} \frac{\sin k \omega \tau_0}{k \omega \tau_0} \end{aligned} \quad (35)$$

Substitution of Eq. (35) into Eq. (31) yields an exact expression for output signal to noise ratio which is, however, not very convenient from a computational point of view. The difficulty lies in the need to evaluate

the last integral of Eq. (35) between finite limits. Simple bounds on this integral can be set by observing that the integrand satisfies the inequality

$$0 \leq \sum_{\ell=1}^{M-1} \sum_{k=1}^{M-1} (M-\ell)(M-k) \frac{\sin \ell \omega \tau_0}{\ell \omega \tau_0} \frac{\sin k \omega \tau_0}{k \omega \tau_0} \leq \sum_{\ell=1}^{M-1} \sum_{k=1}^{M-1} \frac{M-\ell}{\ell \tau_0} \frac{M-k}{k \tau_0} \frac{1}{\omega^2} \quad (36)$$

Thus

$$\begin{aligned} 4 \int_{-\infty}^{\infty} d\omega \sum_{\ell=1}^{M-1} \sum_{k=1}^{M-1} (M-\ell)(M-k) \frac{\sin \ell \omega \tau_0}{\ell \omega \tau_0} \frac{\sin k \omega \tau_0}{k \omega \tau_0} &= 8 \int_{\omega_0}^{\infty} d\omega \sum_{\ell=1}^{M-1} \sum_{k=1}^{M-1} \frac{M-\ell}{\ell \tau_0} \frac{M-k}{k \tau_0} \frac{1}{\omega^2} \\ &\leq 4 \int_{-\omega_0}^{\omega_0} d\omega \sum_{\ell=1}^{M-1} \sum_{k=1}^{M-1} (M-\ell)(M-k) \frac{\sin \ell \omega \tau_0}{\ell \omega \tau_0} \frac{\sin k \omega \tau_0}{k \omega \tau_0} \\ &\leq 4 \int_{-\infty}^{\infty} d\omega \sum_{\ell=1}^{M-1} \sum_{k=1}^{M-1} (M-\ell)(M-k) \frac{\sin \ell \omega \tau_0}{\ell \omega \tau_0} \frac{\sin k \omega \tau_0}{k \omega \tau_0} \end{aligned} \quad (37)$$

Now

$$4 \int_{-\infty}^{\infty} d\omega \sum_{\ell=1}^{M-1} \sum_{k=1}^{M-1} (M-\ell)(M-k) \frac{\sin \ell \omega \tau_0}{\ell \omega \tau_0} \frac{\sin k \omega \tau_0}{k \omega \tau_0} = \frac{4\pi}{\tau_0^2} \sum_{\ell=1}^{M-1} \sum_{k=1}^{M-1} \frac{M-\ell}{\ell} \frac{M-k}{k} \min(\ell \tau_0, k \tau_0) \quad (38)^1$$

where $\min(\ell \tau_0, k \tau_0)$ denotes the smaller of the two numbers $\ell \tau_0$ and $k \tau_0$.

Simplifying further,

$$\frac{4\pi}{\tau_0^2} \sum_{\ell=1}^{M-1} \sum_{k=1}^{M-1} \frac{M-\ell}{\ell} \frac{M-k}{k} \min(\ell \tau_0, k \tau_0) = \frac{4\pi}{\tau_0} \sum_{\ell=1}^{M-1} \frac{(M-\ell)^2}{\ell} + \frac{8\pi}{\tau_0} \sum_{\ell=2}^{M-1} \sum_{k=1}^{\ell-1} \frac{(M-\ell)(M-k)}{\ell} \quad (39)$$

¹Bierens de Haan, Nouvelles Tables D'Intégrales Définies, Table 157, No. 1.

$$\begin{aligned}
8 \int_{\omega_0}^{\infty} d\omega \sum_{\ell=1}^{M-1} \sum_{k=1}^{M-1} \frac{M-\ell}{\ell \tau_0} \frac{M-k}{k \tau_0} \frac{1}{\omega^2} &= \frac{8}{\tau_0^2 \omega_0} \sum_{\ell=1}^{M-1} \sum_{k=1}^{M-1} \frac{M-\ell}{\ell} \frac{M-k}{k} \\
&= \frac{8}{\tau_0^2 \omega_0} \left(\sum_{\ell=1}^{M-1} \frac{M-\ell}{\ell} \right)^2
\end{aligned} \tag{40}$$

With substitution of Eqs. (39) and (40) into Eq. (37) one obtains

$$\begin{aligned}
\frac{4\pi}{\tau_0} \sum_{\ell=1}^{M-1} \frac{(M-\ell)^2}{\ell} + \frac{8\pi}{\tau_0} \sum_{\ell=2}^{M-1} \sum_{k=1}^{\ell-1} \frac{(M-\ell)(M-k)}{\ell} - \frac{8}{\tau_0} \frac{1}{\tau_0 \omega_0} \left[\sum_{\ell=1}^{M-1} \frac{M-\ell}{\ell} \right]^2 \\
\leq 4 \int_{-\omega_0}^{\omega_0} d\omega \sum_{\ell=1}^{M-1} \sum_{k=1}^{M-1} (M-\ell)(M-k) \frac{\sin \ell \omega \tau_0}{\ell \omega \tau_0} \frac{\sin k \omega \tau_0}{k \omega \tau_0} \\
\leq \frac{4\pi}{\tau_0} \sum_{\ell=1}^{M-1} \frac{(M-\ell)^2}{\ell} + \frac{8\pi}{\tau_0} \sum_{\ell=2}^{M-1} \sum_{k=1}^{\ell-1} \frac{(M-\ell)(M-k)}{\ell}
\end{aligned} \tag{41}$$

Finally, using Eqs. (41) and (35) in Eq. (31),

$$\begin{aligned}
\sqrt{\frac{T\omega_0}{2\pi}} M \frac{S}{N} \frac{1}{\sqrt{1 + \frac{4}{M\omega_0\tau_0} \sum_{\ell=1}^M \frac{M-\ell}{\ell} \text{Si}(\ell\omega_0\tau_0) + \frac{2\pi}{M^2} \frac{1}{\omega_0\tau_0} \sum_{\ell=1}^{M-1} \frac{(M-\ell)^2}{\ell} + \frac{4\pi}{M^2} \frac{1}{\omega_0\tau_0} \sum_{\ell=2}^{M-1} \sum_{k=1}^{\ell-1} \frac{(M-\ell)(M-k)}{\ell}}} \\
\leq \frac{\Delta(\text{DC output})}{D(y_1)} \leq
\end{aligned}$$

$$\begin{aligned}
\sqrt{\frac{T\omega_0}{2\pi}} M \frac{S}{N} \frac{1}{\sqrt{1 + \frac{4}{M\omega_0\tau_0} \sum_{\ell=1}^M \frac{M-\ell}{\ell} \text{Si}(\ell\omega_0\tau_0) + \frac{2\pi}{M^2} \frac{1}{\omega_0\tau_0} \sum_{\ell=1}^{M-1} \frac{(M-\ell)^2}{\ell} + \frac{4\pi}{M^2} \frac{1}{\omega_0\tau_0} \sum_{\ell=2}^{M-1} \sum_{k=1}^{\ell-1} \frac{(M-\ell)(M-k)}{\ell} \\
- \frac{4}{(\omega_0\tau_0)^2 M^2} \left[\sum_{\ell=1}^{M-1} \frac{M-\ell}{\ell} \right]^2}}
\end{aligned} \tag{L2}$$

The symbol $\text{Si}(x) = \int_0^x \frac{\sin y}{y} dy$ denotes the sine integral.

If $\omega_0 \tau_0 \rightarrow \infty$, i.e., the frequency range $0 \leq \omega \leq \omega_0$ processed by the detector is large compared to $\frac{1}{\tau_0}$, the upper and lower bounds converge towards each other and

$$\frac{\Delta(\text{DC output})}{D(y_4)} \rightarrow \sqrt{\frac{T\omega_0}{2\pi}} M \frac{S}{N} \quad (43)$$

Under the condition $\frac{S(\omega)}{N(\omega)} = \frac{S}{N}$, the output signal to noise ratio of a likelihood ratio detector is

$$\frac{\Delta(\text{DC output})}{D(\text{output})} = \sqrt{\frac{T}{2\pi}} \frac{S}{N} \sqrt{\int_0^{\omega_0} |G(\omega)|^2 d\omega} \quad (44)^1$$

$G(\omega)$, the array gain, approaches M for $\omega \gg \frac{1}{\tau_0}$. Hence for $\omega_0 \gg \frac{1}{\tau_0}$ the ratio of the output signal to noise ratios given by Eqs. (43) and (44) tends to unity. This is, of course, reasonable since there is virtually no noise correlation from hydrophone to hydrophone over most of the frequency range processed.

Fig. 2 shows a plot of the output signal to noise ratio (normalized with respect to $\sqrt{\frac{T\omega_0}{2\pi}} M \frac{S}{N}$) versus $\frac{\omega_0}{2\pi}$ for a five-element linear array with two-foot spacing between hydrophones. Even if $\frac{\omega_0}{2\pi}$, the upper limit of the frequency range being processed, is as low as 1000 cps the bounds of Eq. (42) coincide closely so that the curves accurately determine system performance. Also shown on the same figure is the output signal to noise ratio (again normalized with respect to $\sqrt{\frac{T\omega_0}{2\pi}} M \frac{S}{N}$) of a likelihood ratio detector using the same array of hydrophones. The oscillatory

¹See Report No. 3, Eq. (30).

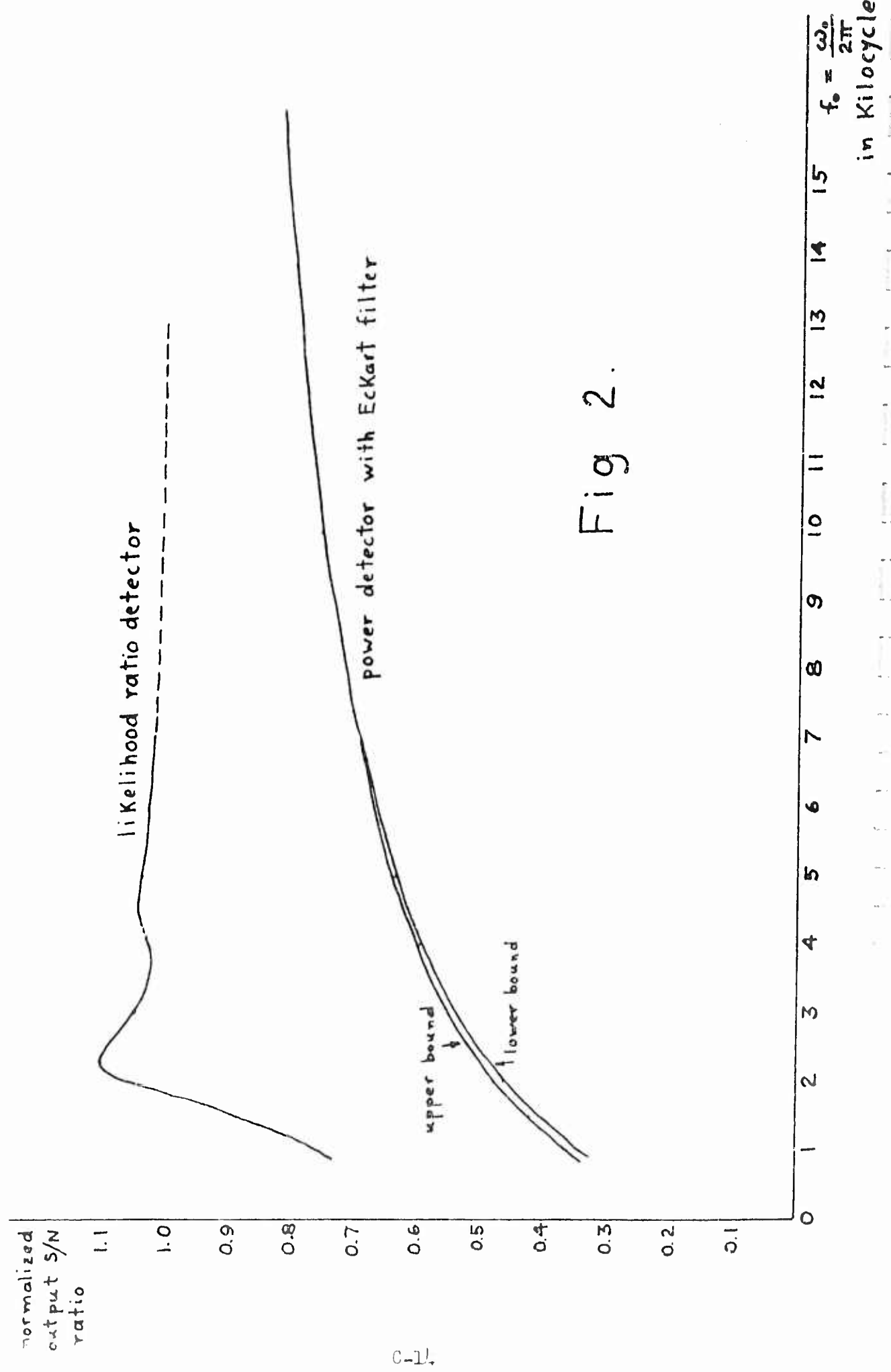


Fig 2.

behavior of this curve is due to very pronounced oscillation of the array gain $G(\omega)$ about the average value 5. From a practical point of view the most important conclusion to be drawn from Fig. 2 is that the output signal to noise ratio of the likelihood ratio detector does not exceed that of the power detector with Eckart filter by a factor significantly in excess of 2 if the processed frequency range extends beyond 1000 cps.

IV. Conclusions

This report compares the performance of a likelihood ratio detector with that of a power detector preceded by an Eckart filter. Signal and noise are assumed to be independent Gaussian random processes and the signal to noise ratio at each hydrophone of the receiving array is assumed to be small.

In the absence of noise correlation from hydrophone to hydrophone the likelihood ratio detector is shown to be formally equivalent to the power detector with Eckart filter. For the case of appreciable noise correlation between hydrophones, calculations are carried out under the following supplementary assumptions:

- 1) Signal and noise spectra satisfy $\frac{S(\omega)}{N(\omega)} = \frac{\bar{S}}{\bar{N}}$, a constant, over the frequency range processed by the detection system.
- 2) The receiving array is linear and has M equally spaced hydrophones.

Numerical results for a five-element array with 2-ft. spacing between hydrophones show that the output signal to noise ratio of the likelihood ratio detector exceeds that of the power detector with Eckart filter, but by a factor never significantly greater than 2 if the processed frequency range extends beyond 1000 cps. As the upper limit of the processed frequency range approaches infinity, the ratio of the performance figures (output signal to noise ratios) of the two instrumentations tends to unity.



LIKELIHOOD RATIO DETECTION OF GAUSSIAN SIGNALS
WITH NOISE VARYING FROM ELEMENT TO ELEMENT
OF THE RECEIVING ARRAY

by

Peter M. Schultheiss

Progress Report No. 11

General Dynamics/Electric Boat Research

(53-00-10-0231)

January 1964

DEPARTMENT OF ENGINEERING
AND APPLIED SCIENCE
YALE UNIVERSITY

I. Introduction

This report continues the study of the detection of weak directional signals in the presence of a very much stronger isotropic background noise. As in several earlier reports, both signal and noise will be taken as Gaussian random processes, but in contrast to most of the earlier work the noise level will be assumed to vary from hydrophone to hydrophone. The problem of variable noise levels was treated in Report No. 2 for the case of a power detector using clipped or unclipped data. It was shown that the performance of the system employing clipped data can be distinctly superior to that of a system using unclipped data when the variation of noise levels becomes sufficiently large. The purpose of the present investigation is to determine whether clipping is an efficient method for handling variations in noise levels or whether substantial improvements might be attainable through use of some more complicated procedure. Since the likelihood ratio detector is optimal under most reasonable performance criteria, it will (as in several earlier reports) be used as the standard of comparison.

The nature and degree of difficulty of the problem to be studied varies drastically with the assumptions concerning the variations in noise level from hydrophone to hydrophone. Of particular importance are two questions: 1) Does the noise level at each hydrophone remain essentially constant over the time interval T available for detection? 2) Can the noise level at each hydrophone be monitored continuously and therefore assumed to be known during the detection process?

In practice the time T is likely to be sufficiently small so that it is not unreasonable to regard the noise level at each hydrophone as fixed over T seconds. Furthermore, in all cases where a significant detection

problem exists, the signal to noise ratio at each hydrophone is small so that the total average received power differs only insignificantly from the average noise power. It should, in general, be possible to measure the average received power to a reasonable degree of accuracy in a time short compared to T . Hence the analytically simplest assumption, that the noise level at each hydrophone is known and remains fixed during the observation interval, appears to be quite realistic.

II. General Results

Under the assumptions stated above the analysis of the likelihood ratio detector given by Bryn¹ and extended in Report No. 3 requires only minor modifications. It is now no longer possible to work with the normalized noise correlation matrix Q_1 used in Report No. 3. However, if the same average signal power is received by each hydrophone, it is a simple matter to show that the output signal to noise ratio assumes the form of Eq. (1), an expression entirely analogous to that obtained in Report No. 3 [Eq. (25)].

$$\frac{\Delta(\text{DC output})}{D(\text{output})} = \sqrt{\sum_n \left\{ \text{Tr} [P_2(n) Q_2^{-1}(n)] \right\}^2} \quad (1)$$

Here $P_2(n)$ and $Q_2(n)$ are the matrices of unnormalized correlation coefficients of signal and noise respectively. In other words P_2 has the elements $\langle A_i(n) A_j(n) \rangle_S$ and Q_2 the elements $\langle A_i(n) A_j(n) \rangle_N$ where $\{A_i(n)\}$ is the set of Fourier cosine coefficients of the signal received by the i^{th} hydrophone (See Report No. 3, page 2).

¹F. Bryn, "Optimal Signal Processing of Three Dimensional Arrays Operating on Gaussian Signals and Noise," J.A.S.A. 34, No. 3, March 1962, pp. 289-297.

The computational problem is simplified greatly if one assumes negligible noise correlation from hydrophone to hydrophone. The effect of noise correlation on detector performance has been studied extensively in earlier reports, and there is no reason to expect the introduction of variable noise levels to alter the general conclusions drastically. The simplifying assumption is therefore made in order to focus attention on those aspects of the detection problem which depend strongly on the variations in noise level.

In the absence of noise correlation from hydrophone to hydrophone, the matrix $Q_2(n)$ is diagonal and may be written in the form

$$Q_2(n) = N(\omega_n) \Delta\omega \begin{bmatrix} N_1 & & 0 \\ & N_2 & \\ 0 & & \ddots \\ & & & N_M \end{bmatrix} \quad (2)$$

$N(\omega)$ is the normalized noise spectrum, so that $\int_0^\infty N(\omega) d\omega = 1$. N_i

stands for the average noise power received by the i^{th} hydrophone. If the array is steered on target, as will be assumed,

$$P_2(n) = \bar{S} S(\omega) \Delta\omega \begin{bmatrix} 1 & 1 & \dots & 1 \\ 1 & 1 & \dots & 1 \\ \vdots & & & \\ 1 & 1 & \dots & 1 \end{bmatrix} \quad (3)$$

$S(\omega)$ is the normalized signal spectrum, and \bar{S} stands for the average signal power at each hydrophone.

Equation (1) may now be rewritten as follows:

$$\frac{\Delta(\text{DC output})}{D(\text{output})} = \bar{S} \sqrt{\sum_n \left[\frac{S(\omega_n)}{N(\omega_n)} \sum_{i=1}^M \frac{1}{N_i} \right]^2} \quad (4)$$

If T is sufficiently large so that $S(\omega)$ and $N(\omega)$ are essentially constant over the frequency interval $\Delta\omega = \frac{2\pi}{T}$, Eq. (4) can be approximated by the integral [See Report No. 3, Eq. (29)]

$$\frac{\Delta(\text{DC output})}{D(\text{output})} = \sqrt{\frac{T}{2\pi}} \left[\sum_{i=1}^M \frac{S_i}{N_i} \right] \sqrt{\int_0^\infty \left[\frac{S(\omega)}{N(\omega)} \right]^2 d\omega} \quad (5)^1$$

Comparing with Report No. 3, Eq. (32), one sees that this expression is equal to the output signal to noise ratio of a likelihood ratio detector with input signal to noise ratio

$$\frac{S}{N} = \frac{1}{M} \sum_{i=1}^M \frac{S_i}{N_i} \quad (6)$$

at each hydrophone.²

With the same noise level at each hydrophone and no noise correlation from hydrophone to hydrophone, one finds that the likelihood ratio detector is formally equivalent to a simple power detector preceded by an Eckart filter [See Report No. 10, Eq. (24)]. With varying noise levels the equivalent instrumentation is a power detector with Eckart filter and adjustable gain k_i in each hydrophone circuit. A block diagram of the required instrumentation is shown in Fig. 1. The analysis of this circuit requires only a minor extension of the argument contained in Report No. 10. Thus y_2 is now given by

$$y_2(t) = \int_0^\infty d\tau w(\tau) \sum_{i=1}^M k_i x_i(t - \tau) \quad (7)$$

¹If only the frequency range $\omega_1 \leq \omega \leq \omega_2$ is processed by the detector the limits of integration become ω_1 and ω_2 .

²Note that in Report No. 3 the symbols $S(\omega)$ and $N(\omega)$ represent unnormalized spectra.

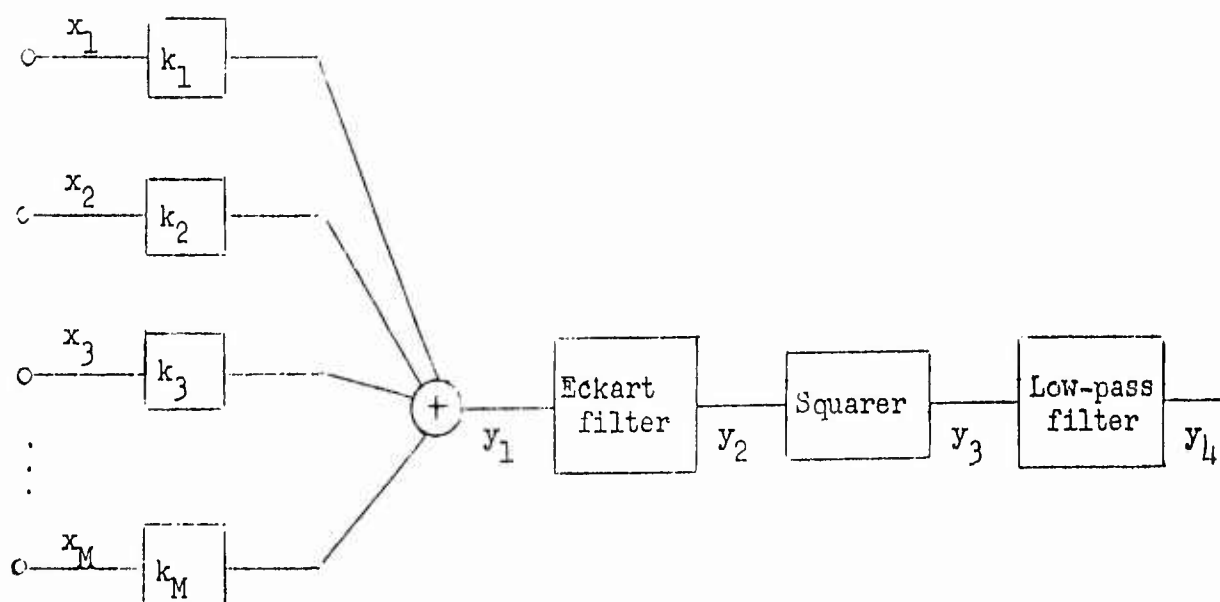


Fig. 1

This leads to

$$\Delta(\text{DC output}) = \frac{1}{2} \left[\sum_{i=1}^M k_i \right]^2 \mathcal{S} \int_{-\infty}^{\infty} d\omega S(\omega) |H(\omega)|^2 \quad (8)$$

and

$$D^2(y_4) = \frac{\pi}{T} \int_{-\infty}^{\infty} d\omega |H(\omega)|^4 \left| \sum_{i=1}^M \sum_{h=1}^M k_i k_h G_{ih}(\omega) \right|^2 \quad (9)$$

where $H(\omega)$ is the frequency response function of the Eckart filter and $G_{ih}(\omega)$ is the unnormalized cross-spectral density between the i^{th} and h^{th} hydrophones. [See Report No. 10, Eqs. (6) and (19).]

Hence the output signal to noise ratio is

$$\frac{\Delta(\text{DC output})}{D(y_4)} = \frac{\sqrt{T}}{2\sqrt{\pi}} \frac{\left[\sum_{i=1}^M k_i \right]^2 \mathcal{S} \int_{-\infty}^{\infty} d\omega S(\omega) |H(\omega)|^2}{\sqrt{\int_{-\infty}^{\infty} d\omega |H(\omega)|^4 \left| \sum_{i=1}^M \sum_{h=1}^M k_i k_h G_{ih}(\omega) \right|^2}} \quad (10)$$

The frequency response function of the Eckart filter satisfies the equation

$$|H(\omega)|^2 = \frac{S(\omega)}{N^2(\omega)} \quad (11)$$

Substituting Eq. (11) into Eq. (10) and recognizing that the integrands in numerator and denominator are even functions of ω

$$\frac{\Delta(\text{DC output})}{D(y_4)} = \sqrt{\frac{T}{2\pi}} \frac{\left[\sum_{i=1}^M k_i \right]^2 \int_0^\infty d\omega \left[\frac{S(\omega)}{N(\omega)} \right]^2}{\sqrt{\int_0^\infty d\omega \frac{S^2(\omega)}{N^4(\omega)} \left| \sum_{i=1}^M \sum_{h=1}^M k_i k_h G_{ih}(\omega) \right|^2}} \quad (12)$$

In the absence of noise correlation from hydrophone to hydrophone

$$G_{ih}(\omega) = \begin{cases} N_i N(\omega) & \text{for } h = i \\ 0 & \text{for } h \neq i \end{cases} \quad (13)$$

Hence

$$\begin{aligned} \frac{\Delta(\text{DC output})}{D(y_4)} &= \sqrt{\frac{T}{2\pi}} \frac{\left[\sum_{i=1}^M k_i \right]^2 \int_0^\infty d\omega \left[\frac{S(\omega)}{N(\omega)} \right]^2}{\sqrt{\int_0^\infty d\omega \left[\frac{S(\omega)}{N(\omega)} \right]^2 \left| \sum_{i=1}^M k_i^2 N_i \right|^2}} \\ &= \sqrt{\frac{T}{2\pi}} \frac{\left[\sum_{i=1}^M k_i \right]^2}{\sum_{i=1}^M k_i^2 N_i} \sqrt{\int_0^\infty d\omega \left[\frac{S(\omega)}{N(\omega)} \right]^2} \end{aligned} \quad (14)$$

Equation (14) is identical with Eq. (5) if

$$\frac{\left[\sum_{i=1}^M k_i \right]^2}{\sum_{i=1}^M k_i^2 N_i} = \sum_{i=1}^M \frac{1}{N_i} \quad (15)$$

Equation (15) is satisfied when

$$k_i = \frac{1}{N_i} \quad (16)$$

Thus the k_i in Fig. 1 are simply gain control circuits which discriminate against hydrophones with high noise level. The total average power out of the gain control k_i varies with $\frac{1}{N_i}$.

III. Comparison of Likelihood Ratio Detector and Clipped Power Detector

In Report No. 2 the performance of a power detector operating on clipped data is compared with that of a power detector operating on unclipped data. For ease in comparison with the earlier results it is therefore convenient to relate the performance figure of the likelihood ratio detector [Eq. (5)] to the equivalent figure of merit of an unclipped power detector.

With $G_{ih}(\omega)$ given by Eq. (13), $|H(\omega)| = 1$, and $k_i = 1$ for all i . Eq. (10) becomes

$$\frac{\Delta(\text{DC output})}{D(y_h)} = \sqrt{\frac{T}{2\pi}} M^2 \frac{\int_0^\infty d\omega S(\omega)}{\sqrt{\int_0^\infty d\omega N^2(\omega) \left| \sum_{i=1}^M N_i \right|^2}} = \sqrt{\frac{T}{2\pi}} M^2 \frac{S}{\sum_{i=1}^M N_i} \frac{1}{\sqrt{\int_0^\infty d\omega N^2(\omega)}} \quad (17)$$

Thus the ratio of Eq. (5) to Eq. (17), i.e., the ratio of the performance figure of the likelihood ratio detector to that of the unclipped power detector is

performance figure of likelihood ratio detector
performance figure of unclipped power detector

$$\frac{1}{M^2} \left(\sum_{i=1}^M N_i \right) \left(\sum_{i=1}^M \frac{1}{N_i} \right) \sqrt{\left[\int_0^\infty \left[\frac{S(\omega)}{N(\omega)} \right]^2 d\omega \right] \left[\int_0^\infty N^2(\omega) d\omega \right]} \quad (18)$$

When all of the N_i are equal Eq. (18) reduces to

$$\frac{\text{performance figure of likelihood ratio detector}}{\text{performance figure of unclipped power detector}} = \sqrt{\frac{\int_0^\infty \left[\frac{S(\omega)}{N(\omega)} \right]^2 d\omega}{\int_0^\infty N^2(\omega) d\omega}} \quad (19)$$

This gives the improvement attainable with likelihood ratio techniques in the absence of noise variations from hydrophone to hydrophone, a factor which has been discussed in several earlier reports.

The quantity of interest here is the dependence of Eq. (18) on the variation of N_i from hydrophone to hydrophone. It is given by

$$F = \frac{1}{M^2} \left(\sum_{i=1}^M N_i \right) \left(\sum_{i=1}^M \frac{1}{N_i} \right) = \frac{1}{M^2} \sum_{i=1}^M \sum_{j=1}^M \frac{N_i}{N_j} \quad (20)$$

For numerical computations it will be assumed that the average noise power at each hydrophone can assume just two values, a low value N_L and a higher value N_H . The probability that any given hydrophone has average noise power N_H is p and the noise power levels at different hydrophones are regarded as statistically independent.

If k of the hydrophones are in the high noise state

$$\sum_{i=1}^M \sum_{j=1}^M \frac{N_i}{N_j} = k^2 + (M-k)^2 + k(M-k) \left(\frac{N_H}{N_L} + \frac{N_L}{N_H} \right) \quad (21)$$

Hence R_1 , the expected value of F , assumes the form

$$R_1 = E(F) = \frac{1}{M^2} \sum_{k=0}^M \left[k^2 + (M-k)^2 + k(M-k) \left(\frac{N_H}{N_L} + \frac{N_L}{N_H} \right) \right] \frac{M!}{k! (M-k)!} p^k (1-p)^{M-k} \quad (22)$$

Figure 2 shows R_L as a function of N_H/N_L for $p = \frac{1}{2}$ and $M = 2, 5, 10$ and ∞ . Also shown is the improvement ratio R_c of a clipped power detector relative to an unclipped power detector, normalized to unity at $N_H/N_L = 1$. This curve was computed from Report No. 2, Eq. (34), with $p = \frac{1}{2}$ and $c = N_H/N_L$ (low input signal to noise ratio). In Report No. 2 it was assumed in effect that precisely pM hydrophones were in the high noise state (perhaps because of known spatial patterns of flow noise). This is equivalent to the assumption $M \rightarrow \infty$. Thus R_L rises somewhat more rapidly with N_H/N_L than the equivalent improvement ratio for the clipped power detector. However the ratio $\frac{R_L (M=\infty)}{R_c}$ is less than 2 over the entire range investigated. Therefore the gain to be made by going to a likelihood ratio detector is probably insufficient to justify replacement of the simple clippers with the more complicated gain control circuits demanded by the likelihood ratio detector.

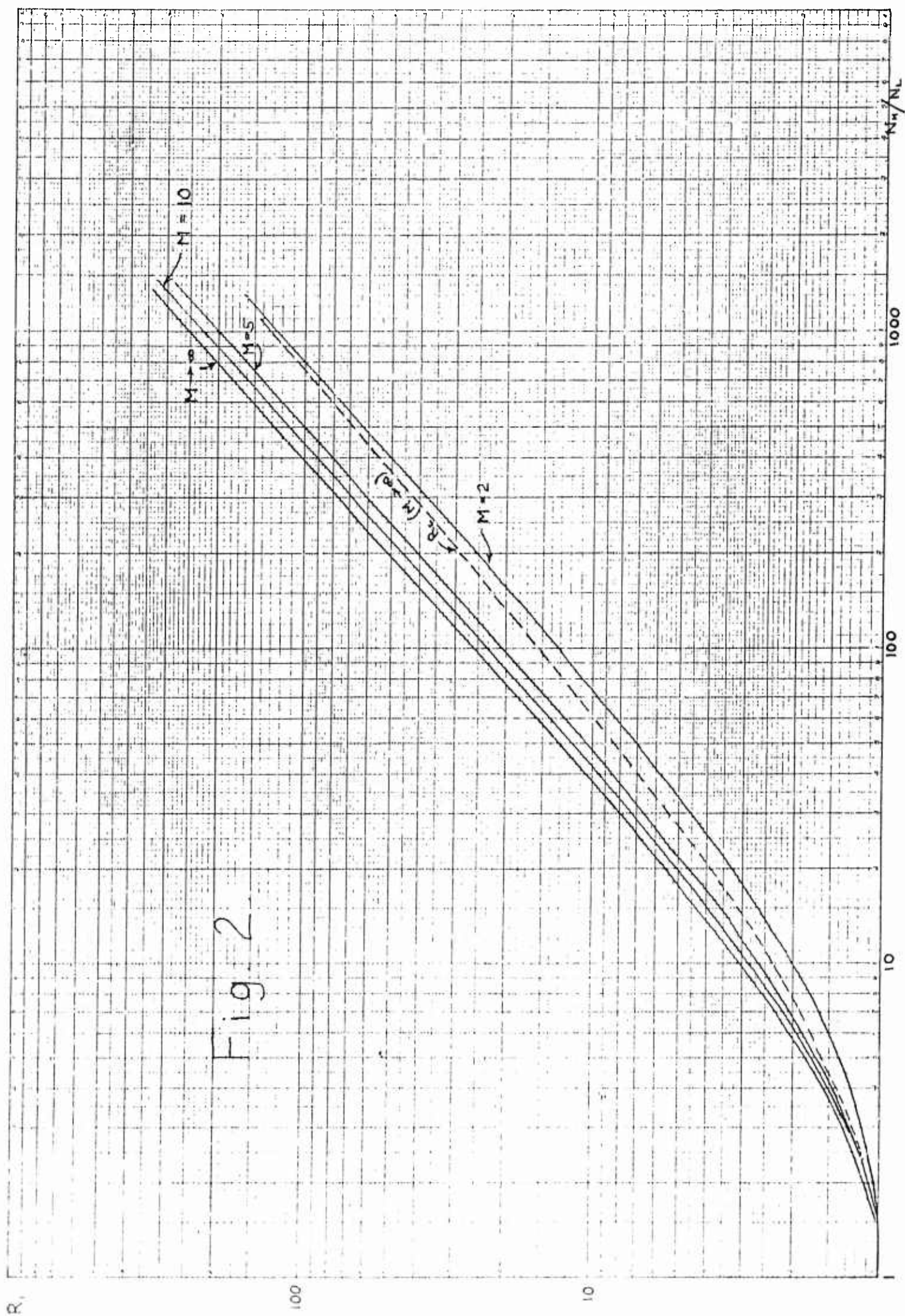
The improvement ratio R_L is the expected value of the ratio of the performance figures of the likelihood ratio and power detectors. An equally logical basis of comparison would be the ratio of the expected values of the performance figures. This leads to the definition

$$R_2 = \frac{1}{K} \frac{E(\text{performance figure of likelihood ratio detector})}{E(\text{performance figure of unclipped power detector})} \quad (23)$$

whereas R_L was defined by

$$R_L = \frac{1}{K} E \left\{ \frac{\text{performance figure of likelihood ratio detector}}{\text{performance figure of unclipped power detector}} \right\} \quad (24)$$

In both of these equations K is the improvement ratio for equal noise power at each hydrophone and is given by Eq. (19).



From Eqs. (5) and (17)

$$R_2 = \frac{E\left(\sum_{i=1}^M \frac{1}{N_i}\right)}{M^2 E\left(\frac{1}{\sum_{i=1}^M N_i}\right)} \quad (25)$$

With the same assumptions concerning the distribution of the N_i as were made in the computation of R_1 one obtains

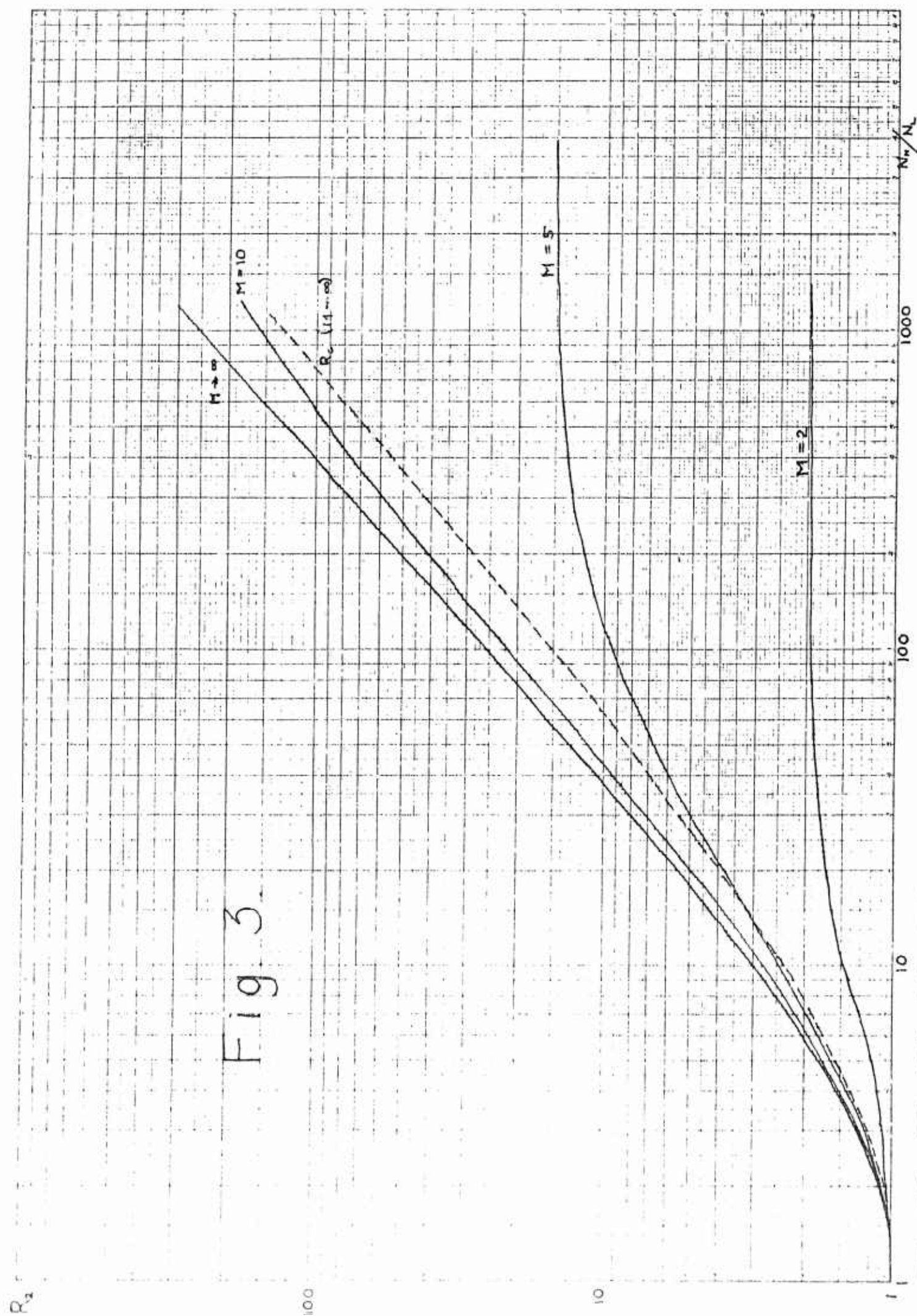
$$E\left(\sum_{i=1}^M \frac{1}{N_i}\right) = M E\left(\frac{1}{N_i}\right) = M\left(\frac{p}{N_H} + \frac{1-p}{N_L}\right) \quad (26)$$

and

$$E\left(\frac{1}{\sum_{i=1}^M N_i}\right) = \sum_{k=0}^M \frac{1}{k N_H + (M-k)N_L} \frac{M!}{k! (M-k)!} p^k (1-p)^{M-k} \quad (27)$$

Figure 3 shows R_2 plotted as a function of N_H/N_L for $p = \frac{1}{2}$ and $M = 2, 5, 10$ and ∞ . The curve for $M = \infty$ is, of course, identical with the corresponding curve of Fig. 2, so that the comparison with R_c remains unchanged. However, for finite M the various curves of Fig. 3 approach asymptotic values of 2^{M-1} for large N_H/N_L . This is due to the fact that there is a finite probability (2^{-M}) that all hydrophones will be in the low noise state. Hence $E\left(\frac{1}{\sum_{i=1}^M N_i}\right)$ approaches the finite constant $\frac{2^{-M}}{M N_L}$ as $N_H/N_L \rightarrow \infty$.

Report No. 2 considered a variety of possible distributions for N_i aside from the one analyzed thus far. Equivalent computations for the improvement ratio of the likelihood ratio detector (with $M \rightarrow \infty$) show



results entirely consistent with those given in Figs. 2 and 3. In each case investigated the improvement ratio of the likelihood ratio detector rises somewhat, but not drastically, faster with N_H/N_L than that of the clipped power detector. For example, if N_1 has the continuous probability density

$$f(N_1) = \begin{cases} \frac{1}{N_1} \left(\ln \frac{N_H}{N_L} \right)^{-1} & \text{for } N_L \leq N_1 \leq N_H \\ 0 & \text{elsewhere} \end{cases} \quad (28)$$

and if the various N_1 are statistically independent, one finds (for $M \rightarrow \infty$)

$$R_1 = R_2 = \frac{\left(\frac{N_H}{N_L} - 1 \right)^2}{\frac{N_H}{N_L} \left(\ln \frac{N_H}{N_L} \right)^2} \quad (29)$$

The improvement ratio for the clipped power detector is [from Report No. 2, Eq. (25)]

$$R_c = 4 \frac{\left(\sqrt{\frac{N_H}{N_L}} - 1 \right)^2 \left(\frac{N_H}{N_L} - 1 \right)}{\frac{N_H}{N_L} \left(\ln \frac{N_H}{N_L} \right)^3} \quad (30)$$

Thus for large N_H/N_L

$$\frac{R_1}{R_c} = \frac{R_2}{R_c} \approx \frac{1}{4} \ln \frac{N_H}{N_L} \quad (31)$$

Hence

$$\frac{R_1}{R_c} \approx 1.73 \quad \text{for } \frac{N_H}{N_L} = 1000$$

IV. Conclusions

This report analyzes the effectiveness of likelihood ratio techniques for the detection of weak directional Gaussian signals in isotropic Gaussian noise when the average noise power varies from hydrophone to hydrophone. The following basic assumptions are made:

- 1) The noise disturbances received by different hydrophones are uncorrelated.
- 2) The average noise power at each hydrophone can be measured in a time short compared to the time T available for detection.
- 3) The average noise power at each hydrophone remains fixed during the observation time T .
- 4) The average noise powers at different hydrophones are statistically independent.

Under these conditions the likelihood ratio detector reduces to a power detector with Eckart filter incorporating in each hydrophone circuit a gain control that varies the gain of the channel inversely with the noise power received by the corresponding hydrophone.

The performance index (output signal to noise ratio) of the likelihood ratio detector is better than that of the clipped power detector under all conditions, but the relative advantage increases only slowly with increases in the variation of noise from hydrophone to hydrophone. Thus one comes to the conclusion that clipping, while not an optimal procedure, is quite efficient in combating the effects of noise variation from hydrophone to hydrophone. The gains to be made by the use of likelihood ratio techniques are relatively small in all cases investigated.



MINIMUM VARIANCE ESTIMATION OF RELATIVE DELAY
BETWEEN TWO RANDOM SIGNALS IN NOISE

by

Richard A. McDonald

Progress Report No. 12

General Dynamics/Electric Boat Research
(53-00-10-0231)

March 1964

DEPARTMENT OF ENGINEERING
AND APPLIED SCIENCE
YALE UNIVERSITY

I. Introduction

As implied in the title, a signal is received in two channels, and the problem is to estimate relative delay between the two received versions. This estimate of delay is wanted in order to determine the bearing of a point source generating the signal at some distance away in the transmission medium.

It is assumed that the signal generated by the source is random in nature, and for simplicity in the following work, it is also necessary to assume that the signal process is stationary Gaussian bandlimited white noise. It will further be assumed that the signal in each channel is corrupted by independent stationary Gaussian bandlimited white noise. Figure 1 is a sketch of the system being studied.

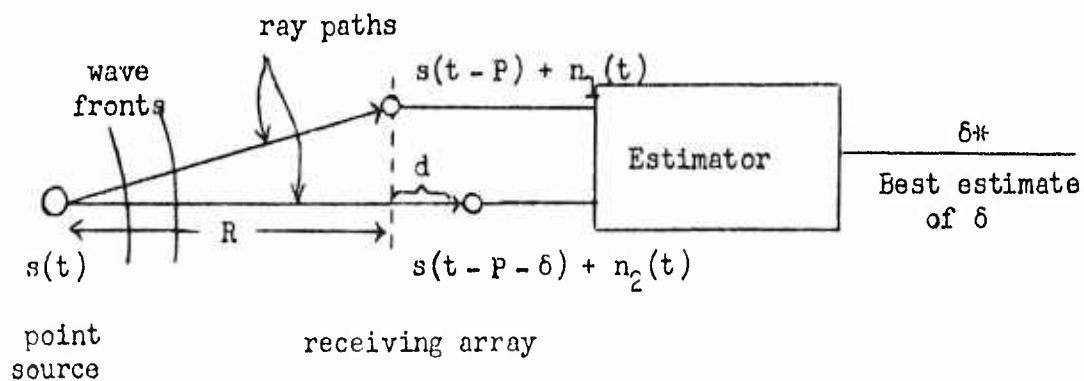


Figure 1 Receiving, Estimating System

The relative delay $\delta = \frac{d}{c}$ is the time required for the signal to travel the additional distance d in the medium. The delay P is the gross travel time of the signal to the array and will not enter into

further discussions. Difference in attenuation of the signal before entering the two channels is neglected. However, different noise levels in the two channels are assumed. The choice of bandlimited white signal and noise means that frequency dependence of attenuation has been neglected. This assumption will be poor at large bandwidths or long range of transmission. Usually a random component of delay and a non-stationary signal level are present in systems of this sort due to inhomogeneities of the transmission medium, multipath, etc. However, these are neglected in the present analysis. Some discussion of these effects will appear in a final section of this report. Also in the final section will appear further discussion of the other assumptions.

II. Notation and Model

It is assumed that the signal and noise are observed in each channel over the period of time T . The time origin will be chosen so as to neglect the gross delay P indicated in Fig. 1. Then we write for the signal in the two channels

$$\begin{aligned} x(t) &= s(t) + n_1(t) \\ y(t) &= s(t - \delta) + n_2(t) \end{aligned} \tag{1}$$

Under our assumptions, $x(t)$ and $y(t)$ are each completely characterized over a long interval T by $2TW$ samples taken at intervals of $\frac{1}{2W}$ seconds. Here W is the bandwidth in cycles per second. We make the definitions

$$\begin{aligned} x_1 &= x \left(\frac{1}{2W} \right) \\ y_1 &= y \left(\frac{1}{2W} \right) \end{aligned} \tag{2}$$

The data available to the estimator is then the two row vectors x and y or the composite vector $\ell = (x, y)$ where

$$\begin{aligned} x &= (x_1, x_2, \dots, x_{2TW}) \\ y &= (y_1, y_2, \dots, y_{2TW}) \end{aligned} \quad (3)$$

A well-known theorem¹ from the theory of estimation sets a lower bound on the variance of an estimate of the parameter of a distribution when a sample from a process with that distribution is available. We shall formulate our problem in this vein. Subsequent discussion will show that certain realizable estimation schemes attain this limiting performance. Under the assumptions, all the statistical parameters of the joint distribution of the components of ℓ are known except the relative delay which is to be estimated. We write the joint probability density as $P(\ell; k)$ where ℓ is the previously defined vector, and k is defined such that

$$\frac{k}{2W} = \delta \quad (4)$$

The best estimate of the normalized variable k is denoted k^* and the theorem states that

$$E \left\{ (k^* - k)^2 \right\} \geq \frac{1}{E \left\{ \left(\frac{\partial}{\partial k} [\log P(\ell; k)] \right)^2 \right\}} \quad (5)$$

¹See H. Cramér, Mathematical Methods of Statistics, Princeton University Press, 1946. The material is discussed in chapter 32 and following.

The theorem is valid for unbiased estimates, i.e., estimates such that $E\{k^* \} = k$, and for regular estimation, i.e., for distribution functions which do not have discontinuities as functions of k . These conditions apply to the present case.

In the section which follows, the Gaussian probability function $P(\ell; k)$ will be written down and the operations indicated in Eq. (5) will be carried out. In the end the normalization to the variable k will be reversed so that the error will be stated in more familiar terms.

III. Minimum Variance of Estimate of Relative Delay

The Gaussian probability function $P(\ell; k)$ is easily written in general form.

$$P(\ell; k) = \frac{1}{(2\pi)^n |M_k|^{1/2}} \exp \left\{ -\frac{1}{2} \ell M_k^{-1} \ell^T \right\} \quad (6)$$

Here $n = 2TW$ is used for convenience, and the covariance matrix M_k is defined below.

$$M_k = \begin{bmatrix} a_{11} & a_{12} & \dots & a_{1n} & b_{11} & b_{12} & \dots & b_{1n} \\ a_{21} & a_{22} & \dots & & b_{21} & b_{22} & \dots & \\ \vdots & \vdots & \vdots & & \vdots & \vdots & \vdots & \\ a_{n1} & & & a_{nn} & b_{n1} & & & b_{nn} \\ \hline b_{11} & b_{21} & \dots & b_{n1} & c_{11} & c_{12} & \dots & c_{1n} \\ b_{12} & b_{22} & \dots & & c_{21} & c_{22} & \dots & \\ \vdots & \vdots & \vdots & & \vdots & \vdots & \vdots & \\ b_{1n} & & & b_{nn} & c_{n1} & & & c_{nn} \end{bmatrix} \quad (7)$$

$$\left. \begin{aligned} a_{ii} &= S + N_1 \\ c_{ii} &= S + N_2 \end{aligned} \right\} \quad \text{all } i \quad (8)$$

$$a_{ij} = c_{ij} = 0 \quad \text{all } i \neq j$$

$$\begin{aligned} b_{ij} &= E \left\{ x_i y_j \right\} = E \left\{ s \left(\frac{i}{2W} \right) s \left(\frac{j-k}{2W} \right) \right\} \\ &= S \frac{\sin [\pi(j-k-i)]}{\pi(j-k-i)} \end{aligned} \quad (9)$$

Note that only in the elements b_{ij} does the functional dependence of P upon k appear.

We proceed by carrying out the operations of $P(\ell; k)$ indicated in Eq. (5). First,

$$\log P(\ell; k) = -n \log 2\pi - \frac{1}{2} \log |M_k| - \frac{1}{2} \ell M_k^{-1} \ell' \quad (10)$$

The next step, that of differentiation, is tedious and so the details are relegated to an appendix. It is convenient to evaluate the derivative only at integral values of k . In fact, further attention will be concentrated only on the case $k = 0$, although other integral values are possible. Later discussion will show that this is not a serious restriction.

As shown in the appendix,

$$\left. \frac{\partial}{\partial k} \log P(\ell; k) \right|_{k=0} = -y m x' \quad (11)$$

where

$$m = \begin{bmatrix} 0 & \frac{S}{B} & -\frac{S}{2B} & \frac{S}{3B} & \dots \\ -\frac{S}{B} & 0 & \frac{S}{B} & \frac{S}{2B} & \dots \\ \frac{S}{2B} & & & & \\ \vdots & & & & \\ \vdots & & & & \end{bmatrix} \quad (12)$$

and

$$B = (S + N_1)(S + N_2) - S^2 \quad (13)$$

Now, it is necessary to compute $E \left\{ (y m x')^2 \right\}$ in order to substitute into Eq. (5). The product $y m x'$ is a summation of $n^2 - n$ terms, each one a product of the form

$$+ \frac{x_i y_j}{|(i-j)|B}, \quad i \neq j.$$

The square of $y m x'$ is a summation with $(n^2 - n)^2$ terms consisting of each term in $y m x'$ times itself and every other term. If the expectation of the sum is taken term by term, each may be expanded according to the following principle.²

$$E \left\{ (x_i y_j)(x_h y_\ell) \right\} = \underbrace{E \left\{ x_i y_j \right\}}_{(1)} \underbrace{E \left\{ x_h y_\ell \right\}}_{(2)} + \underbrace{E \left\{ x_i x_h \right\}}_{(2)} \underbrace{E \left\{ y_j y_\ell \right\}}_{(2)} + \underbrace{E \left\{ x_i y_\ell \right\}}_{(3)} \underbrace{E \left\{ x_h y_j \right\}}_{(3)} \quad (14)$$

²See Davenport and Root, Random Signals and Noise, McGraw-Hill, 1958, § 8.7.

Under the assumptions of the problem, and with $k = 0$, all the expectations of two-fold products shown in Eq. (14) are zero unless the indices of the two variables are the same. For equal indices we have

$$\begin{aligned} E\{x_i^2\} &= S + N_1 \\ E\{y_i^2\} &= S + N_2 \\ E\{x_i y_i\} &= S \end{aligned} \tag{15}$$

Because the diagonal terms of m are all zero [See Eq. (12)], terms of type ① in Eq. (14) do not contribute to $E\{(y m x')^2\}$. Terms of type ② contribute only if $i = h$ and $j = l$, or in other words, for products of terms of $y m x'$ with themselves. Terms of type ③ will contribute only if $i = l$ and $h = j$, or in other words, for products of terms of $y m x'$ with symmetrical positions about the major diagonal. We shall carry through one sample set of terms. Let us consider the expectation of the products of the term from $y m x'$ corresponding to the first non-zero element in the first row of m , with itself and with its diagonally symmetric term. The self term contributes $(S + N_1)(S + N_2) S^2/B^2$ and the cross product contributes $- S^4/B^2$. The net contribution is S^2/B . For terms further from the diagonal, a factor $(i - j)^2$ appears in the denominator. The net contributions of all self and cross products may then be arranged into a matrix for convenience. This gives

$$E\{(y_{mx'})^2\} = \frac{S^2}{(S+N_1)(S+N_2) - S^2} \mathcal{S} \left\{ \begin{bmatrix} 0 & 1 & \frac{1}{4} & \frac{1}{9} & \dots \\ 1 & 0 & 1 & \frac{1}{4} & \dots \\ \frac{1}{4} & 1 & 0 & 1 & \dots \\ \vdots & & & & \end{bmatrix} \right\} \quad (16)$$

The factor $S^2 / [(S+N_1)(S+N_2) - S^2]$ is common to all the terms, and the operation $\mathcal{S}\{\}$ has been invented for convenience to indicate the sum of all elements of a matrix.

The summation is finite because the matrix is $n \times n$. We may write the summation in the form

$$\left[2(n-1) + \frac{2(n-2)}{4} + \frac{2(n-3)}{9} + \dots + \frac{2}{(n-1)^2} \right]$$

This may be manipulated to obtain

$$2n \left[1 + \frac{1}{4} + \frac{1}{9} + \dots + \frac{1}{(n-1)^2} \right] - 2 \left[1 + \frac{1}{2} + \frac{1}{3} + \dots + \frac{1}{n-1} \right]$$

The bracketed series in the first term converges³ for large n to $\pi^2/6$.

The bracketed series in the second term diverges⁴ but may be approximated for large n by $\log(n-1) + \gamma$, where $\gamma \simeq .5772$ is Euler's constant.

Hence we write

³See Pierce, A Short Table of Integrals, fourth ed., Ginn and Co., 1956, No. 832.

⁴See Pierce, No. 794.

$$E\left\{(y_{mx'})\right\} \approx \frac{2 S^2}{(S + N_1)(S + N_2) - S^2} \left[n \frac{\pi^2}{6} - \log(n-1) - .5772 \right] \quad (17)$$

for large n . Obviously if n is large enough only the first term in the bracket need be kept.

Now, substitution into Eq. (5) yields

$$E\left\{(k^* - k)^2\right\} \geq \frac{(S + N_1)(S + N_2) - S^2}{2 S^2} \cdot \frac{1}{n \frac{\pi^2}{6} - \log(n-1) - .5772} \quad (18)$$

Substitution of $n = 2WT$ and $\delta = \frac{k}{2W}$ yields minimum estimation error

for time delay δ in terms of observation time T and bandwidth W . We have

$$E\left\{(\delta^* - \delta)^2\right\} \geq \frac{(S + N_1)(S + N_2) - S^2}{S^2} \cdot \frac{1}{8W^2} \cdot \frac{1}{\frac{WT\pi^2}{3} - \log(2WT-1) - .5772} \quad (19)$$

If the usual assumptions of $WT \gg 1$ and $\frac{S}{N_1}$ or $\frac{S}{N_2} \ll 1$ are made, the expression may be simplified considerably. Then we have

$$E\left\{(\delta^* - \delta)^2\right\} \geq \frac{N_1 N_2}{S^2} \cdot \frac{3}{8\pi^2} \cdot \frac{1}{W^2} \cdot \frac{1}{WT} \quad (20)$$

Corresponding to the restriction $k = 0$, there is for Eq. (20) the restriction $\delta = 0$. However, this is not a serious restriction because the equivalent situation is attainable by insertion of a known amount c delay into $x(t)$, or altering the time origin of the $x(t)$ samples.

Since the result given by Eq. (20) is supposed to be an absolute minimum for the error, it is useful to compare it with results obtained

elsewhere. In Progress Report No. 9, T. Usher, Jr., has an equation for minimum bearing error for a split beam system. To make a comparison, we use his Eq. (52). To put his result into the same terms as ours, we make the following substitutions or changes:

- 1) We have two hydrophones. Set $M = 1$.
- 2) Multiply by $\frac{c}{d}$ to convert to time delay error.
- 3) Square expression to get mean squared error.
- 4) Set bandwidth ω_L of averager equal to $\frac{\pi}{T}$. This is obtained by assuming that the averaging filter of the split beam system has a weighting function which is constant for an interval T and zero elsewhere.
- 5) Set $g_s(\omega)/g_n(\omega) = 1$, $0 \leq \omega \leq 2\pi W$; zero elsewhere. This conforms to our assumption of bandlimited white signal and noise.
- 6) Let $N_1 = N_2 = N$ in Eq. (20).

When all of these changes are made, the two expressions are equal.

IV. Maximum Likelihood Estimator

If the minimum estimation error given by the statistical theory is attainable, it can be attained by the method of maximum likelihood.⁵ To estimate by the method of maximum likelihood, it is necessary to solve the equation

$$\frac{\partial}{\partial k} \log P(\ell; k) = 0 \quad (21)$$

for the value of k as a function of the value of the sample vector. Unfortunately, it has not been possible to perform the differentiation indicated in Eq. (21) continuously as a function of k . Since the differentiation has been performed for $k = 0$, it is clear that a

⁵H. Cramér, op. cit., Chapter 33.

nearly equivalent method of estimation is to "steer" the array either physically or by insertion of time delay until the time delay is zero. This may be detected when the value of $\dot{y}m x' = 0$. Then by Eqs. (11) and (21), the maximum likelihood estimate of the additional delay is zero. However, since this is not strictly the maximum likelihood solution sought, it is necessary to evaluate the error of this method of estimation. A brief investigation has shown that evaluation of this error is tedious, and involves finding the distribution of zero crossings of a random process.

Since it has already been shown that another estimation method is as good as the method of maximum likelihood could be, it is not necessary to go into the details of the analysis here.

V. Conclusions

The foregoing results show that the ideal system in the sense of our assumptions has an optimum performance specified by Eq. (20). Furthermore, under the same set of conditions, realizable schemes such as the split beam system attain the same optimum performance. Although this is comforting, it leaves unanswered the question of performance under other conditions. The realizable schemes have been evaluated under other conditions. For instance, the split beam system has been extensively analyzed in Progress Report No. 9. However, it is not known how this performance compares with the optimum attainable under the same conditions. It is proposed to discuss the assumptions made in this report and to suggest ways in which the analysis could be made more general.

To begin with, the assumption of bandlimited Gaussian white signal and noise is quite restrictive. Unfortunately, the entire analysis

works because of this set of assumptions. The band-limitation allows sampling, thus reducing the data to a sequence of numbers. The Gaussian, white assumption gives the probability density function very simple properties. The one hope of improving upon this assumption is to sample in the frequency domain instead of in the time domain. However, this will make the statistical properties a much more complicated function of time delay.

Another assumption has been made that the signal level is stationary. However, it is often observed that received signal strength varies as a function of time, although usually at frequencies which are very low compared to the system bandwidth. One possible representation of this situation is multiplicative noise. That is, we write

$$\begin{aligned} x(t) &= a(t) s(t) + n_1(t) \\ y(t) &= b(t - \delta) s(t - \delta) + n_2(t) \end{aligned} \tag{22}$$

where $a(t) \geq 0$, $b(t) \geq 0$ are slowly varying random processes, independent of $s(t)$, $n_1(t)$ and $n_2(t)$. It is helpful to assume $E\{a^2(t)\} = 1$, $E\{b^2(t)\} = 1$, so that the average signal to noise ratios are still S/N_1 and S/N_2 . It can be shown that if $s(t)$ is Gaussian white noise, still the product $a(t) s(t)$ or $b(t) s(t)$ will not in general be either Gaussian or white. However, as long as the signal to noise ratios are very small compared to unity, then $x(t)$ and $y(t)$ may still be assumed Gaussian white. Then the rest of the analysis will carry through in a simple fashion, with the only change appearing

in the values of the coefficients b_{ij} given in Eq. (9). It is clear that

$$b_{ij} = E\left\{x_i y_j\right\} = E\left\{s\left(\frac{i}{2W}\right) s\left(\frac{j-k}{2W}\right)\right\} E\left\{a\left(\frac{i}{2W}\right) b\left(\frac{j-k}{2W}\right)\right\}$$

$$= S \frac{\sin[\pi(j-k-i)]}{\pi(j-k-i)} R_{ab}\left(\frac{j-k-i}{2W}\right) \quad (23)$$

Note that the values of b_{ij} are still zero for $k = 0, 1, 2, \dots$ if $j-k-i \neq 0$. This is then easily carried through. It is obvious that the only change this will make in the result is the values of the coefficients in the matrix m . These may be readily calculated with any particular choice for the function R_{ab} .

Another empirically observed phenomenon which has been neglected is the random component of time delay which is often present. To the extent that this time delay is identical in both channels, it introduces no error whatsoever. However, if there is lack of complete correlation between the time delay in the two channels, errors will result. If this delay is slowly varying to the extent that it remains nearly fixed over the observation period T , then the error in delay must be added directly to whatever random errors are generated in the estimation system. Hence this may be accounted for without disturbing the analysis. Should higher frequency components of random time delay occur, they will affect the result by reducing the value of $E\left\{s\left(\frac{i}{2W}\right) s\left(\frac{j-k}{2W}\right)\right\}$ used to compute b_{ij} in Eq. (9). This will have an effect equivalent to reduced input signal to noise ratio.

Finally it has been assumed that the complete time waveforms of $x(t)$ and $y(t)$ are available to the estimator. In practice this

information is usually clipped and sampled before being presented to the estimator. Under our assumptions the sampling produces no loss of information. However, if used in combination with the clipping, considerable information is thrown away. It would be very helpful to carry out an analysis similar to the one above but using only the sampled clipped information. Then the loss of information could be evaluated in terms of increase in minimum estimation error, and the performance of practical systems under these circumstances could also be evaluated to obtain a realistic figure of merit.

The main problem in performing the analysis for clipped sampled information is to write the joint probability density function for the clipped samples in a general form such that the differentiation, etc., may be easily performed.

Appendix Differentiation of $\log P(\ell; k)$ with respect to k

From eq. (10) we have

$$\log P(\ell; k) = - 2TW \log 2\pi - \frac{1}{2} \log |M_k| - \frac{1}{2} \ell M_k^{-1} \ell' \quad (A-1)$$

①

②

③

The terms are labeled ①, ②, and ③ and will be considered separately.

Term ① is independent of k ; hence its derivative is zero. It will be shown that the derivative of ② is zero for integral values of k .

First we note that M_k is considerably simplified for integral k .

Denote integral k by $k = K$, and M_K may be written

$$M_K = \begin{bmatrix} \begin{array}{cccc} S+N_1 & 0 & 0 & \dots & 0 \\ 0 & S+N_1 & & & \\ 0 & & S+N_1 & & \\ \vdots & & & \ddots & \\ 0 & & & & S+N_1 \end{array} & \begin{array}{c} \overbrace{0 \dots 0}^{K \text{ columns}} \\ 0 \dots 0 \quad S \quad 0 \dots 0 \\ 0 \dots 0 \quad 0 \quad S \dots 0 \\ \vdots \\ 0 \quad \quad \quad 0 \quad S \\ \vdots \\ 0 \quad \quad \quad 0 \quad 0 \\ \vdots \\ 0 \quad \quad \quad 0 \quad 0 \end{array} \\ \begin{array}{c} \underbrace{0 \dots 0}_{K \text{ rows}} \\ \vdots \\ 0 \dots 0 \\ S \quad 0 \\ \vdots \\ 0 \dots S \quad 0 \quad 0 \dots 0 \\ 0 \dots 0 \quad S \quad 0 \dots 0 \end{array} & \begin{array}{c} S+N_2 \quad 0 \quad 0 \quad 0 \\ 0 \quad S+N_2 \quad 0 \quad 0 \\ 0 \quad 0 \quad S+N_2 \quad 0 \\ \vdots \\ \vdots \\ 0 \quad \quad \quad \quad S+N_2 \end{array} \end{bmatrix} \quad (A-2)$$

A similar picture applies for negative integers K except that the minor non-zero diagonals are shifted in the opposite direction. Now suppose K is changed incrementally to $k = K + \Delta k$. If all but the linear terms in k are neglected, $M_{K+\Delta k}$ can be written approximately

$$M_{K+\Delta k} \approx \begin{bmatrix} \begin{array}{ccc} S+N_1 & 0 & \\ 0 & \swarrow \searrow & \\ & \swarrow \searrow & \\ & & 0 \end{array} & \begin{array}{ccccc} \frac{S\Delta k}{2} & -S\Delta k & S & S\Delta k & -\frac{S\Delta k}{2} \\ & \swarrow \searrow & \swarrow \searrow & \swarrow \searrow & \swarrow \searrow \\ & & \swarrow \searrow & \swarrow \searrow & \swarrow \searrow \\ & & & \swarrow \searrow & \swarrow \searrow \\ & & & & -\frac{S\Delta k}{2} \\ & & & & S\Delta k \\ & & & & S \\ & & & & -S\Delta k \\ & & & & \frac{S\Delta k}{2} \end{array} \\ \hline \begin{array}{ccccc} \frac{S\Delta k}{2} & -S\Delta k & S & S\Delta k & -\frac{S\Delta k}{2} \\ & \swarrow \searrow & \swarrow \searrow & \swarrow \searrow & \swarrow \searrow \\ & & \swarrow \searrow & \swarrow \searrow & \swarrow \searrow \\ & & & \swarrow \searrow & \swarrow \searrow \\ & & & & -\frac{S\Delta k}{2} \\ & & & & S\Delta k \\ & & & & S \\ & & & & -S\Delta k \\ & & & & \frac{S\Delta k}{2} \end{array} & \begin{array}{ccc} S+N_2 & 0 & \\ 0 & \swarrow \searrow & \\ & \swarrow \searrow & \\ & & 0 \end{array} \end{bmatrix}$$

(A-3)

Then the derivative is evaluated by means of the definition.

$$\frac{\partial}{\partial k} \left| M_k \right| \Big|_{k=K} = \lim_{\Delta k \rightarrow 0} \frac{|M_{K+\Delta k}| - |M_K|}{\Delta k} \quad (A-4)$$

For this a general evaluation of $|M_K|$ as well as $|M_{K+\Delta k}|$ is required.

We begin with $|M_K|$ for $K = 0$. Note the following:

1)

$$\begin{vmatrix} S+N_1 & S \\ S & S+N_2 \end{vmatrix} = (S+N_1)(S+N_2) - S^2$$

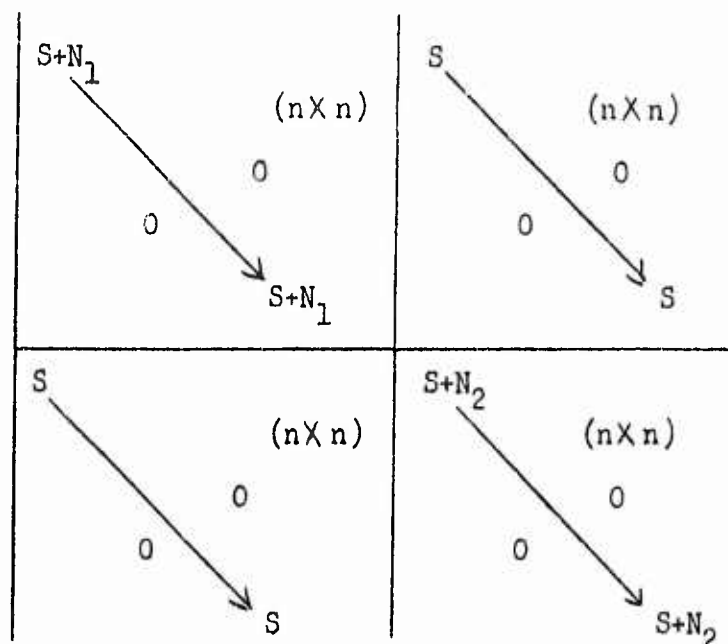
2)

$$\begin{vmatrix} S+N_1 & 0 & S & 0 \\ 0 & S+N_1 & 0 & S \\ S & 0 & S+N_2 & 0 \\ 0 & S & 0 & S+N_2 \end{vmatrix} = (S+N_1) \begin{vmatrix} S+N_1 & 0 & S \\ 0 & S+N_2 & 0 \\ S & 0 & S+N_2 \end{vmatrix} + S \begin{vmatrix} 0 & S & 0 \\ S+N_1 & 0 & S \\ S & 0 & S+N_2 \end{vmatrix}$$

$$= (S+N_1)(S+N_2) \begin{vmatrix} S+N_1 & S \\ S & S+N_2 \end{vmatrix} - S^2 \begin{vmatrix} S+N_1 & S \\ S & S+N_2 \end{vmatrix}$$

$$= \left[(S+N_1)(S+N_2) - S^2 \right]^2$$

3) For size $2n \times 2n$ we denote matrix sizes for convenience of reader.



Without showing all the steps, expansion of the above determinant is made along the first column, yielding two non-zero terms. The first term, proportional to $(S+N_1)$, is expanded along its n^{th} row ($n+1^{\text{st}}$ of original). The second term, proportional to S , is expanded along its first row. Then terms are combined to give

$$\left\{ (S+N_1)(S+N_2) - S^2 \right\}$$

$S+N_1$ $(n-1 \times n-1)$ \searrow 0 $S+N_1$	S $(n-1 \times n-1)$ \searrow 0 S
S $(n-1 \times n-1)$ \searrow 0 S	$S+N_2$ $(n-1 \times n-1)$ \searrow 0 $S+N_2$

From here it is an easy step to the conclusion that

$$|M_0| = \left\{ (S+N_1)(S+N_2) - S^2 \right\}^n \quad (A-5)$$

In a similar fashion, if K is some integer other than zero, either negative or positive, but less than n , a general result may be obtained. The details will not be shown here. The result is

$$|M_K| = \left\{ (S+N_1)(S+N_2) - S^2 \right\}^{n-|K|} (S+N_1)^{|K|} (S+N_2)^{|K|} \quad (A-6)$$

Similarly, $|M_{K+\Delta k}|$ may be evaluated. For compact notation, terms with powers of Δk greater than or equal to two will be dropped. Again the only case considered in detail is the case $K = 0$. Beginning directly with the $2n \times 2n$ case, we have

$$M_{0+\Delta k} = \begin{bmatrix} \begin{array}{c} S+N_1 \\ \searrow \\ 0 \end{array} \begin{array}{c} (n \times n) \\ 0 \end{array} \begin{array}{c} S \quad S\Delta k \quad \frac{-S\Delta k}{2} \quad \dots \\ \swarrow \quad \searrow \quad \swarrow \quad \searrow \\ -S\Delta k \quad \quad \quad S\Delta k \\ \vdots \quad \quad \quad \vdots \\ \vdots \quad \quad \quad -S\Delta k \quad \quad S \end{array} \\ \begin{array}{c} S \quad -S\Delta k \quad \frac{S\Delta k}{2} \quad \dots \\ \swarrow \quad \searrow \quad \swarrow \quad \searrow \\ S\Delta k \quad \quad \quad \frac{S\Delta k}{2} \\ \frac{-S\Delta k}{2} \quad \quad \quad -S\Delta k \\ \vdots \quad \quad \quad \vdots \\ \vdots \quad \quad \quad \frac{-S\Delta k}{2} \quad \quad S\Delta k \quad \quad S \end{array} \\ \begin{array}{c} S+N_2 \\ \searrow \\ 0 \end{array} \begin{array}{c} (n \times n) \\ 0 \end{array} \end{bmatrix}$$

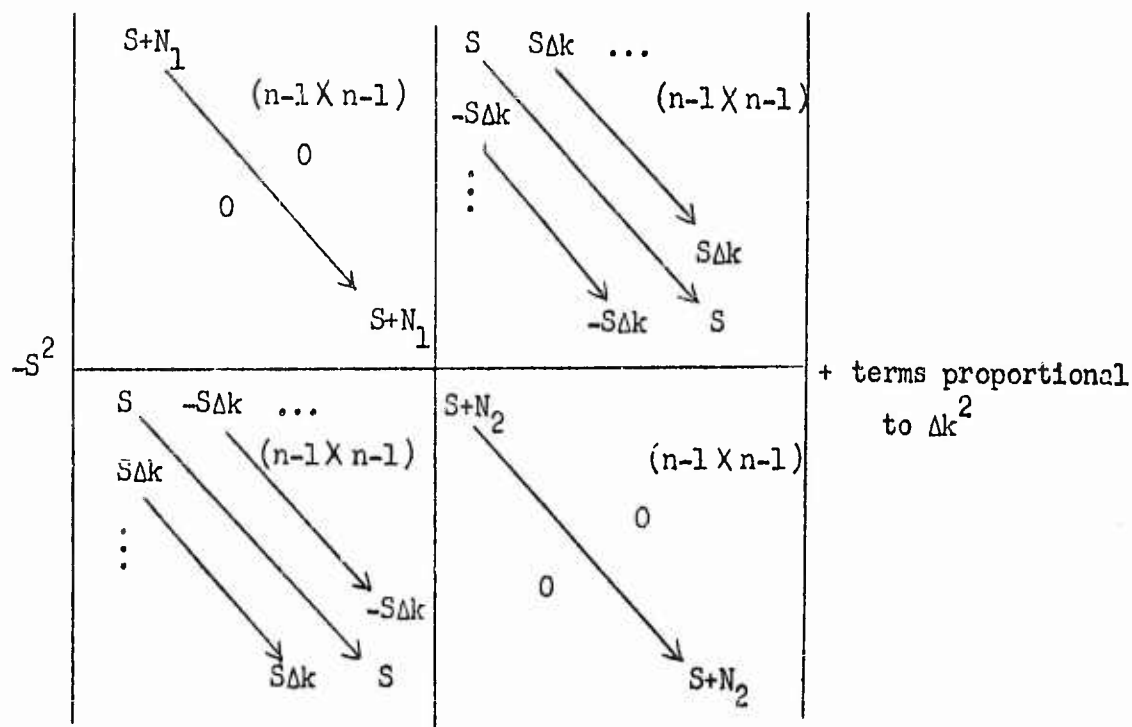
Expansion along the first column yields a series of terms of the form

$$(S+N_1) \begin{vmatrix} \textcircled{1} \end{vmatrix} + S \begin{vmatrix} \textcircled{2} \end{vmatrix} - S\Delta k \begin{vmatrix} \textcircled{3} \end{vmatrix} + \frac{S\Delta k}{2} \begin{vmatrix} \textcircled{4} \end{vmatrix} - \frac{S\Delta k}{3} \begin{vmatrix} \textcircled{5} \end{vmatrix} + \dots$$

First the determinant $\begin{vmatrix} \textcircled{1} \end{vmatrix}$ is expanded along its n^{th} row ($(n+1)^{\text{st}}$ of original). This gives a number of terms, one of which is

$$(S+N_1)(S+N_2) \begin{vmatrix} S+N_1 & & & & \\ & (n-1 \times n-1) & & & \\ & & 0 & & \\ & & & \ddots & \\ & & & & S+N_1 \\ S & -S\Delta k & \dots & & \\ S\Delta k & & & (n-1 \times n-1) & \\ \vdots & & & & \ddots \\ & & & & -S\Delta k & S \\ S+N_2 & & & & & (n-1 \times n-1) \\ & & & & & 0 \\ & & & & & & S+N_2 \end{vmatrix}$$

The other terms resulting from the expansion of $\begin{vmatrix} \textcircled{1} \end{vmatrix}$ all have a complete n^{th} column of terms which are either zero or proportional to Δk as well as a coefficient in front proportional to Δk . Hence they are proportional at least to Δk^2 and may be neglected. A similar sequence of steps results when $\begin{vmatrix} \textcircled{2} \end{vmatrix}$ is expanded along its first row. The result is



When $|\textcircled{3}|$, $|\textcircled{4}|$, $|\textcircled{5}|$, etc., are expanded along their n^{th} column, all the terms have an entire row proportional to Δk , so that the contributions are proportional at least to Δk^2 . Then we write

$$|M_{O+\Delta k}| = |M_O| + \text{terms proportional to } \Delta k^2 \text{ or higher powers of } \Delta k \quad (\text{A-7})$$

Further investigation for cases $K \neq 0$ yields the result, not proven here, that

$$|M_{K+\Delta k}| = |M_K| + \text{terms proportional to } \Delta k^2 \text{ or higher powers of } \Delta k \quad (\text{A-8})$$

Substitution of this result into Eq. (A-4) and evaluation of the limit then gives

$$\left. \frac{\partial}{\partial k} |M_k| \right|_{k=K} = 0 \quad (\text{A-9})$$

Now there remains the problem of differentiation of term $\textcircled{3}$ in Eq. (A-1). Again the definition of derivative will be used.

$$\frac{\partial}{\partial k} \left(-\frac{1}{2} \ell M_K^{-1} \ell' \right) \bigg|_{k=K} = \lim_{\Delta k \rightarrow 0} \frac{\frac{1}{2} \ell M_K^{-1} \ell' - \frac{1}{2} \ell M_{K+\Delta k}^{-1} \ell'}{\Delta k} \quad (\text{A-10})$$

First some algebraic manipulations are performed.

$$\frac{1}{2} \ell M_K^{-1} \ell' - \frac{1}{2} \ell M_{K+\Delta k}^{-1} \ell' = \frac{1}{2} \ell \left[M_K^{-1} - M_{K+\Delta k}^{-1} \right] \ell' \quad (\text{A-11})$$

The difference shown in the brackets may be approximated for small Δk by a standard matrix technique.⁶ Let

$$M_{K+\Delta k} = M_K + D_K \quad (\text{A-12})$$

From Eqs. (A-3) and (A-2), D_K may be written approximately, keeping only linear terms in Δk . It will be seen that only these terms count when $\lim \Delta k \rightarrow 0$ is taken.

$$D_K \approx \left[\begin{array}{ccc|ccc} 0 & 0 & \dots & 0 & -S\Delta k & 0 & S\Delta k & \dots \\ 0 & & & & & & & \\ \vdots & & & & & & & \\ 0 & \dots & & 0 & & & & \end{array} \right] \quad \begin{array}{l} \nearrow S\Delta k \\ \nearrow 0 \\ \nearrow -S\Delta k \end{array}$$

$$\left[\begin{array}{ccc|ccc} & & & 0 & 0 & \dots & 0 \\ & & & 0 & & & \\ & & & \vdots & & & \\ -S\Delta k & & & & & & \\ 0 & & & & & & \\ S\Delta k & & & & & & \\ & & & S\Delta k & 0 & -S\Delta k & \\ 0 & \dots & & 0 & \dots & & 0 \end{array} \right] \quad \begin{array}{l} \nearrow S\Delta k \\ \nearrow 0 \\ \nearrow -S\Delta k \end{array} \quad (\text{A-13})$$

⁶See, for instance, Fraser, Duncan, and Collar, Elementary Matrices, Cambridge University Press, 1957, § 4-11.

Now let us define

$$M_{K+\Delta k}^{-1} = M_K^{-1} + \delta_K \quad (A-14)$$

Then, by definition of the unit matrix I,

$$M_{K+\Delta k} \left[M_K^{-1} + \delta_K \right] = I \quad (A-15)$$

Rearranging and pre-multiplying by M_K^{-1} gives

$$M_K^{-1} M_{K+\Delta k} \delta_K = M_K^{-1} \left[I - M_{K+\Delta k} M_K^{-1} \right]$$

The left-hand side is approximately δ_K . Equation (A-12) may be substituted into the right-hand side to obtain

$$\delta_K \approx - M_K^{-1} D_K M_K^{-1} \quad (A-16)$$

Substitution of the various results back into Eq. (A-10) then gives

$$\left. \frac{\partial}{\partial k} \left(-\frac{1}{2} \ell M_K^{-1} \ell' \right) \right|_{k=K} = \lim_{\Delta k \rightarrow 0} \frac{\frac{1}{2} \ell M_K^{-1} D_K M_K^{-1} \ell'}{\Delta k} \quad (A-17)$$

Since D_K is the only matrix in which dependence on Δk appears, the limiting operation may be moved inside.

$$\left. \frac{\partial}{\partial k} \left(-\frac{1}{2} \ell M_K^{-1} \ell' \right) \right|_{k=K} = \frac{1}{2} \ell M_K^{-1} \left(\lim_{\Delta k \rightarrow 0} \frac{D_K}{\Delta k} \right) M_K^{-1} \ell' \quad (A-18)$$

Now all of the terms of the product shown in Eq. (A-18) may be written out. The vector ℓ is defined in Eq. (3). From Eq. (A-13), we write

$$\lim_{\Delta k \rightarrow 0} \frac{D_K}{\Delta k} = \begin{bmatrix} \begin{array}{c|c} \begin{array}{ccc} 0 & 0 & \dots \\ 0 & & \\ \vdots & & \end{array} & \begin{array}{c} \text{K columns} \\ \begin{array}{ccccccc} 0 & \frac{s}{2} & -s & 0 & s & -\frac{s}{2} & \dots \\ & \searrow & \searrow & \searrow & \searrow & \searrow & \searrow \\ & & -\frac{s}{2} & s & 0 & -s & \frac{s}{2} \end{array} \end{array} \\ \hline \begin{array}{c} \text{K rows} \\ \begin{array}{ccccccc} \frac{s}{2} & & & & & & \\ -s & & & & & & \\ 0 & & & & & & \\ s & & & & & & \\ -\frac{s}{2} & & & & & & \\ \vdots & & & & & & \end{array} \end{array} & \begin{array}{c} \begin{array}{ccc} 0 & 0 & \dots \\ 0 & & \\ \vdots & & \end{array} \\ 0 \end{array} \end{bmatrix}$$

(A-19)

It is not difficult to show that the inverse of M_K is as follows:

$$M_K^{-1} = \begin{bmatrix} \begin{array}{cc|cc} \frac{S+N_2}{B} & 0 & 0 & -\frac{S}{B} \\ 0 & \frac{S+N_2}{B} & 0 & 0 \end{array} & \begin{array}{cc} K \text{ columns} & K \text{ columns} \\ 0 & 0 \end{array} \\ \hline \begin{array}{cc|cc} 0 & \frac{1}{S+N_1} & 0 & 0 \\ 0 & \frac{1}{S+N_1} & 0 & 0 \end{array} & \begin{array}{cc} K \text{ rows} & K \text{ rows} \\ 0 & 0 \end{array} \\ \hline \begin{array}{cc|cc} 0 & 0 & \frac{1}{S+N_2} & 0 \\ 0 & 0 & \frac{1}{S+N_2} & 0 \end{array} & \begin{array}{cc} K \text{ rows} & K \text{ rows} \\ 0 & 0 \end{array} \\ \hline \begin{array}{cc|cc} -\frac{S}{B} & 0 & 0 & \frac{S+N_1}{B} \\ 0 & -\frac{S}{B} & 0 & \frac{S+N_1}{B} \end{array} & \begin{array}{cc} K \text{ rows} & K \text{ rows} \\ 0 & 0 \end{array} \end{bmatrix} \quad (A-20)$$

where $B = (S+N_1)(S+N_2) - S^2$. This can be proved by multiplying by M_K , given in Eq. (A-2) to obtain the unit matrix.

The matrix multiplication required to evaluate Eq. (A-18) is straightforward, but takes a lot of space. Hence only the result is shown, and only for $K = 0$. Leaving the multiplications by ℓ and ℓ' until last, we get

$$M_0^{-1} \left(\lim \frac{D_K}{\Delta k} \right) M_0^{-1} = m$$

$$= \begin{bmatrix} 0 & \begin{matrix} \frac{S}{B} & -\frac{S}{2B} & \frac{S}{3B} & \dots \\ -\frac{S}{B} & \frac{S}{2B} & -\frac{S}{B} & \frac{S}{2B} \\ \frac{S}{2B} & -\frac{S}{B} & \frac{S}{2B} & -\frac{S}{B} \\ \vdots & \vdots & \vdots & \vdots \end{matrix} \\ \begin{matrix} 0 & -\frac{S}{B} & \frac{S}{2B} & \dots \\ \frac{S}{B} & -\frac{S}{2B} & \frac{S}{B} & -\frac{S}{2B} \\ -\frac{S}{2B} & \frac{S}{B} & -\frac{S}{2B} & \frac{S}{B} \\ \frac{S}{3B} & -\frac{S}{2B} & \frac{S}{B} & -\frac{S}{2B} \\ \vdots & \vdots & \vdots & \vdots \end{matrix} & 0 \end{bmatrix} \quad (A-21)$$

A similar set of results could be derived for $K \neq 0$, but since they are not really used in the main body of the report, the space is not taken here.

Finally, Eq. (A-18) may be evaluated.

$$\frac{\partial}{\partial k} \left(-\frac{1}{2} e M_K^{-1} e' \right) = \frac{1}{2} s m e' \quad (A-22)$$

Further simplification is obtained if the upper right hand corner of m is defined as a new matrix m . The result is

$$m = \begin{bmatrix} 0 & \frac{S}{B} & -\frac{S}{2B} & \frac{S}{3B} & \dots \\ -\frac{S}{B} & & & & \\ \frac{S}{2B} & & & & \\ -\frac{S}{3B} & & & & \\ \vdots & & & & \end{bmatrix} \begin{matrix} \searrow \frac{S}{3B} \\ \searrow -\frac{S}{2B} \\ \searrow \frac{S}{B} \\ \searrow 0 \end{matrix} \quad (A-23)$$

and

$$\left. \frac{\partial}{\partial k} \log P(l; k) \right|_{k=0} = y m x' \quad (A-24)$$



BEARING UNCERTAINTY FOR SPLIT-BEAM SONAR ARRAYS
DUE TO SCATTERING IN A RANDOM MEDIUM

by

Theron Usher, Jr.

Progress Report No. 13

General Dynamics/Electric Boat Research

(53-00-10-0231)

March 1964

DEPARTMENT OF ENGINEERING
AND APPLIED SCIENCE
YALE UNIVERSITY

I. Introduction

The problem of single frequency wave propagation in a weakly inhomogeneous medium has been considered at length by Chernov.⁽¹⁾ The results that are applicable for this report are found mainly in Chapters V and VI of Reference (1). Chernov assumes perturbed plane wave propagation through a medium in which the refractive index fluctuates in a random isotropic fashion throughout the medium. He develops expressions for the correlation of the amplitude and phase fluctuations of the scattered wave at different points in the medium.

Recently Lord⁽²⁾ has applied Chernov's results to the determination of the bearing uncertainty for a discrete linear difference array receiving a single-frequency signal.

In this report Chernov's results are applied to the operation of a split-beam system of transducers identical to that considered in Progress Report No. 9.⁽³⁾ The bearing uncertainty due to the scattering of a single frequency plane-wave signal is derived. It would be desirable to derive the bearing uncertainty for a wide-band random signal, but the analysis poses some difficulties. It will be seen in the following sections that the variance of the propagation time through the medium is not a function of frequency, but there is no assurance that the exact values of the time delays for all frequencies are precisely the same, or even show correlation over a reasonable band of frequencies. Possibly further study of Chernov's work could resolve this question. However, the results for wide-band signals should be no worse than those for single-frequency signals.

II. Review of Results from Chernov

Chernov assumes a single frequency plane wave for the acoustic pressure of the form in Eq. (1) propagating through a medium in which the refractive index varies in a random fashion about a mean value.

$$p(t) = p_0(t) \epsilon^{j\psi} = p_0(t) \epsilon^{\beta + j\gamma} \quad (1)$$

In Eq. (1) β and γ are the amplitude and phase fluctuations respectively, and $p_0(t)$ is the plane wave solution in a homogeneous medium, given by Eq. (2).

$$p_0(t) = \epsilon^{-j(\omega t - kr)} = \epsilon^{-j\omega\left(t - \frac{r}{c}\right)} \quad (2)$$

The variances of the phase and amplitude fluctuations are given in Eqs. (3) and (4).

$$\langle \gamma^2 \rangle = \frac{\pi^{1/2}}{2} \langle \mu^2 \rangle \frac{\omega^2}{c^2} \ar(1 + \frac{1}{D} \arctan D) \quad (3)$$

$$\langle \beta^2 \rangle = \frac{\pi^{1/2}}{2} \langle \mu^2 \rangle \frac{\omega^2}{c^2} \ar(1 - \frac{1}{D} \arctan D) \quad (4)$$

$$(ka \gg 1)$$

In Eqs. (3) and (4) $\langle \mu^2 \rangle$ is the variance of the refractive index and a is the correlation distance for the fluctuations of the refractive index. For the derivation of Eqs. (3) and (4), the correlation function for the fluctuations of the refractive index at two different points in space is assumed to have the form

$$\langle \mu_1 \mu_2 \rangle = \langle \mu^2 \rangle e^{-\frac{\xi^2 + \eta^2 + \zeta^2}{a^2}} \quad (5)$$

where ξ , η , and ζ are the differences of the coordinates for each of the two points. Also, the wave parameter D in Eqs. (3) and (4) is given by

$$D = \frac{4r}{ka^2} = \frac{4r}{a} \cdot \frac{1}{ka} \quad (6)$$

The normalized cross-correlation between amplitude and phase at the same point in the medium is found to be

$$R_{\beta\gamma} = \frac{\langle \beta\gamma \rangle}{\left[\langle \beta^2 \rangle \langle \gamma^2 \rangle \right]^{1/2}} = \frac{1}{2} \frac{\ln(1+D^2)}{\sqrt{D^2 - (\arctan D)^2}} \quad (7)$$

For $D \gg 1$ Eq. (7) becomes

$$R_{\beta\gamma} \approx \frac{\ln D}{D} \rightarrow 0 \quad (8)$$

The problem of evaluating the autocorrelation between the amplitude fluctuations and the phase fluctuations at two different points in the medium is divided into two distinctly different parts. First the autocorrelation is evaluated for the situation in which the two points are located in line with the path of propagation. The normalized longitudinal autocorrelation for amplitude and phase is given by

$$R_{\beta_{1,2}} = R_{\gamma_1\gamma_2} = \frac{\langle \beta_1 \beta_2 \rangle}{\langle \beta^2 \rangle} = \frac{\langle \gamma_1 \gamma_2 \rangle}{\langle \gamma^2 \rangle} = \frac{1}{1 + \left(\frac{2\Delta r}{ka^2} \right)^2} \quad (9)$$

$\left(\begin{array}{l} D \gg 1 \\ ka \gg 1 \end{array} \right)$

where Δr is the separation of the two points.

Next, the autocorrelation is evaluated for the situation in which the two points are located along a line perpendicular to the path of propagation. The normalized transverse autocorrelation functions are

$$R_{\beta 1,2} = \frac{\epsilon^{-\frac{\ell^2}{a^2}} - \frac{1}{D} \left[\frac{\pi}{2} - \text{Si} \left(\frac{1}{D} \frac{\ell^2}{a^2} \right) \right]}{1 - \frac{1}{D} \arctan D} \quad (10)$$

$$R_{\gamma 1,2} = \frac{\epsilon^{-\frac{\ell^2}{a^2}} + \frac{1}{D} \left[\frac{\pi}{2} - \text{Si} \left(\frac{1}{D} \frac{\ell^2}{a^2} \right) \right]}{1 + \frac{1}{D} \arctan D} \quad (11)$$

$$\text{for } ka \gg 1 \\ D > 1$$

If D is very large,

$$R_{\beta 1,2} = R_{\gamma 1,2} \approx R_{\mu} = \epsilon^{-\frac{\ell^2}{a^2}} \quad (12)$$

In Eqs. (10), (11) and (12), ℓ is the separation of the two points.

Note that the longitudinal correlation is high over a distance

$$\Delta r \leq \frac{ka}{2} \cdot a$$

which is much larger than the distance $\ell \leq a$ over which the transverse correlation is high.

Values for a , c , and $\langle \mu^2 \rangle$ to be used in this report are:

$$a = 2 \text{ ft. (from Chernov)}$$

$$c = 5000 \text{ ft/sec}$$

$$\langle \mu^2 \rangle = 5 \times 10^{-9} \text{ (from Chernov)}$$

III. Response of a Split Beam System

In this section the results of Section II are utilized in the analysis of the split-beam system shown in Fig. 1.

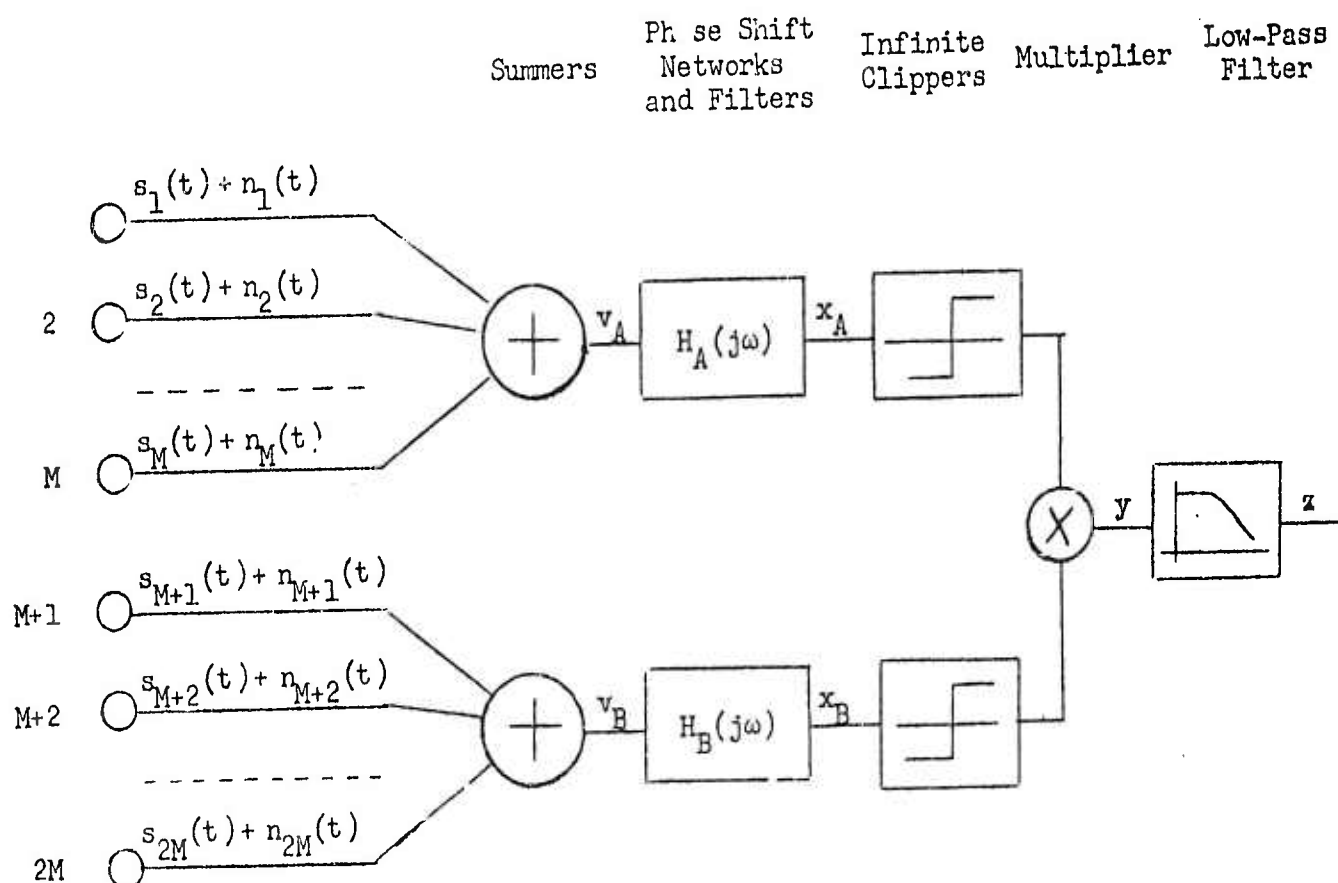


Figure 1 Typical Split-Beam System

The assumptions concerning noise properties are the same as those in Progress Report No. 9. The signal from the i^{th} transducer is expressed in Eq. (13).

$$s_i(t) = \text{Re} \left\{ A e^{-j[\omega t - (i-1)\omega T - \psi_1]} \right\} \quad (13)$$

In Eq. (13) A is the complex number representing the magnitude and initial phase of the unperturbed wave at the first transducer, T is the time delay

of the unperturbed wave between adjacent transducers. The function ψ_1 is the complex random fluctuation of amplitude and phase defined in Eq. (1).

The outputs of the summing amplifiers in Fig. 1 are

$$v_A(t) = \sum_{i=1}^M \left[\operatorname{Re} \left\{ A \epsilon^{-j[\omega t - (i-1)\omega T - \psi_i]} \right\} + n_i(t) \right] \quad (14)$$

$$v_B(t) = \sum_{k=1}^M \left[\operatorname{Re} \left\{ A \epsilon^{-j[\omega t - (k+M-1)\omega T - \psi_{k+M}]} \right\} + n_{k+M}(t) \right] \quad (15)$$

The average value of the output of the multiplier is given by⁽³⁾

$$\bar{y} = \frac{2}{\pi} \arcsin \left[\frac{R_{x_A x_B}(0)}{\left\{ R_{x_A}(0) R_{x_B}(0) \right\}^{1/2}} \right] \quad (16)$$

For low signal-to-noise ratios at the transducers, the values of $R_{x_A}(0)$ and $R_{x_B}(0)$ depend on the noise parameters only, and $R_{x_A x_B}(0)$ depends on the signal parameters only.

The "on target" null response of the array is thus determined solely by $R_{x_A x_B}(0)$, and for this reason the cross-correlation function receives our attention. In the following analysis the overbar indicates averaging over the time variable, and the brackets $\langle \rangle$ indicate averaging over the space variables. The functions $x_A(t)$ and $x_B(t)$ are

$$x_A(t) = \sum_{i=1}^M \left[\operatorname{Re} \left\{ A H_A(j\omega) \epsilon^{-j[\omega t - (i-1)\omega T - \psi_i]} \right\} + n_i'(t) \right] \quad (17)$$

$$x_B(t) = \sum_{k=1}^M \left[\operatorname{Re} \left\{ A H_B(j\omega) \epsilon^{-j[\omega t - (k+M-1)\omega T - \psi_{k+M}]} \right\} + n_{k+M}'(t) \right] \quad (18)$$

The crosscorrelation between $x_A(t)$ and $x_B(t)$ is

$$\begin{aligned} R_{x_A x_B}(0) &= \overline{x_A(t) x_B(t)} \\ &= \sum_{i=1}^M \sum_{k=1}^M \operatorname{Re} \left\{ A H_A(j\omega) \epsilon^{-j[\omega t - (i-1)\omega T - \psi_i]} A^* H_B^*(j\omega) \epsilon^{j[\omega t - (k+M-1)\omega T - \psi_{k+M}^*]} \right\} \end{aligned} \quad (19)$$

Since $H_A(j\omega) = j\omega H_B(j\omega)$, Eq. (19) simplifies to

$$R_{x_A x_B}(0) = \sum_{i=1}^M \sum_{k=1}^M \left| A H_B(j\omega) \right|^2 \omega \epsilon^{\beta_i + \beta_{k+M}} \sin[\gamma_{k+M} - \gamma_i + (k+M-i)\omega T] \quad (20)$$

Note that $R_{x_A x_B}(0)$ is still a random variable involving the space coordinates.

As might be expected, for $T = 0$, if β and γ are independent,

$$\left\langle R_{x_A x_B}(0) \right\rangle_{T=0} = 0$$

because

$$\left\langle \epsilon^{\beta_i + \beta_{k+M}} \sin(\gamma_{k+M} - \gamma_i) \right\rangle = \left\langle \epsilon^{\beta_i + \beta_{k+M}} \right\rangle \left\langle \sin(\gamma_{k+M} - \gamma_i) \right\rangle = 0 \quad (21)$$

In order to make further deductions from Eq. (20) and to justify Eq. (21), it is necessary to consider the values of some of the parameters reviewed in Section II. It is desirable to have the parameter $D \gg 1$, in order to simplify analysis. From Eq. (6) it can be seen that D takes on its minimum value when range r is minimum and the upper processing frequency is highest. For $D > 100$ the following relation holds between range and frequency. Range is given in kiloyards.

$$\frac{4(3000r)c}{\omega a^2} > 100 \quad , \quad r > \frac{\omega}{150,000} \quad (22)$$

From Table (1) in Report 9 the upper half-power frequencies are listed for optimum processing as a function of range. From this table

$$\omega_{\text{upper}} = 210,000 r^{-1/2} \quad (23)$$

The simultaneous solution of Eqs. (22) and (23) gives

$$r > \left(\frac{210,000}{150,000} \right)^{2/3} = 1.25 \text{ kyd.} \quad \text{for} \quad D > 100 \quad (24)$$

Detection for ranges less than 1.25 kyd should not pose significant problems.

The upper limit on the normalized correlation between the β and γ components of the complex ψ function is found from Eq. (8).

$$R_{\beta\gamma} < \frac{\ln 100}{100} = .046 \quad \text{for} \quad D > 100 \quad (25)$$

Also inherent in the analysis is the assumption of forward scattering for which $ka > 1$. Thus

$$\omega > \frac{c}{a} = 2500 \text{ rad/sec.} \quad (26)$$

From Table 1, Report 9, the lower half power points for the optimum filter are found from the relation

$$\omega_{\text{lower}} = 63,000 r^{-1/2} \quad (27)$$

Thus the upper bound on range for which the assumptions are reasonably valid is

$$r < \left(\frac{63,000}{2500} \right)^2 = 630 \text{ kyd} \quad \text{for} \quad ka > 1 \quad (28)$$

The maximum values of the variances for γ and β are also of interest for the condition of optimum filtering. Combining Eq. (23) with Eqs. (3) and (4), we have

$$\overline{\gamma^2} = \overline{\beta^2} < \frac{\pi^{1/2}}{2} \mu^2 \frac{(210,000 r^{-1/2})^2}{c^2} a(3000 r) = 4.7 \times 10^{-2} \quad (29)$$

Actually, the above result should be equally valid for any filter function, since the upper cutoff frequency for the optimum filter is closely related to the cutoff frequency for the signal spectrum.

IV. Bearing Uncertainty

Two attacks are possible for determining the bearing uncertainty. First, the square of the cross-correlation function for $T = 0$ in Eq. (20) is averaged over the space coordinates.

$$\left\langle R^2 \right\rangle_{T=0} = \left| A H_B(j\omega) \right|^4 \omega^2 \sum_{i=1}^M \sum_{k=1}^M \sum_{p=1}^M \sum_{q=1}^M \times \left\langle \beta_i + \beta_{k+M} + \beta_p + \beta_{q+M} \sin(\gamma_{k+M} - \gamma_i) \sin(\gamma_{q+M} - \gamma_p) \right\rangle \quad (30)$$

Since the mean square values of β and γ are small, Eq. (30) reduces to

$$\begin{aligned}
 \left\langle R \right|_{T=0}^2 &\approx |A H_B(j\omega)|^4 \omega^2 \sum_i \sum_k \sum_p \sum_q \left\langle \left[1 + (\beta_i + \beta_{k+M} + \beta_p + \beta_{q+M}) \right] (\gamma_{k+M} - \gamma_i)(\gamma_{q+M} - \gamma_p) \right\rangle \\
 &\approx |A H_B(j\omega)|^4 \omega^2 \sum_i \sum_k \sum_p \sum_q \left\langle (\gamma_{k+M} - \gamma_i)(\gamma_{q+M} - \gamma_p) \right\rangle \\
 &= 2 |A H_B(j\omega)|^4 \omega^2 \left\{ \sum_{i=1}^M \sum_{p=1}^M \langle \gamma_i \gamma_p \rangle - \sum_{i=1}^M \sum_{k=1}^M \langle \gamma_i \gamma_{k+M} \rangle \right\} \quad (31)
 \end{aligned}$$

Next, the derivative of R with respect to T is evaluated at $T = 0$ and averaged over the space coordinates.

$$\begin{aligned}
 \left\langle \frac{dR}{dT} \right|_{T=0} &= |A H_B(j\omega)|^2 \omega^2 \sum_{i=1}^M \sum_{k=1}^M (k+M-i) \left\langle \epsilon^{\beta_i + \beta_{k+M}} \cos(\gamma_{k+M} - \gamma_i) \right\rangle \\
 &\approx |A H_B(j\omega)|^2 \omega^2 M^3 \quad (32)
 \end{aligned}$$

The bearing uncertainty is defined in Eq. (33) (by analogy from Eq. (31), Report No. 9).

$$\sigma_\theta = \frac{c}{d} \left\langle R \right|_{T=0}^2 \right\rangle^{1/2} \left\langle \frac{dR}{dT} \right|_{T=0} \right\rangle^{-1} \quad (33)$$

From Eqs. (3), (4), and (12) and the array geometry we can specify the values of the individual terms in Eq. (31).

$$\langle \gamma_i \gamma_p \rangle = \frac{\pi^{1/2}}{2} \left\langle \mu^2 \right\rangle \frac{\omega^2}{c^2} \ar R_{(p-i)} = \frac{\pi^{1/2}}{2} \left\langle \mu^2 \right\rangle \frac{\omega^2}{c^2} \ar \epsilon - \frac{(p-i)^2 d^2}{2} \quad (34)$$

$$\langle \gamma_1 \gamma_{k+M} \rangle = \frac{\pi^{1/2}}{2} \langle \mu^2 \rangle \frac{\omega^2}{c^2} \ar R_{(k+M-1)} = \frac{\pi^{1/2}}{2} \langle \mu^2 \rangle \frac{\omega^2}{c^2} \ar \epsilon - \frac{(k+M-1)d^2}{a^2} \quad (35)$$

Combination of the results in Eqs. (31) through (35) yields

$$\sigma_0 = \left(\pi^{1/2} \langle \mu^2 \rangle a \right)^{1/2} \frac{r^{1/2}}{M^{3/2} (Md)} \left[\sum_{i=1}^M \sum_{p=1}^M R_{(p-i)} - \sum_{i=1}^M \sum_{k=1}^M R_{(k+M-1)} \right]^{1/2} \quad (36)$$

Transverse autocorrelations are used because the average wavefront is parallel to the line of the array.

The expansion of the series in Eq. (36) yields

$$\begin{aligned} \sigma_0 = & \left(\pi^{1/2} \langle \mu^2 \rangle a \right)^{1/2} \frac{r^{1/2}}{M^{3/2} (Md)} \left[1 + \left(2 - \frac{3}{M} \right) R_{(1)} + \left(2 - \frac{6}{M} \right) R_{(2)} + \dots \right. \\ & + \left(\frac{6}{M} - 1 \right) R_{(M-2)} + \left(\frac{3}{M} - 1 \right) R_{(M-1)} - R_{(M)} - \left(1 - \frac{1}{M} \right) R_{M+1} \\ & \left. - \left(1 - \frac{2}{M} \right) R_{(M+2)} - \dots - 2R_{(2M-2)} - R_{(2M-1)} \right]^{1/2} \quad (37) \end{aligned}$$

Only the first few terms of the series in Eq. (37) have significant value, since the value of the normalized autocorrelation approaches zero very rapidly with increasing argument.

Since there are M^2 terms in both double series of Eq. (36), the bearing uncertainty satisfies the following inequality, in which the constant K is equal to $\left(\pi^{1/2} \langle \mu^2 \rangle a \right)^{1/2}$.

$$K \frac{r^{1/2}}{M^{3/2} (Md)} < \sigma_0 < K \frac{r^{1/2}}{M(Md)} \quad (38)$$

An alternate approach for evaluating the bearing uncertainty involves solving for the time delay from Eq. (20) which yields a null response.

$$\sum_{i=1}^M \sum_{k=1}^M \sin(\gamma_{k+M} - \gamma_i + (k+M-i) \omega T_{\text{null}}) = 0 \quad (39)$$

and

$$T_{\text{null}} = \frac{\sum_{i=1}^M \sum_{k=1}^M (\gamma_i - \gamma_{k+M})}{\omega M^3} \quad (40)$$

The time delay for null response is now a random variable over the space coordinates.

Since $T = \frac{d}{c} \theta$ for small angles, the bearing uncertainty can be directly related to the standard deviation of T_{null} .

$$\sigma_{\theta} = \frac{c}{d} \left\langle T_{\text{null}}^2 \right\rangle^{1/2} = \frac{c \left[\sum_{i=1}^M \sum_{k=1}^M \sum_{p=1}^M \sum_{q=1}^M \left\langle (\gamma_i - \gamma_{k+M})(\gamma_p - \gamma_{q+M}) \right\rangle \right]^{1/2}}{\omega M^2 (Md)} \quad (41)$$

Simplification of Eq. (41) yields a result identical to that in Eq. (33).

V. Numerical Examples

Two numerical examples are chosen for which the bearing uncertainty is calculated. For both cases

$$\left(n^{1/2} \left\langle \mu^2 \right\rangle \right)^{1/2} = 1.33 \times 10^{-4} \text{ ft}^{1/2}$$

For the first example, $M = 1$, $d = 200$ ft and $r = 30,000$ ft or 10 kyd. From Eq. (35)

$$\begin{aligned}\sigma_{\theta_1} &= 1.33 \times 10^{-4} \frac{(30,000)^{1/2}}{200} (1 - 0) = 1.15 \times 10^{-4} \text{ rad.} \\ &= 6.6 \times 10^{-3} \text{ degrees}\end{aligned}\quad (42)$$

For the second example, $M = 25$, $d = 2$ ft and $r = 30,000$ ft or 10 kyd.

$$\begin{aligned}\sigma_{\theta_2} &= 1.33 \times 10^{-4} \frac{(30,000)^{1/2}}{25^{3/2} (50)} \left[1 + \left(2 - \frac{3}{25} \right) \epsilon^{-1} + \left(2 - \frac{6}{25} \right) \epsilon^{-4} + \dots \right]^{1/2} \\ &= 4.85 \times 10^{-6} \text{ rad} = 2.8 \times 10^{-4} \text{ degrees}\end{aligned}\quad (43)$$

VI. Conclusions

The numerical results in Section V show that the bearing uncertainties introduced by scattering in the medium are extremely small. It is possible that the assumed value of $\langle \mu^2 \rangle$ is too small, but the value of $\langle \mu^2 \rangle$ would have to be several orders of magnitude larger in order to have calculated results agree with the bearing errors for actual situations. This alternative seems unlikely.

The transducer configuration described in Lord's analysis⁽²⁾ has exactly the same geometry as the one in this report, but the assumed method of processing the transducer outputs is different than the method analyzed here. His results are expressed in the following equation, using the symbols defined in this report.

$$\sigma_{\theta} \approx \left(2\pi^{1/2} \langle \mu^2 \rangle_a \right)^{1/2} \frac{r^{1/2}}{M(Md)} \left[\sum_{i=1}^M \sum_{p=1}^M R_{(p-i)} - \sum_{i=1}^M \sum_{k=1}^M R_{(k+M-i)} \right]^{1/2} \quad (44)$$

His results are greater than the results in Eq. (36) by a factor of $2^{1/2}M$. The $2^{1/2}$ arises from the fact that the bearing uncertainty depends on $\left(\langle \beta^2 \rangle + \langle \gamma^2 \rangle \right)$ and not just $\langle \gamma^2 \rangle$, and the factor M apparently arises from the processing method.

REFERENCES

- (1) Chernov, L. A., Wave Propagation in a Random Medium, McGraw-Hill Book Company, 1960.
- (2) Lord, G. E., "Variance of the Bearing Angle of a Discrete Linear Difference Array in a Random Transmission Medium," Applied Physics Laboratory, University of Washington, 1963.
- (3) Usher, T., "Random Bearing Errors in Split Beam Systems," Progress Report No. 9, General Dynamics/Electric Boat Research (53-00-10-0231), Yale University, December 1963.



LIKELIHOOD RATIO DETECTION FOR LONG OBSERVATION TIMES

by

Allen H. Levesque

Progress Report No. 14

General Dynamics/Electric Boat Research

(53-00-10-0231)

May 1964

DEPARTMENT OF ENGINEERING
AND APPLIED SCIENCE

YALE UNIVERSITY

I. Introduction

This report deals with the problem of finding an approximation to the optimum receiver for the detection of a signal of unknown frequency in gaussian noise.

It is well known that the likelihood ratio (LR) detector is the optimum processor for the detection of a signal in random noise. When the desired signal is a function of certain unknown parameters, the LR must be averaged over all possible values of the unknown parameters. This averaged LR, considered as a function of the received signal $v(t)$, specifies the operations which the optimum detector must perform on $v(t)$, that is, the form of the optimum detector. In most cases of practical interest, however, the averaging of the LR cannot be carried out in closed form.

In such cases the averaged LR, or some monotonic function of the averaged LR, is obtained in the form of a power series involving linear, quadratic, and higher order operations on $v(t)$. A satisfactory approximation to the form of the optimum detector may then be obtained from the lowest order term in the power series expansion, if it is assumed that higher order terms in the series can safely be neglected. This assumption is the subject of this report.

Optimum detection is generally considered for cases in which weak or threshold signals are to be enhanced to a detectable level by long processing time. In these cases, higher order terms in the power series for the detector operations are usually neglected on the basis of low

pre-detection signal-to-noise ratio (SNR).^{*} It is the object of this report to show that for certain cases this is not sufficient grounds for dropping all higher-order terms. It will be shown that a low pre-detection SNR can be offset by long post-detection integration time, and certain higher-order terms in the power series can thereby be made appreciable with respect to the lowest-order term.

Three signal cases are considered:

- 1) A broadband gaussian stochastic signal whose spectral density is flat over a band of width Ω rad/sec.
- 2) A narrowband gaussian stochastic signal with bandwidth Ω_b rad/sec and center frequency ω_c rad/sec. Here ω_c is equally likely to lie anywhere in the band Ω , and Ω_b is assumed to be much smaller than Ω .
- 3) A steady sinusoid of unknown frequency and phase, lying anywhere in the band Ω with uniform probability.

For each of the three cases, the noise is assumed to be gaussian and spectrally flat over the band Ω .

Case 3) is seen to be the problem treated in Progress Report No. 8.² Here we shall see that the assumption made on page 5 of that report can be inaccurate for long post-detection integration time, in spite of a low pre-detection SNR.

^{*}See, for example, Middleton,¹ discussion on p. 821.

II. Power Series Expansion for LR Detection

Here we shall derive the power series expansion which prescribes the operations to be performed on the received signal by the optimum detector. The symbols and conventions used here will in general conform to those used in Progress Report No. 8. The reader may refer to Section II of that report for a discussion of the basic assumptions and for other comment pertinent to this derivation.

The received signal, in the form of a vector of time samples, is

$$\underline{v} = \underline{s} + \underline{n} \quad (1)$$

where \underline{s} is the "desired signal" and \underline{n} is the noise. When the noise is gaussian with zero mean and covariance matrix \underline{K} , the averaged LR is given by

$$\ell(\underline{v}) = \left\langle \exp \left(-\frac{1}{2} \underline{s}' \underline{K}^{-1} \underline{s} + \underline{s}' \underline{K}^{-1} \underline{v} \right) \right\rangle_{\underline{s}} \quad (2)$$

where $\langle \rangle_{\underline{s}}$ indicates a statistical average over the unknown signal parameters. At this point we shall restrict ourselves to the consideration of white noise backgrounds, in which case the noise covariance matrix is diagonal. In this case the first quadratic form in the exponent in Eq. (1) becomes

$$-\frac{1}{2} \underline{s}' \underline{K}^{-1} \underline{s} = -\frac{1}{2N} \sum_{i=1}^n s_i^2 \quad (3)$$

where N is the variance of the noise, s_i is a sample of the desired signal at the time instant t_i , and n is the total number of time samples. The summation in Eq. (3) is seen to be proportional to the total energy content of the desired signal during the observation time of the signal.

Since we shall only be concerned with frequency and phase as unknown signal parameters, the summation in Eq. (3) will be unaffected by the averaging operation $\langle \rangle_S$. From this argument, then, we can rewrite Eq. (2) as

$$\ell(\underline{v}) = \exp\left(-\frac{1}{2} \underline{s}' \underline{K}^{-1} \underline{s}\right) \left\langle \exp(\underline{s}' \underline{K}^{-1} \underline{v}) \right\rangle_S \quad (4)$$

Using a power series expansion for the exponential, we have

$$\ell(\underline{v}) = \exp\left(-\frac{1}{2} \underline{s}' \underline{K}^{-1} \underline{s}\right) \left\langle 1 + (\underline{s}' \underline{K}^{-1} \underline{v}) + \frac{1}{2!} (\underline{s}' \underline{K}^{-1} \underline{v})^2 + \frac{1}{3!} (\underline{s}' \underline{K}^{-1} \underline{v})^3 + \dots \right\rangle_S \quad (5)$$

We shall be dealing with cases of "incoherent" signals (in the sense of Section II of the aforementioned report) in which the odd powers of $\underline{s}' \underline{K}^{-1} \underline{v}$ go to zero in the averaging operation $\langle \rangle_S$. The averaged LR thus becomes

$$\ell(\underline{v}) = \exp\left(-\frac{1}{2} \underline{s}' \underline{K}^{-1} \underline{s}\right) \left\langle 1 + \frac{1}{2!} (\underline{s}' \underline{K}^{-1} \underline{v})^2 + \frac{1}{4!} (\underline{s}' \underline{K}^{-1} \underline{v})^4 + \dots \right\rangle_S \quad (6)$$

We now take $\log \ell(\underline{v})$ as the test statistic in the optimum detector:

$$\begin{aligned} \log \ell(\underline{v}) = & -\frac{1}{2} \underline{s}' \underline{K}^{-1} \underline{s} + \frac{1}{2} \left\langle (\underline{s}' \underline{K}^{-1} \underline{v})^2 \right\rangle \\ & + \frac{1}{4!} \left\langle (\underline{s}' \underline{K}^{-1} \underline{v})^4 \right\rangle - \frac{1}{8} \left\langle (\underline{s}' \underline{K}^{-1} \underline{v})^2 \right\rangle^2 \\ & + O(\underline{s}^6) \end{aligned} \quad (7)$$

Equation (7) is exact through $O(\underline{s}^4)$. In Eq. (7) and hereafter, the symbol $\langle \rangle$ will imply $\langle \rangle_S$.

III. Deflections of Terms in the Power Series

In any specific detection problem we would want to approximate the operation of the detector by one or more of the terms in Eq. (7) involving the received signal \underline{v} . The contributions of the various higher-order terms to $\log \ell(\underline{v})$ could then be neglected or replaced by suitable bias terms.

In order to justify such approximations, however, we must examine the changes in the various terms in going from the "noise-only" condition to the "signal-plus-noise" condition. Here we shall calculate the change in the average values of the terms. For convenience this change will be called a deflection and will be denoted by $\Delta E[]$. In particular, the following deflections will be obtained in general form:

$$\Delta E[O(\underline{s}^2)] = \Delta E\left[\frac{1}{2} \langle (\underline{s}' \underline{K}^{-1} \underline{v})^2 \rangle\right] \quad (8)$$

$$\Delta E[O(\underline{s}^4)] = \Delta E\left[\frac{1}{4!} \langle (\underline{s}' \underline{K}^{-1} \underline{v})^4 \rangle - \frac{1}{8} \langle (\underline{s}' \underline{K}^{-1} \underline{v})^2 \rangle^2\right] \quad (9)$$

These two deflections will then be evaluated for the three signal cases outlined in Section I.

For future reference, we shall also obtain

$$\Delta E\left[\frac{1}{6!} \langle (\underline{s}' \underline{K}^{-1} \underline{v})^6 \rangle\right] \quad (10)$$

This term is the most significant term in $O(\underline{s}^6)$.

Deflection of $O(\underline{s}^2)$

We note that

$$\begin{aligned} \langle (\underline{s}' \underline{K}^{-1} \underline{v})^2 \rangle &= \langle \underline{v}' \underline{K}^{-1} \underline{s} \underline{s}' \underline{K}^{-1} \underline{v} \rangle \\ &= \underline{v}' \underline{K}^{-1} \langle \underline{s} \underline{s}' \rangle \underline{K}^{-1} \underline{v} \\ &= \underline{v}' \underline{\bar{G}} \underline{v} \end{aligned} \quad (11)$$

Thus the deflection of $O(\underline{s}^2)$ is given by

$$\Delta E \left[O(\underline{s}^2) \right] = E_{S+N} \left[\frac{1}{2} \underline{v}' \underline{\bar{G}} \underline{v} \right] - E_N \left[\frac{1}{2} \underline{v}' \underline{\bar{G}} \underline{v} \right] \quad (12)$$

The first average gives

$$\begin{aligned} E_{S+N} \left[\frac{1}{2} \underline{v}' \underline{\bar{G}} \underline{v} \right] &= \frac{1}{2} \langle (\underline{s}' + \underline{n}') \underline{\bar{G}} (\underline{s} + \underline{n}) \rangle_{S+N} \\ &= \frac{1}{2} \langle \underline{s}' \underline{\bar{G}} \underline{s} \rangle_S + \langle \underline{s}' \underline{\bar{G}} \underline{n} \rangle_{S+N} + \frac{1}{2} \langle \underline{n}' \underline{\bar{G}} \underline{n} \rangle_N \\ &= \frac{1}{2} \sum_i \sum_j \langle s_i s_j \rangle_S \bar{G}_{ij} + \frac{1}{2} \sum_i \sum_j K_{ij} \bar{G}_{ij} \\ &= \frac{1}{2} \text{tr} (\underline{K} \underline{\bar{G}})^2 + \frac{1}{2} \text{tr} \underline{K} \underline{\bar{G}} \end{aligned} \quad (13)$$

The second average in Eq. (12) gives

$$\begin{aligned} E_N \left[\frac{1}{2} \underline{v}' \underline{\bar{G}} \underline{v} \right] &= \frac{1}{2} \langle \underline{n}' \underline{\bar{G}} \underline{n} \rangle_N \\ &= \frac{1}{2} \text{tr} \underline{K} \underline{\bar{G}} \end{aligned} \quad (14)$$

Thus

$$\boxed{\Delta E \left[O(\underline{s}^2) \right] = \frac{1}{2} \text{tr} (\underline{K} \underline{\bar{G}})^2} \quad (15)$$

Deflection of $O(\underline{s}^4)$

We will now calculate $\Delta E[O(\underline{s}^4)]$. The derivation can be simplified by noting that the average $E_{S+N}[\]$ contains $S \times S$ terms, $S \times N$ terms and $N \times N$ terms, and that the $N \times N$ terms drop out by subtraction in calculating the deflection. Thus we need only calculate the $S \times S$ and $S \times N$ terms. From Eqs. (9) and (11),

$$\Delta E[O(\underline{s}^4)] = \Delta E \left[\frac{1}{4!} \left\langle (\underline{v}' \underline{G} \underline{v})^2 \right\rangle - \frac{1}{8} (\underline{v}' \underline{\bar{G}} \underline{v})^2 \right] \quad (16)$$

where

$$\underline{G} = \underline{K}^{-1} \underline{s} \underline{s}' \underline{K}^{-1} \quad (17)$$

The deflection is calculated as follows:

$$\begin{aligned} \Delta E[O(\underline{s}^4)] &= \frac{1}{4!} \left\langle \frac{S}{(\underline{s}' \underline{G} \underline{s})^2} + 6 \frac{S}{(\underline{s}' \underline{G} \underline{s})} \frac{N}{(\underline{n}' \underline{G} \underline{n})} \right\rangle \\ &\quad - \frac{1}{8} \left[\frac{S}{(\underline{s}' \underline{\bar{G}} \underline{s})^2} + 4 \frac{S+N}{(\underline{s}' \underline{\bar{G}} \underline{n})^2} + 2 \frac{S}{(\underline{s}' \underline{\bar{G}} \underline{s})} \frac{N}{(\underline{n}' \underline{\bar{G}} \underline{n})} \right] \\ &= \frac{1}{4!} \left\langle \frac{S}{\text{tr}^2(\underline{s} \underline{s}' \underline{G})} + 6 \text{tr} \left(\left\langle \underline{s} \underline{s}' \right\rangle \underline{G} \right) \text{tr} (\underline{K} \underline{G}) \right\rangle \\ &\quad - \frac{1}{8} \left[\frac{S}{\text{tr}^2(\underline{s} \underline{s}' \underline{\bar{G}})} + 4 \text{tr} (\underline{K} \underline{\bar{G}})^3 + 2 \text{tr} (\underline{K} \underline{\bar{G}})^2 \text{tr} (\underline{K} \underline{\bar{G}}) \right] \quad (18) \end{aligned}$$

Equation (18) can be simplified by noting again that we shall be considering only white noise backgrounds, for which $\underline{K} = N \underline{I}$. Thus,

$$\left\langle 6 \text{tr} \left(\left\langle \underline{s} \underline{s}' \right\rangle \underline{G} \right) \text{tr} (\underline{K} \underline{G}) \right\rangle = \left\langle \frac{6}{N} \text{tr} \left(\left\langle \underline{s} \underline{s}' \right\rangle \underline{G} \right) \left(\sum_{i=1}^n s_i^2 \right) \right\rangle \quad (19)$$

Again noting that the averaging over frequency and phase will not affect the summation, which is proportional to the total energy in the desired signal, we can write

$$\begin{aligned}
 \left\langle 6 \operatorname{tr} \left(\left\langle \underline{s} \underline{s}' \right\rangle \underline{G} \right) \operatorname{tr} (\underline{K} \underline{G}) \right\rangle &= \left\langle 6 \operatorname{tr} \left(\left\langle \underline{s} \underline{s}' \right\rangle \underline{G} \right) \right\rangle \operatorname{tr} (\underline{K} \underline{G}) \\
 &= 6 \operatorname{tr} \left(\left\langle \underline{s} \underline{s}' \right\rangle \underline{G} \right) \operatorname{tr} (\underline{K} \underline{G}) \\
 &= 6 \operatorname{tr} (\underline{K} \underline{G})^2 \operatorname{tr} (\underline{K} \underline{G})
 \end{aligned} \tag{20}$$

and now

$$\Delta E \left[O(\underline{s}^4) \right] = \frac{1}{4!} \left\langle \frac{S}{\operatorname{tr}^2(\underline{s} \underline{s}' \underline{G})} \right\rangle - \frac{1}{8} \frac{S}{\operatorname{tr}^2(\underline{s} \underline{s}' \underline{G})} - \frac{1}{2} \operatorname{tr} (\underline{K} \underline{G})^3 \tag{21}$$

Finally we make use of the following matrix relationship. If matrices A and B are square and of the same order, and either A or B is the tensor product of a vector with itself, then

$$\operatorname{tr}^n(\underline{A} \underline{B}) = \operatorname{tr} (\underline{A} \underline{B})^n \tag{22}$$

(The proof of this statement is found in Appendix A.) In this case (s s') is such a tensor product and we can write

$$\Delta E \left[O(\underline{s}^4) \right] = \frac{1}{4!} \operatorname{tr} \left\langle \frac{S}{\underline{s} \underline{s}' \underline{G} \underline{s} \underline{s}' \underline{G}} \right\rangle - \frac{1}{8} \frac{S}{\operatorname{tr} (\underline{s} \underline{s}' \underline{G})^2} - \frac{1}{2} \operatorname{tr} (\underline{K} \underline{G})^3 \tag{23}$$

The average $\langle \rangle$ applies to matrices G, and the overline average, $\overline{}$, applies to matrices (s s').

Broadband White Noise

We shall consider only cases of broadband white noise with variance N .

For such a case,

$$\begin{aligned}\underline{K} &= N \underline{I} \\ \underline{G} &= \frac{1}{N^2} \underline{s} \underline{s}' = \frac{1}{N^2} \left\{ s_i s_j \right\} \\ \bar{\underline{G}} &= \frac{1}{N^2} \langle \underline{s} \underline{s}' \rangle = \frac{1}{N^2} \left\{ \langle s_i s_j \rangle \right\}\end{aligned}\tag{24}$$

Using Eqs. (24) we have

$$\begin{aligned}\Delta E \left[O(\underline{s}^2) \right] &= \frac{1}{2} \text{tr} (\underline{K} \bar{\underline{G}})^2 \\ &= \frac{1}{2N^2} \text{tr} \langle \underline{s} \underline{s}' \rangle^2\end{aligned}$$

Thus

$$\Delta E \left[O(\underline{s}^2) \right] = \frac{1}{2N^2} \sum_i \sum_j \langle s_i s_j \rangle^2\tag{25}$$

Similarly

$$\begin{aligned}\Delta E \left[O(\underline{s}^4) \right] &= \frac{1}{4! N^4} \sum_h \left\langle \sum_i \sum_j \sum_k \frac{v_h v_i s_i s_j v_j v_k s_k s_h}{v_h v_i s_i s_j v_j v_k s_k s_h} \right\rangle \\ &= \frac{1}{8N^4} \sum_h \sum_i \sum_j \sum_k \frac{v_h v_i \langle s_i s_j \rangle v_j v_k \langle s_k s_h \rangle}{v_h v_i s_i s_j v_j v_k s_k s_h} \\ &= \frac{1}{2N^3} \sum_i \sum_j \sum_k \langle s_i s_j \rangle \langle s_j s_k \rangle \langle s_k s_i \rangle\end{aligned}\tag{26}$$

$$\begin{aligned}
\Delta E \left[O(\underline{s}^4) \right] &= \frac{1}{4! N^4} \sum_h \sum_i \sum_j \sum_k \langle s_h s_i s_j s_k \rangle^2 \\
&\quad - \frac{1}{8N^4} \sum_h \sum_i \sum_j \sum_k \langle s_h s_i s_j s_k \rangle \langle s_i s_j \rangle \langle s_k s_h \rangle \\
&\quad - \frac{1}{2N^3} \sum_i \sum_j \sum_k \langle s_i s_j \rangle \langle s_j s_k \rangle \langle s_k s_i \rangle
\end{aligned} \tag{27}$$

All the summations are from 1 to n, the total number of time samples.

We will also calculate the average $E_S \left[\frac{1}{6!} \langle (\underline{s}' \underline{K}^{-1} \underline{v})^6 \rangle \right]$. This quantity is the most significant term in $\Delta E \left[O(\underline{s}^6) \right]$; the complete calculation of $\Delta E \left[O(\underline{s}^6) \right]$ will not be carried out here.

$$\begin{aligned}
E_S \left[\frac{1}{6!} \langle (\underline{s}' \underline{K}^{-1} \underline{v})^6 \rangle \right] &= \frac{1}{6!} \frac{S}{\langle (\underline{s}' \underline{G} \underline{s})^3 \rangle} \\
&= \frac{1}{6! N^6} \left\langle \sum_h \sum_i \sum_j \sum_k \sum_\ell \sum_m \frac{v_h v_i v_j v_k v_\ell v_m}{v_h v_i v_j v_k v_\ell v_m} s_h s_i s_j s_k s_\ell s_m \right\rangle
\end{aligned}$$

Thus

$$E_S \left[\frac{1}{6!} \langle (\underline{s}' \underline{K}^{-1} \underline{v})^6 \rangle \right] = \frac{1}{6! N^6} \sum_h \sum_i \sum_j \sum_k \sum_\ell \sum_m \langle s_h s_i s_j s_k s_\ell s_m \rangle^2 \tag{28}$$

The three specific signal cases outlined in Section I will now be considered in the following three sections.

IV. Broadband Gaussian Stochastic Signal

Let us consider the case in which both the noise and the desired signal are gaussian random processes, with flat spectra over the same frequency band, Ω rad/sec wide. If the signal has total average power $A^2/2$, then

$$\langle \underline{s} \underline{s}' \rangle = \frac{A^2}{2} \underline{I} \quad (29)$$

From Eq. (25),

$$\Delta E \left[O(\underline{s}^2) \right] = \frac{A^4}{8N^2} n \quad (30)$$

The number of samples is dictated by sampling theory:

$$\begin{aligned} n &= \frac{\Omega}{\pi} T \\ &= 2 \bar{\Phi} T \end{aligned} \quad (31)$$

In Eq. (31), $\bar{\Phi}$ is the noise (and signal) bandwidth in cps, and T is the observation time of the received signal. If the spectral level of the noise is N_0 v^2 /rad/sec,

$$\Delta E \left[O(\underline{s}^2) \right] = \frac{A^4}{4N_0^2 \Omega^2} \bar{\Phi} T \quad (32)$$

Letting

$$\frac{A^2}{2N_0 \Omega} = R_1 \quad (33)$$

we write finally

$$\Delta E \left[O(\underline{s}^2) \right] = R_1^2 \bar{\Phi} T \quad (34)$$

Since R_i is the pre-detection or "input" SNR, the deflection of the $O(\underline{s}^2)$ terms in this case is seen to be the square of the input SNR times the observation time, normalized with respect to the inverse of the bandwidth.

Now the deflection of $O(\underline{s}^4)$ is calculated using Eq. (27). If the signal is a gaussian random process,

$$\langle s_h s_i s_j s_k \rangle = \langle s_h s_i \rangle \langle s_j s_k \rangle + \langle s_h s_j \rangle \langle s_i s_k \rangle + \langle s_h s_k \rangle \langle s_i s_j \rangle \quad (35)$$

Thus

$$\begin{aligned} \Delta E \left[O(\underline{s}^4) \right] &= \frac{1}{4! N^4} \sum_h \sum_i \sum_j \sum_k \left[3 \langle s_h s_i \rangle^2 \langle s_j s_k \rangle^2 + 6 \langle s_h s_i \rangle \langle s_j s_k \rangle \langle s_h s_j \rangle \langle s_i s_k \rangle \right] \\ &\quad - \frac{1}{8N^4} \sum_h \sum_i \sum_j \sum_k \left[\langle s_i s_j \rangle^2 \langle s_k s_h \rangle^2 + 2 \langle s_h s_i \rangle \langle s_j s_k \rangle \langle s_i s_j \rangle \langle s_k s_h \rangle \right] \\ &\quad - \frac{1}{2N^3} \sum_i \sum_j \sum_k \langle s_i s_j \rangle \langle s_j s_k \rangle \langle s_k s_i \rangle \\ &= - \frac{1}{2N^3} \sum_i \sum_j \sum_k \langle s_i s_j \rangle \langle s_j s_k \rangle \langle s_k s_i \rangle \quad (36) \end{aligned}$$

If the signal spectrum is white with total average power $A^2/2$,

$$\begin{aligned} \Delta E \left[O(\underline{s}^4) \right] &= - \frac{A^6}{16N^3} n \\ &= - \frac{A^6}{8N_o^3 \Omega^3} \Phi^T \end{aligned}$$

and thus

$$\boxed{\Delta E \left[O(\underline{s}^4) \right] = - R_i^3 \Phi^T T} \quad (37)$$

It is of interest to compare this result with Eq. (34). If R_1 is much smaller than unity, the deflection of $O(\underline{s}^4)$ may be considered negligible with respect to the deflection of $O(\underline{s}^2)$.

V. Narrowband Gaussian Signal

In this section the desired signal is assumed to be a narrowband gaussian random process with total average power $A^2/2$, bandwidth Ω_b ad/sec, and center frequency ω_c rad/sec, where ω_c may lie anywhere in a frequency band Ω rad/sec wide. For simplicity, the signal spectrum is assumed to be flat over Ω_b and the p.d.f. for ω_c flat over Ω . These relationships are indicated in Fig. 1. The center frequency of the Ω -band is ω_0 .

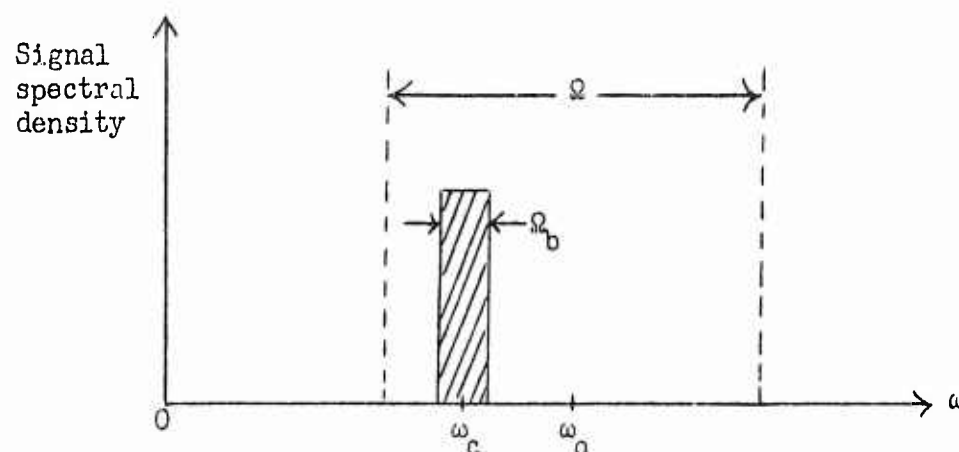


Figure 1

The a.c.f. of the signal, a function of ω_c , is

$$R_s(t_i - t_j) = \frac{A^2}{2} \text{sinc } \bar{\Omega}_b(t_i - t_j) \cos \omega_c(t_i - t_j) \quad (38)$$

where

$$\text{sinc } x = \frac{\sin x}{\pi x}$$

and

$$\bar{\Omega}_b = \frac{\Omega_b}{2\pi}$$

Averaging the right side of Eq. (38) with respect to the p.d.f. of ω_c over the Ω -band, we have

$$\langle \underline{s} \underline{s}' \rangle = \left\{ \frac{A^2}{2} \text{sinc } \bar{\Phi}_b(t_i - t_j) \text{sinc } \bar{\Phi}(t_i - t_j) \cos \omega_o(t_i - t_j) \right\} \quad (39)$$

From Eq. (25),

$$\Delta E \left[O(\underline{s}^2) \right] = \frac{A^4}{8N^2} \sum_i \sum_j \text{sinc}^2 \bar{\Phi}_b(t_i - t_j) \text{sinc}^2 \bar{\Phi}(t_i - t_j) \cos^2 \omega_o(t_i - t_j) \quad (40)$$

As an approximation, for $\omega_o \gg \Omega$ and $\omega_o T \gg 1$, we replace $\cos^2 \omega_o(t_i - t_j)$ by its average value, $\frac{1}{2}$, and

$$\Delta E \left[O(\underline{s}^2) \right] \approx \frac{A^4}{16N^2} \sum_i \sum_j \text{sinc}^2 \bar{\Phi}_b(t_i - t_j) \text{sinc}^2 \bar{\Phi}(t_i - t_j) \quad (41)$$

The double summation is then replaced by a double integration

$$\begin{aligned} \Delta E \left[O(\underline{s}^2) \right] &\approx \frac{A^4}{16N^2} \cdot \frac{\Omega^2}{\pi^2} \int_0^T dt \int_0^T d\sigma \text{sinc}^2 \bar{\Phi}_b(t - \sigma) \text{sinc}^2 \bar{\Phi}(t - \sigma) \\ &\approx \frac{A^4}{16N_o^2 \Omega^2} \int_0^{\bar{\Phi}T} dx \int_0^{\bar{\Phi}T} dy \text{sinc}^2 b(x - y) \text{sinc}^2(x - y) \end{aligned} \quad (42)$$

where

$$b = \frac{\bar{\Phi}_b}{\bar{\Phi}}$$

If the integration time is long with respect to the inverse of the signal bandwidth and the signal bandwidth is narrow with respect to the overall band of frequency uncertainty, that is, $\bar{\Phi}T \gg \bar{\Phi}_bT \gg 1$, then a reasonable further approximation is

$$\Delta E \left[O(\underline{s}^2) \right] \approx \frac{A^4}{4N_0^2 \Omega^2} \bar{\Phi} T$$

or

$$\Delta E \left[O(\underline{s}^2) \right] \approx R_1^2 \bar{\Phi} T \quad (43)$$

The calculation of $\Delta E \left[O(\underline{s}^4) \right]$ for this signal case is considerably more involved than for the broadband signal case considered in Section IV; therefore only the final result will be presented here, the details of the calculation being left to Appendix B.

Again assuming that the signal is very narrowband and that the integration time is long, that is, $\bar{\Phi} T \gg \bar{\Phi}_b T \gg 1$, the work of Appendix B shows that

$$\Delta E \left[O(\underline{s}^4) \right] \approx \frac{1}{6} R_1^4 \left[\frac{2}{b} (\bar{\Phi} T)^2 + \frac{3}{b^2} (\bar{\Phi} T) \right] - \frac{1}{2} R_1^4 \left[(\bar{\Phi} T)^2 + \frac{3}{4b} (\bar{\Phi} T) \right] - R_1^4 (\bar{\Phi} T) \quad (44)$$

On comparing Eq. (44) with Eq. (43) it is seen that $\Delta E \left[O(\underline{s}^4) \right]$ depends upon a higher power of the input SNR than does $\Delta E \left[O(\underline{s}^2) \right]$, as was true in the broadband gaussian signal case. However, while $\Delta E \left[O(\underline{s}^2) \right]$ depends linearly upon integration time, $\Delta E \left[O(\underline{s}^4) \right]$ contains terms which grow as the square of integration time. We see therefore that for any value of R_1 , however small, the magnitude of the deflection of $O(\underline{s}^4)$ can be made equal to or greater than that of $O(\underline{s}^2)$ by making the integration time sufficiently long.

Example

As an example, let $R_1 = .1$ and $b = .1$. From Eqs. (43) and (44),

$$\Delta E \left[O(\underline{s}^2) \right] \approx (.01) \bar{\Phi} T$$

$$\Delta E \left[O(\underline{s}^4) \right] \approx (.0003)(\bar{\Phi} T)^2 + (.004) \bar{\Phi} T$$

If we let $\bar{\Phi} T = 100$, we have

$$\Delta E \left[O(\underline{s}^2) \right] = 1.0$$

$$\Delta E \left[O(\underline{s}^4) \right] = 3.4$$

And if $\bar{\Phi} T = 200$,

$$\Delta E \left[O(\underline{s}^2) \right] = 2.0$$

$$\Delta E \left[O(\underline{s}^4) \right] = 12.8$$

We see therefore that for this case of a narrowband gaussian signal whose center frequency is uncertain over a wider frequency band, terms $O(\underline{s}^4)$ and terms of higher order in Eq. (7) cannot be considered negligible simply on the basis of low input SNR. Such an approximation might be highly inaccurate if the post-detection integration time is long, as required in threshold situations.

VI. Sinusoid of Unknown Frequency and Phase

Here we assume that the desired signal is a sinusoid whose amplitude is constant over the observation time of the received signal. The phase of the sinusoid is unknown and its frequency is known only to lie within a frequency band Ω rad/sec wide. For convenience, the phase and frequency are assumed to have uniform p.d.f.'s over $0, 2\pi$ and over the Ω -band, respectively.

This case can be treated as a limiting form of the narrowband signal case considered in Section V if we let the signal bandwidth $\Phi_b \rightarrow 0$. If Φ_b is vanishingly small, the sinusoid will have a constant amplitude over any single observation interval, and the amplitude will have a Rayleigh p.d.f. over the ensemble of all such observation intervals. The total signal power, averaged statistically over the ensemble, is $A^2/2$. It can easily be shown that the sinusoid will have an r.m.s. amplitude A ; therefore through second-order statistics (in \underline{s}), this case is identical to that considered in Progress Report No. 8.

From Eq. (39), if $\Phi_b \rightarrow 0$,

$$\langle \underline{s} \underline{s}' \rangle = \left\{ \frac{A^2}{2} \text{sinc } \Phi (t_i - t_j) \cos \omega_0 (t_i - t_j) \right\} \quad (45)$$

Letting $b \rightarrow 0$ in Eq. (42) does not alter the approximation embodied in Eq. (43), and

$$\Delta E \left[O(\underline{s}^2) \right] \approx R_1^2 (\Phi T) \quad (46)$$

The deflection of $O(\underline{s}^4)$ can be obtained by letting $\Phi_b \rightarrow 0$ (and hence $b \rightarrow 0$) at appropriate points in the derivation in Appendix B. This procedure is carried out in detail in Appendix C, and only the results are stated here. From Appendix C, we have

$$\Delta E \left[O(\underline{s}^4) \right] = \frac{16}{4!} R_1^4 (\Phi T)^3 - R_1^4 (\Phi T)^2 - R_1^3 (\Phi T) \quad (47)$$

Again, if Eqs. (46) and (47) are compared, it is seen that the deflection of $O(\underline{s}^4)$ depends upon higher powers of the integration time and can become appreciably large with respect to $\Delta E \left[O(\underline{s}^2) \right]$ when the integration time is made long.

Deflection of Higher-Order Terms

It is of interest to see the manner in which deflections of higher-order terms in the power series depend upon input SNR and post-detection integration time. For this purpose, the average $E_S \left\langle \frac{1}{6!} (\underline{s}' \underline{K}^{-1} \underline{v})^6 \right\rangle$ is calculated in Appendix D for the sinusoidal signal case. This term is the most significant contribution to $\Delta E \left[O(\underline{s}^6) \right]$ in this case for long integration time. From this result the behavior of corresponding terms in higher-order deflections is deduced. From Appendix D,

$$E_S \left\langle \frac{1}{6!} (\underline{s}' \underline{K}^{-1} \underline{v})^6 \right\rangle \approx \frac{1}{3} R_1^6 (\Phi T)^5 \quad (48)$$

and for a p^{th} -order term,

$$E_S \left\langle \frac{1}{p!} (\underline{s}' \underline{K}^{-1} \underline{v})^p \right\rangle \approx \frac{2^{\frac{p}{2}}}{(\frac{p}{2} + 1)!} R_1^p (\Phi T)^{p-1} \quad (49)$$

$p \text{ even}$

VII. Conclusions and Remarks

This report has considered, by means of some specific cases, the question of the contribution of higher-order terms in a power series expansion of $\log \ell(\underline{y})$, the output of an optimum detector.

The results of Section IV showed that if the desired signal is a gaussian random process with a flat spectrum over a known frequency band, the deflections of terms of all orders grow linearly with integration time and the higher-order deflections have as coefficients progressively higher powers of the input SNR. Therefore when the input SNR is much smaller than unity, the major contribution to $\log \ell(\underline{y})$ is from the $O(\underline{s}^2)$ term and higher-order terms can be neglected. This was the approximation made by Tuteur³ in which the operation of the optimum detector for such a signal was represented by the lowest-order term in the series (equivalent to squaring the received signal and integrating over the observation interval $0, T$). It is clear that this approximation is justified for low input SNR, regardless of the length of T .

In Section V the gaussian signal was assumed to be narrowband with an unknown center frequency, where the band of center frequency uncertainty was assumed considerably larger than the signal bandwidth. In that case it was found that terms of higher-order than $O(\underline{s}^2)$ could not be neglected when the integration time became appreciably long.

The same observation applies to the limiting case of a sinusoidal signal, considered in Section VI. In these latter two cases, then, if one were to construct an approximation to the optimum detector with the power series in mind, a certain number of higher-order terms in Eq. (7),

and the corresponding operations on the received signal, would have to be incorporated into the detector. The number of terms to be included would depend upon the input SNR and the integration time.

This is not suggested as a technique for constructing the optimum detector, but it is of interest to consider the implication of including certain higher-order operations. Suppose as an example that the desired signal is a narrowband incoherent signal whose center frequency is equally likely to be any one of m known frequencies. The lowest-order term in the series [See Eqs. (7), (11)] is then

$$\frac{1}{2} \langle \underline{v}' \underline{G} \underline{v} \rangle = \frac{1}{2m} \sum_{i=1}^m \underline{v}' \underline{G}_i \underline{v}$$

where \underline{G}_i is a function of the i^{th} frequency. This expression indicates a quadratic operation on the received signal at each of the m frequencies, followed by a summation of all these quantities. The most significant $O(s^4)$ term becomes

$$\frac{1}{4!} \langle (\underline{v}' \underline{G} \underline{v})^2 \rangle = \frac{1}{4!m} \sum_{i=1}^m (\underline{v}' \underline{G}_i \underline{v})^2$$

Adding to these the corresponding terms at higher orders of s , it is seen that the optimum detector calls for the calculation of $\underline{v}' \underline{G}_i \underline{v}$ at each frequency, followed by a nonlinear operation on $\underline{v}' \underline{G}_i \underline{v}$ and finally a summation of the m quantities. This suggests band-splitting with a bank of m filters and detection of the separate filter outputs, which is the scheme one would intuitively choose to detect a narrowband signal with unknown frequency.

Some recent results indicate that such a band-splitting scheme represents a very good approximation to the optimum detector for such a signal. Reports on these results are forthcoming.

Appendix A A Special Trace Relationship

Matrices A and B are square matrices of the same order. We wish to show that if B is a tensor product of a vector b times itself, i.e., if

$$\underline{B} = \underline{b} \times \underline{b} = \underline{b} \underline{b}' = \left\{ b_i b_j \right\} \quad (\text{A-1})$$

then

$$\text{tr}(\underline{A} \underline{B})^2 = \text{tr}^2(\underline{A} \underline{B}) \quad (\text{A-2})$$

Proceeding formally, we have

$$\begin{aligned} \text{tr}(\underline{A} \underline{B})^2 &= \text{tr}(\underline{A} \underline{B} \underline{A} \underline{B}) \\ &= \text{tr} \left\{ \sum_i \sum_j \sum_k A_{hi} B_{ij} A_{jk} B_{km} \right\} \\ &= \sum_{h=m} \left[\sum_i \sum_j \sum_k A_{hi} B_{ij} A_{jk} B_{km} \right] \\ &= \sum_h \sum_i \sum_j \sum_k A_{hi} B_{ij} A_{jk} B_{kh} \\ &= \sum_h \sum_i \left(\sum_i A_{hi} B_{ij} \right) \left(\sum_k A_{jk} B_{kh} \right) \end{aligned} \quad (\text{A-3})$$

If

$$B_{ij} = b_i b_j$$

and

$$B_{kh} = b_k b_h$$

$$\begin{aligned}
\text{tr}(\underline{A} \underline{B})^2 &= \sum_h \sum_j \left(\sum_i A_{hi} b_i b_j \right) \left(\sum_k A_{jk} b_k b_h \right) \\
&= \left(\sum_h \sum_i A_{hi} b_i b_h \right) \left(\sum_j \sum_k A_{jk} b_k b_j \right) \\
&= \text{tr}^2(\underline{A} \underline{B})
\end{aligned} \tag{A-4}$$

No special properties, such as symmetry, are required of the matrix \underline{A} .

In general,

$$\begin{aligned}
\text{tr}(\underline{A} \underline{B})^m &= \sum_{i_1=i_{2m+1}} \left\{ \sum_{i_2} \sum_{i_3} \dots \sum_{i_{2m}} A_{i_1 i_2} B_{i_2 i_3} A_{i_3 i_4} B_{i_4 i_5} \dots A_{i_{2m-1} i_{2m}} B_{i_{2m} i_{2m+1}} \right\} \\
&= \sum_{i_1} \sum_{i_2} \dots \sum_{i_{2m}} \left[A_{i_1 i_2} A_{i_3 i_4} \dots A_{i_{2m-1} i_{2m}} B_{i_2 i_3} B_{i_4 i_5} \dots B_{i_{2m} i_1} \right]
\end{aligned} \tag{A-5}$$

If

$$B_{jk} = b_j b_k$$

$$\begin{aligned}
\text{tr}(\underline{A} \underline{B})^m &= \left(\sum_{i_1} \sum_{i_2} A_{i_1 i_2} b_{i_1} b_{i_2} \right) \left(\sum_{i_3} \sum_{i_4} A_{i_3 i_4} b_{i_3} b_{i_4} \right) \dots \\
&\quad \left(\sum_{i_{2m-1}} \sum_{i_{2m}} A_{i_{2m-1} i_{2m}} b_{i_{2m-1}} b_{i_{2m}} \right) \\
&= \text{tr}^m(\underline{A} \underline{B})
\end{aligned} \tag{A-6}$$

Appendix B Deflection of $O(\underline{s}^4)$ --Narrowband Gaussian Signal

The total deflection of terms of order \underline{s}^4 , as given by Eq. (27), is

$$\begin{aligned} \Delta E \left[O(\underline{s}^4) \right] &= \frac{1}{4! N^4} \sum_h \sum_i \sum_j \sum_k \langle s_h s_i s_j s_k \rangle^2 \\ &\quad - \frac{1}{8N^4} \sum_h \sum_i \sum_j \sum_k \langle s_h s_i s_j s_k \rangle \langle s_i s_j \rangle \langle s_k s_h \rangle \\ &\quad - \frac{1}{2N^3} \sum_i \sum_j \sum_k \langle s_i s_j \rangle \langle s_j s_k \rangle \langle s_k s_i \rangle \end{aligned} \quad (B-1)$$

For convenience the three terms in Eq. (B-1) will be considered separately.

First Term

The signal spectrum has total average power $A^2/2$ and is flat over a narrow band Ω_b rad/sec wide, centered at the unknown frequency ω_c rad/sec. Since $s(t)$ is a sample function of a gaussian random process,

$$\begin{aligned} \langle s_h s_i s_j s_k \rangle &= \left\langle \overline{s_h s_i} \overline{s_j s_k} + \overline{s_h s_j} \overline{s_i s_k} + \overline{s_i s_j} \overline{s_h s_k} \right\rangle_{\omega_c} \\ &= \frac{A^4}{4} \left\langle \text{sinc } \Phi_b(t_h - t_i) \cos \omega_c(t_h - t_i) \text{sinc } \Phi_b(t_j - t_k) \cos \omega_c(t_j - t_k) \right. \\ &\quad + \text{sinc } \Phi_b(t_h - t_j) \cos \omega_c(t_h - t_j) \text{sinc } \Phi_b(t_i - t_k) \cos \omega_c(t_i - t_k) \\ &\quad \left. + \text{sinc } \Phi_b(t_i - t_j) \cos \omega_c(t_i - t_j) \text{sinc } \Phi_b(t_h - t_k) \cos \omega_c(t_h - t_k) \right\rangle_{\omega_c} \end{aligned} \quad (B-2)$$

where

$$\Phi_b = \frac{\Omega_b}{2\pi} \quad \text{cps} \quad (B-3)$$

The center frequency ω_c has a flat p.d.f. over a band Ω rad/sec wide, and the band is centered on the frequency ω_o . Thus if the average is taken over ω_c ,

$$\begin{aligned} \langle s_h s_i s_j s_k \rangle = \frac{A^4}{8} & \left[\text{sinc } \overline{\Phi}_b(t_h - t_i) \text{sinc } \overline{\Phi}_b(t_j - t_k) \text{sinc } \overline{\Phi}(t_h - t_i + t_j - t_k) \cos \omega_o(t_h - t_i + t_j - t_k) \right. \\ & + \text{sinc } \overline{\Phi}_b(t_h - t_i) \text{sinc } \overline{\Phi}_b(t_j - t_k) \text{sinc } \overline{\Phi}(t_h - t_i - t_j + t_k) \cos \omega_o(t_h - t_i - t_j + t_k) \\ & + \text{sinc } \overline{\Phi}_b(t_h - t_j) \text{sinc } \overline{\Phi}_b(t_i - t_k) \text{sinc } \overline{\Phi}(t_h - t_j + t_i - t_k) \cos \omega_o(t_h - t_j + t_i - t_k) \\ & + \text{sinc } \overline{\Phi}_b(t_h - t_j) \text{sinc } \overline{\Phi}_b(t_i - t_k) \text{sinc } \overline{\Phi}(t_h - t_j - t_i + t_k) \cos \omega_o(t_h - t_j - t_i + t_k) \\ & + \text{sinc } \overline{\Phi}_b(t_i - t_j) \text{sinc } \overline{\Phi}_b(t_h - t_k) \text{sinc } \overline{\Phi}(t_i - t_j + t_h - t_k) \cos \omega_o(t_i - t_j + t_h - t_k) \\ & \left. + \text{sinc } \overline{\Phi}_b(t_i - t_j) \text{sinc } \overline{\Phi}_b(t_h - t_k) \text{sinc } \overline{\Phi}(t_i - t_j - t_h + t_k) \cos \omega_o(t_i - t_j - t_h + t_k) \right] \end{aligned} \quad (B-4)$$

where

$$\overline{\Phi} = \frac{\Omega}{2\pi} \text{ cps} \quad (B-5)$$

The first term in Eq. (B-1) then becomes

$$\begin{aligned}
 & \frac{1}{L! N!} \sum_h \sum_i \sum_j \sum_k \langle s_{h_i} s_{j_k} s_{j_k} \rangle^2 \\
 & \approx \frac{A^8}{64 \cdot L! N!} \sum_h \sum_i \sum_j \sum_k \left[3 \operatorname{sinc}^2 \bar{\Phi}_b(t_h - t_i) \operatorname{sinc}^2 \bar{\Phi}_b(t_j - t_k) \operatorname{sinc}^2 \bar{\Phi}(t_h - t_i + t_j - t_k) \cos^2 \omega_0(t_h - t_i + t_j - t_k) \right. \\
 & \quad + 3 \operatorname{sinc}^2 \bar{\Phi}_b(t_h - t_i) \operatorname{sinc}^2 \bar{\Phi}_b(t_j - t_k) \operatorname{sinc}^2 \bar{\Phi}(t_h - t_i - t_j + t_k) \cos^2 \omega_0(t_h - t_i - t_j + t_k) \\
 & \quad + 2 \operatorname{sinc} \bar{\Phi}_b(t_h - t_i) \operatorname{sinc} \bar{\Phi}_b(t_j - t_k) \operatorname{sinc} \bar{\Phi}_b(t_i - t_j) \operatorname{sinc}^2 \bar{\Phi}(t_h - t_i + t_j - t_k) \cos^2 \omega_0(t_h - t_i + t_j - t_k) \\
 & \quad + 2 \operatorname{sinc} \bar{\Phi}_b(t_h - t_i) \operatorname{sinc} \bar{\Phi}_b(t_j - t_k) \operatorname{sinc} \bar{\Phi}_b(t_i - t_j) \operatorname{sinc}^2 \bar{\Phi}(t_h - t_i - t_j + t_k) \cos^2 \omega_0(t_h - t_i - t_j + t_k) \\
 & \quad \left. + 2 \operatorname{sinc} \bar{\Phi}_b(t_h - t_i) \operatorname{sinc} \bar{\Phi}_b(t_i - t_k) \operatorname{sinc} \bar{\Phi}_b(t_j - t_j) \operatorname{sinc}^2 \bar{\Phi}(t_h - t_i + t_j - t_k) \cos^2 \omega_0(t_h - t_i + t_j - t_k) \right] \\
 & \quad \left. + 2 \operatorname{sinc} \bar{\Phi}_b(t_h - t_i) \operatorname{sinc} \bar{\Phi}_b(t_i - t_k) \operatorname{sinc} \bar{\Phi}_b(t_j - t_j) \operatorname{sinc}^2 \bar{\Phi}(t_h - t_i - t_j + t_k) \cos^2 \omega_0(t_h - t_i - t_j + t_k) \right] \\
 & \quad (B-6)
 \end{aligned}$$

Other cross-product terms from the square of the right side of Eq. (B-4) contain cosine factors of the form $\cos 2\omega_0(t_h - t_i)$ or $\cos 2\omega_0(t_j - t_k)$. Such terms will go to approximately zero in the summation over h, i, j, k and are simply left out of Eq. (B-6).

From symmetry considerations the first two four-dimensional sums in Eq. (B-6) will yield the same result; the last three terms will also yield identical results. Thus only two summations need be carried out. Starting with the first term in Eq. (B-6), we have

$$\begin{aligned}
 & \sum_h \sum_i \sum_j \sum_k 3 \operatorname{sinc}^2 \frac{\Phi T}{b} (t_h - t_i) \operatorname{sinc}^2 \frac{\Phi T}{b} (t_j - t_k) \operatorname{sinc}^2 \frac{\Phi T}{b} (t_h - t_i + t_j - t_k) \cos^2 \omega_0 (t_h - t_i + t_j - t_k) \\
 & \approx \frac{3}{2} (16) \int_0^{\Phi T} ds \int_0^{\Phi T} dt \int_0^{\Phi T} du \int_0^{\Phi T} dv \operatorname{sinc}^2 b(s-t) \operatorname{sinc}^2 b(u-v) \operatorname{sinc}^2 (s-t+u-v) \\
 & \approx 24 \int_0^{\Phi T} ds \int_0^{\Phi T} dt \int_0^{\Phi T} du \operatorname{sinc}^2 b(s-t) \operatorname{sinc}^2 b(u-s+t-u) \quad \text{for } 0 \leq s-t+u \leq \Phi T \\
 & = 24 \int_0^{\Phi T} ds \int_0^{\Phi T} dt \int_0^{\Phi T} du \operatorname{sinc}^4 b(s-t) \quad \text{(B-7)} \\
 & \approx 24 \frac{\Phi T}{b^2} \int_0^{b\Phi T} dx \int_0^{b\Phi T} dy \operatorname{sinc}^4 (x-y)^* \\
 & \approx 24 \left(\frac{\Phi T}{b^2} \right) \left(\frac{2}{3} \right) \int_0^{b\Phi T} dx \quad \text{for } 0 \leq x \leq b\Phi T \\
 & \approx 24 \left(\frac{\Phi T}{b^2} \right) \left(\frac{2}{3} \right) (b \Phi T) = \frac{16}{b} (\Phi T)^2 \quad \text{(B-8)}
 \end{aligned}$$

*See Reference 4, Table 157, Integral No. 27.

where $b = \bar{\Phi}_b / \bar{\Phi}$. The approximations are good for long integration time, that is, for

$$\bar{\Phi} T \gg \bar{\Phi}_b T \gg 1$$

Taking the third term in Eq. (B-6),

$$\sum_h \sum_i \sum_j \sum_k 2 \operatorname{sinc} \bar{\Phi}_b(t_h - t_1) \operatorname{sinc} \bar{\Phi}_b(t_j - t_k) \operatorname{sinc} \bar{\Phi}_b(t_1 - t_j) \operatorname{sinc} \bar{\Phi}_b(t_h - t_k)$$

$$\operatorname{sinc}^2 \bar{\Phi}(t_h - t_1 + t_j - t_k) \cos^2 \omega_0(t_h - t_1 + t_j - t_k)$$

$$\approx 16 \int_0^{\bar{\Phi} T} ds \int_0^{\bar{\Phi} T} dt \int_0^{\bar{\Phi} T} du \int_0^{\bar{\Phi} T} dv \operatorname{sinc} b(s-t) \operatorname{sinc} b(u-v) \operatorname{sinc} b(t-u) \operatorname{sinc} b(s-v) \operatorname{sinc}^2(s-t+u-v)$$

$$\approx 16 \int_0^{\bar{\Phi} T} ds \int_0^{\bar{\Phi} T} dt \int_0^{\bar{\Phi} T} du \operatorname{sinc}^2 b(s-t) \operatorname{sinc}^2 b(t-u) \quad \text{for } 0 \leq s-t+u \leq \bar{\Phi} T \quad (\text{B-9})$$

$$= \frac{16}{b^3} \int_0^{b\bar{\Phi} T} dx \int_0^{b\bar{\Phi} T} dy \int_0^{b\bar{\Phi} T} dz \operatorname{sinc}^2(x-y) \operatorname{sinc}^2(y-z)$$

$$\approx \frac{16}{b^3} \int_0^{b\bar{\Phi} T} dx \int_0^{b\bar{\Phi} T} dy \operatorname{sinc}^2(x-y) \quad \text{for } 0 \leq y \leq b\bar{\Phi} T$$

$$\approx \frac{16}{b^3} (b \bar{\Phi} T)$$

$$= \frac{16}{b^2} (\bar{\Phi} T) \quad (\text{B-10})$$

Thus the first term in Eq. (B-1) becomes

$$\frac{1}{4! N^4} \sum_h \sum_i \sum_j \sum_k \langle s_h s_i s_j s_k \rangle^2 \approx \frac{1}{4! N^4} \cdot \frac{A^8}{64} \left[\frac{32}{b} (\overline{\Phi T})^2 + \frac{48}{b^2} (\overline{\Phi T}) \right]$$

or

$$\boxed{\frac{1}{4! N^4} \sum_h \sum_i \sum_j \sum_k \langle s_h s_i s_j s_k \rangle^2 \approx \frac{1}{6} (R_i)^4 \left[\frac{2}{b} (\overline{\Phi T})^2 + \frac{3}{b^2} (\overline{\Phi T}) \right]} \quad (B-11)$$

Second Term

The average $\langle s_h s_i s_j s_k \rangle$ is given by Eq. (B-4), and $\langle s_h s_i \rangle$ and $\langle s_j s_k \rangle$ are obtained using Eq. (39), Section V. Multiplying these together to form the second term in Eq. (B-1), and summing over h, i, j, k , we find that only four of the cross-products will produce non-zero results.

Summing the first of these four cross-products, we have

$$\begin{aligned} & - \frac{A^8}{32 \cdot 8N^4} \sum_h \sum_i \sum_j \sum_k \text{sinc } \overline{\Phi}_b(t_h - t_i) \text{sinc } \overline{\Phi}_b(t_j - t_k) \text{sinc } \overline{\Phi}(t_h - t_i + t_j - t_k) \cos \omega_o(t_h - t_i + t_j - t_k) \\ & \quad \cdot \text{sinc } \overline{\Phi}_b(t_h - t_i) \text{sinc } \overline{\Phi}(t_h - t_i) \cos \omega_o(t_h - t_i) \\ & \quad \cdot \text{sinc } \overline{\Phi}_b(t_j - t_k) \text{sinc } \overline{\Phi}(t_j - t_k) \cos \omega_o(t_j - t_k) \\ & = - \frac{A^8}{32 \cdot 8N^4} \sum_h \sum_i \sum_j \sum_k \text{sinc}^2 \overline{\Phi}_b(t_h - t_i) \text{sinc}^2 \overline{\Phi}_b(t_j - t_k) \text{sinc } \overline{\Phi}(t_h - t_i) \text{sinc } \overline{\Phi}(t_j - t_k) \\ & \quad \cdot \text{sinc } \overline{\Phi}(t_h - t_i + t_j - t_k) \cos \omega_o(t_h - t_i) \cos \omega_o(t_j - t_k) \\ & \quad \cdot \cos \omega_o(t_h - t_i + t_j - t_k) \end{aligned}$$

$$\begin{aligned}
&= - \frac{A^8}{64 \cdot 8N^4} \sum_h \sum_i \sum_j \sum_k \left[\text{sinc}^2 \bar{\Phi}_b(t_h - t_i) \text{sinc}^2 \bar{\Phi}_b(t_j - t_k) \text{sinc} \bar{\Phi}(t_h - t_i) \text{sinc} \bar{\Phi}(t_j - t_k) \right. \\
&\quad \cdot \text{sinc} \bar{\Phi}(t_h - t_i + t_j - t_k) \cos^2 \omega_0(t_h - t_i + t_j - t_k) \\
&\quad + \text{sinc}^2 \bar{\Phi}_b(t_h - t_i) \text{sinc}^2 \bar{\Phi}_b(t_j - t_k) \text{sinc} \bar{\Phi}(t_h - t_i) \text{sinc} \bar{\Phi}(t_j - t_k) \\
&\quad \cdot \text{sinc} \bar{\Phi}(t_h - t_i + t_j - t_k) \cos \omega_0(t_h - t_i - t_j + t_k) \cos \omega_0(t_h - t_i + t_j - t_k) \left. \right] \\
&= - \frac{A^8}{128 \cdot 8N^4} (16) \int_0^{\bar{\Phi}T} ds \int_0^{\bar{\Phi}T} dt \int_0^{\bar{\Phi}T} du \int_0^{\bar{\Phi}T} dv \text{sinc}^2 b(s-t) \text{sinc}^2 b(u-v) \text{sinc}(s-t) \text{sinc}(u-v) \\
&\quad \cdot \text{sinc}(s-t+u-v) \\
&\approx - \frac{A^8}{128 \cdot 8N^4} (16) \int_0^{\bar{\Phi}T} ds \int_0^{\bar{\Phi}T} dt \int_0^{\bar{\Phi}T} du \text{sinc}^4 b(s-t) \text{sinc}^2(u-t) \\
&\quad 0 \leq s-t+u \leq \bar{\Phi}T \\
&\approx - \frac{A^8}{128 \cdot 8N^4} (16) (\bar{\Phi}T) \int_0^{\bar{\Phi}T} ds \int_0^{\bar{\Phi}T} dt \text{sinc}^4 b(s-t) \text{sinc}^2(s-t) \\
&\approx - \frac{A^8}{128 \cdot 8N^4} (16) (\bar{\Phi}T)^2 \\
&= - \frac{A^8}{64N^4 \Omega^2} (\bar{\Phi}T)^2 \tag{B-12}
\end{aligned}$$

Again the approximations assume $\bar{\Phi}T \gg b\bar{\Phi}T \gg 1$. The second of the four cross-product terms will also yield the result given by Eq. (B-12).

The third cross-product gives

$$\begin{aligned}
 & - \frac{A^8}{32 \cdot 8N^4} \sum_h \sum_i \sum_j \sum_k \operatorname{sinc} \bar{\Phi}_b(t_i - t_j) \operatorname{sinc} \bar{\Phi}_b(t_h - t_k) \operatorname{sinc} \bar{\Phi}(t_i - t_j - t_h + t_k) \cos \omega_o(t_i - t_j - t_h + t_k) \\
 & \quad \cdot \operatorname{sinc} \bar{\Phi}_b(t_h - t_i) \operatorname{sinc} \bar{\Phi}(t_h - t_i) \cos \omega_o(t_h - t_i) \\
 & \quad \cdot \operatorname{sinc} \bar{\Phi}_b(t_j - t_k) \operatorname{sinc} \bar{\Phi}(t_j - t_k) \cos \omega_o(t_j - t_k) \\
 & = - \frac{A^8}{64 \cdot 8N^4} \sum_h \sum_i \sum_j \sum_k \operatorname{sinc} \bar{\Phi}_b(t_i - t_j) \operatorname{sinc} \bar{\Phi}_b(t_h - t_k) \operatorname{sinc} \bar{\Phi}_b(t_h - t_i) \operatorname{sinc} \bar{\Phi}_b(t_j - t_k) \\
 & \quad \cdot \operatorname{sinc} \bar{\Phi}(t_h - t_i) \operatorname{sinc} \bar{\Phi}(t_j - t_k) \operatorname{sinc} \bar{\Phi}(t_i - t_j - t_h + t_k) \\
 & \quad \cdot \cos \omega_o(t_i - t_j - t_h + t_k) \left[\cos \omega_o(t_h - t_i + t_j - t_k) + \cos \omega_o(t_h - t_i - t_j + t_k) \right] \\
 & \approx - \frac{A^8}{128 \cdot 8N^4} (16) \int_0^{\bar{\Phi}T} ds \int_0^{\bar{\Phi}T} dt \int_0^{\bar{\Phi}T} du \int_0^{\bar{\Phi}T} dv \operatorname{sinc} b(t-u) \operatorname{sinc} b(s-v) \operatorname{sinc} b(s-t) \operatorname{sinc} b(u-v) \\
 & \quad \cdot \operatorname{sinc}(s-t) \operatorname{sinc}(u-v) \operatorname{sinc}(t-u-s+v) \\
 & \approx - \frac{A^8}{64N^4} \int_0^{\bar{\Phi}T} ds \int_0^{\bar{\Phi}T} dt \int_0^{\bar{\Phi}T} du \operatorname{sinc} b(t-u) \operatorname{sinc} b(s-t) \operatorname{sinc}(s-t) \operatorname{sinc}(s-t) \\
 & \quad \cdot \operatorname{sinc} b(s-t) \operatorname{sinc} b(t-u) \operatorname{sinc} b(s-u) \\
 & \qquad \qquad \qquad 0 \leq s+u-t \leq \bar{\Phi}T \\
 & = - \frac{A^8}{64N^4} \int_0^{\bar{\Phi}T} ds \int_0^{\bar{\Phi}T} dt \int_0^{\bar{\Phi}T} du \operatorname{sinc}^2 b(s-t) \operatorname{sinc}^2 b(t-u) \operatorname{sinc}^2(s-t) \operatorname{sinc} b(s-u) \\
 & \approx - \frac{A^8}{64N^4} \int_0^{\bar{\Phi}T} ds \int_0^{\bar{\Phi}T} du \operatorname{sinc}^3 b(s-u) \quad (B-13)
 \end{aligned}$$

*See Reference 4, Table 156, Integral No. 7.

$$\begin{aligned}
&\approx - \frac{A^8}{64N^4} \left(\frac{1}{b^2} \right) \left(\frac{3}{4} b \bar{\Phi T} \right) \\
&= - \frac{A^8}{64N_o^4 \Omega^4} \frac{3}{4b} (\bar{\Phi T}) \quad (B-14)
\end{aligned}$$

The fourth cross-product term will also yield the result given by Eq.

(B-14), and we have

$$- \frac{1}{8N^4} \sum_h \sum_i \sum_j \sum_k \langle s_h s_i s_j s_k \rangle \langle s_h s_i \rangle \langle s_j s_k \rangle \approx - \frac{A^8}{32N_o^4 \Omega^4} \left[(\bar{\Phi T})^2 + \frac{3}{4b} (\bar{\Phi T}) \right]$$

or

$$- \frac{1}{8N^4} \sum_h \sum_i \sum_j \sum_k \langle s_h s_i s_j s_k \rangle \langle s_h s_i \rangle \langle s_j s_k \rangle \approx - \frac{1}{2} R_i^4 \left[(\bar{\Phi T})^2 + \frac{3}{4b} (\bar{\Phi T}) \right]$$

(B-15)

Third Term

The third and last term in Eq. (B-1) is

$$\begin{aligned}
&- \frac{1}{2N^3} \sum_i \sum_j \sum_k \langle s_i s_j \rangle \langle s_j s_k \rangle \langle s_k s_i \rangle \\
&= - \frac{A^6}{16N^3} \sum_i \sum_j \sum_k \text{sinc } \bar{\Phi}_b(t_i - t_j) \text{sinc } \bar{\Phi}(t_i - t_j) \cos \omega_o(t_i - t_j) \\
&\quad \cdot \text{sinc } \bar{\Phi}_b(t_j - t_k) \text{sinc } \bar{\Phi}(t_j - t_k) \cos \omega_o(t_j - t_k) \\
&\quad \cdot \text{sinc } \bar{\Phi}_b(t_k - t_i) \text{sinc } \bar{\Phi}(t_k - t_i) \cos \omega_o(t_k - t_i)
\end{aligned}$$

$$\begin{aligned}
&= -\frac{A^6}{32N^3} \sum_i \sum_j \sum_k \text{sinc } \bar{\Phi}_b(t_i - t_j) \text{sinc } \bar{\Phi}_b(t_j - t_k) \text{sinc } \bar{\Phi}_b(t_k - t_i) \\
&\quad \cdot \text{sinc } \bar{\Phi}(t_i - t_j) \text{sinc } \bar{\Phi}(t_j - t_k) \text{sinc } \bar{\Phi}(t_k - t_i) \\
&\quad \cdot \left[\cos^2 \omega_0(t_j - t_k) + \frac{1}{2} \cos 2\omega_0(t_i - t_k) + \frac{1}{2} \cos 2\omega_0(t_i - t_j) \right] \\
&\approx -\frac{A^6}{64N^3} (8) \int_0^{\bar{\Phi}T} ds \int_0^{\bar{\Phi}T} dt \int_0^{\bar{\Phi}T} du \text{sinc } b(s-t) \text{sinc } b(t-u) \text{sinc } b(u-s) \\
&\quad \cdot \text{sinc}(s-t) \text{sinc}(t-u) \text{sinc}(u-s) \\
&\approx -\frac{A^6}{8N^3} \int_0^{\bar{\Phi}T} ds \int_0^{\bar{\Phi}T} dt \text{sinc}^3 b(s-t) \text{sinc}^2(s-t) \\
&\approx -\frac{A^6}{8N_0^3 \Omega^3} (\bar{\Phi}T) \\
&= -R_i^3(\bar{\Phi}T)
\end{aligned} \tag{B-16}$$

Thus the total deflection of $O(\underline{s}^4)$ is approximately

$$\begin{aligned}
\Delta E \left[O(\underline{s}^4) \right] &\approx \frac{1}{6} R_i^4 \left[\frac{2}{b} (\bar{\Phi}T)^2 + \frac{3}{b^2} (\bar{\Phi}T) \right] \\
&\quad - \frac{1}{2} R_i^4 \left[(\bar{\Phi}T)^2 + \frac{3}{11b} (\bar{\Phi}T) \right] \\
&\quad - R_i^3(\bar{\Phi}T)
\end{aligned} \tag{B-17}$$

Appendix C Deflection of $O(\underline{s}^4)$ --Sinusoidal Signal

The deflection for this case is obtained by letting $b = 0$ at various steps in the derivation of Appendix B.

With $b = 0$ in Eq. (B-7),

$$\begin{aligned} \sum_h \sum_i \sum_j \sum_k 3 \operatorname{sinc}^2 \bar{\Phi}(t_h - t_i + t_j - t_k) \cos^2 \omega_o(t_h - t_i + t_j - t_k) &\approx 24 \int_0^{\bar{\Phi}T} ds \int_0^{\bar{\Phi}T} dt \int_0^{\bar{\Phi}T} du \quad (1) \\ &\text{for } 0 \leq s-t+u \leq \bar{\Phi}T \\ &= 24 \cdot 2 \int_0^{\bar{\Phi}T} ds \int_0^s dt \int_0^{\bar{\Phi}T-s+t} du \quad (1) \\ &= 48 \int_0^{\bar{\Phi}T} ds \int_0^s dt [\bar{\Phi}T - s + t] \\ &= 48 \int_0^{\bar{\Phi}T} ds \left[\bar{\Phi}T s - \frac{s^2}{2} \right] \\ &= 16 (\bar{\Phi}T)^3 \quad (C-1) \end{aligned}$$

Letting $b = 0$ in Eq. (B-9), we have

$$\begin{aligned} \sum_h \sum_i \sum_j \sum_k 2 \operatorname{sinc}^2 \bar{\Phi}(t_h - t_i + t_j - t_k) \cos^2 \omega_o(t_h - t_i + t_j - t_k) &\approx 16 \int_0^{\bar{\Phi}T} ds \int_0^{\bar{\Phi}T} dt \int_0^{\bar{\Phi}T} du \quad (1) \\ &= \frac{32}{3} (\bar{\Phi}T)^3 \quad (C-2) \end{aligned}$$

Thus we have

$$\frac{1}{4!N^4} \sum_h \sum_i \sum_j \sum_k \langle s_h s_i s_j s_k \rangle^2 \approx \frac{A^8}{64 \cdot 4! N_0^4 \Omega^4} 64(\Phi_T)^3$$

and

$$\boxed{\frac{1}{4!N^4} \sum_h \sum_i \sum_j \sum_k \langle s_h s_i s_j s_k \rangle^2 \approx \frac{2}{3} R_i^4 (\Phi_T)^3} \quad (C-3)$$

Letting $b = 0$ in the derivation leading to Eq. (B-12) leaves that result unchanged. Letting $b = 0$ in Eq. (B-13), we have

$$\begin{aligned} & - \frac{A^8}{32 \cdot 8N^4} \sum_h \sum_i \sum_j \sum_k \text{sinc } \Phi(t_i - t_j - t_h + t_k) \text{sinc } \Phi(t_h - t_i) \text{sinc } \Phi(t_j - t_k) \\ & \quad \cdot \cos \omega_0(t_i - t_j - t_h + t_k) \cos \omega_0(t_h - t_i) \cos \omega_0(t_j - t_k) \\ & \approx - \frac{A^8}{64N^4} \int_0^{\Phi_T} ds \int_0^{\Phi_T} du \quad (1) \\ & = - \frac{A^8}{64N_0^4 \Omega^4} (\Phi_T)^2 \\ & = - \frac{1}{4} R_i^4 (\Phi_T)^2 \end{aligned} \quad (C-4)$$

This is identical to the result given by Eq. (B-12), thus

$$\boxed{- \frac{1}{8N^4} \sum_h \sum_i \sum_j \sum_k \langle s_h s_i s_j s_k \rangle \langle s_h s_i \rangle \langle s_j s_k \rangle \approx - R_i^4 (\Phi_T)^2} \quad (C-5)$$

The derivation leading to Eq. (B-16) is not affected by letting $b = 0$, thus

$$-\frac{1}{2N^3} \sum_i \sum_j \sum_k \langle s_i s_j \rangle \langle s_j s_k \rangle \langle s_k s_i \rangle \approx -R_1^3(\bar{\Phi}_T) \quad (C-6)$$

Finally, combining Eqs. (C-3), (C-5) and (C-6), we can write

$$\Delta E \left[O(\underline{s}^4) \right] \approx \frac{2}{3} R_1^4(\bar{\Phi}_T)^3 - R_1^4(\bar{\Phi}_T)^2 - R_1^3(\bar{\Phi}_T) \quad (C-7)$$

Appendix D Deflections of Higher-Order Terms--Sinusoidal Signal

The largest contribution to $\Delta E [O(\underline{s}^6)]$ for this case is made by the average

$$E_S \left[\frac{1}{6!} \left\langle (\underline{s}^T \underline{K}^{-1} \underline{v})^6 \right\rangle \right] = \frac{1}{6! N^6} \sum_h \sum_i \sum_j \sum_k \sum_\ell \sum_m \left\langle s_h s_i s_j s_k s_\ell s_m \right\rangle^2 \quad (D-1)$$

The desired signal $s(t)$ is (though a limiting case of zero bandwidth) a sample function of a gaussian random process. Therefore

$$\left\langle s_h s_i s_j s_k s_\ell s_m \right\rangle = \left\langle \overline{s_h s_i} \overline{s_j s_k} \overline{s_\ell s_m} + \overline{s_h s_j} \overline{s_i s_k} \overline{s_\ell s_m} + \dots + \overline{s_h s_k} \overline{s_i s_\ell} \overline{s_j s_m} \right\rangle_{\omega_c} \quad (D-2)$$

The right side of Eq. (D-1) contains a total of $1 \cdot 3 \cdot 5 = 15$ terms.* Since the signal bandwidth is vanishingly small,

$$\begin{aligned} \left\langle s_h s_i s_j s_k s_\ell s_m \right\rangle &= \frac{A^6}{8} \left\langle \cos \omega_c(t_h - t_i) \cos \omega_c(t_j - t_k) \cos \omega_c(t_\ell - t_m) \right. \\ &\quad + \cos \omega_c(t_h - t_j) \cos \omega_c(t_i - t_k) \cos \omega_c(t_\ell - t_m) \\ &\quad + \dots + \cos \omega_c(t_h - t_k) \cos \omega_c(t_i - t_\ell) \cos \omega_c(t_j - t_m) \left. \right\rangle_{\omega_c} \\ &= \frac{A^6}{8} \left\langle \frac{1}{4} \left[\cos \omega_c(t_h - t_i + t_j - t_k + t_\ell - t_m) + \cos \omega_c(t_h - t_i + t_j - t_k - t_\ell + t_m) \right. \right. \\ &\quad + \cos \omega_c(t_h - t_i - t_j + t_k + t_\ell - t_m) + \cos \omega_c(t_h - t_i - t_j + t_k - t_\ell + t_m) \left. \right] \\ &\quad + \dots + \frac{1}{4} \left[\cos \omega_c(t_h - t_k + t_i - t_\ell + t_j - t_m) + \cos \omega_c(t_h - t_k + t_i - t_\ell - t_j + t_m) \right. \\ &\quad + \cos \omega_c(t_h - t_k - t_i + t_\ell + t_j - t_m) + \cos \omega_c(t_h - t_k - t_i + t_\ell - t_j + t_m) \left. \right] \left. \right\rangle_{\omega_c} \end{aligned}$$

*See Laning and Battin,⁵ pp. 82-85, for a discussion of moments of a multivariate normal distribution.

$$\begin{aligned}
&= \frac{A^6}{32} \left[\text{sinc } \Phi(t_h - t_1 + t_j - t_k + t_\ell - t_m) \cos \omega_0(t_h - t_1 + t_j - t_k + t_\ell - t_m) \right. \\
&\quad + \text{sinc } \Phi(t_h - t_1 + t_j - t_k - t_\ell + t_m) \cos \omega_0(t_h - t_1 + t_j - t_k - t_\ell + t_m) \\
&\quad \left. + \dots + \text{sinc } \Phi(t_h - t_k - t_1 + t_\ell - t_j + t_m) \cos \omega_0(t_h - t_k - t_1 + t_\ell - t_j + t_m) \right] \\
&\hspace{15em} (D-3)
\end{aligned}$$

The right side of Eq. (D-3) contains sixty terms, but it can be shown that the terms can have only fifteen distinguishable arguments and that the fifteen types of term each occur with multiplicity four. Hence Eq. (D-3) can be rewritten with only fifteen terms and with a coefficient $A^6/8$ instead of $A^6/32$; when this modified expression is squared and used in Eq. (D-1), we have

$$\begin{aligned}
&E_S \left[\frac{1}{6!} \left\langle \left(\underline{s}^T \underline{K}^{-1} \underline{v} \right)^6 \right\rangle \right] \\
&= \frac{A^{12}}{64 \cdot 6! N^6} \sum_h \sum_i \sum_j \sum_k \sum_\ell \sum_m \left[\text{sinc}^2 \Phi(t_h - t_1 + t_j - t_k + t_\ell - t_m) \cos^2 \omega_0(t_h - t_1 + t_j - t_k + t_\ell - t_m) \right. \\
&\quad + \text{sinc}^2 \Phi(t_h - t_1 + t_j - t_k - t_\ell + t_m) \cos^2 \omega_0(t_h - t_1 + t_j - t_k - t_\ell + t_m) \\
&\quad + \dots \\
&\quad + \text{sinc}^2 \Phi(t_h - t_k - t_1 + t_\ell - t_j + t_m) \cos^2 \omega_0(t_h - t_k - t_1 + t_\ell - t_j + t_m) \\
&\quad \left. + \text{cross-product terms} \right] \\
&\hspace{15em} (D-4)
\end{aligned}$$

All the cross-product terms will yield approximately zero when the 6-d summation is carried out. Due to symmetry of the arguments, the fifteen squared terms in Eq. (D-4) will all yield the same 6-d sum. Thus, more simply,

$$\begin{aligned}
& E_S \left[\frac{1}{6!} \left\langle (\underline{s}' \underline{K}^{-1} \underline{v})^6 \right\rangle \right] \\
& \approx \frac{15 A^{12}}{64 \cdot 6! N^6} \sum_h \sum_i \sum_j \sum_k \sum_\ell \sum_m \left[\text{sinc}^2 \Phi(t_h - t_i + t_j - t_k + t_\ell - t_m) \cos^2 \omega_0(t_h - t_i + t_j - t_k + t_\ell - t_m) \right] \\
& \approx \frac{15 A^{12}}{128 \cdot 6! N^6} (64) \int_0^{\Phi_T} ds \int_0^{\Phi_T} dt \int_0^{\Phi_T} du \int_0^{\Phi_T} dv \int_0^{\Phi_T} dw \int_0^{\Phi_T} dx \text{sinc}^2(s+t+u-v-w-x) \quad (D-5)
\end{aligned}$$

The integral in Eq. (D-5) was approximated by replacing $\text{sinc}^2(s+\dots-x)$ with $\delta(s+\dots-x)$, a Dirac delta function. The integration is tedious and is not reproduced here. The result is

$$\begin{aligned}
E_S \left[\frac{1}{6!} \left\langle (\underline{s}' \underline{K}^{-1} \underline{v})^6 \right\rangle \right] & \approx \frac{15 A^{12}}{128 \cdot 6! N^6} (64) \left(\frac{1}{2} \right) (\Phi_T)^5 \\
& = \frac{15 A^{12}}{4 \cdot 6! N_0^6 \Omega^6} (\Phi_T)^5
\end{aligned}$$

Thus

$$\boxed{E_S \left[\frac{1}{6!} \left\langle (\underline{s}' \underline{K}^{-1} \underline{v})^6 \right\rangle \right] \approx \frac{1}{3} R_1^6 (\Phi_T)^5} \quad (D-6)$$

Extension to Higher-Order Terms

Calculation of the average

$$E_S \left[\frac{1}{p!} \left\langle (\underline{s}' \underline{K}^{-1} \underline{v})^p \right\rangle \right] \quad p = 2, 4, 6, \dots$$

requires approximation of an integral of the form

$$\begin{aligned}
& \int_0^X dx_1 \dots \int_0^X dx_p \text{sinc}^2(x_1 - x_2 + x_3 - x_4 + \dots + x_{p-1} - x_p) \\
& \approx \int_0^X dx_1 \dots \int_0^X dx_p \delta(x_1 - x_2 + x_3 - x_4 + \dots + x_{p-1} - x_p) = V \quad (D-7)
\end{aligned}$$

For the values of p considered in this report, the value of V was found to be

$$V = \frac{2}{\frac{p}{2} + 1} x^{p-1}, \quad p = 2, 4, 6 \quad (D-8)$$

This writer has been unable to prove that Eq. (D-8) holds for values of p greater than 6, but we may conjecture that it does hold. If so, then for long integration time,

$$E_S \left[\frac{1}{p!} \left\langle (\underline{s}' \underline{K}^{-1} \underline{v})^p \right\rangle \right] \approx \frac{2^p}{p!} R_1^p [1 \cdot 3 \cdot 5 \cdots (p-1)] \frac{(\overline{\Phi T})^{p-1}}{\frac{p}{2} + 1}, \quad p \text{ even} \quad (D-9)$$

$$E_S \left[\frac{1}{p!} \left\langle (\underline{s}' \underline{K}^{-1} \underline{v})^p \right\rangle \right] \approx \frac{2^{\frac{p}{2}}}{(\frac{p}{2} + 1)!} R_1^p (\overline{\Phi T})^{p-1}, \quad p \text{ even} \quad (D-10)$$

It can be seen from Eq. (D-10) that the fractional coefficient is always smaller than unity and monotonically approaches zero as p becomes very large.

List of Symbols

$\frac{A^2}{2}$	= signal power
$\{B_{ij}\}$	= a matrix
\underline{G}	= coefficient matrix in optimum detection
\bar{G}	= coefficient matrix, averaged over signal parameters
\underline{I}	= identity matrix
\underline{K}	= noise covariance matrix
$\ell(\underline{v})$	= likelihood ratio
N	= noise power
N_o	= noise spectrum level in $v^2/\text{rad/sec}$
n	= number of time samples
\underline{n}	= noise vector
$n(t)$	= noise process
$O(x)$	= "at most on the order of x "
R_i	= pre-detection or "input" signal-to-noise ratio
$R_s(\tau)$	= autocorrelation function of narrowband signal
S	= set of unknown signal parameters
\underline{s}	= desired signal vector
$s(t)$	= desired signal process
T	= observation time of received signal
\underline{v}	= received signal vector
$v(t)$	= received signal process

$\delta(x)$ = Dirac delta function

Φ = bandwidth of signal frequency uncertainty in cps

Φ_b = bandwidth of narrowband signal in cps

Ω = bandwidth of signal frequency uncertainty in rad/sec

Ω_b = bandwidth of narrowband signal in rad/sec

ω_c = center frequency of narrowband signal in rad/sec

ω_o = center of band of signal frequency uncertainty in rad/sec

$E[x]$ = average value of x

$\Delta E[O(x)]$ = "deflection" of $O(x)$, i.e., change in average value of $O(x)$ in going from noise-only condition to signal plus-noise condition

$\text{tr } \underline{A}$ = trace of matrix \underline{A} = sum of diagonal terms

$\langle \rangle_N$ = conditional statistical average--only noise present

$\langle \rangle_S$ = statistical average over unknown signal parameters

$\langle \rangle_{S+N}$ = conditional statistical average--signal and noise present

Abbreviations

a.c.f. = autocorrelation function

LR = likelihood ratio

p.d.f. = probability density function

SNR = signal-to-noise ratio

References

1. Middleton, D., An Introduction to Statistical Communication Theory, McGraw-Hill Book Company, New York, 1960.
2. Levesque, A. H., "Optimal Detection of a Sinusoid with Unknown Frequency and Phase," Progress Report No. 8, General Dynamics/Electric Boat Research, Yale University, November, 1963.
3. Tuteur, F. B., "Detection of Wide-Band Signals Modulated by a Low-Frequency Sinusoid," Progress Report No. 5, General Dynamics/Electric Boat Research, Yale University, June, 1963.
4. Bierens de Haan, D., Nouvelles Tables d'Intégrales Définies, G. E. Stechert and Company, New York, 1939.
5. Laning, J. H., and R. H. Battin, Random Processes in Automatic Control, McGraw-Hill Book Company, 1956.



OPTIMAL DETECTION OF A COHERENT SINUSOID
WITH UNKNOWN FREQUENCY

by

Allen H. Levesque

Progress Report No. 15

General Dynamics/Electric Boat Research
(53-00-10-0231)

June 1964

DEPARTMENT OF ENGINEERING
AND APPLIED SCIENCE
YALE UNIVERSITY

I. Introduction

A previous report¹ dealt with the problem of optimally detecting a sinusoidal signal of unknown phase whose frequency was known only to lie within a prescribed band. The results of that investigation were negative; they indicated that the sinusoid was no more detectable than a gaussian random signal having a flat spectral density over the same frequency band. Those results, however, were viewed with suspicion. Later work² showed that the small-signal approximation used in truncating the power series for the optimum detector structure would not hold for long integration times and that this faulty approximation accounted for the pessimistic results.

In this report a different approach is taken to the problem of optimally detecting a signal of unknown frequency. This work leads to an accurate approximation to the optimum detector structure for cases of large post-detection SNR. In order to keep the development simple and to avoid questions of non-gaussian statistics, the desired signal is assumed to be a steady sinusoid with known amplitude and phase^{*} and unknown frequency; the unknown frequency is assumed to have a discrete probability distribution. The extension to more realistic signal models is straightforward, but involved.

^{*}Given the frequency of the signal, the phase structure is assumed to be completely known. By definition this is termed a "coherent" signal, since $\langle \underline{s} \rangle_S \neq 0$.

II. Likelihood Ratio Detection of a Signal with an Unknown Parameter

The optimum detector for the detection of a signal in a background of random noise is a likelihood ratio (hereafter LR) detector. If the desired signal contains unknown parameters, the detector must compute a LR which is statistically averaged over all the possible values of the signal parameters. If \underline{v} is the received signal in the form of a vector of time samples and the signal contains only one unknown parameter θ , the averaged LR is given by

$$\ell(\underline{v}) = \langle L(\underline{v}, \theta) \rangle_{\theta} \quad (1)$$

where $L(\underline{v}, \theta)$ is the LR for a particular value of θ .

If the parameter θ has a discrete probability distribution over a finite set of values,

$$\ell(\underline{v}) = \sum_{i=1}^m p_i L(\underline{v}, \theta_i) \quad (2)$$

where m is the total number of possible values of θ and p_i is the probability of the i^{th} value. In general the quantities $\log L(\underline{v}, \theta_i)$ can be generated more conveniently than $L(\underline{v}, \theta_i)$. With this in mind the average LR can be written as

$$\ell(\underline{v}) = \sum_{i=1}^m p_i \exp \left[\log L(\underline{v}, \theta_i) \right] \quad (3)$$

Thus the optimum detector calculates the quantities $\log L(\underline{v}, \theta_i)$, forms the sum in Eq. (3), and compares this with a pre-set threshold k . If the threshold is exceeded, the decision is made that the desired signal is present in the received data. This test is indicated by

$$\sum_{i=1}^m p_i \exp \left[\log L(\underline{v}, \theta_i) \right] \geq k \quad (4)$$

The decision scheme can be visualized in geometric terms if the test quantities $\log L(\underline{v}, \theta_i)$ are taken as coordinates in an m -dimensional hyperspace. The space is divided into two regions, which may be called the "signal" and "no signal" regions. The boundary between these two regions is determined from Eq. (4) by the equality

$$\sum_{i=1}^m p_i \exp \left[\log L(\underline{v}, \theta_i) \right] = k \quad (5)$$

For a given received signal \underline{v} , the coordinates $\log L(\underline{v}, \theta_i)$ define a point in the m -dimensional space. If the point lies in the "signal" region, the decision is made that the desired signal is present with noise. If the point lies in the "no signal" region, the decision is made that noise only is present. A specific case will now be considered.

III. LR Detection of a Coherent Sinusoid - Two-Frequency Case

III.1 The Decision Plane

If the desired signal is a sinusoid with known amplitude and phase and with a frequency ω that can take on any one of m discrete values, then from Eq. (3),

$$\ell(\underline{v}) = \sum_{i=1}^m p_i \exp \left[\log L(\underline{v}, \omega_i) \right] \quad (6)$$

As an example, let $m = 2$ and $p_1 = p_2 = \frac{1}{2}$. Equation (6) now gives

$$\ell(\underline{v}) = \frac{1}{2} \exp \left[\log L(\underline{v}, \omega_1) \right] + \frac{1}{2} \exp \left[\log L(\underline{v}, \omega_2) \right] \quad (7)$$

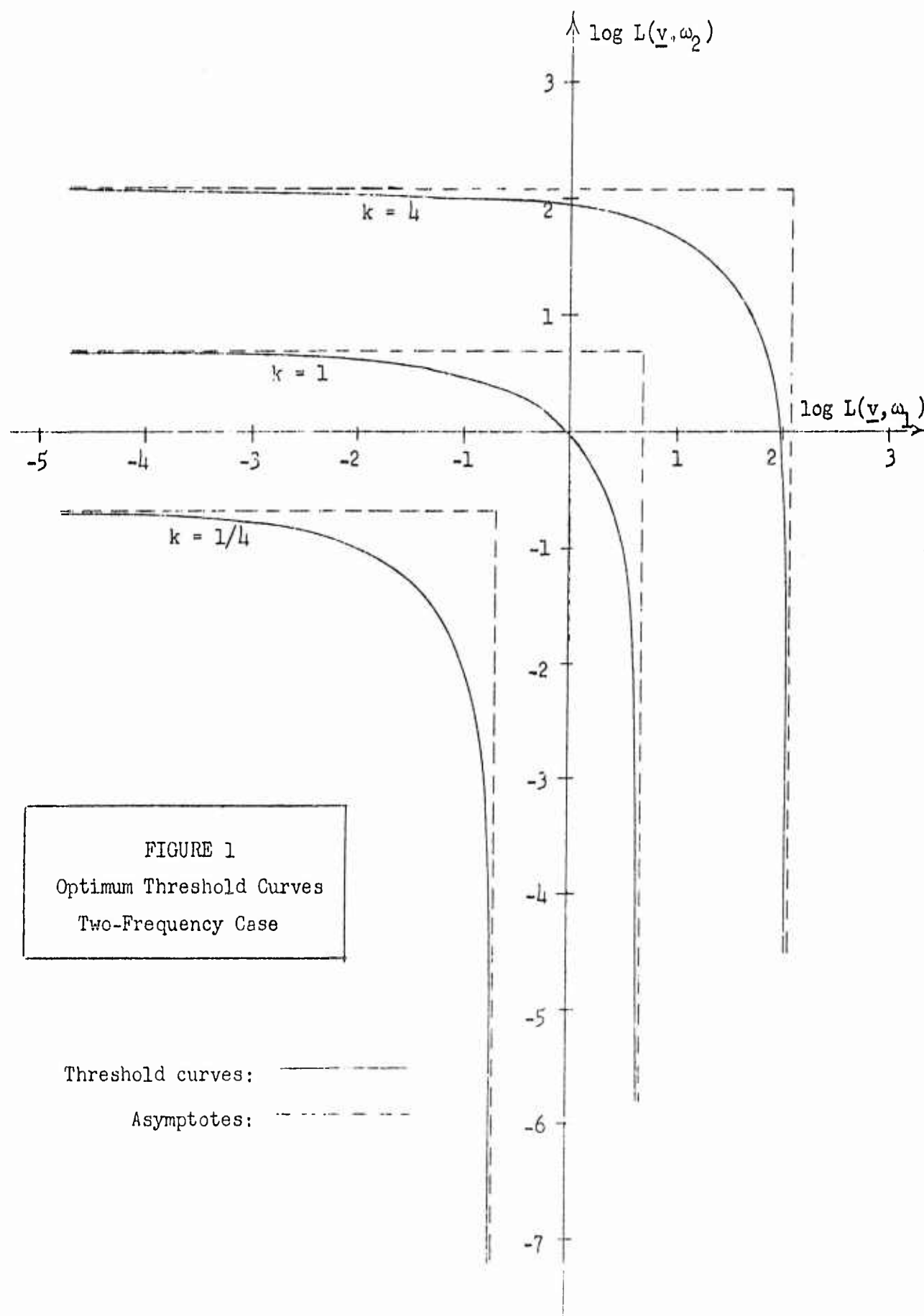
Using Eq. (5), the boundary between the two decision regions is given by

$$\frac{1}{2} \exp \left[\log L(\underline{v}, \omega_1) \right] + \frac{1}{2} \exp \left[\log L(\underline{v}, \omega_2) \right] = k \quad (8)$$

or

$$\log L(\underline{v}, \omega_2) = \log \left\{ 2k - \exp \left[\log L(\underline{v}, \omega_1) \right] \right\} \quad (9)$$

Threshold curves given by Eq. (9) are plotted in Fig. 1 for several values of k . It should be noted that the curves all become asymptotically parallel to the coordinate axes. In practice one of these curves is chosen to divide the plane into "signal" and "no signal" decision regions. For a received signal vector \underline{v} , $\log L(\underline{v}, \omega_1)$ and $\log L(\underline{v}, \omega_2)$ are calculated and these quantities define a point in this decision plane. If the point lies above or to the right of the chosen threshold curve, the decision is made that the desired signal is present. If the point lies below and to the left of the curve, the decision is made that noise only is present.



If the number of possible values of the frequency is made larger, the decision plane of Fig. 1 is replaced by an m -dimensional decision space, and the threshold curve is replaced by an m -dimensional decision surface.

III.2 Detection in Gaussian Noise

If the noise is additive and gaussian with a covariance matrix \underline{K} , the LR for a given value of signal frequency is

$$L(\underline{v}, \omega_1) = \exp \left[-\frac{1}{2} \underline{s}'(\omega_1) \underline{K}^{-1} \underline{s}(\omega_1) + \underline{s}'(\omega_1) \underline{K}^{-1} \underline{v} \right] \quad (10)$$

For convenience let

$$L_1 = L(\underline{v}, \omega_1)$$

and

$$\underline{s}_1 = \underline{s}(\omega_1)$$

Then, for the case in which the signal frequency may take on one of two discrete values, the test quantities are given by

$$\log L_1 = -\frac{1}{2} \underline{s}_1' \underline{K}^{-1} \underline{s}_1 + \underline{s}_1' \underline{K}^{-1} \underline{v} \quad (11)$$

$$\log L_2 = -\frac{1}{2} \underline{s}_2' \underline{K}^{-1} \underline{s}_2 + \underline{s}_2' \underline{K}^{-1} \underline{v} \quad (12)$$

Thus the operation of the optimum detector in this case consists of a general cross-correlation of the received signal with the desired signal at each of the possible signal frequencies.

In order to calculate the detectability of the signal, the conditional p.d.f.'s of $\log L_1$ and $\log L_2$ must be obtained. Since the noise is gaussian and Eqs. (11) and (12) describe linear operations on the received signal, the quantities $\log L_1$ and $\log L_2$ are gaussian random variables. The required mean values of $\log L_1$ are calculated as follows:

$$\begin{aligned}
\langle \log L_1 \rangle_N &= -\frac{1}{2} \underline{s}_1' \underline{K}^{-1} \underline{s}_1 + \langle \underline{s}_1' \underline{K}^{-1} \underline{v} \rangle_N \\
&= -\frac{1}{2} \underline{s}_1' \underline{K}^{-1} \underline{s}_1 + \underline{s}_1' \underline{K}^{-1} \langle \underline{v} \rangle_N \\
&= -\frac{1}{2} \underline{s}_1' \underline{K}^{-1} \underline{s}_1
\end{aligned} \tag{13}$$

$$\begin{aligned}
\langle \log L_1 \rangle_{S_1+N} &= -\frac{1}{2} \underline{s}_1' \underline{K}^{-1} \underline{s}_1 + \langle \underline{s}_1' \underline{K}^{-1} (\underline{s}_1 + \underline{n}) \rangle_{S_1+N} \\
&= -\frac{1}{2} \underline{s}_1' \underline{K}^{-1} \underline{s}_1 + \underline{s}_1' \underline{K}^{-1} \underline{s}_1 + \underline{s}_1' \underline{K}^{-1} \langle \underline{n} \rangle_N \\
&= \frac{1}{2} \underline{s}_1' \underline{K}^{-1} \underline{s}_1
\end{aligned} \tag{14}$$

$$\begin{aligned}
\langle \log L_1 \rangle_{S_2+N} &= -\frac{1}{2} \underline{s}_1' \underline{K}^{-1} \underline{s}_1 + \langle \underline{s}_1' \underline{K}^{-1} (\underline{s}_2 + \underline{n}) \rangle_N \\
&= -\frac{1}{2} \underline{s}_1' \underline{K}^{-1} \underline{s}_1 + \underline{s}_1' \underline{K}^{-1} \underline{s}_2
\end{aligned} \tag{15}$$

The variances of $\log L_1$ are

$$\begin{aligned}
\text{var}_N [\log L_1] &= \left\langle \left(-\frac{1}{2} \underline{s}_1' \underline{K}^{-1} \underline{s}_1 + \underline{s}_1' \underline{K}^{-1} \underline{v} \right)^2 \right\rangle_N - \frac{1}{4} (\underline{s}_1' \underline{K}^{-1} \underline{s}_1)^2 \\
&= \langle \underline{s}_1' \underline{K}^{-1} \underline{v} \underline{v}' \underline{K}^{-1} \underline{s}_1 \rangle_N \\
&= \underline{s}_1' \underline{K}^{-1} \langle \underline{v} \underline{v}' \rangle_N \underline{K}^{-1} \underline{s}_1 \\
&= \underline{s}_1' \underline{K}^{-1} \underline{K} \underline{K}^{-1} \underline{s}_1 \\
&= \underline{s}_1' \underline{K}^{-1} \underline{s}_1
\end{aligned} \tag{16}$$

$$\begin{aligned}
\text{var}_{S_1+N} \left[\log L_1 \right] &= \left\langle \left(-\frac{1}{2} \underline{s}_1' \underline{K}^{-1} \underline{s}_1 + \underline{s}_1' \underline{K}^{-1} (\underline{s}_1 + \underline{n}) \right)^2 \right\rangle_N - \frac{1}{4} (\underline{s}_1' \underline{K}^{-1} \underline{s}_1)^2 \\
&= \left\langle \left(\frac{1}{2} \underline{s}_1' \underline{K}^{-1} \underline{s}_1 + \underline{s}_1' \underline{K}^{-1} \underline{n} \right)^2 \right\rangle_N - \frac{1}{4} (\underline{s}_1' \underline{K}^{-1} \underline{s}_1)^2 \\
&= \frac{1}{4} (\underline{s}_1' \underline{K}^{-1} \underline{s}_1)^2 + \underline{s}_1' \underline{K}^{-1} \underline{s}_1 \underline{s}_1' \underline{K}^{-1} \langle \underline{n} \rangle_N \\
&\quad + \underline{s}_1' \underline{K}^{-1} \langle \underline{n} \underline{n}' \rangle_N \underline{K}^{-1} \underline{s}_1 - \frac{1}{4} (\underline{s}_1' \underline{K}^{-1} \underline{s}_1)^2 \\
&= \underline{s}_1' \underline{K}^{-1} \underline{s}_1
\end{aligned} \tag{17}$$

$$\begin{aligned}
\text{var}_{S_2+N} \left[\log L_1 \right] &= \left\langle \left[-\frac{1}{2} \underline{s}_1' \underline{K}^{-1} \underline{s}_1 + \underline{s}_1' \underline{K}^{-1} (\underline{s}_2 + \underline{n}) \right]^2 \right\rangle_N - \frac{1}{4} (\underline{s}_1' \underline{K}^{-1} \underline{s}_1)^2 \\
&= -\underline{s}_1' \underline{K}^{-1} \underline{s}_1 \underline{s}_1' \underline{K}^{-1} \underline{s}_2 + (\underline{s}_1' \underline{K}^{-1} \underline{s}_2)^2 + \underline{s}_1' \underline{K}^{-1} \langle \underline{n} \underline{n}' \rangle_N \underline{K}^{-1} \underline{s}_1 \\
&= -\underline{s}_1' \underline{K}^{-1} \underline{s}_1 \underline{s}_1' \underline{K}^{-1} \underline{s}_2 + (\underline{s}_1' \underline{K}^{-1} \underline{s}_2)^2 + \underline{s}_1' \underline{K}^{-1} \underline{s}_1
\end{aligned} \tag{18}$$

If the noise is assumed to have a flat spectrum over a frequency band encompassing all possible values of the signal frequency,

$$\underline{s}_1' \underline{K}^{-1} \underline{s}_2 = \frac{1}{N} \sum_{i=1}^n s_1(t_i) s_2(t_i) \tag{19}$$

and

$$\underline{s}_1' \underline{K}^{-1} \underline{s}_1 = \frac{1}{N} \sum_{i=1}^n s_1^2(t_i) \tag{20}$$

where N is the variance of the noise.

If the spectral level of the noise is $N_0 v^2/\text{rad/sec}$, then from results of sampling analysis,

$$\frac{1}{N} \sum_{i=1}^n s_1(t_i) s_2(t_i) \approx \frac{1}{\pi N_0} \int_0^T dt s_1(t) s_2(t) \approx 0 \quad (21)$$

where T is the observation time of the received signal. The zero result in Eq. (21) follows from the fact that $s_1(t)$ and $s_2(t)$ are sinusoids of different frequencies.

Similarly,

$$\frac{1}{N} \sum_{i=1}^n s_1^2(t_i) \approx \frac{1}{\pi N_0} \int_0^T dt s_1^2(t) \quad (22)$$

It will be convenient to define a detection index:

$$d \equiv \frac{1}{\pi N_0} \int_0^T dt s^2(t) \quad (23)$$

where $s(t)$ may be either $s_1(t)$ or $s_2(t)$, since the signal is assumed to have the same amplitude at either frequency. It should be noted that the detection index is proportional to the power in the receiver signal and to the observation time and inversely proportional to the spectral level of the noise. This detection index may also be regarded as the post-detection SNR.

With the aid of Eqs. (19) through (23), the averages in Eqs. (13), (14) and (15) may now be written as

$$\langle \log L_1 \rangle_N = -\frac{d}{2} \quad (24)$$

$$\left\langle \log L_1 \right\rangle_{S_1+N} = \frac{d}{2} \quad (25)$$

$$\left\langle \log L_1 \right\rangle_{S_2+N} = -\frac{d}{2} \quad (26)$$

Similarly,

$$\left\langle \log L_2 \right\rangle_N = -\frac{d}{2} \quad (27)$$

$$\left\langle \log L_2 \right\rangle_{S_1+N} = -\frac{d}{2} \quad (28)$$

$$\left\langle \log L_2 \right\rangle_{S_2+N} = \frac{d}{2} \quad (29)$$

Similarly,

$$\text{var}_N \left[\log L_2 \right] = d \quad (30)$$

$$\text{var}_{S_1+N} \left[\log L_2 \right] = d \quad (31)$$

$$\text{var}_{S_2+N} \left[\log L_2 \right] = d \quad (32)$$

To construct the joint p.d.f.'s for the test quantities, the correlation coefficient is required:

$$\begin{aligned} \frac{1}{d} \left\langle \left(\log L_1 + \frac{d}{2} \right) \left(\log L_2 + \frac{d}{2} \right) \right\rangle_N &= \frac{1}{d} \left\langle \underline{s}_1' \underline{K}^{-1} \underline{v} \underline{v}' \underline{K}^{-1} \underline{s}_2 \right\rangle_N \\ &= \frac{1}{d} \underline{s}_1' \underline{K}^{-1} \left\langle \underline{v} \underline{v}' \right\rangle_N \underline{K}^{-1} \underline{s}_2 \\ &= \frac{1}{d} \underline{s}_1' \underline{K}^{-1} \underline{s}_2 \\ &= 0 \end{aligned} \quad (33)$$

Thus the test quantities $\log L_1$ and $\log L_2$ are uncorrelated, and, since they are gaussian random variables, independent. With the following change of variables,

$$x_1 = \log L_1$$

$$x_2 = \log L_2$$

the joint p.d.f.'s can be written as

$$f(x_1, x_2 / \underline{0}) = \frac{1}{2\pi d} \exp \left[- \frac{\left(x_1 + \frac{d}{2}\right)^2 + \left(x_2 + \frac{d}{2}\right)^2}{2d} \right] \quad (34)$$

$$f(x_1, x_2 / \underline{s}_1) = \frac{1}{2\pi d} \exp \left[- \frac{\left(x_1 - \frac{d}{2}\right)^2 + \left(x_2 + \frac{d}{2}\right)^2}{2d} \right] \quad (35)$$

$$f(x_1, x_2 / \underline{s}_2) = \frac{1}{2\pi d} \exp \left[- \frac{\left(x_1 + \frac{d}{2}\right)^2 + \left(x_2 - \frac{d}{2}\right)^2}{2d} \right] \quad (36)$$

The centers of these three density functions are plotted in the decision plane of Fig. 2, together with a typical optimum threshold curve. It is particularly interesting to note that if the threshold curve remains fixed and the detection index d becomes large, the precise shape of the threshold curve near the origin of the decision plane becomes less important with regard to the conditional probabilities of error. This is because the region near the "corner" of the curve becomes a region of steadily smaller probability measure with respect to the three p.d.f.'s as d increases.* With this in mind the decision scheme may be simplified when d is large by replacing the optimum threshold curve with its straight-line

*The mean value of each of the test quantities has a magnitude equal to $d/2$, and a standard deviation equal to \sqrt{d} ; thus as d becomes larger, each of the density functions becomes narrower with respect to its mean value.

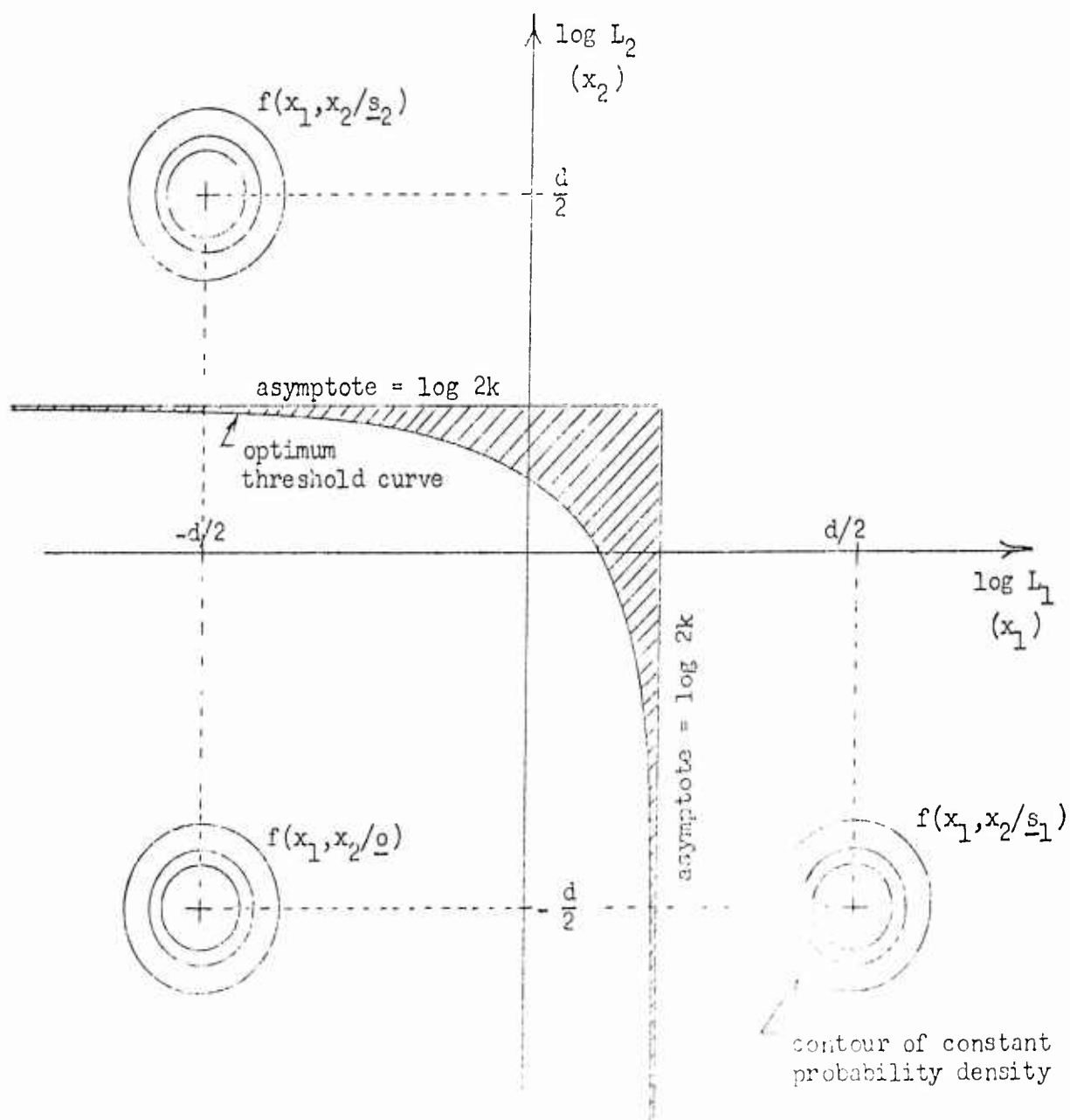


FIGURE 2
Optimum Threshold Curve and Its Band-Splitting Approximation
Two-Frequency Case

asymptotes, also shown in Fig. 2. The decision scheme corresponding to this new threshold curve can be stated as follows: If either $\log L_1$ or $\log L_2$ is above the threshold value $\log 2k$, the decision is made that a signal is present. Thus a threshold test is performed at each of the possible frequencies at which the signal may appear and a final decision about the presence of the signal is made on the basis of the individual tests. This type of decision scheme will be referred to in a general way as a "band-splitting" scheme.* As d is made increasingly large, the region (shown shaded in Fig. 2) between the optimum threshold curve and the band-splitting threshold curve, makes a steadily smaller contribution to the conditional probabilities of error. Therefore it can be stated that the optimum detector becomes asymptotically a band-splitting detector as the detection index d is made increasingly large.

A different situation prevails as d approaches zero, however. Figure 3 shows, for a low value of d , the arrangement of centers of the p.d.f.'s with respect to a typical optimum threshold curve. As d is made very small, the shape of the threshold curve for large magnitudes of $\log L_1$ and $\log L_2$ becomes less significant in the determination of the error probabilities. Only the shape of the threshold curve in the region of the closely spaced p.d.f.'s is important, and a straight line with slope -1 can serve as a good approximation to the curve in that region. Such a straight-line threshold is also pictured in Fig. 3.

It is shown in Appendix A that if $\log \langle L(\underline{y}, \omega) \rangle$ is expanded in a power series and the lowest-order coherent term in the series is used to

*The term "band splitting" is more appropriate where a continuous frequency band is being searched for a signal by means of a bank of band-pass filters. For convenience a set of correlation detectors will be regarded as a special case of the filter bank.

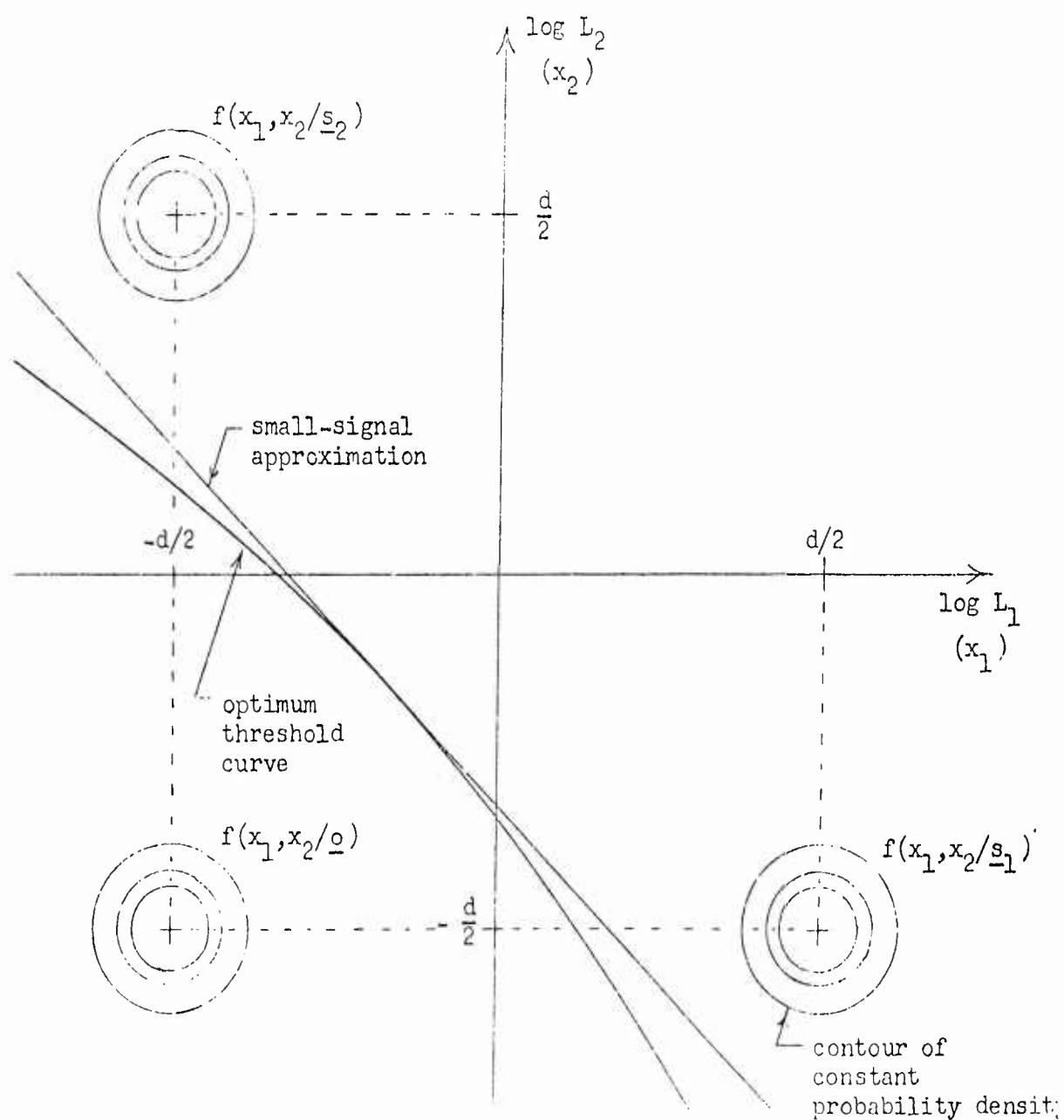


FIGURE 3
Optimum Threshold Curve and Its Small-Signal Approximation
Two-Frequency Case

approximate the operation of the optimum detector, then that approximation corresponds precisely to a straight-line threshold as pictured in Fig. 3. That is, for this case of a coherent sinusoid having one of two known frequencies, a power series analysis with small-signal approximations leads to the test

$$\log L_1 + \log L_2 \gtrless 2 \log k - \frac{d}{2} \quad (37)$$

It is now clear that the approximation leading to Eq. (37) is valid only if the detection index d is much smaller than unity, and it must be noted that it is not sufficient that the pre-detection SNR be small, since d also depends on the integration time, as shown by Eq. (23). In the threshold situation, where d is made much larger than unity by means of a long integration time, the band-splitting detector will provide a better approximation to the optimum detector.

The detector structure implied by Eq. (37) will be referred to hereafter as a "sum-and-test" detector.

III.3 Detector Probabilities - Two-Frequency Case

The conditional false-alarm and false-dismissal probabilities will be calculated for the optimum detector and for the sub-optimum detector derived by the small-signal analysis of Appendix A. Signal detectability curves will then be obtained.

Optimum Detector

The conditional false alarm probability α can be visualized with the aid of Fig. 2. It is the probability that the point $(\log L_1, \log L_2)$ lies above or to the right of the optimum threshold curve, given that noise only is present. From Eq. (34),

$$\alpha = \int_{\log 2k}^{\infty} dx_2 \frac{1}{\sqrt{2\pi d}} \exp \left[-\frac{1}{2d} \left(x_2 + \frac{d}{2} \right)^2 \right] \\ + \int_{-\infty}^{\log 2k} dx_2 \frac{1}{\sqrt{2\pi d}} \exp \left[-\frac{1}{2d} \left(x_2 + \frac{d}{2} \right)^2 \right] \int_{\log [2k - \exp(x_2)]}^{\infty} dx_1 \frac{1}{\sqrt{2\pi d}} \exp \left[-\frac{1}{2d} \left(x_1 + \frac{d}{2} \right)^2 \right] \quad (38)$$

After a change of variables,

$$\alpha = \frac{1}{\sqrt{2\pi}} \int_{\sqrt{\frac{d}{4}} + \frac{1}{\sqrt{d}} \log 2k}^{\infty} dv \exp \left(-\frac{v^2}{2} \right) + \frac{1}{\sqrt{2\pi}} \int_{-\infty}^{\sqrt{\frac{d}{4}} + \frac{1}{\sqrt{d}} \log 2k} dv \exp \left(-\frac{v^2}{2} \right) \frac{1}{\sqrt{2\pi}} \int_{\sqrt{\frac{d}{4}} + \frac{1}{\sqrt{d}} \log [2k - \exp(\sqrt{d}v - \frac{d}{2})]}^{\infty} du \exp \left(-\frac{u^2}{2} \right) \quad (39)$$

The double integration in Eq. (39) cannot be carried out in closed form, but it may be numerically evaluated to any desired degree of accuracy.

To facilitate computations in this report, the optimum threshold curve will be replaced by the band-splitting threshold for large values of d . A graphical estimation of the detectability for low values of d will then be carried out. For the band-splitting approximation, the conditional false alarm probability is given by

$$\alpha \approx \frac{1}{\sqrt{2\pi}} \int_{\sqrt{\frac{d}{4}} + \frac{1}{\sqrt{d}} \log 2k}^{\infty} dv \exp \left(-\frac{v^2}{2} \right) + \frac{1}{\sqrt{2\pi}} \int_{-\infty}^{\sqrt{\frac{d}{4}} + \frac{1}{\sqrt{d}} \log 2k} dv \exp \left(-\frac{v^2}{2} \right) \frac{1}{\sqrt{2\pi}} \int_{\sqrt{\frac{d}{4}} + \frac{1}{\sqrt{d}} \log 2k}^{\infty} du \exp \left(-\frac{u^2}{2} \right)$$

$$\alpha \approx \frac{1}{2} \left[1 - \Phi \left(\sqrt{\frac{d}{4}} + \frac{1}{\sqrt{d}} \log 2k \right) \right] \left[\frac{3}{2} + \frac{1}{2} \Phi \left(\sqrt{\frac{d}{4}} + \frac{1}{\sqrt{d}} \log 2k \right) \right] \quad (40)$$

where

$$\Phi(x) = \frac{1}{\sqrt{2\pi}} \int_{-x}^x dt \exp\left(-\frac{t^2}{2}\right) \quad (41)$$

The function $\Phi(x)$ is the Normal Probability Integral, available in tables.³

The conditional false dismissal probability is the probability that the point $(\log L_1, \log L_2)$ lies to the left of and below the optimum threshold curve in Fig. 2. Given that the two signal frequencies are equally likely, this probability can be calculated with respect to either one of the signal-plus-noise distributions. Thus

$$\beta = \int_{-\infty}^{\log 2k} dx_2 \frac{1}{\sqrt{2\pi d}} \exp\left[-\frac{1}{2d}\left(x_2 - \frac{d}{2}\right)^2\right] \int_{-\infty}^{\log[2k - \exp(x_2)]} dx_1 \frac{1}{\sqrt{2\pi d}} \exp\left[-\frac{1}{2d}\left(x_1 + \frac{d}{2}\right)^2\right] \quad (42)$$

After a change of variables,

$$\beta = \frac{1}{\sqrt{2\pi}} \int_{-\infty}^{\frac{1}{\sqrt{d}} \log 2k - \frac{\sqrt{d}}{2}} dv \exp\left(-\frac{v^2}{2}\right) \cdot \frac{1}{\sqrt{2\pi}} \int_{-\infty}^{\frac{\sqrt{d}}{2} + \frac{1}{\sqrt{d}} \log[2k - \exp(\frac{d}{2} + \sqrt{d}v)]} du \exp\left(-\frac{u^2}{2}\right) \quad (43)$$

Again, for the band-splitting approximation the false dismissal probability is approximated by

$$\beta \approx \frac{1}{\sqrt{2\pi}} \int_{-\infty}^{\frac{1}{\sqrt{d}} \log 2k - \frac{\sqrt{d}}{2}} dv \exp\left(-\frac{v^2}{2}\right) \cdot \frac{1}{\sqrt{2\pi}} \int_{-\infty}^{\frac{\sqrt{d}}{2} + \frac{1}{\sqrt{d}} \log 2k} du \exp\left(-\frac{u^2}{2}\right) \quad (44)$$

$$\beta \approx \frac{1}{2} \left[1 - \Phi\left(\frac{1}{\sqrt{d}} \log 2k - \frac{\sqrt{d}}{2}\right) \right] \left[1 + \Phi\left(\frac{\sqrt{d}}{2} + \frac{1}{\sqrt{d}} \log 2k\right) \right] \quad (45)$$

From Eqs. (40) and (45), the conditional detection probability $1 - \beta$ is plotted in Fig. 4 as a function of $\sqrt{d'}$ for fixed values of the conditional false-alarm probability α . The curves are estimated for the region of $1 - \beta$ below 80 per cent. Detection probabilities on the order of 99 per cent or better will usually be desired, and this is well within the range where the band-splitting detector provides a very accurate approximation to the optimum detector.

Sum-And-Test Detector

From Eq. (34) and with the aid of Fig. 3,

$$\alpha = \int_{\frac{1}{\sqrt{2}}(d/2 + \log k)}^{\infty} du \frac{1}{\sqrt{2nd'}} \exp \left(-\frac{u^2}{2d'} \right) \quad (46)$$

After a change of variable,

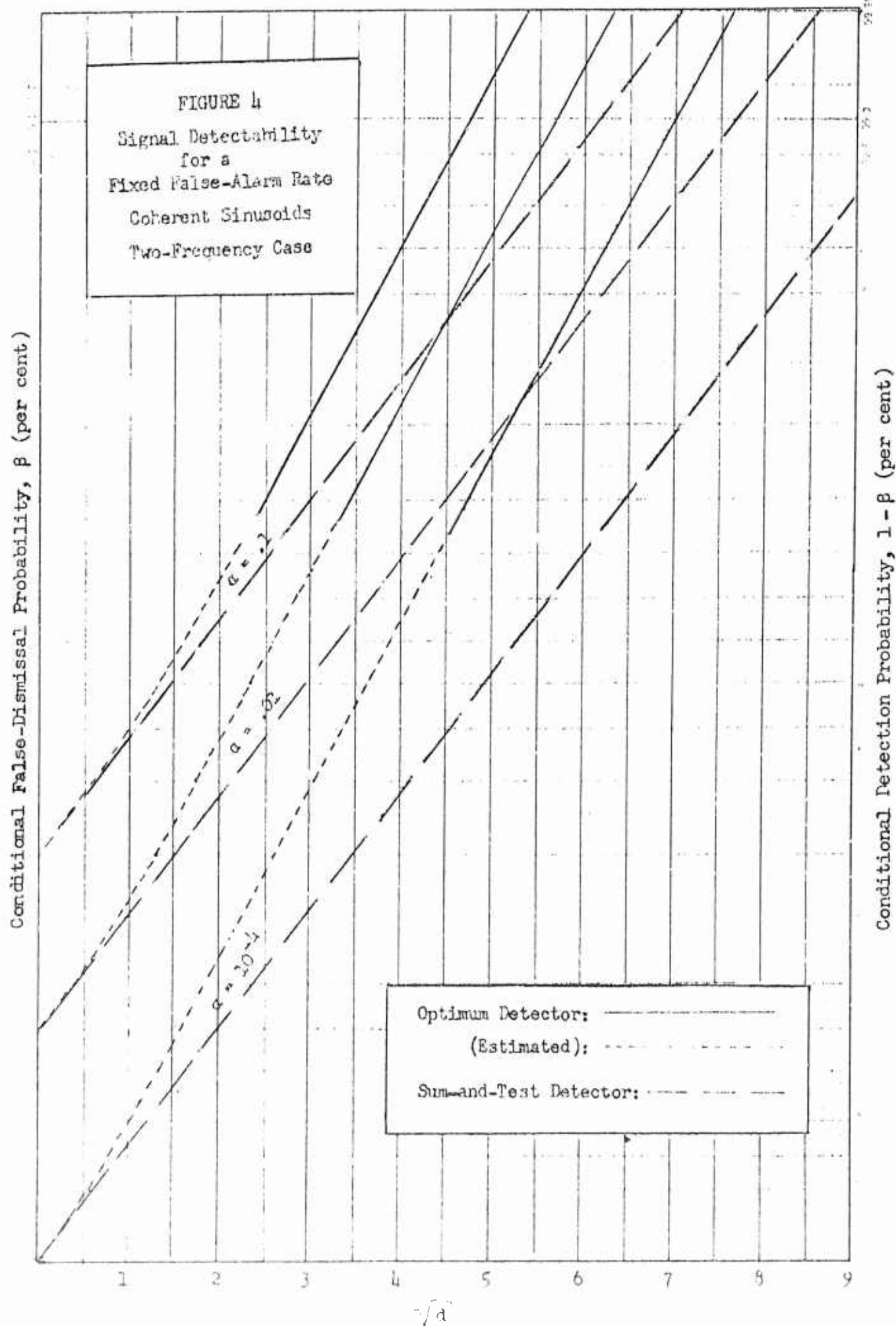
$$\alpha = \frac{1}{\sqrt{2\pi}} \int_{\sqrt{\frac{d'}{8}} + \frac{1}{\sqrt{2d'}} \log k}^{\infty} dz \exp \left(-\frac{z^2}{2} \right)$$

$$\alpha = \frac{1}{2} \left[1 - \Phi \left(\sqrt{\frac{d'}{8}} + \frac{1}{\sqrt{2d'}} \log k \right) \right] \quad (47)$$

Similarly,

$$\beta = \frac{1}{2} \left[1 - \Phi \left(\sqrt{\frac{d'}{8}} - \frac{1}{\sqrt{2d'}} \log k \right) \right] \quad (48)$$

From Eqs. (47) and (48), values of $1 - \beta$ are plotted in Fig. 4 as a function of $\sqrt{d'}$ for three fixed false-alarm rates. It is seen that the



conditional detection probability for this sub-optimum scheme steadily falls away from that of the optimum detector as the detection index increases. As the uncertainty about the frequency of the desired signal is increased to a larger number of possible values, the difference between the performance of the sum-and-test detector and that of the optimum detector becomes more pronounced.

IV. Detection of a Coherent Sinusoid - m-Frequency Case

IV.1 The Detection Space

The work of the previous section has shown that in the detection of a coherent sinusoid with an unknown frequency which can have one of two values, the optimum detector becomes asymptotically a band-splitting type of detector as the post-detection SNR becomes large. If the unknown signal frequency is equally likely to have any one of m possible values, the decision space becomes an m -dimensional hyperspace, and the threshold surface dividing the space into "signal" and "no signal" regions is obtained from Eq. (15), with $L(\underline{v}, \theta_i) = L(\underline{v}, \omega_i) \equiv L_i$, as

$$\frac{1}{m} \sum_{i=1}^m \exp(\log L_i) = k \quad (49)$$

As the detection index is made very large and a received signal is tested, two different situations will occur, depending upon the presence or absence of a signal:

- 1) If no signal is present, all m of the test quantities $\log L_i$ will have large negative mean values, equal to $-d/2$ [See Eq. (24)].
- 2) If signal is present, $m-1$ of the test quantities will have mean values equal to $-d/2$, and one test

quantity will have a mean value equal to $d/2$ [See Eqs. (26) and (25)].

Thus it is of interest to examine the shape of the threshold surface in regions of the hyperspace where the test quantities have large negative values. If Eq. (49) is solved for one of the test quantities in terms of the others,

$$\exp(\log L_1) = mk - \exp(\log L_2) - \dots - \exp(\log L_m) \quad (50)$$

or

$$\log L_1 = \log \left[mk - \exp(\log L_2) - \dots - \exp(\log L_m) \right] \quad (51)$$

When $\log L_2, \dots, \log L_m$ have large negative values, the exponentials in Eq. (51) become very small, and

$$\log L_1 \approx \log mk \quad (52)$$

Thus the asymptotes of the optimum threshold curve are hyperplanes perpendicular to each of the m coordinate axes of the decision space. These asymptote planes are analogous to the asymptote lines of the two-dimensional case.

It is seen then that as the detection index becomes large the precise shape of the threshold surface near the origin of the decision space becomes less important with respect to error probabilities and the optimum threshold surface may be approximated by a set of m hyperplanes. The decision scheme corresponding to this approximation can be stated as follows: If one or more of the test quantities $\log L_1, \log L_2, \dots, \log L_m$ are above the threshold $\log mk$, the decision is made that a signal is present. If all m test quantities are below $\log mk$, the decision is made that noise only is present. As in the two-frequency case, this detection scheme will be referred to as a "band-splitting" scheme.

It can be stated in general, then, that the optimum detector for the detection of a coherent sinusoid whose unknown frequency is given by a discrete probability distribution becomes asymptotically a band-splitting detector as the detection index d becomes large.

For small values of post-detection SNR, the work of Appendix A shows that the optimum detector can be approximated by a sum-and-test detector. For the m -frequency case the approximation leads to the test

$$\sum_{i=1}^m \log L_i \gtrsim m \log k - (m-1) \frac{d}{2} \quad (53)$$

The threshold surface corresponding to this sub-optimum scheme is given by

$$\sum_{i=1}^m \log L_i = m \log k - (m-1) \frac{d}{2} \quad (54)$$

and this is seen to be a hyperplane in the m -dimensional decision space. This is analogous to the straight-line threshold shown in Fig. 3 for the small-signal approximation in the two-frequency case.

IV.2 Detection Probabilities - m -Frequency Case

Optimum Detector

For large values of d the optimum detector will be approximated by the band-splitting detector to simplify the computation of the error probabilities. For small values of d the detectability will then be estimated.

The conditional false-alarm probability is the probability that one or more of the test quantities exceeds the threshold $\log mk$, given that noise only is present. That is,

$$\alpha = P \left[\begin{array}{l} \text{At least one of the test quantities } \log L_i \text{ is} \\ \text{above its threshold, given that noise only is} \\ \text{present} \end{array} \right]$$

$$= 1 - P \left[\begin{array}{l} \text{All the test quantities } \log L_i \text{ are below} \\ \text{their thresholds, given that noise only} \\ \text{is present} \end{array} \right]$$

The conditional false-dismissal probability is

$$\beta = P \left[\begin{array}{l} \text{All the test quantities } \log L_i \text{ are below their} \\ \text{thresholds, given that a signal is present at} \\ \text{any one of the possible frequencies} \end{array} \right]$$

It is shown in Appendix B that

$$\alpha = 1 - (1 - \alpha_i)^m \quad (55)$$

and

$$\beta = \beta_i (1 - \alpha_i)^{m-1} \quad (56)$$

where

$$\alpha_i = P \left[\begin{array}{l} \log L_i \text{ is above its threshold, given that no} \\ \text{signal is present at the frequency } \omega_i \end{array} \right]$$

$$\beta_i = P \left[\begin{array}{l} \log L_i \text{ is below its threshold, given that a} \\ \text{signal is present at the frequency } \omega_i \end{array} \right]$$

The probabilities α_i are assumed equal for all $i = 1, 2, \dots, m$, and the probabilities β_i are assumed equal for all $i = 1, 2, \dots, m$. The error probabilities α and β can be bounded as

$$\alpha \leq m \alpha_i \quad (57)$$

and

$$\beta \leq \beta_i \quad (58)$$

These bounds are tight for $m \alpha_i \ll 1$. It is seen from Eqs. (57) and (58) that if the threshold for each $\log L_i$ is held fixed and the frequency

uncertainty is increased, the false alarm probability will be approximately proportional to m , while the false dismissal probability will remain approximately unchanged.

The conditional p.d.f.'s for $\log L_i$ are needed. Let $x_i = \log L_i$. Then, from Eqs. (24), (25), (26), (30), (31) and (32),

$$f(x_i/o \text{ or } s_j) = \frac{1}{\sqrt{2\pi d}} \exp \left[-\frac{1}{2d} \left(x_i + \frac{d}{2} \right)^2 \right] \quad (59)$$

$i \neq j$

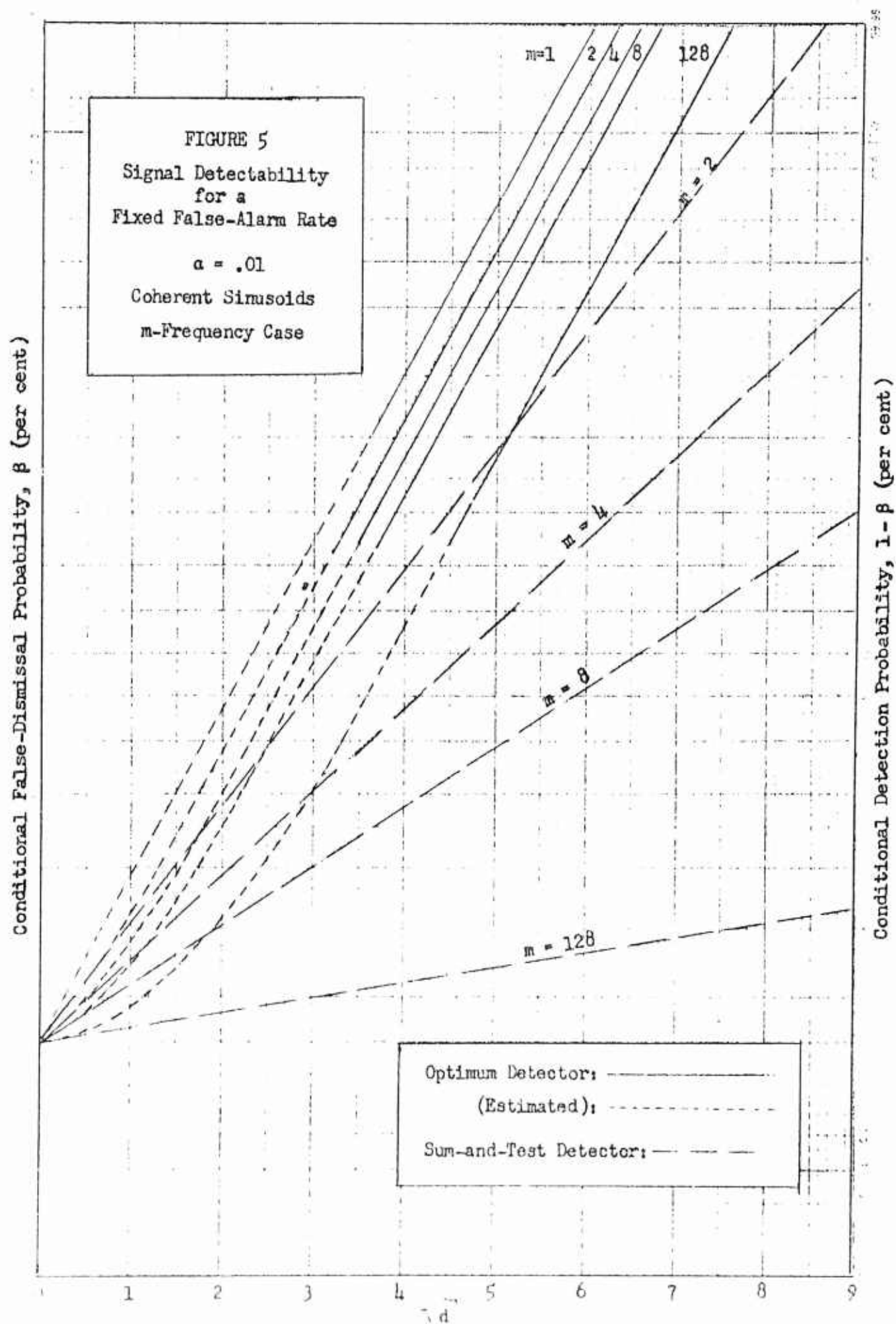
and

$$f(x_i/s_i) = \frac{1}{\sqrt{2\pi d}} \exp \left[-\frac{1}{2d} \left(x_i - \frac{d}{2} \right)^2 \right] \quad (60)$$

If the threshold for each test quantity is $\log mk$,

$$\left\{ \begin{array}{l} \alpha_i \\ \beta_i \end{array} \right\} = \frac{1}{2} \left[1 - \Phi \left(\sqrt{\frac{d}{4}} \pm \frac{1}{\sqrt{d}} \log mk \right) \right] \quad (61)$$

From Eqs. (55), (56) and (61), the conditional detection probability $1 - \beta$ can be calculated as a function of \sqrt{d} for a fixed value of the conditional false alarm probability α and for any number m of signal frequencies. Results of these calculations for $\alpha = .01$ and $m = 1, 2, 4, 8$ and 128 are shown in Fig. 5. It can be seen from the figure that the set of detection curves for different values of m becomes a set of parallel straight lines as \sqrt{d} becomes large, with the detectability becoming poorer as m increases, as would be expected. The asymptotic form of the detectability curves for small error probabilities can easily be derived using the bounds of Eqs. (57) and (58). For small values of $m\alpha_i$ the bounds become very good approximations and using Eq. (57) together with Eq. (61), one can write



$$\alpha \approx \frac{m}{2} \left[1 - \Phi \left(\sqrt{\frac{d}{4}} + \frac{1}{\sqrt{d}} \log mk \right) \right] \quad (62)$$

The conditional detectability $1 - \beta$ is to be calculated as a function of \sqrt{d} for a fixed value of α , therefore let $\alpha = \alpha^*$ where α^* is the chosen fixed false-alarm rate. Now, from Eq. (62),

$$\frac{1}{\sqrt{d}} \log mk \approx \Phi^{-1} \left(1 - \frac{2\alpha^*}{m} \right) - \sqrt{\frac{d}{4}} \quad (63)$$

where $\Phi^{-1}(z)$ denotes the "inverse Normal Probability Integral," that is, the number x for which $z = \Phi(x)$ [See Eq. (41)].

From Eqs. (58) and (61), an approximation is obtained for the conditional false-dismissal probability as

$$\beta \approx \frac{1}{2} \left[1 - \Phi \left(\sqrt{\frac{d}{4}} - \frac{1}{\sqrt{d}} \log mk \right) \right] \quad (64)$$

Inserting Eq. (63) into Eq. (64), one obtains

$$\beta \approx \frac{1}{2} \left\{ 1 - \Phi \left[\sqrt{d} - \Phi^{-1} \left(1 - \frac{2\alpha^*}{m} \right) \right] \right\} \quad (65)$$

The conditional detection probability is then approximately

$$1 - \beta \approx \frac{1}{2} \left\{ 1 + \Phi \left[\sqrt{d} - \Phi^{-1} \left(1 - \frac{2\alpha^*}{m} \right) \right] \right\} \quad \sqrt{d} \gg 1 \quad (66)$$

The right-hand side of Eq. (66) is seen to be of the general form

$$c_1 \Phi \left[c_2 \sqrt{d} + c_3 \right] + c_4 \quad (67)$$

where C_1, C_2, C_3 and C_4 are constants. This general form represents a linear function of \sqrt{d} on the normal probability scale of Fig. 5. Thus the asymptotes of the detectability curves for the optimum detector, given by Eq. (66), plotted for various values of m or various values of α^* are a family of parallel straight lines, the horizontal displacement of each line being determined by the quantity $\Phi^{-1}(1 - 2\alpha^*/m)$. If α^* is held fixed and m is increased,

$$\Phi^{-1}\left(1 - \frac{2\alpha^*}{m}\right) \rightarrow \infty \quad \text{as } \begin{matrix} m \rightarrow \infty \\ \alpha^* = \text{const.} \end{matrix}$$

Thus the detection curve moves steadily to the right as m increases, representing steadily poorer detectability with increasing uncertainty about the signal frequency, as is seen in Fig. 5. The same trend is observed if m is held fixed and α^* is decreased; that is,

$$\Phi^{-1}\left(1 - \frac{2\alpha^*}{m}\right) \rightarrow \infty \quad \text{as } \begin{matrix} \alpha^* \rightarrow 0 \\ m = \text{const.} \end{matrix}$$

This is the trend exhibited by the optimum detector curves in Fig. 4 for the two-frequency case.

Sum-And-Test Detector

For the sum-and-test detector, the test quantity is

$$y = \sum_{i=1}^m \log L_i \quad (68)$$

When noise only is present, each of the quantities $\log L_i$ has a mean value $-d/2$ and a variance d . Thus

$$f(y/\underline{o}) = \frac{1}{\sqrt{2\pi md}} \exp \left[-\frac{1}{2md} \left(y + \frac{md}{2} \right)^2 \right] \quad (69)$$

When a signal is present at one of the m possible frequencies, $m-1$ of the quantities $\log L_i$ will have a mean value $-d/2$ and one will have a mean value $d/2$. Thus

$$f(y/\underline{s}_1) = \frac{1}{\sqrt{2\pi md}} \exp \left\{ -\frac{1}{2md} \left[y + (m-2)\frac{d}{2} \right]^2 \right\} \quad (70)$$

If y is compared with a threshold $m \log k - (m-1)\frac{d}{2}$, the conditional error probabilities are given by

$$\left\{ \begin{array}{l} \alpha \\ \beta \end{array} \right\} = \frac{1}{2} \left[1 - \Phi \left(\sqrt{\frac{d}{4m}} \pm \sqrt{\frac{m}{d}} \log k \right) \right] \quad (71)$$

Curves of conditional detection probability $1-\beta$ as a function of \sqrt{d} are shown in Fig. 5 for the sum-and-test detector. The curves are plotted for $\alpha = .01$ and values of $m = 1, 2, 4, 8$ and 128 . As was seen for the optimum detector, the signal detectability with the sum-and-test detector becomes poorer as m increases. An expression for $1-\beta$ as a function of \sqrt{d} and any fixed false-alarm rate $\alpha = \alpha^*$ and for any value of m can be found as follows: From Eq. (71),

$$\alpha^* = \frac{1}{2} \left[1 - \Phi \left(\sqrt{\frac{d}{4m}} + \sqrt{\frac{m}{d}} \log k \right) \right] \quad (72)$$

Thus

$$\sqrt{\frac{m}{d}} \log k = \Phi^{-1}(1 - 2\alpha^*) - \sqrt{\frac{d}{4m}} \quad (73)$$

From Eqs. (71) and (73),

$$1 - \beta = \frac{1}{2} \left\{ 1 + \bar{\Phi} \left[\sqrt{\frac{d}{m}} - \bar{\Phi}^{-1}(1 - 2\alpha^*) \right] \right\} \quad (74)$$

where $\bar{\Phi}^{-1}(\)$ has the same meaning as in Eq. (63). The right-hand side of Eq. (74) is seen to be of the general form of expression (67) and thus represents a linear function of \sqrt{d} on the normal probability scale of Fig. 5. Since \sqrt{d} enters Eq. (74) in the form $\sqrt{d/m}$, the slope of the detectability curve will vary with m , decreasing as m increases. Thus if a family of detectability curves for the sum-and-test detector is plotted for a fixed value of α , the slope of each curve will approach zero as m becomes increasingly large, as is seen in Fig. 5. The horizontal displacement of the curves is governed by $\bar{\Phi}^{-1}(1 - 2\alpha^*)$ and thus a family of curves plotted for a fixed value of m consists of a set of parallel lines, with the detectability becoming steadily poorer as α^* is made smaller; this is seen in Fig. 4.

Figure 5 shows that as the uncertainty about signal frequency increases, the performance of the sum and-test detector declines more rapidly than that of the optimum detector. In the operation of the sum-and-test detector, an increase in the number of possible values of the signal frequency requires an identical increase in the number of noisy correlator outputs to be summed before the threshold test; thus the post-detection SNR varies inversely with m , as is seen in Eq. (71). However, the optimum detector, when visualized in terms of its asymptotic form, the band-splitting detector, effectively searches out the "best" (that is, the largest) of the m outputs and then uses this in the threshold test.

Increasing m simply increases the number of test quantities among which the detector must search, but the detector will still seek out the "best" output for use in the threshold test. As more outputs are to be examined, the conditional false alarm probability increases, therefore the threshold must be adjusted slightly upward to maintain the same false alarm rate; this change in threshold level leads to a slightly lower conditional detection probability.

A useful basis for comparison of the optimum detector with the sum-and-test detector is that of pre-detection SNR or post-detection integration time required for a desired level of performance. This comparison is made in Fig. 6 in a plot of $r = d_{\text{sum}}/d_{\text{opt}}$ vs. m , for $\alpha = \beta = .01$, where

d_{sum} = detection index required with the sum-and-test detector for error probabilities $\alpha = \beta = .01$.

d_{opt} = detection index required with the optimum detector for error probabilities $\alpha = \beta = .01$.

Since the detection index d is seen from Eq. (23) to depend linearly upon the pre-detection SNR and linearly upon the integration time, the ratio r may be interpreted as either a ratio of required input SNR for a fixed integration time or a ratio of required integration times for a fixed input SNR. It is seen from the figure that the ratio r increases indefinitely as the number of possible values of the signal frequency increases.

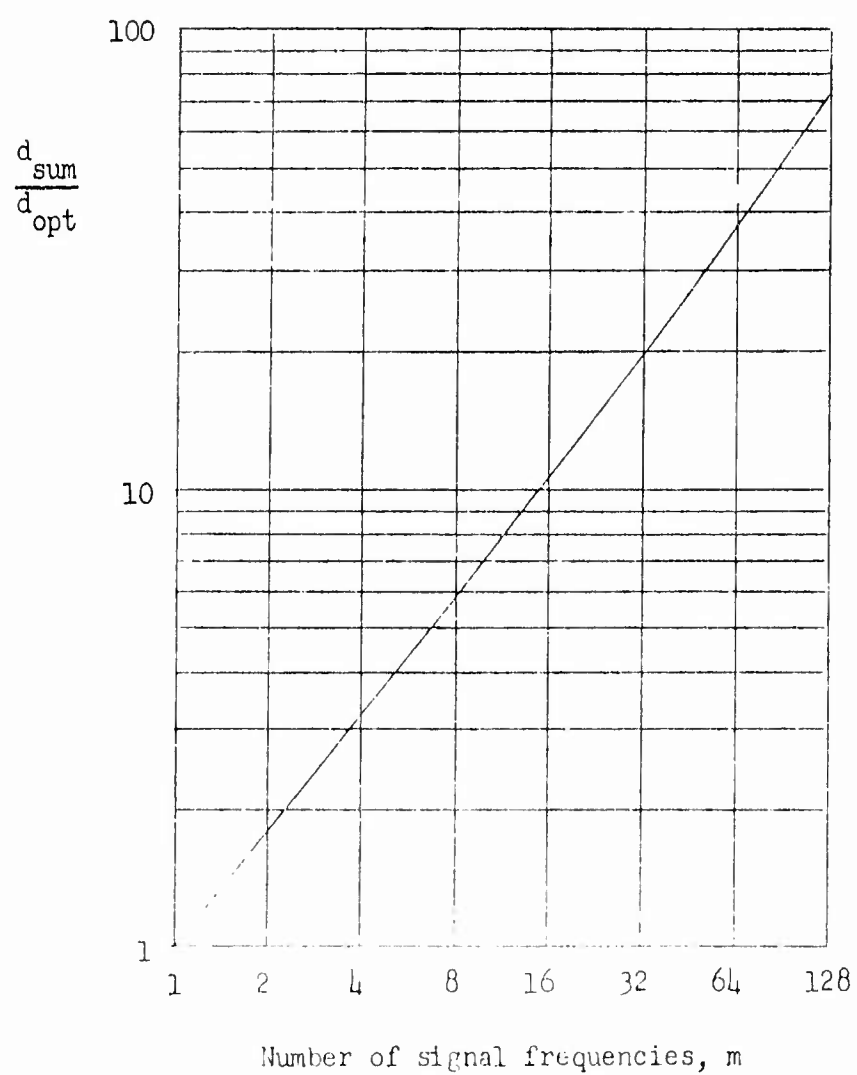


FIGURE 6

Comparison of Optimum Detector with Sum-and-Test Detector:
Ratio of Required Detection Indices for $\alpha = \beta = .01$

V. Conclusions and Comments

The work of this report has shown that the optimum receiver for the detection of a coherent sinusoid with a discrete frequency distribution becomes asymptotically a band-splitting detector as the post-detection SNR is made large. The band-splitting detection scheme is exactly equivalent to the classical method of maximum likelihood for testing a statistical hypothesis.* This can be seen if the band-splitting threshold test is written in the following form:

$$\max_{\omega_1} \log L(\underline{v}, \omega_1) \geq \log mk$$

or

$$\max_{\omega_1} L(\underline{v}, \omega_1) \geq mk$$

The method of maximum likelihood is not generally an optimum decision strategy in any sense but gives satisfactory performance in many cases where insufficient a priori information is available to allow construction of an optimum strategy. It is moreover a decision strategy that one would intuitively choose to detect a signal of unknown frequency. It is especially satisfying to see that the optimum-detector approach, as followed in this report, also leads to the use of a maximum likelihood detector and to see that this detector is very nearly optimum in the range of post-detection SNR which is of particular interest.

This work can be extended directly to the case of an incoherent signal whose frequency (or center frequency) is given by a discrete probability distribution. For such a case the threshold test would again be given by Eq. (4) and the threshold surface by Eq. (5), with $\theta_1 = \omega_1$ in both cases. The individual test quantity $\log L(\underline{v}, \omega_1)$ generally cannot

*Reference 4 provides a comprehensive treatment of the subject of hypothesis testing.

be obtained in closed form for an incoherent signal; however, in a weak-signal situation $\log L(\underline{v}, \omega_1)$ can be expanded in a power series and satisfactorily approximated by a quadratic form. This quadratic form would of course have non-gaussian statistics, but as the observation time is made long, the statistics would become gaussian by the central-limit theorem. Thus for weak received signal and a long observation time, the m-frequency incoherent signal case can be handled by much the same procedure as is outlined in this report. The form of the optimum detector would again approach that of the band-splitting detector for large post-detection SNR.

If the unknown signal frequency is given by a p.d.f. over a continuous range of values, the test quantities $\log L_1$ form a non-enumerable set and the optimum decision scheme can no longer be visualized in terms of a coordinate space. It can be seen, however, that as the frequency distribution becomes continuous the band-splitting detector becomes a band-sweeping detector, which calculates $\log L(\underline{v}, \omega)$ as a continuous function of ω over the band of frequency uncertainty; if this function exceeds a preset threshold at any value of ω , the decision is made that the desired signal is present. The specific problem of detecting a narrowband gaussian signal with unknown center frequency will be treated in a later report.

Appendix A A Small-Signal Approximation to the Optimum Detector

In the optimum detection of a signal with unknown parameters, the detector must calculate the average LR

$$\ell(\underline{v}) = \left\langle \exp \left(-\frac{1}{2} \underline{s}' \underline{K}^{-1} \underline{s} + \underline{s}' \underline{K}^{-1} \underline{v} \right) \right\rangle \quad (\text{A-1})$$

where $\langle \rangle$ implies $\langle \rangle_{\underline{s}}$. If the exponential in Eq. (A-1) is expanded in a power series, the average over signal parameters taken term by term, and the function $\log \ell(\underline{v})$ expanded in a second power series, the result is

$$\log \ell(\underline{v}) = -\frac{1}{2} \langle \underline{s}' \underline{K}^{-1} \underline{s} \rangle + \langle \underline{s}' \underline{K}^{-1} \underline{v} \rangle + \frac{1}{2} \left[\langle (\underline{s}' \underline{K}^{-1} \underline{v})^2 \rangle - \langle \underline{s}' \underline{K}^{-1} \underline{v} \rangle^2 \right] + O(\underline{s}^3) \quad (\text{A-2})$$

In the weak-signal situation, the major contribution to $\log \ell(\underline{v})$ is from the coherent term $\langle \underline{s}' \underline{K}^{-1} \underline{v} \rangle$. As an approximation, the terms of the order \underline{s}^2 can be replaced by their averages taken with noise only present. These averages, together with the term $-\frac{1}{2} \langle \underline{s}' \underline{K}^{-1} \underline{s} \rangle$, are then taken as bias terms in threshold test. The three bias terms are thus

$$\begin{aligned} -\frac{1}{2} \langle \underline{s}' \underline{K}^{-1} \underline{s} \rangle &= \left\langle \sum_i \sum_j s_i s_j K_{ij}^{-1} \right\rangle \\ &= \sum_i \sum_j \langle s_i s_j \rangle K_{ij}^{-1} \\ &= \text{tr} \left(\langle \underline{s} \underline{s}' \rangle \underline{K}^{-1} \right) \end{aligned} \quad (\text{A-3})$$

$$\begin{aligned}
-\frac{1}{2} \overline{\langle (\underline{s}' \underline{K}^{-1} \underline{v})^2 \rangle} &= \overline{\langle \underline{v}' \underline{K}^{-1} \underline{s} \underline{s}' \underline{K}^{-1} \underline{v} \rangle} \\
&= \overline{\underline{v}' \underline{K}^{-1} \langle \underline{s} \underline{s}' \rangle \underline{K}^{-1} \underline{v}} \\
&= \sum_i \sum_j \overline{v_i v_j} \left(\underline{K}^{-1} \langle \underline{s} \underline{s}' \rangle \underline{K}^{-1} \right)_{ij} \\
&= \text{tr} \left(\underline{K} \underline{K}^{-1} \langle \underline{s} \underline{s}' \rangle \underline{K}^{-1} \right) \\
&= \text{tr} \left(\langle \underline{s} \underline{s}' \rangle \underline{K}^{-1} \right) \tag{A-4}
\end{aligned}$$

$$\begin{aligned}
-\frac{1}{2} \overline{\langle \underline{s}' \underline{K}^{-1} \underline{v} \rangle^2} &= -\frac{1}{2} \overline{\underline{v}' \underline{K}^{-1} \langle \underline{s} \rangle \langle \underline{s}' \rangle \underline{K}^{-1} \underline{v}} \\
&= -\frac{1}{2} \sum_i \sum_j \overline{v_i v_j} \left(\underline{K}^{-1} \langle \underline{s} \rangle \langle \underline{s}' \rangle \underline{K}^{-1} \right)_{ij} \\
&= -\frac{1}{2} \text{tr} \left(\langle \underline{s} \rangle \langle \underline{s}' \rangle \underline{K}^{-1} \right) \\
&= -\frac{1}{2} \sum_i \sum_j \langle s_i \rangle \langle s_j' \rangle K_{ij}^{-1} \\
&= -\frac{1}{2} \langle \underline{s}' \rangle \underline{K}^{-1} \langle \underline{s} \rangle \tag{A-5}
\end{aligned}$$

Therefore,

$$\log \ell(\underline{v}) \approx \langle \underline{s}' \rangle \underline{K}^{-1} \underline{v} - \frac{1}{2} \langle \underline{s}' \rangle \underline{K}^{-1} \langle \underline{s} \rangle \tag{A-6}$$

If the signal is a sinusoid of known amplitude and phase with an unknown frequency given by a discrete distribution, then

$$\langle \underline{s} \rangle = \sum_{i=1}^m p_i \underline{s}(\omega_i) \quad (\text{A-7})$$

If the m frequencies are equally probable,

$$\langle \underline{s} \rangle = \frac{1}{m} \sum_{i=1}^m \underline{s}(\omega_i) = \frac{1}{m} \sum_{i=1}^m \underline{s}_i \quad (\text{A-8})$$

If, in addition, the noise is white with variance N ,

$$\log \ell(\underline{v}) \approx \frac{1}{mN} \sum_{i=1}^m \underline{s}_i' \underline{v} - \frac{1}{2mN} \sum_{i=1}^m \sum_{j=1}^m \underline{s}_i' \underline{s}_j \quad (\text{A-9})$$

Since \underline{s}_i and \underline{s}_j represent sinusoids of different frequencies,

$$\begin{aligned} \frac{1}{N} \underline{s}_i' \underline{s}_j &\approx 0 & i \neq j \\ &= \frac{1}{N} \sum_{k=1}^n s_i^2(t_k) = d & i = j \end{aligned} \quad (\text{A-10})$$

Thus,

$$\begin{aligned} \log \ell(\underline{v}) &\approx \frac{1}{mN} \sum_{i=1}^m \underline{s}_i' \underline{v} - \frac{d}{2m} \\ &= \frac{1}{m} \sum_{i=1}^m \left[\frac{1}{N} \underline{s}_i' \underline{v} - \frac{d}{2} \right] + \left(1 - \frac{1}{m} \right) \frac{d}{2} \end{aligned} \quad (\text{A-11})$$

From Eqs. (11) and (12),

$$\log \ell(\underline{v}) \approx \frac{1}{m} \sum_{i=1}^m \log L_i + \left(1 - \frac{1}{m} \right) \frac{d}{2} \quad (\text{A-12})$$

Therefore the weak-signal approximation leads to the threshold test

$$\sum_{i=1}^m \log L_i \gtrless m \log k - (m-1) \frac{d}{2} \quad (\text{A-13})$$

As an example, let $m = 2$. The detector then performs the threshold test

$$\log L_1 + \log L_2 \gtrless 2 \log k - \frac{d}{2}$$

If $\log L_1$ and $\log L_2$ are considered as coordinates in a two-dimensional decision space, the curve dividing the space into "signal" and "no signal" regions is given by

$$\log L_1 + \log L_2 = 2 \log k - \frac{d}{2} \quad (\text{A-14})$$

This is seen to be a straight line with slope -1.

Appendix B Error Probabilities for a Band-Splitting Detector with
Independent Outputs

The conditional error probabilities are derived for a band-splitting detection scheme. The following events are defined:

S_0 = Event that noise only is present

S_i = Event that signal is present with frequency ω_i , $i = 1, 2, \dots, m$

E_0 = Event that all m outputs lie below the fixed threshold value

E_i = Event that the i^{th} output exceeds its threshold value,
 $i = 1, 2, \dots, m$

False Alarm

The conditional false alarm probability is given by

$\alpha = P$ [at least one output exceeds its threshold value, given
that noise only is present]

$$= 1 - \prod_{i=1}^m [1 - P(E_i/S_0)] \quad (\text{B-1})$$

If the m outputs are independent, the probability of an event E_i is not affected by the presence or absence of signal at any frequency other than ω_i .

Thus

$$P(E_i/S_0) = P(E_i/S_i^*) \quad (\text{B-2})$$

The right-hand side of Eq. (B-2) is seen to be the conditional false alarm probability for the threshold test at the i^{th} frequency, that is

$$P(E_i/S_i^*) = \alpha_i = P \left[\begin{array}{l} \text{the } i^{\text{th}} \text{ output exceeds its threshold, given} \\ \text{that no signal is present with the} \\ \text{frequency } \omega_i \end{array} \right] \quad (\text{B-3})$$

Thus, from Eqs. (B-1), (B-2), and (B-3),

$$\alpha = 1 - \prod_{i=1}^m (1 - \alpha_i) \quad (\text{B-4})$$

If α_i has the same value for $i = 1, 2, \dots, m$, then

$$\alpha = 1 - (1 - \alpha_i)^m \quad (\text{B-5})$$

False Dismissal

The conditional false dismissal probability is given by

$$\begin{aligned} \beta &= P \left[\begin{array}{l} \text{all } m \text{ outputs lie below the fixed threshold value,} \\ \text{given that the signal is present at any one of the} \\ \text{possible frequencies} \end{array} \right] \\ &= P(E_0 / S_1 + S_2 + \dots + S_m) \end{aligned} \quad (\text{B-6})$$

If all m outputs are independent and have the same mean and variance, the probability of the event E_0 in the presence of signal is independent of the signal frequency. Thus

$$P(E_0 / S_1 + S_2 + \dots + S_m) = P(E_0 / S_i) \quad i = 1, 2, \dots, m \quad (\text{B-7})$$

From Eqs. (B-6) and (B-7) and the definition of E_0 ,

$$\begin{aligned} \beta &= P(E_0 / S_i) \quad i = 1, 2, \dots, m \\ &= P(E_1^{*}, E_2^{*}, \dots, E_m^{*} / S_i) \quad i = 1, 2, \dots, m \end{aligned} \quad (\text{B-8})$$

Since the outputs are independent,

$$\beta = \prod_{j=1}^m P(E_j^{*} / S_i) \quad i = 1, 2, \dots, m \quad (\text{B-9})$$

For $i = j$,

$$P(E_j^*/S_j) = \beta_j = P \left[\begin{array}{l} \text{the } j^{\text{th}} \text{ output is below its threshold, given} \\ \text{that a signal is present at the frequency } \omega_j \end{array} \right]$$

and for $i \neq j$,

$$P(E_j^*/S_i) = P(E_j^*/S_j^*) = 1 - \alpha_j \quad (\text{B-10})$$

The first equality in Eq. (B-10) follows from the fact that the event E_j^* is independent of the presence or absence of signal at any frequency other than ω_j . Since β_j is assumed to have the same value for all $j = 1, 2, \dots, m$ and α_j the same value for all $j = 1, 2, \dots, m$, Eq. (B-9) can be rewritten as

$$\beta = \beta_j (1 - \alpha_j)^{m-1}$$

(B-11)

List of Symbols

d	= detection index or post-detection SNR
\underline{K}	= noise covariance matrix
k	= a threshold
$L(\underline{v}, \omega_1)$	= likelihood ratio, given the signal frequency ω_1
$\ell(\underline{v})$	= average likelihood ratio
m	= number of possible values of the signal frequency
N	= noise variance
N_0	= noise spectrum level, $v^2/\text{rad/sec}$
n	= number of time samples
\underline{n}	= noise vector
$O(x)$	= "at most on the order of x "
r	= ratio of detection indices
\underline{s}	= desired signal vector
$s(t)$	= desired signal process
T	= observation time of received signal
\underline{v}	= received signal vector
α	= conditional false-alarm probability--noise only present
α^{th}	= a fixed value of α
θ	= an unknown signal parameter
β	= conditional false-dismissal probability--signal and noise present
$\Phi(x)$	= Normal Probability Integral

$\bar{\Phi}^{-1}(x)$ = Inverse Normal Probability Integral

ω_1 = a signal frequency

$\text{tr } \underline{A}$ = trace of matrix \underline{A} = sum of diagonal terms

$\langle \rangle_N$ = conditional average--noise only present

$\langle \rangle_{S_1+N}$ = conditional average--a signal and noise present

Abbreviations

LR = likelihood ratio

p.d.f. = probability density function

SNR = signal-to-noise ratio

References

1. Levesque, A. H., "Optimal Detection of a Sinusoid with Unknown Frequency and Phase," Progress Report No. 8, General Dynamics/Electric Boat Research, Yale University, November 1963.
2. Levesque, A. H., "Likelihood Ratio Detection for Long Observation Times," Progress Report No. 14, General Dynamics/Electric Boat Research, Yale University, May 1964.
3. National Bureau of Standards, Tables of Normal Probability Functions, Applied Mathematics Series, No. 23, Washington, 1953.
4. Lehmann, E. L., Testing Statistical Hypotheses, J. Wiley and Sons, New York, 1959.



AN ANALYSIS OF BEARING ERRORS
DUE TO CLIPPING AND SAMPLING
IN THE PUFFS SONAR SYSTEM

by

Theron Usher, Jr.

Progress Report No. 16

General Dynamics/Electric Boat Research

(53-00-10-0231)

June 1964

DEPARTMENT OF ENGINEERING
AND APPLIED SCIENCE

YALE UNIVERSITY

I. Introduction

The description of the PUFFS sonar system which follows applies to the block diagram of the system found in Fig. 1.

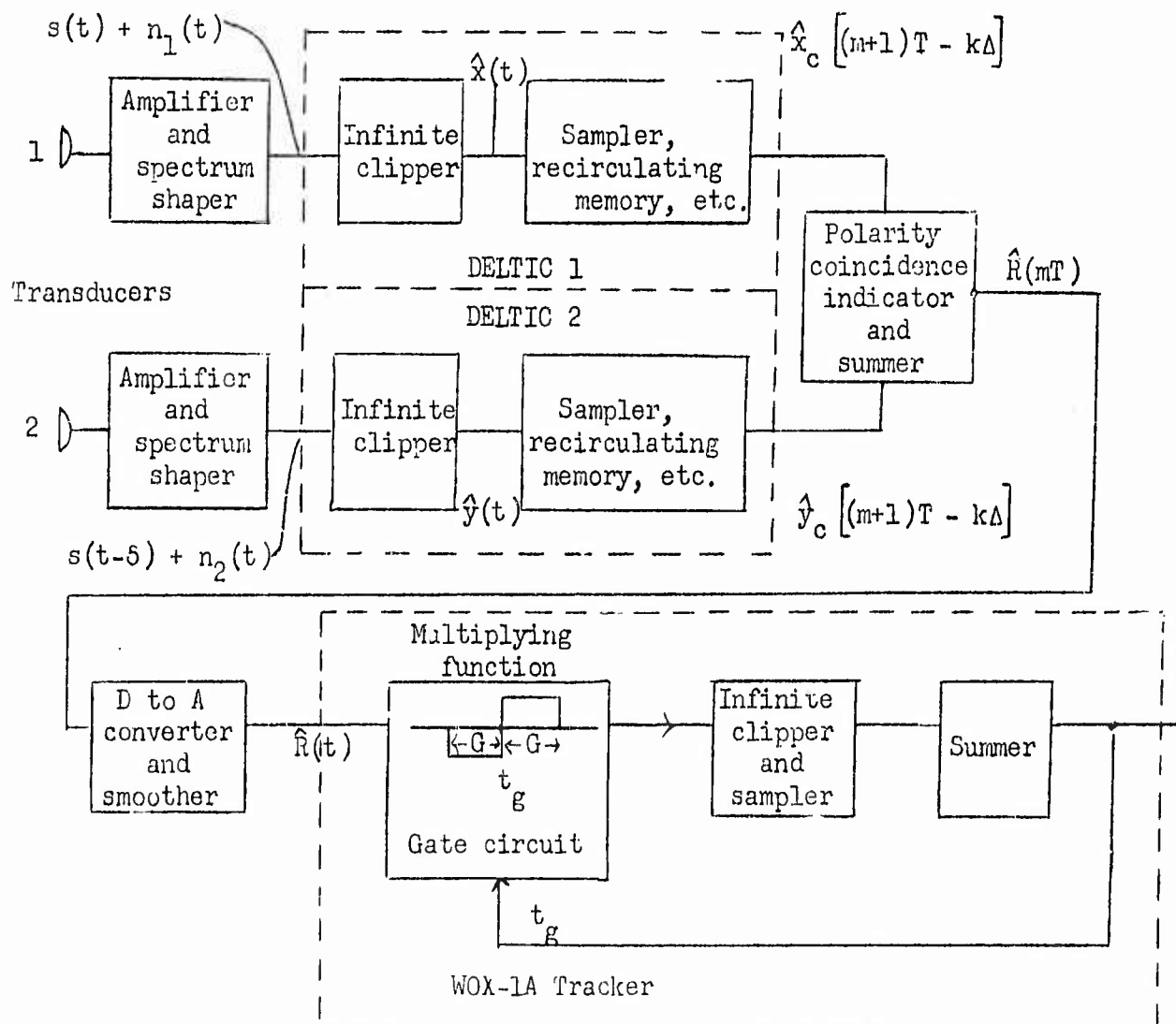


Figure 1 PUFFS Sonar System

The electrical outputs of the transducers are passed through identical amplifiers and filters in each channel. The frequency response characteristic of the amplifier and filter combination is chosen to more-or-less enhance the signal-to-noise properties of the received signal.⁽¹⁾ The amplifier output in the upper channel contains a signal component generated by a target in the water and a contaminating noise component. The amplifier output in the lower channel contains a delayed version of the signal in the upper channel in addition to a noise component.

The outputs of both amplifiers are then processed by Delay Line Time Compressors (DELTIC), which are described in the literature.^{(2), (3)} A DELTIC has two modes of operation, the loading mode and the storage mode.

In the loading mode, the DELTIC samples the clipped version of the input signal at uniform intervals of time. The sample pulse circulates around an acoustical delay line and appears at the output just before the next sample is taken. The next sample pulse then circulates around the acoustical delay line with the previous sample pulse, and the process is repeated. At the beginning of the K^{th} sampling interval the first sample pulse has recirculated and precessed an amount of time almost equal to a sample period. When the $(K+1)^{\text{th}}$ sample is taken, the first sample pulse is discarded. Each time a new sample is taken, the K^{th} previous sample is discarded so that the acoustic delay line holds the previous $(K-1)$ samples in the proper time sequence, but with their time scale compressed by a factor K .

In the storage mode the DELTIC merely recirculates K pulses through the acoustic delay line without the precession encountered in the loading mode. The acoustical delay is increased slightly to accomplish this, and the input samples are discontinued.

In the PUFFS system shown in Fig. 1, DELTIC 2 is operated continuously in the loading mode. DELTIC 1 is operated alternately in the loading and storage modes. The loading mode lasts for K sample periods and the storage mode for K sample periods.

During each sample period occurring in the storage mode time of DELTIC 1, the sequence of positive and negative unit pulses from both DELTIC units are multiplied and the products summed. In this fashion an approximation to the correlation function between the signals in both channels is obtained.

The nonlinear tracker is also described in the literature.⁽⁴⁾ The K-point correlation estimate is smoothed and fed to a device which measures the area of the correlation function for a given time interval centered to the right of a given time coordinate, and subtracts from that the area of the function for the same time interval to the left of the given time coordinate. If the sign of the difference is positive, the time coordinate is shifted in the positive direction a fixed amount, and the same measurement is taken on the K point correlation estimate generated during the following storage-mode time of DELTIC 1. For a negative difference, the tracker time coordinate moves the fixed amount in the negative direction for the next measurement.

In this fashion the tracker automatically seeks a time coordinate for which the output of the gate circuit has an average value of zero. The tracker output should then be a good estimate of the time at which the peak of the correlation function for $\hat{x}(t)$ and $\hat{y}(t)$ occurs, and therefore an estimate of the relative time delay between the signal components in both channels.

At least two analyses to determine the random bearing errors generated by the PUFFS system have been carried out. (5), (6) Ostrander and Rae assume linear processing of the input signals, without clipping or sampling. They obtain a relationship for the random bearing error generated by a gate circuit centered at the peak of the correlation function. In their analysis the width of the gate is assumed to be small relative to the correlation time of the signal. The tracker operation is not considered in the analysis.

In reference (6) the infinite clipping is mentioned, but sampling is not considered. The gate circuit has a width approximately equal to the correlation time of the signal and the nonlinear tracker operation is included in the analysis. The analysis in reference (6) also contains a treatment of the problem of determining maximum bearing rates. If the target is moving such that the bearing rate is constant, the operation of the WOX-1A tracker produces a steady error between actual bearing and estimated bearing. In reference (6), the bearing rate that causes the sum of the steady error and three times standard deviation of the random component to equal the bearing error for maximum output of the gate circuit is defined as the maximum bearing rate. This seems to be a useful rule-of-thumb definition.

In following sections, the effects of infinite clipping, sampling, and the nonlinear operation of the tracker are combined and analyzed to determine the random bearing error. The results are compared to those given by Ostrander and Rae in order to evaluate the degradation caused by clipping and sampling.

II. Correlation Estimate of the DELTIC

From Fig. 1, the outputs of the amplifiers following the hydrophones are given by $s(t) + n_1(t)$ and $s(t-\delta) + n_2(t)$ respectively. It is assumed that the frequency response characteristics of both amplifiers are adjusted to enhance the detection of the signal components.⁽¹⁾ The outputs of the infinite clippers are given by

$$\hat{x}(t) = \text{sgn} \left\{ s(t) + n_1(t) \right\} \quad (1)$$

$$\hat{y}(t) = \text{sgn} \left\{ s(t-\delta) + n_2(t) \right\} \quad (2)$$

As explained in the previous section, the output of the sampler and recirculating memory of each DELTIC is actually a time-compressed series of pulses. The sampler obtains samples T seconds apart and these pulses are recirculated so that K pulses are compressed into one sample period.

For DELTIC 2, which is continuously operated in the loading mode, the compressed output may be expressed by

$$\hat{y}_c \left[(m+1)T - k\Delta \right] = \hat{y} \left[(m-k)T \right] \quad (3)$$

For DELTIC 1, the operation is alternately in the loading mode and the storage mode. Since computation of the estimated cross-correlation function only takes place in the period for the storage mode, the compressed output of interest is

$$\hat{x}_c \left[(m+1)T - k\Delta \right] = \hat{x} \left[-kT \right] \quad (4)$$

In addition,

$$k, m = 0, 1, 2, \dots, (K-1)$$

and

$$T = K \Delta \quad (5)$$

The polarity coincidence indicator and summer in Fig. 1 operates on the pulses in each interval T of the compressed functions \hat{x}_c and \hat{y}_c so as to produce a running estimate of the correlation function of the clipped signals $\hat{x}(t)$ and $\hat{y}(t)$. The estimate is given by

$$\begin{aligned}\hat{R}(mT) &= \frac{1}{K} \sum_{k=0}^{K-1} \hat{x}_c \left[(m+1)T - k\Delta \right] \hat{y}_c \left[(m+1)T - k\Delta \right] \\ &= \frac{1}{K} \sum_{k=0}^{K-1} \hat{x} \left[-kT \right] \hat{y} \left[(m-k)T \right] \quad m = 0, 1, 2, \dots, K-1\end{aligned}\quad (6)$$

The relationship of $\hat{R}(mT)$, hereafter designated by \hat{R}_m , to the properties of the functions at the inputs of the infinite clippers in Fig. 1 is found by substituting Eqs. (1) and (2) into Eq. (6) and finding the mean value of the result:

$$E\left[\hat{R}_m\right] = \frac{1}{K} \sum_{k=0}^{K-1} E\left[\text{sgn}\left\{s(-kT) + n_1(-kT)\right\} \text{sgn}\left\{s(mT - \delta - kT) + n_2(mT - kT)\right\}\right] \quad (7)$$

The value of each term in Eq. (7) is given by the well-known inverse sine relationship⁽⁷⁾ found in Eq. (8).

$$E\left[\hat{R}_m\right] = \frac{2}{\pi} \arcsin \left\{ \frac{S}{(S + N_1)^{1/2} (S + N_2)^{1/2}} \rho_s(mT - \delta) \right\} \quad (8)$$

In Eq. (8) S , N_1 , and N_2 are signal and noise powers respectively and ρ_s is the normalized autocorrelation function for the signal after the spectrum shaping by the amplifier in Fig. 1. It is assumed that $n_1(t)$ and $n_2(t)$ are uncorrelated, and that signal and noise are gaussian and stationary.

If the noise powers are equal and if $S \ll N$ as is the case for threshold detection, Eq. (8) reduces to

$$E[\hat{R}_m] = \frac{2}{\pi} \frac{S}{N} \rho_S(mT - \delta) \quad (9)$$

$$m = 0, 1, \dots, K-1$$

From Eq. (9) it can be seen that the expected value of the K-point correlation estimate is very simply related to the autocorrelation of the signal for threshold situations.

III. Expected Gate Circuit Output

The K-point correlation estimate derived in Section II is actually a time series. This time series is smoothed to a continuous curve before it is applied to the gate circuit of the tracker. For the purposes in this report, it will be assumed that the K-point correlation estimate is smoothed by a triangular interpolating function. The input to the gate circuit is then

$$\hat{R}(t) = \sum_{m=0}^{K-1} \hat{R}_m f\left(\frac{t}{T} - m\right) \quad (10)$$

where

$$f(\alpha) = \begin{cases} 1 - |\alpha| & \alpha \leq 1 \\ 0 & \alpha > 1 \end{cases} \quad (11)$$

The function $f(\alpha)$ is shown in Fig. 2.

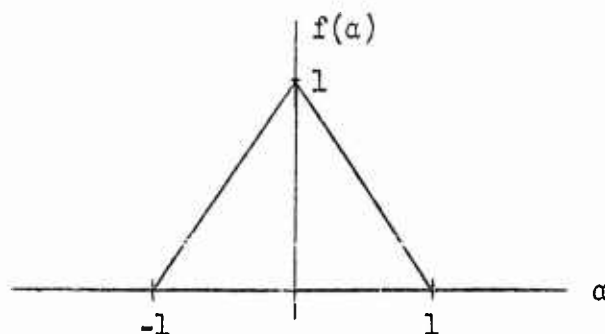


Figure 2 Triangular Interpolating Function

The output of the gate circuit is defined by

$$\begin{aligned}
 F(t_g) &= - \int_{-G+t_g}^{t_g} \hat{R}(t) dt + \int_{t_g}^{G+t_g} \hat{R}(t) dt \\
 &= \sum_{m=0}^{K-1} \hat{R}_m \left[- \int_{-G+t_g}^{t_g} f\left(\frac{t}{T} - m\right) dt + \int_{t_g}^{G+t_g} f\left(\frac{t}{T} - m\right) dt \right] \\
 &= T \sum_{m=0}^{K-1} \hat{R}_m \left[- \int_{\frac{-G+t_g}{T} - m}^{\frac{t_g}{T} - m} f(a) da + \int_{\frac{t_g}{T} - m}^{\frac{G+t_g}{T} - m} f(a) da \right] \quad (12)
 \end{aligned}$$

Using the result in Eq. (9) for $\frac{S}{N} \ll 1$, we find that the expected value of the output of the gate circuit is given by

$$E[F(t_g)] = \bar{F} = \frac{2}{\pi} T \frac{S}{N} \sum_{m=0}^{K-1} \rho_S(mT - \delta) \left[- \int_{\frac{-G+t_g}{T} - m}^{\frac{t_g}{T} - m} f(a) da + \int_{\frac{t_g}{T} - m}^{\frac{G+t_g}{T} - m} f(a) da \right] \quad (13)$$

Also of interest later in the system analysis is the slope of $E[F(t_g)]$ at the primary null response of the gate. The primary null response occurs for $t_g \approx \delta$. The slope is computed for two cases, δ being an integral multiple of T , and δ being an odd half-integral multiple of T . For these cases the null response occurs exactly at $t_g = \delta$. Thus

$$\left. \frac{dF}{dt_g} \right|_{t_g = \delta} = \frac{2}{\pi} \frac{S}{N} \sum_{m=0}^{K-1} \rho_s(mT - \delta) \left[f\left(\frac{-G + \delta}{T} - m\right) + f\left(\frac{G + \delta}{T} - m\right) - 2f\left(\frac{\delta}{T} - m\right) \right] \quad (14)$$

If $G \ll T$, the value of Eq. (14) is greatly determined by the shape of the interpolating function, and since the choice of this function is arbitrary, the results would not be very useful. If G is an integral multiple of T , the value of Eq. (14) is not dependent on the shape of the interpolating function, as long as the function is zero for integral values of α .

If $\frac{\delta}{T}$ is an integer m_0 , then $m_0 T - \delta = 0$ and Eq. (14) for integral values of $\frac{G}{T}$ becomes

$$\left. \frac{dF}{dt_g} \right|_{t_g = \delta} = -2 \cdot \frac{2}{\pi} \frac{S}{N} \left[1 - \rho_s(G) \right] \quad (15)$$

$$\frac{G}{T} = 1, 2, 3, \dots$$

In the derivation of Eq. (15) it is also assumed that $m_0 - \frac{G}{T} \geq 0$ and

$$m_0 + \frac{G}{T} \leq K-1.$$

If $\frac{\delta}{T}$ is an odd half-integer $m_0 + \frac{1}{2}$, then $m_0 T - \delta = \frac{1}{2} T$, and Eq. (14) for integral values of $\frac{G}{T}$ reduces to

$$\left. \frac{d\bar{F}}{dt_g} \right|_{t_g=\delta} = -\frac{2}{\pi} \frac{3}{N} \left[2\rho_s\left(\frac{1}{2}T\right) - \rho_s\left(G - \frac{1}{2}T\right) - \rho_s\left(G + \frac{1}{2}T\right) \right] \quad (16)$$

In the derivation of Eq. (16) the facts that $f(\alpha)$ and $\rho_s(\tau)$ are even functions, and that $f\left(\pm \frac{1}{2}\right) = \frac{1}{2}$ are utilized. Equations (15) and (16) hold for other interpolating functions just as long as $f(\alpha) = 0$ for $|\alpha| > 1$, and $f\left(\pm \frac{1}{2}\right) = \frac{1}{2}$.

IV. Variance of Gate Circuit Output

The variance of the gate circuit output is needed with the results from the previous section to compute the bearing error represented at the output of the gate circuit. It will be assumed that threshold conditions exist such that $S \ll N$. This makes the mathematical derivation of the variance of the gate circuit tractable since only noise χ noise terms are considered.

The square of the output of the gate circuit is

$$F^2(t_g) = T^2 \sum_{\ell=0}^{K-1} \sum_{m=0}^{K-1} \hat{R}_\ell \hat{R}_m \left[\begin{array}{cc} \frac{t_g}{T} - \ell & \frac{G+t_g}{T} - \ell \\ -\int_{\frac{-G+t_g}{T} - \ell}^{\frac{t_g}{T} - \ell} f(\alpha) d\alpha & + \int_{\frac{t_g}{T} - \ell}^{\frac{G+t_g}{T} - \ell} f(\alpha) d\alpha \end{array} \right] \left[\begin{array}{cc} \frac{t_g}{T} - m & \frac{G+t_g}{T} - m \\ -\int_{\frac{-G+t_g}{T} - m}^{\frac{t_g}{T} - m} f(\alpha) d\alpha & + \int_{\frac{t_g}{T} - m}^{\frac{G+t_g}{T} - m} f(\alpha) d\alpha \end{array} \right] \quad (17)$$

The expected value of $F^2(t_g)$ is the variance required, since the computation is done in the absence of signal. The only random variables in Eq. (17) are \hat{R}_ℓ and \hat{R}_m . The integrals depend only on the assumed interpolating functions. The computation of $E[\hat{R}_\ell \hat{R}_m]$ follows from Eqs. (1), (2), and (6).

$$E[\hat{R}_j \hat{R}_m] = \frac{1}{K^2} \sum_{j=0}^{K-1} \sum_{k=0}^{K-1} E \left[\text{sgn}\{n_1(-jT)\} \text{sgn}\{n_2(\ell T - jT)\} \text{sgn}\{n_1(-kT)\} \text{sgn}\{n_2(mT - kT)\} \right] \quad (18)$$

Since $n_1(t)$ and $n_2(t)$ are uncorrelated, and if both have the same spectral characteristics, Eq. (18) simplifies to

$$E[\hat{R}_j \hat{R}_m] = \frac{1}{K^2} \sum_{j=0}^{K-1} \sum_{k=0}^{K-1} \left(\frac{2}{\pi} \right)^2 \arcsin\left\{ \rho_n[(k-j)T] \right\} \arcsin\left\{ \rho_n[(k-j-m+\ell)T] \right\} \quad (19)$$

Equation (19) appears extremely complicated, but many terms for the summation indices m and j are absent because the multipliers in Eq. (17) vanish.

Combining the results of Eq. (19) with those in Eq. (17), we have

$$\sigma_F^2(t_g) = \left(\frac{2}{\pi} \frac{T}{K} \right)^2 \sum_{\ell} \sum_m A\left(\frac{G}{T}, \frac{t_g}{T} - \ell \right) A\left(\frac{G}{T}, \frac{t_g}{T} - m \right) \sum_j \sum_k \mu_{k-j} \mu_{k-j-m+\ell} \quad (20)$$

where

$$A\left(\frac{G}{T}, \frac{t_g}{T} - m \right) = - \int_{\frac{-G+t_g}{T} - m}^{\frac{t_g}{T} - m} f(\alpha) d\alpha + \int_{\frac{t_g}{T} - m}^{\frac{G+t_g}{T} - m} f(\alpha) d\alpha \quad (21)$$

and

$$\mu_k = \arcsin \left\{ \rho_n(kT) \right\} \quad (22)$$

The weighting function A is evaluated in Table 1 for several integer values of $\frac{G}{T}$ at half-integer values of $\left(\frac{t_g}{T} - m \right)$. Note that the weighting functions have odd symmetry. Since the correlation functions $\mu_{k-j-m+\ell}$

are functions of $(m - \ell)$, it is convenient to evaluate the double summation over ℓ and m by considering terms of the type $(m - \ell) = 0$, $(m - \ell) = \pm 1$, $(m - \ell) = \pm 2$, etc. Letting $(m - \ell) = a$, we have

$$\sigma_F^2(t_g) = \left(\frac{2}{\pi} \frac{T}{K}\right)^2 \sum_{m=0}^{K-1} \sum_a A\left(\frac{G}{T}, \frac{t_g}{T} - m + a\right) A\left(\frac{G}{T}, \frac{t_g}{T} - m\right) \sum_{j=0}^{K-1} \sum_{k=0}^{K-1} \mu_{k-j} \mu_{k-j-a} \quad (23)$$

The limits for the summation index a are not defined because only a few values of m and ℓ in Eq. (20) produce non-zero values of the product of the weighting functions. It is assumed that the double summation over m and a in Eq. (23) includes all non-zero values of $A\left(\frac{G}{T}, \frac{t_g}{T} - m + a\right) A\left(\frac{G}{T}, \frac{t_g}{T} - m\right)$.

$\frac{G}{T} \backslash \frac{t_g}{T} - m$	-4	-3.5	-3	-2.5	-2	-1.5	-1.0	-.5	0
1	0	0	0	0	0	$\frac{1}{8}$	$\frac{1}{2}$	$\frac{5}{8}$	0
2	0	0	0	$\frac{1}{8}$	$\frac{1}{2}$	$\frac{7}{8}$	1	$\frac{3}{4}$	0
3	0	$\frac{1}{8}$	$\frac{1}{2}$	$\frac{7}{8}$	1	1	1	$\frac{3}{4}$	0

Table 1 Values of weighting function for triangular interpolating function

The product $A\left(\frac{G}{T}, \frac{t_g}{T} - m + a\right) A\left(\frac{G}{T}, \frac{t_g}{T} - m\right)$ is shown in Table 2 for $\frac{G}{T} = 1$ and various values of a . The indicated summation over index m in Eq. (23) is also executed in Table 2. The coefficients generated are dependent on the position of the gate center, t_g , relative to the estimate points. Two conditions are considered: the gate center halfway between

two correlation estimate points, and the gate center coincident with an estimate point. It is interesting to note that the sum of coefficients for all values of a is always zero.

$a \backslash \frac{t_g}{T} - m$	-2	-1.5	-1.0	-.5	0	.5	1.0	1.5	2.0	$\sum_m \frac{t_g}{T} =$ half integer	$\sum_m \frac{t_g}{T} =$ integer
0	0	$\frac{1}{64}$	$\frac{1}{4}$	$\frac{25}{64}$	0	$\frac{25}{64}$	$\frac{1}{4}$	$\frac{1}{64}$	0	$\frac{3}{16}$	$\frac{1}{2}$
1	0	$\frac{5}{64}$	0	$-\frac{25}{64}$	0	$\frac{5}{64}$	0	0	0	$-\frac{15}{64}$	0
2	0	$-\frac{5}{64}$	$-\frac{1}{4}$	$-\frac{5}{64}$	0	0	0	0	0	$-\frac{5}{32}$	$-\frac{1}{4}$
3	0	$-\frac{1}{64}$	0	0	0	0	0	0	0	$-\frac{1}{64}$	0

Table 2 Non-zero products of weighting functions
for different a . $G/T = 1$

From Table 2, for the case in which t_g is coincident with an estimate point (t_g/T an integer), Eq. (23) reduces to

$$\sigma_{F_1}^2 = \left(\frac{2}{\pi} \frac{T}{K} \right)^2 \sum_{j=0}^{K-1} \sum_{k=0}^{K-1} \frac{1}{2} \mu_{k-j} (\mu_{k-j} - \mu_{k-j+2}) \quad (24)$$

For t_g halfway between estimate points (t_g/T a half-integer), we have

$$\sigma_{F_2}^2 = \left(\frac{2}{\pi} \frac{T}{K} \right)^2 \sum_{j=0}^{K-1} \sum_{k=0}^{K-1} \mu_{k-j} \left(\frac{26}{32} \mu_{k-j} - \frac{15}{32} \mu_{k-j+1} - \frac{10}{32} \mu_{k-j+2} - \frac{1}{32} \mu_{k-j+3} \right) \quad (25)$$

Combining the coefficients for positive and negative values of a is possible because μ is an even function.

If K is very large, and if μ_k is essentially zero for k much smaller than K , then it can easily be shown by expansion of a double series of the type in Eq. (24) that

$$\sum_{j=0}^{K-1} \sum_{k=0}^{K-1} \mu_{k-j} (\mu_{k-j} \pm \mu_{k-j+2r}) \approx K \left[\sum_{k=0}^{K-1} (\mu_k \pm \mu_{k+2r})^2 + \sum_{k=1}^{r-1} (\mu_k \pm \mu_{2r-k})^2 + \mu_r (\mu_r \pm \mu_r) \right] \quad (26)$$

and

$$\sum_{j=0}^{K-1} \sum_{k=0}^{K-1} \mu_{k-j} (\mu_{k-j} \pm \mu_{k-j+2r-1}) \approx K \left[\sum_{k=0}^{K-1} (\mu_k \pm \mu_{k+2r-1})^2 + \sum_{k=1}^{r-1} (\mu_k \pm \mu_{2r-1-k})^2 \right] \quad (27)$$

where

$$r = 1, 2, 3, \dots \quad (r \ll K)$$

The approximations in Eqs. (26) and (27) are such that the left-hand sides are slightly less than the right-hand sides because terms are added to the left-hand sides to satisfy the approximations. Only the first few terms in the approximations are significant, however.

Applying the approximations in Eqs. (26) and (27) to Eqs. (24) and (25), we have

$$\sigma_{F_1}^2 \approx \left(\frac{2}{\pi} \frac{T}{K} \right)^2 K \sum_{k=0}^{K-1} \frac{1}{2} (\mu_k - \mu_{k+2})^2 \quad (28)$$

$$\sigma_{F_2}^2 \approx \left(\frac{2}{\pi} \frac{T}{K} \right)^2 K \left\{ \sum_{k=0}^{K-1} \left[\frac{15}{32} (\mu_k - \mu_{k+1})^2 + \frac{10}{32} (\mu_k - \mu_{k+2})^2 + \frac{1}{32} (\mu_k - \mu_{k+3})^2 \right] + \frac{1}{32} (\mu_1 - \mu_2)^2 \right\} \quad (29)$$

For $\frac{G}{T} = 2$, the product of the weighting functions is shown in Table 3.

$\frac{G}{T} \backslash \frac{G}{T}$		sums over m												half integers		integers
		3	-2.5	-2.0	-1.5	-1.0	-.5	0	.5	1.0	1.5	2.0	2.5	3.0	half integers	integers
0		0	$\frac{1}{64}$	$\frac{1}{4}$	$\frac{49}{64}$	1	$\frac{9}{16}$	0	$\frac{9}{16}$	1	$\frac{49}{64}$	$\frac{1}{4}$	$\frac{1}{64}$	0	$\frac{43}{16}$	$\frac{5}{2}$
1		0	$\frac{7}{64}$	$\frac{1}{2}$	$\frac{21}{32}$	0	$-\frac{9}{16}$	0	$\frac{21}{32}$	$\frac{1}{2}$	$\frac{7}{64}$	0	-	-	$\frac{31}{32}$	1
2		0	$\frac{3}{32}$	0	$-\frac{21}{32}$	-1	$-\frac{21}{32}$	0	$\frac{3}{32}$	0	0	-	-	-	$-\frac{9}{8}$	-1
3		0	$-\frac{3}{32}$	$-\frac{1}{2}$	$-\frac{49}{64}$	$-\frac{1}{2}$	$-\frac{3}{32}$	0	-	-	-	-	-	-	$-\frac{61}{64}$	-1
4		0	$-\frac{7}{64}$	$-\frac{1}{4}$	$-\frac{7}{64}$	0	-	-	-	-	-	-	-	-	$-\frac{7}{32}$	$\frac{1}{4}$
5		0	$-\frac{1}{64}$	0	-	-	-	-	-	-	-	-	-	-	$-\frac{1}{64}$	0

Table 3 Non-zero products of weighting functions
for different $\frac{G}{T}$; $\frac{G}{T} = 2$

The two results for the variance of the gate output, corresponding to Eqs. (24) and (25), are

$$\sigma_{F_1}^2 = \left(\frac{2}{\pi} \frac{T}{K} \right)^2 \sum_{j=0}^{K-1} \sum_{k=0}^{K-1} \mu_{k-j} (2.5 \mu_{k-j} + 2 \mu_{k-j+1} - 2 \mu_{k-j+2} - 2 \mu_{k-j+3} - .5 \mu_{k-j+4})$$

$$\left(\frac{G}{T} = 2 \right) \quad (30)$$

and

$$\sigma_{F_2}^2 = \left(\frac{2}{\pi} \frac{T}{K} \right)^2 \sum_{j=0}^{K-1} \sum_{k=0}^{K-1} \mu_{k-j} (2.69 \mu_{k-j} + 1.94 \mu_{k-j+1} - 2.25 \mu_{k-j+2} - 1.91 \mu_{k-j+3}$$

$$- .44 \mu_{k-j+4} - .03 \mu_{k-j+5})$$

$$\left(\frac{G}{T} = 2 \right) \quad (31)$$

Note that the coefficients of the corresponding terms in Eqs. (30) and (31) are much more nearly equal than those in Eqs. (24) and (25). As $\frac{G}{T}$ increases, dependence of the coefficients on the position of the gate center diminishes.

With the approximations in Eqs. (26) and (27), Eq. (30) simplifies to

$$\sigma_{F_1}^2 \approx \left(\frac{2}{\pi} \frac{T}{K} \right)^2 K \left\{ \sum_{k=0}^{K-1} \left[2(\mu_k + \mu_{k+1})^2 + 2(\mu_k - \mu_{k+2})^2 + 2(\mu_k - \mu_{k+3})^2 + .5(\mu_k - \mu_{k+4})^2 \right. \right.$$

$$\left. \left. - 8 \mu_k^2 \right] + 4 \mu_0^2 + 2(\mu_1 - \mu_2)^2 + .5(\mu_1 - \mu_3)^2 \right\} \quad (32)$$

Equation (31) will not be considered further because it is nearly the same as Eq. (30).

It is also interesting to see the effects of the shape of the assumed interpolating function on the value of the variance of the gate output. For this purpose, the rectangular interpolating function shown in Fig. 3 is used.

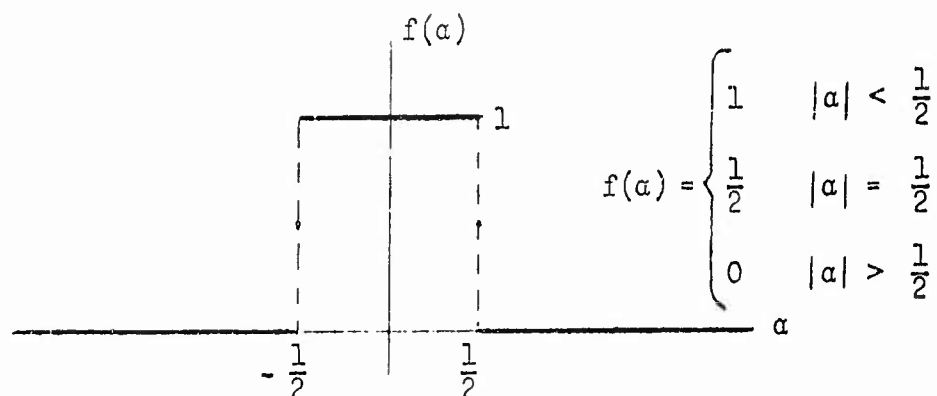


Figure 3 Rectangular Interpolating Function

The weighting function defined in Eq. (21) for the arbitrary interpolating function is evaluated in Table 4 for the rectangular interpolating function.

$\frac{G}{T} \backslash \frac{t_g}{T} - m$	-3.5	-3	-2.5	-2.0	-1.5	-1.0	-.5	0
1	-	-	-	-	0	.5	1.0	0
2	-	-	0	.5	1.0	1.0	1.0	0
3	0	.5	1.0	1.0	1.0	1.0	1.0	0

Table 4 Values of weighting function for rectangular interpolating function

The product $A\left(\frac{G}{T}, \frac{t_g}{T} - m + a\right) A\left(\frac{G}{T}, \frac{t_g}{T} - m\right)$ is shown in Table 5 for $\frac{G}{T} = 1$ and various values of a . In Table 6 the same product is evaluated for $\frac{G}{T} = 2$.

The summation indicated over index m in Eq. (23) is also evaluated for integer and half-integer values of $\frac{t_g}{T}$ in Tables 5 and 6.

$\frac{t}{T} - m$ a	-1.5	-1.0	-.5	0	.5	1.0	1.5	sums	
								half integers	integers
0	0	.25	1.0	0	1.0	.25	0	2.0	.5
1	0	0	-1.0	0	0	-	-	-1.0	0
2	0	-.25	0	-	-	-	-	0	-.25
3	-	-	-	-	-	-	-	0	0

Table 5 Non-zero products of weighting function
for different a; rectangular interpolating
function; $G/T = 1$

$\frac{t}{T} - m$ a	-2.5	-2.0	-1.5	-1.0	-.5	0	0.5	1.0	1.5	2.0	2.5	sums	
												half integers	integers
0	0	.25	1.0	1.0	1.0	0	1.0	1.0	1.0	.25	0	4.0	2.5
1	0	.5	1.0	0	-1.0	0	1.0	.5	0	-	-	1.0	1.0
2	0	0	-1.0	-1.0	-1.0	0	0	-	-	-	-	-2.0	-1.0
3	0	-.5	-1.0	-.5	0	-	-	-	-	-	-	-1.0	-1.0
4	0	-.25	0	-	-	-	-	-	-	-	-	0	-.25

Table 6 Non-zero products of weighting functions for different a;
rectangular interpolating function; $G/T = 2$

From Table 5, the variance of the gate output for integer and half-integer values of t_g/T respectively can be shown to be

$$\sigma_{F_1}^2 \approx \left(\frac{2}{\pi} \frac{T}{K} \right)^2 K \sum_{k=0}^{K-1} \frac{1}{2} (\mu_k - \mu_{k+2})^2 \quad \left(\frac{G}{T} = 1 \right) \quad (33)$$

$$\sigma_{F_2}^2 \approx \left(\frac{2}{\pi} \frac{T}{K} \right)^2 K \sum_{k=0}^{K-1} 2 (\mu_k - \mu_{k+1})^2 \quad \left(\frac{G}{T} = 1 \right) \quad (34)$$

Equation (33) is identical to Eq. (28), but Eq. (34) is considerably different from Eq. (29) and Eq. (33).

From Table 6, for $\frac{G}{T} = 2$, it can be seen that the variance for integer values of t_g/T is identical to that of the corresponding case for the triangular interpolating function. In fact, the variance for integer values of t_g/T for all integer values of $\frac{G}{T}$ can be shown to be independent of the shape of the interpolating function, as long as it is symmetrical and zero for $|a| \geq 1$.

For half-integer values of t_g/T the variance may be shown to be approximately

$$\sigma_{F_2}^2 \approx \left(\frac{2}{\pi} \frac{T}{K} \right)^2 K \left\{ \sum_{k=0}^{K-1} \left[2(\mu_k + \mu_{k+1})^2 + 4(\mu_k - \mu_{k+2})^2 + 2(\mu_k - \mu_{k+3})^2 - 8\mu_k^2 \right] + 4\mu_0^2 + 2(\mu_1 - \mu_2)^2 \right\} \quad (35)$$

An examination of the coefficients in Table 6 $\left(\frac{G}{T} = 2 \right)$ for half-integer values of t_g/T shows that they are closer to those for integer values of t_g/T than those listed in Table 5 $\left(\frac{G}{T} = 1 \right)$. However, the convergence of both sets of values for increasing $\frac{G}{T}$ is not as rapid for

the rectangular interpolating function as it is for the triangular interpolating function. Evidently, the dependence of the variance on the position of t_g relative to the estimate points diminishes as $\frac{G}{T}$ increases and as the interpolating function becomes smoother.

V. Bearing Error at Output of Gate Circuit

From previous work,⁽⁹⁾ bearing error or uncertainty has been defined by a relation similar to the one found in Eq. (36).

$$\sigma_{\theta} = \frac{c}{d} \sigma_F \left| \frac{dF}{dt_g} \right|_0^{-1} \quad (36)$$

In Eq. (36), c is the speed of sound in the medium and d is the separation between transducers in Fig. 1. The relation holds for small bearing angles.

The following equations are the results of substituting Eqs. (28), (29), (32), (33), (34), (35), (15) and (16) into Eq. (36).

For both interpolating functions and integer values of t_g/T , we have

$$\sigma_{\theta_1} = \frac{c}{d} \frac{T}{K^{1/2}} \left(\frac{N}{S} \right) \frac{\left[\sum_{k=0}^{K-1} \frac{1}{2} (\mu_k - \mu_{k+2})^2 \right]^{1/2}}{2[1 - \rho_s(T)]} \quad \left(\frac{G}{T} = 1 \right) \quad (37)$$

and

$$\sigma_{\theta_1} = \frac{c}{d} \frac{T}{K^{1/2}} \left(\frac{N}{S} \right) \frac{\left[\sum_{k=0}^{K-1} \left\{ 2(\mu_k + \mu_{k+1})^2 + 2(\mu_k - \mu_{k+2})^2 + 2(\mu_k - \mu_{k+3})^2 + .5(\mu_k - \mu_{k+4})^2 \right. \right.}{2[1 - \rho_s(2T)]} \quad \left. \left. - 8\mu_k^2 \right\} + 4\mu_0^2 + 2(\mu_1 - \mu_2)^2 + .5(\mu_1 - \mu_3)^2 \right]^{1/2}}{\quad} \quad \left(\frac{G}{T} = 2 \right) \quad (38)$$

For half-integer values of t_g/T , and $\frac{G}{T} = 1$, we have

$$\sigma_{\theta_2} = \frac{c}{d} \frac{T}{K^{1/2}} \left(\frac{N}{S} \right) \frac{\left[\sum_{k=0}^{K-1} \left\{ \frac{15}{32} (\mu_k - \mu_{k+1})^2 + \frac{10}{32} (\mu_k - \mu_{k+2})^2 + \frac{1}{32} (\mu_k - \mu_{k+3})^2 \right\} + \frac{1}{32} (\mu_1 - \mu_2)^2 \right]^{1/2}}{\left[\rho_s \left(\frac{1}{2} T \right) - \rho_s \left(\frac{3}{2} T \right) \right]} \quad (39)$$

(triangular interpolating
function)

and

$$\sigma_{\theta_2} = \frac{c}{d} \frac{T}{K^{1/2}} \left(\frac{N}{S} \right) \frac{\left[\sum_{k=0}^{K-1} 2 (\mu_k - \mu_{k+1})^2 \right]^{1/2}}{\left[\rho_s \left(\frac{1}{2} T \right) - \rho_s \left(\frac{3}{2} T \right) \right]} \quad (40)$$

(rectangular interpolating
function)

Finally, for half-integer values of t_g/T , $\frac{G}{T} = 2$, and the rectangular interpolating function, we have

$$\sigma_{\theta_2} = \frac{c}{d} \frac{T}{K^{1/2}} \left(\frac{N}{S} \right) \frac{\left[\sum_{k=0}^{K-1} \left\{ 2 (\mu_k + \mu_{k+1})^2 + 4 (\mu_k - \mu_{k+2})^2 + 2 (\mu_k - \mu_{k+3})^2 - 8 \mu_k^2 \right\} + 4 \mu_0^2 + 2 (\mu_1 - \mu_2)^2 \right]^{1/2}}{\left[2 \rho_s \left(\frac{1}{2} T \right) - \rho_s \left(\frac{3}{2} T \right) - \rho_s \left(\frac{5}{2} T \right) \right]} \quad (41)$$

In the section that follows, numerical evaluation of Eqs. (37) through (41) is presented.

VI. Numerical Examples

In this section, specific functions are assumed for the normalized correlation functions for signal and noise, typical values are assumed for the parameters of the DELTIC, and the corresponding bearing uncertainties at the output of the gate circuit are computed. The results are compared to those obtained by Ostrander and Rae⁽⁵⁾ for the linear system, and by Usher⁽¹⁰⁾ for a null-output split-beam system. For the purposes of comparison, equivalent observation times and identical array configurations are assumed.

The signal and noise spectral densities are assumed to be identical, except for power level, each being given by

$$G_s(\omega) = \begin{cases} \frac{S}{2\omega_o} & |\omega| \leq \omega_o \\ 0 & |\omega| > \omega_o \end{cases} \quad (42)$$

and

$$G_n(\omega) = \begin{cases} \frac{N}{2\omega_o} & \omega \leq \omega_o \\ 0 & \omega > \omega_o \end{cases} \quad (43)$$

The normalized autocorrelation functions for signal and noise follow.

$$\rho_s(\tau) = \rho_n(\tau) = \frac{\sin \omega_o \tau}{\omega_o \tau} = \text{sinc}\left(\frac{\omega_o \tau}{\pi}\right) \quad (44)$$

These assumptions are fairly realistic in that signal and noise are whitened by the amplifiers and spectrum shapers in Fig. 1 to an upper frequency limit determined by the target range.⁽¹⁰⁾

If $\omega_0 T = \frac{\pi}{2}$, from Eqs. (22) and (44) we have

$$\mu_k = \arcsin \left\{ \text{sinc } \frac{k}{2} \right\} \quad (45)$$

The values of μ_k are listed in Table 7.

k	0	1	2	3	4	5	6	7	8	9
μ_k	1.57	.692	0	-.213	0	.127	0	-.091	0	.078

Table 7 μ_k as a function of k for $\omega_0 T = \frac{\pi}{2}$

The results in Eqs. (37) through (41) have been computed and the normalized bearing uncertainty, $\sigma_\theta \frac{d}{c} \frac{K^{1/2}}{T} \frac{S}{N}$, for the different cases is shown in Table 8.

Gate width G/T	1		2	
Gate center t_g/T	half integer	integer	half integer	integer
triangular interpolation	2.28	1.83	≈ 2.26	1.90
rectangular interpolation	2.76		2.63	

Table 8 $\sigma_\theta \frac{d}{c} \frac{K^{1/2}}{T} \frac{S}{N}$, Normalized bearing uncertainty

for $\omega_0 T = \frac{\pi}{2}$, band-limited white spectrum

If $\omega_0 T = \pi$, Eqs. (22) and (44) yield

$$\mu_k = \arcsin \left\{ \operatorname{sinc} k \right\} = \begin{cases} \frac{\pi}{2} & k = 0 \\ 0 & k \neq 0 \end{cases} \quad (46)$$

The property in Eq. (46) allows a vast simplification of Eqs. (37) through (41) and also allows the investigation in Section IV to be easily extended for values of normalized gate with $\frac{G}{T}$ larger than 2.

From the property in Eq. (46),

$$\mu_{k-j} \mu_{k-j-a} = \begin{cases} \left(\frac{\pi}{2} \right)^2 & k = j \quad a = 0 \\ 0 & \text{otherwise} \end{cases} \quad (47)$$

Equation (23) then reduces to

$$\sigma_F^2(t_g) = \frac{T^2}{K} \sum_{m=0}^{K-1} \left[A \left(\frac{G}{T}, \frac{t_g}{T} - m \right) \right]^2 \quad (48)$$

By extending Tables 1 and 4, squaring, and summing, we can show the following relations. For the triangular interpolating function

$$\sum_{n=0}^{K-1} A^2 = \begin{cases} 2 \frac{G}{T} - \frac{21}{16} & \frac{G}{T} = 2, 3, \dots \text{half integer } \frac{t_g}{T} \\ 2 \frac{G}{T} - \frac{3}{2} & \frac{G}{T} = 1, 2, 3, \dots \text{integer } \frac{t_g}{T} \end{cases} \quad (49)$$

For the rectangular interpolating function

$$\sum_{n=0}^{K-1} A^2 = \begin{cases} 2 \frac{G}{T} & \frac{G}{T} = 1, 2, 3, \dots \text{half integer } \frac{t_g}{T} \\ 2 \frac{G}{T} - \frac{3}{2} & \frac{G}{T} = 1, 2, 3, \dots \text{integer } \frac{t_g}{T} \end{cases} \quad (50)$$

By simplifying Eq. (15) for $\omega_0 T = \pi$, we obtain for integer values of t_g/T

$$\left. \frac{d\bar{F}}{dt_g} \right|_{t_g=\delta} = -2 \frac{2}{\pi} \frac{S}{N} \quad (51)$$

For half integer values of t_g/T and $\omega_0 T = \pi$, Eq. (16) yields

$$\begin{aligned} \left. \frac{d\bar{F}}{dt_g} \right|_{t_g=\delta} &= -2 \frac{2}{\pi} \frac{S}{N} \frac{1}{\pi} \left\{ 2 + (-1)^{G/T} \left[\left(2 \frac{G}{T} - 1 \right)^{-1} - \left(2 \frac{G}{T} + 1 \right)^{-1} \right] \right\} \\ &= -2 \frac{2}{\pi} \frac{S}{N} \frac{2}{\pi} \frac{4 \left(\frac{G}{T} \right)^2 + (-1)^{G/T} - 1}{4 \left(\frac{G}{T} \right)^2 - 1} \end{aligned} \quad (52)$$

Substituting the results of Eqs. (48) through (52) into Eq. (35), we have for integer values of t_g/T , and both interpolating functions,

$$\sigma_{\theta_i} = \frac{\pi}{2\sqrt{2}} \cdot \frac{c}{d} \frac{N}{S} K^{-1/2} T \left(\frac{G}{T} - \frac{3}{4} \right)^{1/2} \quad \frac{G}{T} = 1, 2, 3, \dots \quad (53)$$

For half-integer values of t_g/T ,

$$\sigma_{\theta_h} = \frac{\pi}{2\sqrt{2}} \cdot \frac{\pi}{2} \cdot \frac{4 \left(\frac{G}{T} \right)^2 - 1}{4 \left(\frac{G}{T} \right)^2 + (-1)^{G/T} - 1} \cdot \frac{c}{d} \frac{N}{S} K^{-1/2} T \begin{cases} \times \left(\frac{G}{T} \right)^{1/2} & \text{(rectangular)} \\ \times \left(\frac{G}{T} - \frac{21}{32} \right)^{1/2} & \text{(triangular)} \end{cases} \quad (54)$$

$\frac{G}{T} = 2, 3, 4, \dots$

As $\frac{G}{T}$ increases, the effect of the interpolating function vanishes, but the position of t_g ($t_g = \delta$) makes the result in Eq. (54) higher by a factor $\frac{\pi}{2}$ as a result of the decreased slope of \bar{F} in the vicinity of $t_g = \delta$ for half-integer values of t_g/T .

In order to compare the above results to those obtained by Ostrander and Rae, we note that the total observation time is KT . In terms of bearing uncertainty, the results of Ostrander and Rae⁽⁵⁾ yield Eq. (55), which is written in terms of the symbols used in this report.

$$\sigma_{\theta_L} = \frac{c}{d} \left(\frac{\pi}{KT} \right)^{1/2} \frac{\left[\int_0^\infty \omega^2 G_n(\omega) [G_n(\omega) + 2 G_s(\omega)] d\omega \right]^{1/2}}{\int_0^\infty \omega^2 G_s(\omega) d\omega} \quad (55)$$

For the spectra in Eqs. (42) and (43), and if $\frac{S}{N} \ll 1$, Eq. (55) reduces to

$$\sigma_{\theta_L} = (3\pi)^{1/2} \frac{c}{d} \frac{N}{S} K^{-1/2} T^{-1/2} \omega_0^{-3/2} \quad (56)$$

Equation (56) holds only for small values of G such that the autocorrelation functions for signal and noise may be approximated by

$$\rho(\tau) = 1 + \frac{\tau^2}{2!} \ddot{\rho}(0) \quad \text{for} \quad |\tau| < G \quad (57)$$

For the assumed spectra, the power series approximation is

$$\rho(\tau) = \frac{\sin \omega_0 \tau}{\omega_0 \tau} = 1 - \frac{(\omega_0 \tau)^2}{3!} + \frac{(\omega_0 \tau)^4}{5!} - \dots \quad (58)$$

If $\tau = G$ and $\omega_0 G = \frac{\pi}{2}$, the first two terms of Eq. (58) yield .589, which is a good approximation to the actual value of .638. Thus Eq. (56) is a good approximation for $\omega_0 G \leq \frac{\pi}{2}$.

For the system considered in Table 8, $\omega_0 T = \frac{\pi}{2}$. Eliminating ω_0 from Eq. (56), we have

$$\sigma_{\theta_L} = \frac{2 \cdot 5^{1/2}}{\pi} \frac{c}{d} \frac{N}{S} K^{-1/2} T = 1.56 \frac{c}{d} \frac{N}{S} K^{-1/2} T \quad (59)$$

From the data in Table 8 for $\frac{G}{T} = 1$,

$$\sigma_{\theta} = (1.83 \text{ to } 2.76) \frac{c}{d} \frac{N}{S} K^{-1/2} T \quad (60)$$

The data for $\frac{G}{T} = 2$ is not significantly different. For $\frac{G}{T} = 1$, $\omega_0 G = \frac{\pi}{2}$ in this case and comparison for equal gate widths is valid.

For the system represented by the development leading to Eqs. (53) and (54), $\omega_0 T = \pi$. Eliminating ω_0 from Eq. (56), we have

$$\sigma_{\theta_L} = \frac{3^{1/2}}{\pi} \frac{c}{d} \frac{N}{S} K^{-1/2} T \quad (61)$$

Equation (61) is valid only if $\frac{G}{T} < \frac{1}{2}$. The ratio of the bearing uncertainty in Eqs. (53) and (54) to that in Eq. (61) represents a reasonable performance index that indicates the effect of increasing the gate width. We have as the upper bound

$$\frac{\sigma_{\theta_h}}{\sigma_{\theta_L}} = \frac{\pi^3}{4 \cdot 6^{1/2}} \frac{4\left(\frac{G}{T}\right)^2 - 1}{4\left(\frac{G}{T}\right)^2 + (-1)^{G/T} - 1} \begin{cases} \times \left(\frac{G}{T}\right)^{1/2} & \text{for rectangular interpolation} \\ \times \left(\frac{G}{T} - \frac{21}{32}\right)^{1/2} & \text{for triangular interpolation} \end{cases} \quad (62)$$

and as the lower bound

$$\frac{\sigma_{\theta_1}}{\sigma_{\theta_L}} = \frac{\pi^2}{2 \cdot 6^{1/2}} \left(\frac{G}{T} - \frac{3}{4} \right)^{1/2} \quad (63)$$

Equations (62) and (63) are evaluated and plotted in Fig. 4.

The result for bearing uncertainty for a split-beam system reported by Usher⁽¹⁰⁾ is

$$\sigma_{\theta} = \frac{c}{Md} \left(\frac{SM}{N} \right)^{1/2} (\omega_L)^{1/2} \frac{\left[\int_0^{\infty} \omega^2 |H_B(j\omega)|^4 g_n^2(\omega) d\omega \right]^{1/2}}{\int_0^{\infty} \omega^2 |H_B(j\omega)|^2 g_s(\omega) d\omega} \quad (64)$$

For our system, $M = 1$ and the noise bandwidth of the low-pass filter⁽¹¹⁾ is $\omega_L = \frac{\pi}{KT}$. Also the quantities $|H_B(j\omega)|^2 g_n(\omega)$ and $|H_B(j\omega)|^2 g_s(\omega)$ correspond to the signal and noise spectra assumed in this report. Under these conditions, the results for the split-beam system are identical to those of Ostrander and Rae.⁽⁵⁾

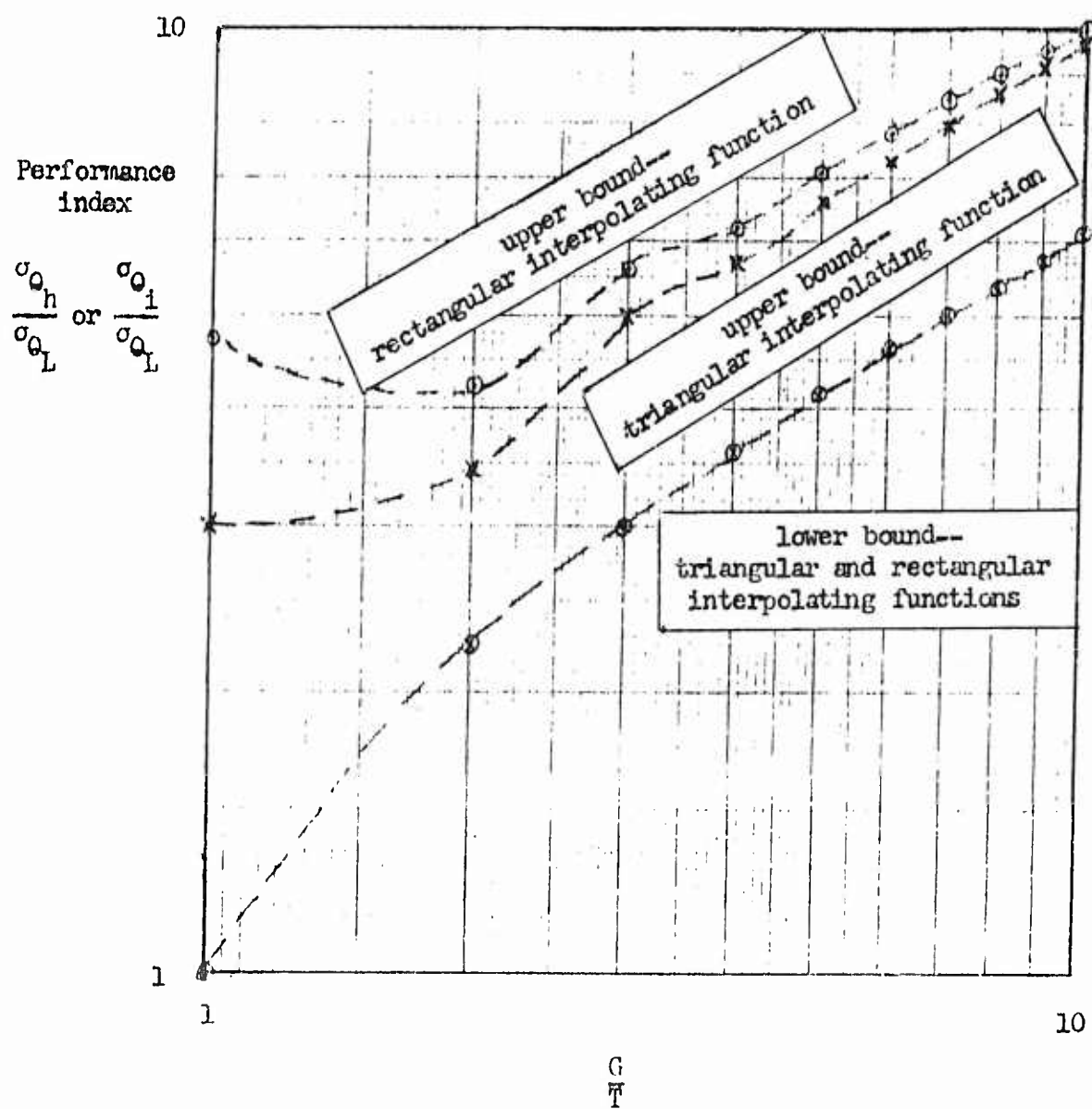


Figure 4

VII. Effect of Nonlinear Tracker (VOX-1A)

The results of Pryor's analysis⁽⁴⁾ can be applied to the system in this report, but some care must be exercised in using Eq. (6) in Reference (4).

The actual step size of the tracker will be defined as Δ_g so that the gate center of the tracker can assume values

$$t_g = \delta + r \Delta_g \quad r = 0, \pm 1, \pm 2, \pm 3, \dots \quad (65)$$

It is assumed that Δ_g is much smaller than T . The gate circuit output has a variance σ_F^2 and the mean value of F for small shifts of the gate center defined by Eq. (65) is approximately

$$\bar{F} \approx r \Delta_g \left. \frac{d\bar{F}}{dt_g} \right|_{t_g = \delta} \quad (66)$$

Expressions for σ_F^2 and the derivative of \bar{F} have been given in previous sections. From Eq. (66), the shift of the input probability distribution each time a step Δ_g is taken is

$$\Delta_g \left. \frac{d\bar{F}}{dt_g} \right|_{t_g = \delta}$$

Following Pryor's analysis,⁽⁴⁾ we are forced to normalize the input standard deviation σ_F by the factor $\left. \frac{d\bar{F}}{dt_g} \right|_{t_g = \delta}$. Equation (67), which

follows, is essentially Eq. (6), Reference (4), modified to apply to the system considered in this report.

$$\sigma_g = \left(\frac{\pi}{8} \right)^{1/4} \left(\Delta_g \sigma_F \left| \left. \frac{d\bar{F}}{dt_g} \right|_{t_g = \delta} \right|^{-1} \right)^{1/2} \quad (67)$$

The bearing uncertainty at the output of the gate circuit, σ_{θ}' , for small bearing angles is $\frac{c}{d} \sigma_g$, and from Eq. (67) is given by

$$\sigma_{\theta}' = \left(\frac{\pi}{8}\right)^{1/4} (\Delta_{\theta} \sigma_{\theta})^{1/2} \quad (68)$$

where

$$\Delta_{\theta} = \frac{c}{d} \Delta_g \quad (69)$$

Equation (68) is valid only where $\Delta_{\theta} \ll \sigma_{\theta}$.

In Section VI for $\frac{G}{T} = 1$, the following relation held for σ_{θ}

$$\sigma_{\theta} \leq \begin{cases} 1.83 \frac{c}{d} \frac{T}{K^{1/2}} \frac{N}{S} & \omega_o T = \frac{\pi}{2} \\ .555 \frac{c}{d} \frac{T}{K^{1/2}} \frac{N}{S} & \omega_o T = \pi \end{cases} \quad (70)$$

From Eq. (69) and the inequality of Δ_{θ} , we have

$$\frac{\Delta_g}{T} \ll \begin{cases} 1.83 \frac{N}{S} K^{-1/2} & \omega_o T = \frac{\pi}{2} \\ .555 \frac{N}{S} K^{-1/2} & \omega_o T = \pi \end{cases} \quad (71)$$

for validity of Eq. (68).

A final complete numerical computation using approximate system parameters is now in order. It will be assumed that

$$K = 500$$

$$T = 50 \times 10^{-6} \text{ sec.}$$

$$\frac{G}{T} = 1$$

$$\omega_c T = \pi$$

$$\frac{\Delta E}{T} = .05$$

$$c = 5000 \text{ ft/sec.}$$

$$d = 100 \text{ ft.}$$

$$\frac{N}{S} = 100 \quad \left(\frac{S}{N} = -20 \text{ db.} \right)$$

From Eq. (61) for the linear and optimal result, we have

$$\sigma_{\theta_L} = \frac{3^{1/2}}{\pi} \frac{5000}{100} (100)(500)^{-1/2} (50 \times 10^{-6}) = 6.14 \times 10^{-3} \text{ rad} = .35 \text{ degrees} \quad (72)$$

Assuming from Fig. 4 that an average performance index of 2 is appropriate for $\frac{G}{T} = 1$, the bearing uncertainty for the output of the gate circuit is

$$\sigma_{\theta} \cong 2(.35) = .7 \text{ degrees} \quad (73)$$

The inequality in Eq. (70) is easily satisfied, so that the bearing uncertainty represented by the output of the WOX-1A tracker from Eqs. (68) and (69) is

$$\sigma_{\theta} = \left(\frac{\pi}{8} \right)^{1/4} \left(\frac{5000}{100} (.05)(50 \times 10^{-6})(57.3)(.7) \right)^{1/2} = .056 \text{ degrees}$$

VIII. Summary and Conclusions

The numerical comparisons carried out in Section VI show that the clipping and sampling operations of the DELTIC processors which were used to compute a sampled estimate of the correlation function caused increased bearing uncertainty relative to that provided by a system without sampling or clipping.

The degradation is not too large, however, if the gate width is not large relative to the correlation time. From the numerical factors in Eq. (59) and Table 8 the ratio of bearing uncertainties ranges from 1.17 to 1.46 for triangular interpolation. The variation is caused by the position of the signal delay time relative to the integral values of T at which the correlation estimates are made. Very nearly the same results are obtained for gate width taking on values equal to the correlation time of the process and also one-half the correlation time of the process. This result shows that there is no advantage gained by making the gate width extremely small.

By doubling the bandwidth of the spectrum, it was possible to obtain numerical results for fairly large values of gate width due to the special nature of the autocorrelation function of signal and noise. Figure 4 shows the ratios of bearing uncertainties for this situation. In this case, for $\frac{G}{T} = 1$, the gate width is equal to the correlation time of the process. Quite widely varying answers are obtained due to the nature of the interpolating functions and the assumed $\frac{\sin \omega_0 \tau}{\omega_0 \tau}$ autocorrelation function for signal and noise.

However, the performance index generally increases as the square root of the gate width, for gate width larger than the correlation time. For $\frac{G}{T} = 1$, the ratio of bearing uncertainties varies between 1.0 and 3.0 for

triangular interpolation. It is expected that the variation would be smaller and less dependent on the position of the gate center for other assumed autocorrelation functions, but the computation would have been much more difficult. An average value of 2 for the ratio of bearing uncertainty for the PUFFS system to that for the system without clipping or sampling seems reasonable.

For the numerical example considered in Section VII, one might say that $\sigma_0 = .7$ degrees corresponds to a bearing error that exceeds the linear range of the gate circuit. For $\frac{G}{T} = 1$, the gate width corresponds to an angle of $\frac{c}{d} G(57.3) = .143^\circ$. An examination of a slightly altered version of Eq. (14) reveals that the maximum of the gate output occurs in the vicinity of $|t_g - \delta| \approx G$ for all $\frac{G}{T}$, and the previous comment might seem to be correct.

However, the slope term $\left. \frac{dF}{dt} \right|_{t_g = \delta}$ in Eq. (36) is used merely as a

calibration constant in computing an apparent bearing inaccuracy from the magnitude of the output signal. Note that $t_g = \delta$ for this computation. The WOX-1A tracker does cause t_g to change in accordance with the output signal of the gate circuit, and it is the tracker output that one must examine to be careful that the error does not exceed, say, one-third of the angle at which the peak output of the tracker occurs. In the example considered, the tracker random bearing error is .056 degrees, which slightly exceeds one-third of the maximum linear range of 0.143 degrees.

It is interesting to note that the WOX-1A tracker is able to reduce the apparent bearing uncertainty because it acts as a nonlinear low-pass filter on the output of the gate circuit and simply makes the effective

observation time much longer than the observation time, KT , for the estimated data feeding into the gate circuit. It should also be noted that the actual observation time for the PUFFS system is one-half that of a continuously operating system, since no autocorrelation estimates are made during the intervals that DELTIC 1 is in the loading mode.

References

- (1) Eckart, Carl, Optimal Rectifier Systems for the Detection of Steady Signals, Marine Laboratory, Scripps Institute of Oceanography, SIO Reference 52-11, University of California, 4 March 1952.
- (2) Anderson, V. C., "Delay Line Time Compressor (DELTIC)," U. S. Patent No. 2,958,039, 25 October 1960.
- (3) Allen, W. B., and E. C. Westerfield, "Digital Compressed-Time Correlators and Matched Filters for Active Sonar," JASA 36, pp. 121-139, January 1964.
- (4) Pryor, C. N., "Analysis of the Puffs Tracker WOX-1A as a General Nonlinear Filter," NAVWEPS Report 7375.
- (5) Ostrander and Rae, "A Method for Estimating Fire Control Accuracies of Submarine PUFFC Systems," ORI, Reports 143 and 143A, 15 April 1963 (CONFIDENTIAL).
- (6) "Final Report on EX-10 Study," pp. 58-90, Raytheon Company, 1 August 1962 (CONFIDENTIAL).
- (7) Karman, W. W., Principles of the Statistical Theory of Communication, p. 153, McGraw-Hill Book Company, 1963.
- (8) Jahnke, Eugene, and Fritz Emde, Tables of Functions, pp. 1-5, Dover Publications, 1945.
- (9) Theoretical Limitations Imposed by System Parameters on Passive Sonar Bearing Accuracy, NAVWEPS Report 4732, The Raytheon Company, 10 August 1962 (CONFIDENTIAL).
- (10) Usher, T. Jr., "Random Bearing Errors in Split-Beam Systems," Progress Report No. 9, General Dynamics/Electric Boat Company Research, Yale University, December 1963.
- (11) McDonald, R. A., "Minimum Variance Estimation of Relative Delay between Two Random Signals in Noise," p. 10, Progress Report No. 12, General Dynamics/Electric Boat Company Research, Yale University, March 1964.

DISTRIBUTION LIST

Defense Documentation Center
Cameron Station (20 copies)
Alexandria, Va. 22314

Bureau of Naval Weapons
Navy Department
Washington 25, D.C.
Attn: RUDC-1

Bureau of Ships
Navy Department
Washington 25, D.C.
Attn: Code 525

Bureau of Ships
Navy Department
Washington 25, D.C.
Attn: Code 450

Bureau of Ships
Navy Department
Washington 25, D.C.
Attn: Leroy Rosen
Code 361D

Bureau of Ships
Navy Department
Washington 25, D.C.
Attn: Code 420

Bureau of Ships (3 copies)
Department of the Navy
Washington 25, D.C.
Attn: N. L. Black
Code 300 FA (FRISCO)

Bureau of Ships
Navy Department
Washington 25, D.C.
Attn: Code 687

Bureau of Ships
Navy Department
Washington 25, D.C.
Attn: Code 1500

Chief, Bureau of Naval Weapons
Washington 25, D.C.
Attn: A. Marans
Code RUSE-4 (FRISCO)

Chief of Naval Operations
Navy Department
Washington 25, D.C.
Attn: OP-311

Chief of Naval Operations
Navy Department
Washington 25, D.C.
Attn: OP-713

Chief of Naval Operations
Navy Department
Washington 25, D.C.
Attn: OP-71

Commandant
Mare Island Naval Shipyard
Vallejo, California
Attn: Design Superintendent

Commandant
Portsmouth Naval Shipyard
Portsmouth, New Hampshire
Attn: Design Superintendent

Commander
Antisubmarine Defense Force
U. S. Pacific Fleet
N. A. S., Navy No. 128
FPO, San Francisco, California

Commander
Submarine Development Group Two
U. S. Naval Submarine Base
Groton, Connecticut

Commander
Submarine Force
U. S. Atlantic Fleet
C/O Fleet Post Office
New York, New York

Commander
Submarine Force
U. S. Pacific Fleet
C/O Fleet Post Office
San Francisco, California

DISTRIBUTION LIST (CONT.)

Commander (Code 753)
U.S.N. Ordnance Test Station
China Lake, California 93557
Attn: Technical Library

Bureau of Naval Weapons (Special
Projects)
Department of the Navy
Washington 25, D.C.
Attn: Mr. Robert Miller

Commanding Officer
Office of Naval Research
Branch Office, Navy 100
C/O Fleet Post Office
New York, New York

Commanding Officer
Submarine School
U. S. Naval Submarine Base
Groton, Connecticut

Commanding Officer (2 copies)
U. S. Naval Underwater Ordnance
Station
Newport, Rhode Island
Attn: Mr. J. F. Kelly & A. da Cruz
Code De2 (FRISCO)

Commanding Officer
Naval War College
Newport, Rhode Island

Commanding Officer & Director
U. S. N. Applied Science Laboratory
U. S. Naval Base
Brooklyn 1, New York
Attn: M. Adelman
Code 9230 (FRISCO)

Commanding Officer & Director
U. S. Naval Electronics Laboratory
San Diego 52, California (2 copies)
Attn: M. J. Sheehy & L. Griffith
Code 3110B (FRISCO)

Commanding Officer & Director
U. S. N. Mine Defense Laboratory
Panama City, Florida
Attn: P. K. White (FRISCO)

Commanding Officer & Director
U. S. Naval Training Device Center
Port Washington, New York
Attn: Technical Library

Commanding Officer & Director
U. S. N. Marine Engineering
Laboratory
Annapolis, Maryland
Attn: T. E. Mansfield
Code 812.2 (FRISCO)

Director
Aeronautical Instrument Laboratory
Naval Air Development Center
Johnsville, Pennsylvania
Attn: L. S. Guarino

Director
David Taylor Model Basin
Washington 25, D.C.
Attn: Code 533

Director (2 copies)
Naval Research Laboratory
Washington 25, D.C.
Attn: Code 2000
Code 5422 (FRISCO)

Director (2 copies)
U. S. Navy Underwater Sound
Laboratory
New London, Connecticut
Attn: Code 920 (FRISCO)
Code 940 (FRISCO)

Director
Special Projects
Department of the Navy
Washington 25, D.C.

Deputy
Comsublant
C/O Fleet Post Office
New York, New York

Naval Air Development Center
ASW Laboratory
Johnsville, Pennsylvania
Attn: ASW System Division

DISTRIBUTION LIST (CONT.)

Naval Ordnance Test Station
China Lake, California
Attn: Code 1422

Office of Naval Research (2 copies)
Navy Department
Washington 25, D.C.
Attn: Code 466
Lcdr. R. N. Crawford, USN

Office of Naval Research
Navy Department
Washington 25, D.C.

Office of Naval Research
Navy Department
Washington 25, D.C.
Attn: Code 463

Office, Chief Signal Officer
Department of the Army
Washington 25, D.C.
Attn: Code SIGRID-5
A. Stombaugh

SACLANT
ASW Research Center
Chief of Naval Operations
(OP 92B2)
Navy Department
Washington 25, D.C.

Superintendent
U. S. Naval Academy
Annapolis, Maryland
Attn: Head, Weapons Dept.

Technical Library
Room 3E 1065
Pentagon
Washington 25, D.C.

British Joint Naval Staff (5 copies)
P. O. Box 165
Benjamin Franklin Station
Washington 25, D.C.
via: Director, Naval Research
Laboratory
Washington 25, D.C.
Attn: Code 2000

Canadian Joint Staff (2 copies)
Washington, D.C.
via: Director, Naval Research
Laboratory
Washington 25, D.C.
Attn: Code 2000

National Academy of Science
Committee on Undersea Warfare
2101 Constitution Avenue, N.W.
Washington 25, D.C.
Attn: Security Officer for
Dr. W. P. Raney
Executive Secretary

General Dynamics/Convair
P.O. Box 1950
San Diego 12, California
Attn: Security Officer for
Engineering Library
Main Zone 6-157

Planning Research Corporation
Universal Bldg. North
1875 Conn. Ave. N.W.
Washington, D.C. 20009
Attn: Security Officer for
W. A. Schoenfeld

Bureau of Naval Weapons
Navy Department
Washington 25, D.C.
Attn: Ree

Commanding Officer
U. S. Naval Ordnance Test
Station
Pasadena, California

University of California
Scripps Institution of Oceanography
La Jolla, California
Attn: Security Officer for
Dr. F. N. Spiess

GENERAL DYNAMICS/Electric Boat Division
 Technical Report U417-64-028
 Processing of Data from Sonar Systems
 (Volume II)
 Dunham Laboratory, Yale University
 September 1, 1964

This is the second in a series of reports dealing with acoustic signal processing. It describes work concerned with the detection and determination of the bearing of a single target in an isotropic noise field. In the cases studied, the data source was assumed to be a single hydrophone or a given array of hydrophones. The problem investigated involved studies of likelihood ratio detection of sinusoidal signals in gaussian noise, in wide-band noise, and determinations of random bearing errors due to processing and also due to medium inhomogeneity for specific types of sonar systems.

GENERAL DYNAMICS/Electric Boat Division
 Technical Report U417-64-028
 Processing of Data from Sonar Systems
 (Volume II)
 Dunham Laboratory, Yale University
 September 1, 1964

This is the second in a series of reports dealing with acoustic signal processing. It describes work concerned with the detection and determination of the bearing of a single target in an isotropic noise field. In the cases studied, the data source was assumed to be a single hydrophone or a given array of hydrophones. The problem investigated involved studies of likelihood ratio detection of sinusoidal signals in gaussian noise, likelihood ratio detection of gaussian signals in wide-band noise, and determinations of random bearing errors due to processing and also due to medium inhomogeneity for specific types of sonar systems.

GENERAL DYNAMICS/Electric Boat Division
 Technical Report U417-64-028
 Processing of Data from Sonar Systems
 (Volume II)
 Dunham Laboratory, Yale University
 September 1, 1964

This is the second in a series of reports dealing with acoustic signal processing. It describes work concerned with the detection and determination of the bearing of a single target in an isotropic noise field. In the cases studied, the data source was assumed to be a single hydrophone or a given array of hydrophones. The problem investigated involved studies of likelihood ratio detection of sinusoidal signals in gaussian noise, likelihood ratio detection of gaussian signals in wide-band noise, and determinations of random bearing errors due to processing and also due to medium inhomogeneity for specific types of sonar systems.

GENERAL DYNAMICS/Electric Boat Division
 Technical Report U417-64-028
 Processing of Data from Sonar Systems
 (Volume II)
 Dunham Laboratory, Yale University
 September 1, 1964

This is the second in a series of reports dealing with acoustic signal processing. It describes work concerned with the detection and determination of the bearing of a single target in an isotropic noise field. In the cases studied, the data source was assumed to be a single hydrophone or a given array of hydrophones. The problem investigated involved studies of likelihood ratio detection of sinusoidal signals in gaussian noise, likelihood ratio detection of gaussian signals in wide-band noise, and determinations of random bearing errors due to processing and also due to medium inhomogeneity for specific types of sonar systems.